Complex Genetic Approaches to Neurodegenerative Diseases

A thesis presented in partial fulfilment of the requirements for the degree of Doctor of Philosophy to the University of London

by

Paresh Rameshchandra Shah

MRC Prion Unit, Institute of Neurology,
University College London

ProQuest LLC
789 East Eisenhower Parkway
P.O. Box 1346
Ann Arbor, MI 48106-1346

Abstract

Neurodegenerative diseases are fatal disorders in which disease pathogenesis results in the progressive degeneration of the central and/or the peripheral nervous systems. These diseases currently affect ~2% of the population but are expected to increase in prevalence as average life expectancy increases. The majority of these diseases have a complex genetic basis. The work presented in this thesis aimed to investigate the genetic basis of two neurodegenerative diseases, amyotrophic lateral sclerosis (ALS) and the human prion diseases kuru and sporadic Creutzfeldt-Jakob disease (sCJD), using novel complex genetic approaches.

ALS is a fatal neurodegenerative disease in which motor neurons are seen to degenerate. It is a complex disease with ~10% of individuals having a family history and the remaining 90% of non-familial cases having some genetic component. The gene *DYNC1H1* is involved in retrograde axonal transport and is a good candidate for ALS. In this thesis the genetic architecture of *DYNC1H1* was elucidated and a mutation screen of exons 8, 13 and 14 was undertaken in familial forms of ALS and other motor neuron diseases. No mutations were found. A linkage disequilibrium (LD) based association study was conducted using two tagging single nucleotide polymorphisms (tSNPs) which were identified as sufficient to represent genetic variation across *DYNC1H1*. These tSNPs were tested for an association with sporadic ALS (SALS) in 261 cases and 225 matched controls but no association was identified.

Kuru is a devastating epidemic prion disease which affected a highly geographically restricted area of the Papua New Guinea highlands, predominantly affected adult women and children. Its incidence has steadily declined since the cessation of its route of transmission, endocannibalism, in the late 1950's. Kuru imposed strong balancing selection on codon 129 of the prion gene (*PRNP*). Analysis of kuru-exposed and unexposed populations showed significant deviations from Hardy-Weinberg equilibrium (HWE) consistent with the known protective effect of codon 129 heterozygosity. Signatures of selection were investigated in the surviving populations, such as deviations from HWE and an increasing cline in codon 129 valine allele frequency, which covaried with disease exposure. A novel *PRNP* G127V polymorphism was detected which, while common in the area of highest kuru incidence, was absent from kuru patients and unexposed population groups. Genealogical analysis revealed that the heterozygous *PRNP* G127V genotype confers strong prion disease resistance, which has been selected by the kuru epidemic.

Finally, *PRNP* copy number was investigated as a possible genetic mechanism for susceptibility to kuru and sCJD. No conclusive copy number changes were identified.

Acknowledgements

Firstly, a massive thank you to my supervisors Professor Elizabeth Fisher and Professor John Collinge. Lizzy, your patience, support and guidance throughout the last three and a half years has gone above-and-beyond the duty of a supervisor and is something that I will always remember. John, thank you for the opportunity to contribute to the outstanding work produced at the MRC Prion Unit. In addition, thanks to Dr Simon Mead – my third supervisor. Simon, your passion for science and your willingness to explain even the most complicated population genetics concepts has been truly influential.

Much of the work in this thesis would not have been possible without the help of several people. Thanks to both Dr Azlina Ahmad-Annuar and Dr Majid Hafezparast for helping me find my feet at the bench at the beginning of my doctorate and your continuing support throughout my studies. I owe a huge debt of thanks to the molecular genetics group at the MRC Prion Unit. James Uphill helped with much of the microsatellite work, Gary Adamson for his help with sequencing and genotyping on the ABI 377, Huda Al-Dujaily and Tracy Campbell for help with extracting DNA from PNG blood samples, John Beck for answering my many questions and Mark Poulter for being the font of all allele discrimination and quantitative PCR knowledge, In addition, thanks to Jerome Whitfield, Mike Alpers and the rest of the PNGIMR field team, for the excellent epidemiology data and samples. Thanks also to Professor Robert Brown and the Day Lab in Boston for your assistance and hospitality during my visit.

The investigations discussed in this thesis would not have been possible without (i) the many thousands of samples collected and shared by various research groups around the world, to whom I am extremely grateful, (ii) all of the families, patients and healthy individuals who donated samples or consented to the collection and use of these samples and (iii) the UK Medical Research Council who funded this project.

I owe much of my perseverance over the last three and a half years to my fellow PhD compatriots, friends and lab mates past and present, without whom, this PhD would have been much more difficult and much less fun. The roll-call is too long to list here but you know who you are and I'll never forget you.

And finally, this thesis is dedicated to my parents who I love more than I have ever dared to say and to Kate, mi vida, without who's love and support none of this would have been possible.

Table of contents

List of figures

List of tables

Abbreviations

µg	Micro grammes
µl	Micro litres
AD	Autosomal dominant
AD	Alzheimer's disease
ALS	Amyotrophic lateral sclerosis
ALS2	Alsin
AMD	Age-related macular degeneration
ANG	Angiogenin
APEX	Apurinic endonuclease
APOE	Apolipoprotein E
APP	Amyloid precursor protein
APS	Ammonium persulphate
AR	Autosomal recessive
AR	Androgen receptor
AT3	Ataxin 3
ATP	Adenosine tri phosphate
BAC	Bacterial artificial chromosome
bp	Base pair
BSA	Bovine serum albumin
BSE	Bovine spongiform encephalopathy
CCA	Congenital contractural arachnodactyly
CCR5	Chemokine (C-C motif) receptor 5
CDCV	Common-disease/common-variant
cDNA	Complementary DNA
CEPH	Centre d'etude du polymorphisme humain
CF	Cystic fibrosis
CFTR	Cystic fibrosis transmembrane regulator
CHMP2B	Chromatin modifying protein/Charged multivesicular body protein 2B
CJD	Creutzfeldt-Jakob disease
cM	CentiMorgan
CNP	Copy number polymorphism
CNS	Central nervous system
CNTF	Ciliary neurotrophic factor
COX1	Cyclooxygenase 1
Cra1	Cramping 1
C_T	Threshold cycle
CYP2D6	Cytochrome p450, subfamily IID, polypeptide 6
DAPI	4',6-Diamidino-2-phenylindole
dATP	Deoxyadenosine triphosphate
DCTN1	Dynactin 1
dCTP	Deoxycytosine triphosphate
ddH20	Purified deionised water
df	Degrees of freedom
dGTP	Deoxyguanosine triphosphate
DLDH	Dementia lacking distinct histopathological features
DM	Dynamic mapping
DMSO	Dimethyl sulphoxide
DNA	Deoxyribonucleic acid
dNTP	Deoxynucleotide triphosphate
DPE	Downstream promoter element
DS	Down syndrome
dTTP	Deoxythymidine triphosphate
DYNC1H1	Cytoplasmic 1 dynein heavy chain 1
EAAT2	Excitatory amino acid transporter 2
EATDT	Extended allelic transmission disequilibrium test
EBV	Epstein bar virus
ECACC	European collection of cell cultures
EDTA	Ethylenediaminetetraacetic acid
EGF	Epidermal growth factor
EGFR	Epidermal growth factor receptor

EI	Exposure index
EM	Expectation maximisation
ENCODE	Encyclopaedia Of DNA Elements
ER	Endoplasmic reticulum
EST	Expressed sequence tag
EtBr	Ethidium bromide
EtOH	Ethanol
FALS	Familial Amyotrophic Lateral Sclerosis
FAM	6-carboxy-fluorescine
fCJD	Familial Creutzfeldt-Jakob disease
FDR	False discovery rate
FFI	Fatal familial insomnia
FISH	Fluorescent in situ hybridization technique
FLD	Frontal lobe degeneration of non-Alzheimer type
FOXP2	Forkhead box P2
FTD	Frontotemporal dementia
G6PD	Glucose 6 phosphate dehydrogenase
GFP	Green fluorescent protein
GRR	Genotype relative risk
GSS	Gerstmann-Sträussler-Scheinker
GTP	Guanosine-Tri-Phosphate
h^2	Heritability
HapMap	International Haplotype Map project
Hbb	Haemoglobulin beta
HD	Hungtington's disease
HEX	Hexachloro-6-carboxyfluorescein
HEXA	Hexosaminidase A
HFE	Haemochromatosis
HGNC	Human Genome Nomenclature Commnittee
HIV	Human immunodeficiency virus
HKA	Hudson-Kreitman-Aguadé
HKA	Hudson–Kreitman–Aguade test
HLA	Human leukocyte antigen
HSP	Hereditary spastic paraplegia
htSNP	Haplotype tagging SNP
HUGO	Human Genome Organisation
HWE	Hardy-Weinberg equilibrium
IARS2	Mitochondrial isoleucine tRNA synthetase
IBD	Inflammmatory bowl disease
IBM	Inclusion body myositis
IFT	Intraflagellar transport
Inr	Transcription initiator
kb	Kilobases
kDa	Kilo Daltons
kV	Kilo volts
LCT	Lasctase
LD	Linkage disequilibrium
LIF	Leukaemia inhibitory factor
LINE	Long interspersed nuclear element
LIS1	Lissencephaly 1
Loa	Legs at odd angles
LOD	Log-of-odds
LRH	Long-range haplotype
M	Molar
MAF	Minor allele frequency
MAO-B	Monoamine oxidase B
MAPT	Microtubule-associated protein tau
Mb	Megabase
MGB	Major groove binding
MGC	Mammalian genome collection
MGI	Mammalian Genome Informatics
MgSO4	Magnesium sulphate
MHC	Major Histocompatibility Complex
Mito	Mitochondrial DNA deletions

MMP3	Matrix metalloproteinase-3
MND	Motor Neuron Disease
mol	Moles
MRC	Medical Research Council
MRCA	Most recent common ancestor
MRI	Magnetic resonance imaging
mRNA	Messenger ribonucleic acid
MT	Microtubule
mtDNA	Mitochondrial DNA
MVB	Multivesicular body
MYCN	Myelocytomatosis viral related oncogene, neuroblastoma derived
NaAce	Sodium acetate
NAIP	Neuronal apoptosis inhibitory protein
NCBI	National Centre for Biotechnology Information
ND2	Subunit 2 of mitochondrial NADH dehydrogenase
NEFH	Neurofilament, heavy chain
NFT	Neurofibril tangles
NGF	Nerve growth factor
NPC	Niemann-Pick type C
nt	Nucleotide
OA	Ocular albinism
OMIM	Online Mendelian Inheritance in Man
OPN1LW	Opsin1 long wave
OPRI	Octapeptide repeat insertion
ORF	Open reading frame
PBS	Phosphate buffered saline
PCR	Polymerase chain reaction
PD	Parkinson's disease
PDR	Polymorphism discovery resource
Pers. comm.	Personal communication
PET	Positron emission tomography
PFA	Paraformaldehyde
PKU	Phenylketonuria
PLP	Proteolipid protein
PMD	Pelizaeus-Merzbacher disease
PNG	Papua New Guinea
PNGIMR	Papua New Guinea Institute of Medical Research
PRKN	Parkin
PRND	Dopple: downstream prion-like gene
PRNP	Prion protein gene
PrP	Prion protein
PrP^{C}	Prion protein (normal cellular isoform)
PRPH	Peripherin
PrP^{Sc}	Prion protein (scrapie isoform)
PSEN1	Presenilin-1
PSP	Progressive supranuclear palsy
QTL	Quantitative trait loci
QTN	Quantitative trait nucleotide
rcf	Relative centrifugal force
RFLPs	Restriction fragment length polymorphisms
RML	Rocky Mountain Laboratories
RNA	Ribonucleic acid
RNAi	RNA interference
rRNA	Ribosomal RNA
RT-PCR	Reverse transcriptase-polymerase chain reaction
SALS	Sporadic amyotrophic lateral sclerosis
SBMA	Spinobulbular muscular atrophy
SCA	Spinocerebellar ataxia
sCJD	Sporadic CJD
SCN9A	Sodium channel, voltage-gated, type IX, alpha
SCNA	α-synuclein
SDS	Sodium dodecyl sulfate
SEM	Standard error of mean
SETX	Senataxin

SINE	Short interspersed repeat element
SMA	Spinal muscular atrophy
SMN1/2	Survival of motor neuron 1/2
SNCA	Alpha synuclein
SNCG	Persyn
SNP	Single nucleotide polymorphism
SOD1	Cu/Zn superoxide dismutase 1
SOD2	Manganese superoxide dismutase
SSC	Sodium chloride sodium citrate
STR	Single tandem repeat
STS	Sequenced tagged site
TBE	Tris-borate EDTA
TDT	Transmission disequilibrium test
TET	Tetrachloro-6-carboxy-fluorescein
T_m	Melting temperature
TNFSF	Tumour necrosis factor superfamily
Tris	2,3-dibromopropyl phosphate
TrkA	Tyrosine kinase
tSNP	Tagging SNP
TSS	Translational start site
UCSC	University California Santa Cruz
UK	United Kingdom
USA	United States of America
UTR	Untranslated region
UV	Ultraviolet
VAPB	Vesicle-associated membrane protein-associated protein B
vCJD	Variant CJD
VCP	Valosin-containing protein
VDR	Vitamin D receptor
VEGF	Vascular endothelial growth factor
WGA	Whole genome association
YAC	Yeast artificial chromosome
λ_R	Relative risk
λ_S	Sibling relative risk

1 Introduction

1.1 Neurodegenerative diseases

Neurodegenerative diseases are a range of fatal disorders in which the disease pathogenesis results in the progressive degeneration of the central and/or the peripheral nervous systems. These diseases, which include Parkinson's disease (PD), Alzheimer's disease (AD), frontotemporal dementia (FTD), amyotrophic lateral sclerosis (ALS) and prion diseases, currently affect approximately 2% of the population in the developed world (Hardy *et al.*, 2006a) and show a propensity to occur with increasing age. As average life expectancy in the developed and developing world continues to increase, so too will the worldwide prevalence of neurodegenerative diseases (Kondo, 1996): conservative models of population growth predict that by 2025, over 1 billion people will be aged greater than 60 years old. This shift will have profound implications on public health and therefore our ability to dissect the aetiology of neurodegenerative disease must match this challenge. Understanding the genetic aetiology of neurodegenerative diseases will improve disease diagnosis, assist genetic counselling in familial cases, inform on an individual's susceptibility to disease, provide targets for therapeutics and inform future public health policy. Until recently, our ability to identify the genetic determinants of neurodegenerative disease has been restricted to rare Mendelian forms. These gene discoveries have illuminated only a small fraction of the causes of more common, apparently sporadic, complex forms of disease. However, recent developments in novel and rapidly advancing study designs, experimental and analysis techniques have begun to shed light on complex neurodegenerative diseases.

1.1.1 Common features of neurodegenerative diseases

In the last decade, several converging lines of investigation have revealed common epidemiological patterns, disease aetiologies and pathogenic mechanisms, underlying neurodegenerative diseases. These shared features suggest that mutual genetic mechanisms may also exist amongst these diseases which may be illuminated using similar techniques. Common features include the abnormal function of the following: protein aggregation and deposition (Skovronsky *et al.*, 2006; Taylor *et al.*, 2002), mitochondrial or oxidative phosphorylation activity (Manfredi *et al.*, 2000; Schon *et al.*, 2003), axonal transport (Roy *et al.*, 2005), endosomal and endocytic function (Bronfman *et al.*, 2007; Nixon, 2005) and the ubiquitin-proteosome system (Ciechanover *et al.*, 2003; Petrucelli *et al.*, 2004; Ross *et al.*, 2004).

In addition many neurodegenerative diseases share common features of genetic epidemiology such as the existence of both familial and sporadic or idiopathic forms of disease. At the same time, familial forms are often rare and sporadic forms of neurodegenerative diseases are often common. The rare exception to this observation are the triplet repeat disorders such as

Huntington's disease and the spinocerebellar ataxias, of which the overwhelming majority are familial, or apparently sporadic but due to cryptic familial inheritance, non-paternity (Davis *et al.*, 1994) or *de novo* repeat expansions (Bozza *et al.*, 1995; Davis *et al.*, 1994; Durr *et al.*, 1995; Futamura *et al.*, 1998; Mandich *et al.*, 1996; Myers *et al.*, 1993). In addition, common to all neurodegenerative diseases is the familial aggregation of disease, which may imply a genetic component to even sporadic disease.

1.1.2 Related genetic mechanisms

Beyond the clinical, epidemiological and pathological features of neurodegenerative diseases, different neurodegenerative disorders may also share a common genetic aetiology: the genetic determinant of one neurodegenerative disease may be a causal or risk factor in another disease. A commonly cited example is ε4 allele of the *alipoprotein E* gene (*APOE*), which is a susceptibility factor for several diseases including: age of onset and dementia in PD (Feldman *et al.*, 2006; Huang *et al.*, 2006; Li *et al.*, 2002; Li *et al.*, 2004; Parsian *et al.*, 2002; Tang *et al.*, 2002a), age of onset in ALS (Li *et al.*, 2004) and age of onset in FTD (Boccardi *et al.*, 2004; Borroni *et al.*, 2005). In addition, the gene *charged multivesicular body protein 2B* (*CHMP2B*), which has been shown to be causative for FTD in both a Danish family and an isolated FTD individual (Skibinski *et al.*, 2005) has also been identified in two cases of ALS (Parkinson *et al.*, 2006). Examples such as these support the view that neurodegenerative diseases, such as FTD and ALS, may have common genetic aetiologies. In addition familial clustering of diseases such as ALS and Creutzfeldt-Jacob disease (CJD) with other neurodegenerative diseases (Majoor-Krakauer *et al.*, 1994; van Duijn *et al.*, 1998) is indicative of a common cause to these diseases which can identify risk factors (Riemenschneider *et al.*, 2004).

1.2 Gene identification in Mendelian forms of neurodegenerative diseases

To date, the overwhelming majority of genes causal for human disease have been identified through linkage analysis. These analyses have commonly required large pedigrees which display clear Mendelian inheritance of a phenotype. Essentially, linkage analysis relies on the co-segregation of a disease causing allele and adjacent DNA markers with the disease phenotype, within a family. Chromosomal segments that do not influence disease segregate randomly. A DNA segment that carries the disease-causing mutation will be shared among affected family members more often than would be predicted by chance and a likelihood score (log-of-odds ratio; LOD) is applied (LOD>3.6 is generally considered the criterion indicating linkage between a genome segment and disease).

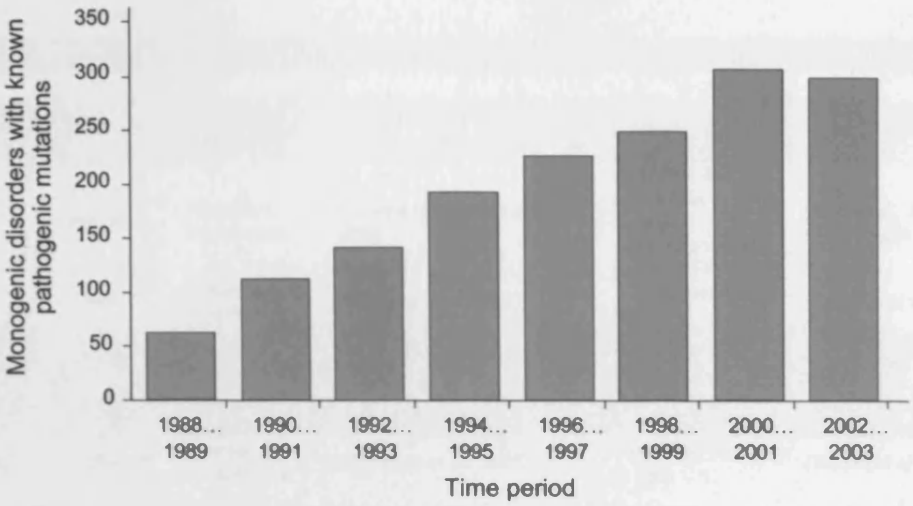

Figure 1.1 Allelic variants showing Mendelian inheritance discovered from 1988 to 2003

Graph depicting the number of pathogenic mutations causing monogenic disorders, recorded in OMIM over 15 years (Modified from Antonarakis *et al.*, 2006).

As Figure 1.1 illustrates, the number of single genes responsible for Mendelian disorders, identified and catalogued in the Online Mendelian Inheritance in Man (OMIM) database increased rapidly between 1988 and 2001. The key to success of linkage analysis has been the near-complete penetrance of simple traits; affected individuals are easily identified and always possess a genetic mutation, which in turn has permitted the collection of the large families required for linkage analysis. However, despite the advances linkage studies have provided in our understanding of the genetic basis of human disease, familial diseases continue to represent the minority of cases in almost all forms of disease. In fact, the majority of human diseases do not demonstrate the characteristics of simple monogenic Mendelian forms and until recently, the accepted dogma has regarded these non-Mendelian forms of disease as sporadic with possibly no genetic component. However, there is a large body of evidence that non-Mendelian diseases have a genetic component and are complex, i.e. are influenced by multiple genes, which interact with each other and with the environment.

1.3 The genetic component of non-Mendelian diseases

Diseases that do not demonstrate Mendelian inheritance may still possess a genetic component.

1.3.1 Familial genetics inform susceptibility loci in sporadic disease

Rare monogenic familial forms of several neurodegenerative diseases have informed our understanding of the genetic aetiology of sporadic disease. Causative genes identified in familial studies of AD, PD, ALS, FTD and CJD for example, have been found to be mutated in a minority of non-Mendelian cases, indicating that at least some sporadic cases have a genetic component (Table 1.1).

Disease	Gene	Familial cases		Sporadic cases	
AD	*APP*	Dominant inheritance	(Tanzi *et al.*, 1987; Goldgaber *et al.*, 1987)	Increases risk	(Brouwers *et al.*, 2006; Guyant-Marechal *et al.*, 2007)
PD	*SNCA*	Dominant inheritance	(Polymeropoulos *et al.*, 1996)	Promoter di-nucleotide repeat associated with increased risk	(Tan *et al.*, 2000; Tan *et al.*, 2003)
	PRKN	Recessive inheritance	(Kitada *et al.*, 1998)	19% sporadic cases	(Lucking *et al.*, 2001)
ALS	*SOD1*	Dominant inheritance	(Rosen *et al.*, 1993)	2-7% sporadic cases	(Andersen *et al.*, 1997; Jackson *et al.*, 1997)
	DCTN1	Dominant inheritance	(Puls *et al.*, 2003)	3 cases to date	(Munch *et al.*, 2004; Munch *et al.*, 2005)
FTD	*CHMP2B*	Dominant inheritance	(Skibinski *et al.*, 2005)	1 possible case to date	(Skibinski *et al.*, 2005)

Table 1.1 Mendelian genes identified with mutations in non-Mendelian diseases

Examples of genes from four Mendelian forms of neurodegenerative diseases that have been implicated in complex forms of the same disease. Maximum of two loci are shown for Alzheimer's disease (AD), Parkinson's disease (PD), amyotrophic lateral sclerosis (ALS) and frontotemporal dementia (FTD). References are not exhaustive.

1.3.2 Familial clustering of disease

The recurrence of an apparently sporadic disease in a family more frequently than could be predicted by population prevalence also provides evidence of a genetic component to non-Mendelian disease. This familial clustering of disease, can be measured by the relative recurrence risk (λ_R) - the risk to relative *R* of an affected proband compared with the population risk. Familial clustering can be interpreted in several ways: disease can be due to shared genetic susceptibility, shared environmental exposure(s), or both. However, familial clustering may be due to other factors such as incomplete penetrance, as has been shown in ALS (Robberecht *et al.*, 1996), or due to the transmission of environmental factors, such as viruses, within families which can mimic or confound true genetic susceptibilities (Szmuness *et al.*, 1973).

Another measure of the contribution of inherited factors to disease risk is heritability (h^2). Estimated from family or twin studies, heritability signifies the fraction of the population variation that can be explained by genetic factors working together in an additive fashion. For diseases such as late onset Alzheimer's disease, heritability may be between 58% and 79% (Gatz *et al.*, 2006).

Twin studies are of particular importance in the estimation of heritability in complex diseases (reviewed in MacGregor *et al.*, 2000) as they exploit the unique degree of genetic sharing among the two types of twin pair: (i) monozygotic twins, who share a common set of genes, and (ii) dizygotic twins, who share on average ~50% of their genes. In addition, the use of twins can control for non-genetic factors, as they share aspects of their early and later environment and these features allow the population-level variation of traits and diseases to be separated into genetic, shared environmental and random environmental components. Conversely, for twins

reared in different environments such as in adoption studies, variances due to environment and gene-environment interactions can also be assessed.

1.4 Complex diseases

Our understanding of complex diseases (also known as complex traits) is founded within the fascinating history of genetics and genetic ideas. In the interest of brevity, the full history of modern genetics and complex diseases is not discussed here (but an excellent account can be found in Strachan *et al.*, 1999). However, to understand what complex diseases are and why the underlying genes have been difficult to elucidate, a brief review of complex genetics is required.

Historically, there have been two traditions within human genetics. The first followed the principles of heredity established by Gregor Mendel who identified that physical traits were inherited discretely. Under this tradition all traits are considered dichotomous (such as polydactyly – either you have an extra finger or you don't) - the off-spring of a set of parents inherit characteristics from one parent or the other and not a blend of the two. This premise also formed the basis of a saltation (or non-gradual) theory of evolution, in which sudden phenotypic changes are seen from one generation to the next. The second tradition was based on the study of variation, such as that carried out by Francis Galton in the late 19th century who observed that human characteristics, such as weight, height and reaction time were quantitative, continuously variable characters. These continuous traits could not be reconciled using Mendelian genetics and did not explain gradual genetic variation (i.e. gradual evolution) seen in many organisms described in the theory of modern synthesis.

In 1918, both traditions were aligned by the mathematician and geneticist Ronald Aylmer Fisher. Fisher proposed that continuous traits are in fact governed by a number of loci, which are inherited in a Mendelian fashion, and that alleles at each locus contribute quantitatively to the overall phenotype. Any variable character that depends on the additive action of a large number of individually small independent causes will be distributed in a normal (Gaussian) distribution in the population, and under this polygenic theory of inheritance, as the number of quantitative trait loci (QTL) increase, the distribution looks increasingly like a Gaussian curve.

However, Fisher's polygenic theory of inheritance could not account for dichotomous characteristics which are not inherited within families. This problem was solved in 1981 by Douglas Scott Falconer who extended the polygenic theory to discontinuous non-Mendelian characters by postulating that (i) an underlying polygenic liability to disease exists within a population and it is this which is continuously distributed and not phenotype and (ii) diseases manifest when the cumulative diseases susceptibility burden exceeds a threshold of liability. By inference, individuals whose genetic liability does not exceed the threshold value do not develop disease (Figure 1.2).

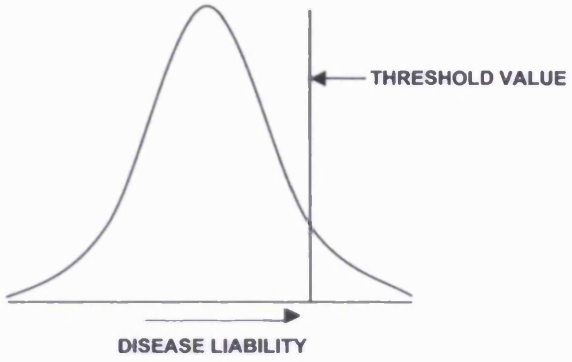

Figure 1.2 The threshold liability model

The model shows the distribution for liability to disease within a population. Individuals to the right of the threshold develop disease whereas those to the left are healthy.

For example, this can be illustrated by the developmental abnormality, cleft lip and palate. Every embryo has a certain susceptibility to cleft lip and palate which follows a Gaussian distribution in the population. During early development the embryonic palatal shelves must become horizontal and fuse together within a specific developmental window of time. The speed at which the plates meet and fuse is unimportant, as long as they meet before a critical developmental stage. If they fuse at or before the critical point then a normal palate forms, and if they do not fuse then a cleft palate results and thus, there is a natural threshold imposed on a continuous trait which is transformed into a dichotomous phenotype.

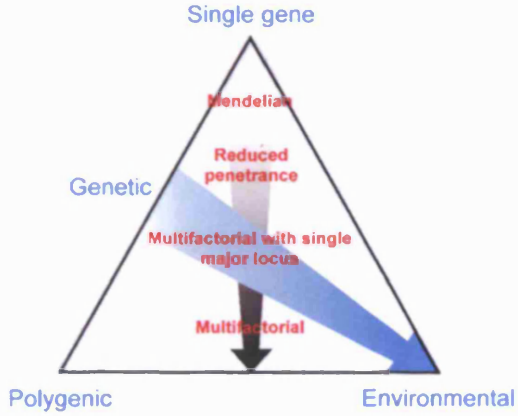

Figure 1.3 The spectrum of human disease

Few characters are purely Mendelian, purely polygenic or purely environmental. Most depend on some mix of major and minor genetic determinants, together with environmental influences. The mix of factors determining any given character could be represented by a point located somewhere within the triangle. (From Strachan *et al.*, 1999)

The threshold liability model also accounts for familial clustering in non-Mendelian disease because liability genes will be more common amongst relatives and therefore all members of the family will be closer to the liability threshold. Not all family members will develop disease as several loci and environmental factors will contribute to phenotype. The challenge for human genetics now is to identify those genes that increase liability to develop disease (susceptibility genes) and those that modify, enhance or reduce a phenotype (modifier genes). In Mendelian diseases, the action of these susceptibility and modifier loci may manifest as reduced

penetrance, meaning that the disease has a reduced likelihood of occurring in individuals who carry the risk genotype. Susceptibility to human disease can therefore be considered a spectrum of genetic and environmental risk, which together can explain Mendelian disease, quantitative traits and complex diseases (Figure 1.3).

1.5 Gene identification strategies in complex diseases

1.5.1 Linkage analysis based approaches

Traditional linkage based approaches have worked well for Mendelian disorders (Antonarakis *et al.*, 2006) and have been carried out successfully on a few complex diseases such as schizophrenia (Stefansson *et al.*, 2002) and type 1 diabetes (Nistico *et al.*, 1996). However, for most complex, polygenic traits, linkage analyses of extended pedigrees, siblings or parent and child trios, have achieved only limited success: Altmuller and colleagues found that in a review of 101 genome-wide linkage studies in 31 complex human diseases, over two-thirds of the studies showed no significance (Altmuller *et al.*, 2001). Where genes have been discovered using linkage analysis they usually explain only a small fraction of the overall heritability of the disease. For example, variants known to affect the risk of inflammatory bowel disease (IBD) together explain a sibling risk of approximately two-fold, compared with a total excess risk of 30-fold (Daly *et al.*, 2004), which indicates that there are additional genes in IBD to be discovered. The lack of success can be attributed to several reasons: (i) linkage is an indirect statistical test, relying on distortions of Mendelian inheritance ratios to infer the nearby location of a disease-causing mutation. When the genetic effect is very large (as in Mendelian disorders), this indirect signal is sufficient. For QTLs with only a small magnitude of effect, the power of linkage may be inadequate. (ii) Large sample sizes can compensate for low magnitude of effect, however assembling large families, each containing multiple affected individuals, is difficult particularly when the disease is rare, has an advanced age of onset and high mortality (as is the case for many neurodegenerative diseases). (iii) In addition, genetic factors such as pleiotropy (one gene which yields multiple phenotypes) and epistasis (the non-additive effect of multiple genes) provide extra complications.

1.5.2 Association studies

In their simplest form, association studies compare the frequency of alleles or genotypes of a particular variant between disease cases and controls. This may be done directly, where a candidate variant, often putatively functional, is tested for enrichment or depletion in disease cases compared to normal controls. For example, resequencing the entirety of a candidate gene in patients and controls, and testing variants such as single nucleotide polymorphisms (SNPs) in cases and controls is a direct test of association as every nucleotide is tested for a potential association with disease. Direct tests are hypothesis-based, with genes and candidate variants

selected for further study either by virtue their location in a region of linkage, or on the basis of other evidence that they might affect disease risk (Carlson *et al.*, 2004a).

In contrast, indirect studies test markers (commonly SNPs) for disease association under the assumption that the marker itself is not causal but that it may be linked by allelic association or linkage disequilibrium (LD) to the true causal variant. Therefore, if a risk polymorphism exists it will either be genotyped directly or be in strong LD with one of the genotyped markers. The benefit of such indirect association studies, also called LD mapping, are that they do not require prior determination of which marker might be functionally important.

1.5.2.1 Linkage disequilibrium

Linkage disequilibrium (LD) has become an important consideration in most association studies for complex diseases. LD describes the non-random correlation between alleles at a pair of genetic markers (commonly SNPs). In contrast to linkage, which describes the association of loci on a chromosome with limited recombination between them, LD describes a situation in which some combinations of alleles occur more or less frequently in a population than would be expected if they were segregating randomly (i.e. in disequilibrium). Whereas linkage analysis relies on informative recombination events within a pedigree, LD utilises informative meioses of an extended pedigree of the complete human population. As a result, the interval shared through identity by decent within a population is much smaller than that shared by linkage in a pedigree, which can aid in the fine mapping of disease loci.

The measure D has been widely used to quantify LD. Consider two adjacent loci — A and B, with two alleles (A,a and B,b) at each locus — the observed frequency of the haplotype that consists of alleles A and B is represented by P_{AB}. Assuming independent assortment of alleles at the two loci, the expected haplotype frequency is $P_A \times P_B$ (where P_A is the frequency of allele A and P_B is the frequency of allele B). From Equation 1.1 it is clear that the primary determinant of LD is recombination which, in addition to recurrent mutation and evolution, serves to errode LD.

Equation 1.1 $$D = P_{AB} - (P_A \times P_B)$$

The utility of LD in association studies relies on the fact there is redundancy in the information gained from typing multiple SNPs in LD: for two SNPs in perfect LD, only one SNP would need to be typed to inform on the genotype of the other. This method of selecting a minimal set of markers to represent the underlying genetic variation is known as tagging. Additionally, SNPs may also be in LD with unknown SNPs that are not genotyped. If the unknown SNP is a causal variant for disease susceptibility, the known genotyped SNP could be used as a proxy to test for an indirect association with disease. The known SNP therefore is a tagging SNP (tSNP) for unknown genetic variation.

Equation 1.2 $D' = D/D_{max}$

Equation 1.3 $r^2 = D^2/P_A P_B P_a P_b$

Although the LD measure D provides a useful explanation as to the extent of LD between two loci, the measures D' and r^2 are more commonly used in association studies (Devlin *et al.*, 1995). D' varies between 0 and 1, is calculated by normalising D by its maximum possible value, D_{max}. $D' = 1$ only if two SNPs have not been separated by recombination. r^2 is more commonly used in the context of association studies and LD mapping and can be calculated by normalising D^2 by the product of all four allele frequencies. r^2 is simply the squared correlation coefficient between the two loci. Perfect LD ($r^2=1$) indicates that markers have not been separated by recombination and have the same allele frequencies. An attractive property of r^2 is that it directly relates to sample size and power. For a study to detect an association between disease and a marker locus, the sample size must be increased by roughly n/r^2 (where n is the number of samples in the study) to have the same power as actually genotyping the susceptibility locus itself (Kruglyak, 1999; Pritchard *et al.*, 2001).

1.5.2.2 Linkage disequilibrium patterns in the human genome

The pattern of LD throughout the human genome has been extensively studied and has been of particular importance in association studies as it impacts on both the efficiency and power of these studies. There are several salient features of LD in the human genome. The first is that LD is inversely correlated with distance. This aspect of LD is intuitive as recombination rates are generally higher between markers at increasing distances and therefore, as LD is eroded by recombination, LD decay is seen over distance (Hartl *et al.*, 2007). However, LD has been shown to be highly variable, extending between a few to several hundred kilobases (kb) (Dawson *et al.*, 2002; Kruglyak, 1999).

Secondly, whereas LD was thought to decay uniformly over distance, several authors have provided evidence to that islands of high LD exist, separated by highly recombining regions (Daly *et al.*, 2001; Rioux *et al.*, 2001). These haplotype blocks of LD, punctuated by hotspots of recombination have been witnessed in multiple studies (Gabriel *et al.*, 2002; International HapMap Consortium, 2003; Jeffreys *et al.*, 2001) however more recent studies have suggested that LD at finer-resolution is more variable than previously thought (Ke *et al.*, 2004). This atomistic picture of LD has been crucial in the design and efficiency of association studies (see below).

Thirdly, LD is heterogeneous amongst populations. Early studies by both Reich and colleagues and Gabriel and colleagues identified that population samples from Africa have markedly less LD than Europeans and Asians (Gabriel *et al.*, 2002; Reich *et al.*, 2001a). In contrast, younger or isolated populations have been shown to have the highest LD, suggesting that within different

populations LD is a reflection of that population's history (i.e. demographic processes influence LD patterns) (Bonnen *et al.*, 2002; Dunning *et al.*, 2000; Kidd *et al.*, 2000). This elevated LD can assist in the mapping of disease genes, as less haplotype diversity is seen and studies require fewer makers. In addition, the genetic architecture in population isolates can also be utilised as groups that have undergone a population bottleneck tend to have a distinct set of common disease alleles and tend to share more environmental features than outbred populations (Peltonen *et al.*, 2000). Taken together, these studies have informed the design of association studies. By identification of the underlying LD structure across a candidate gene or even across the genome, a small number of SNPs could be used to define a large proportion of genetic diversity and be tested for association with disease.

1.5.2.3 Tagging SNPs

The efficacy of using a subset of SNPs to define the majority of variation was first demonstrated by Johnson and colleagues, who found that up to 6 SNPs could define the majority of haplotype diversity in a selection of gene (Johnson *et al.*, 2001). In all, 122 SNPs, spanning 9 genes were reduced to just 34 haplotype tagging SNPs (htSNPs). More recently, tagging strategies moved towards maximising pairwise r^2 as this measure is more informative with respect to association studies (Carlson *et al.*, 2004b). Further efficacy has been gained by the observation that tSNP haplotypes (Figure 1.4) in turn show redundancy (Goldstein *et al.*, 2003a; Weale *et al.*, 2003). In a study by Weale and colleagues, investigating the sodium channel gene *SCN1A*, implicated in epilepsy, this aggressive tagging technique provided a 110-fold saving in genotyping effort. In summary, based on the pattern of LD within a genomic region of interest, a minimal set of tSNPs can be chosen to tag known and unknown variation, providing association studies with efficiencies of both cost and effort.

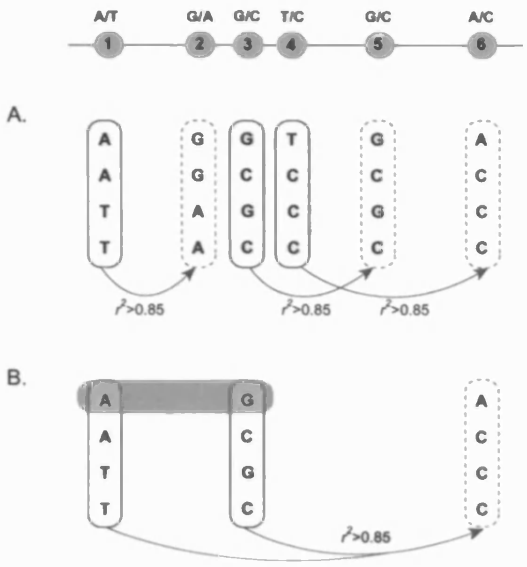

Figure 1.4 Aggressive tagging of variation linked to six loci

Six SNP loci are shown with their corresponding alleles. **A**. Loci 1, 3 and 4 tag SNPs 2, 5 and 6 respectively with a minimum correlation coefficient r^2>0.85. **B**. Redundancy of tSNP haplotypes allows the AG haplotype (red) at tSNPs 1 and 3 to predict the A allele at locus 6.

1.5.3 Association study design

The design of association studies and the technology available to conduct them has changed dramatically since the work presented in this thesis was undertaken. These changes and their effect on study design are examined in later chapters. However, there are some fundamental elements of association study design that are discussed below and in addition, advances in the resources available for future studies are discussed.

1.5.3.1 Study power and sample size

The power of an association study is the statistical probability that the study will detect a true association if one is present. There are several factors that affect study power including sample size, the prevalence and magnitude of effect of the risk factor, and the strength of linkage disequilibrium between the marker and causal variant. Sample size is probably the most common influential factor in association studies, especially in those of rare neurodegenerative diseases where achieving large cohorts would be difficult.

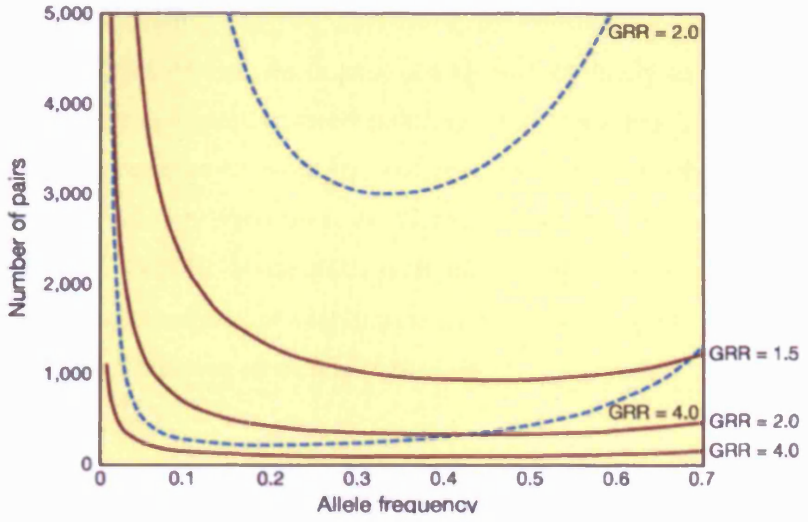

Figure 1.5 Association study sample size predictions

The sample size required for 80% power to detect an association of various genotype relative risks (GRR) with susceptibility alleles of increasing frequency. Dashed line using linkage methodology and solid line using association methodology. (From Risch, 2000).

The effect on samples size due to magnitude of effect (genotype relative risk; GRR) and allele frequency can be witnessed through modelling studies. As Figure 1.5 illustrates association studies can have greater power over linkage when GRR<2 and large sample sizes are required when GRR is small.

1.5.3.2 Sample selection

There are several design considerations related to sample choice and ascertainment that can lead to either spurious association or reduced study power. Population stratification is an important consideration for association studies as allele and haplotype frequencies can differ considerably between populations, resulting in both false positives and negatives associations. This bias can be a potential problem if, for example, disease prevalence varies between populations (i.e. between ethnic groups) as this may result in the over-representation of a subgroup in the case cohort and the more frequent polymorphism in that subgroup will tend to be more associated with disease despite not influencing it (Ardlie *et al.*, 2002; Cardon *et al.*, 2003). Stratification may be overcome by modifying the study design to include family based controls, as is seen in the transmission disequilibrium test (Spielman *et al.*, 1993); typing multiple unlinked genomic control loci to detect stratification and correct for inflation in the test statistic (Devlin *et al.*, 1999; Devlin *et al.*, 2004); or by simply ensuring that cases and control cohorts are matched for ethnicity and environmental covariates (which for most studies can be easily achieved).

Power to detect association may be reduced by inadequate selection of case and control samples. The inadequate selection of case samples may be due to phenotypic heterogeneity or clinical misdiagnosis. The latter may be reduced by ensuring that all cases are diagnosed based on a set of universally adopted diagnostic criteria, such as the El Escorial criteria in ALS

(Brooks, 1994), and the latter may be eliminated by considering intermediate phenotypes (Gottesman *et al.*, 2003). Intermediate disease phenotypes are likely to have fewer extraneous environmental influences compared to those at the endpoint of disease. To overcome phenotypic heterogeneity they are required to be more predictive of disease or disease progression, than disease end-points, which are often used as clinical phenotype. For example, in age-related macular degeneration (AMD), a complex neurodegenerative disease affecting the retinal pigment epithelium, intermediate phenotypes such as photoreceptor segment turnover and macular pigment levels have been identified (Chamberlain *et al.*, 2006).

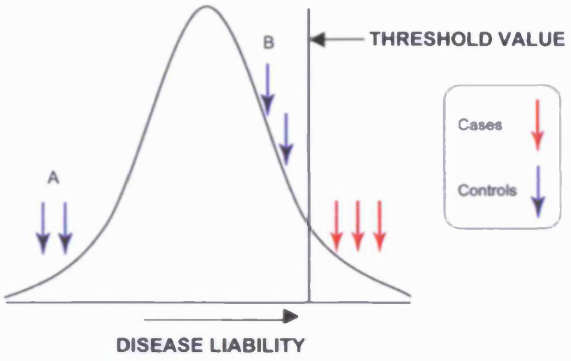

Figure 1.6 Case-control selection using the threshold liability model

Individuals with liability to disease greater than the threshold value will develop disease and be assigned to the case cohort. Control individuals are absent of disease but may either have an extremely low liability to disease (**A**) or be approaching the threshold value (**B**).

There are also several issues with the selection of control samples for case-control association studies of complex diseases. The first can be illustrated using the liability threshold model (Figure 1.6). Generally, the selection of a control cohort is conducted by selecting individuals absent for disease phenotype. However, in complex diseases, where disease may only manifest once the threshold of liability is reached, any individual under the threshold may be selected as a control. If a proportion of the control cohort is comprised of individuals just below the threshold level of liability, this may reduce the power of an association study to detect an association. By choosing controls from the left-hand tail of the distribution (i.e. hyper controls), who have a lower population risk of disease, this power to detect an association may be increased. In most studies where the defined phenotype is the presence/absence of disease or disease end-point, it will impossible to place the control cohort on this distribution, however quantitative intermediate phenotypes (Gottesman *et al.*, 2003) or other indicators of disease risk that vary normally could be used.

1.5.3.3 Candidate gene and whole genome approaches

To date, the majority of case-control association studies for complex diseases have been undertaken on candidate genes. This has largely reflected the limited availability of polymorphism data and the high cost of genotyping for polymorphism ascertainment, making genome-wide methodologies in complex diseases unfeasible for most researchers. Candidate

genes have largely been ascertained in a number of ways: through known causation in Mendelian forms of disease, which are predicted to predispose to complex forms; through regions of linkage from sib-pair studies; through biological plausibility based on phenotypes; model organism mutants, such as mouse models of human disease, or the action of a gene in a pathway relevant to disease pathogenesis. Critically, these methods have relied on prior assumptions. In contrast, genome-wide studies can be undertaken with no prior assumptions as to the location or function of a pathogenic variant; However, these methods, which test up to 500,000 SNPs in one experiment and are therefore likely to detect false positives, also bear a heavy multiple testing penalty.

1.5.3.4 Allelic architecture of complex disease

For most complex diseases the underlying genetic variation remains unknown. The number of relevant disease variants that exist is unknown as are their frequencies in the population: genetic variation could be rare (alleles with frequencies <1% in the population), as is true for most single-gene disorders, it could be more common (frequencies >1% in the population). The frequency spectrum of the alleles for complex diseases is important to consider, because the allele frequencies of variants that predispose to disease and the strength of their phenotypic effects directly relate to the statistical power of genetic association studies, and therefore their likelihood of success.

These underlying allele frequencies are largely unknown because the causal variants remain largely unknown, however theoretical and empirical studies suggest that for complex diseases, some of the causal genetic variants may be common (Chakravarti, 1999; Lander *et al.*, 1994; Reich *et al.*, 2001b). The common disease/common variant (CDCV) hypothesis proposes, that common diseases are a result of common variants (Reich *et al.*, 2001b). Under this model, disease susceptibility is suggested to result from the joint action of several common variants, and unrelated affected individuals share a significant proportion of disease alleles. There are several arguments to support this theory: (i) common diseases are generally not as evolutionarily disadvantageous as single-gene disorders, which often cause early death or markedly decreased reproductive capability; (ii) variants that cause single-gene disorders are highly penetrant, whereas multiple variants are required to cause common diseases and thus, the impact of selective pressure is diluted for the variants for complex traits; (iii) the majority of monogenic diseases are rare, whereas most polygenic diseases are common- population genetic arguments predict that for common diseases, some of the causal genetic variation should have a high frequency in the population, due to the demographic history of the human population (Reich *et al.*, 2001b); and (iv) empirical evidence has suggested that common variants do contribute to the risk of common diseases (Lohmueller *et al.*, 2003).

However, evidence from monogenic disorders suggests that the responsible variants are generally rare, so could the variants that cause common disease not also be predominantly rare? The alternative to CDCV is the disease heterogeneity hypothesis (or multiple rare-variant hypothesis), in which disease susceptibility is due to distinct genetic variants in different individuals and disease-susceptibility alleles have low population frequencies <1% (Smith *et al.*, 2002). This allelic heterogeneity is a potential problem for association studies, unlike the CDCV hypothesis which supports the mapping of loci through association (Pritchard *et al.*, 2002), and may be a more pervasive phenomenon in common disease (Pritchard, 2001). So, what are the prospects for neurodegenerative diseases? Successes in mapping the susceptibility *APOE* ε4 locus associated with increased risk to Alzheimer disease (Corder *et al.*, 1993) has been possible due to high allele frequencies, ranging from 5%–41% in various populations (Fullerton *et al.*, 2000) and large effect size. However, identification of risk factors with smaller effect sizes at lower frequencies will require much larger samples and possibly more sensitive analytic techniques.

As discussed later, allelic heterogeneity and the CDCV hypothesis may be a surmountable problems for complex loci mapping and even some successes have been seen. For example, the gene *NOD2* has been successfully associated with Crohn's disease despite the presence of moderate allelic heterogeneity (Hugot *et al.*, 2001) as has *CAPN10*, a susceptibility locus for type 2 diabetes (Horikawa *et al.*, 2000). In addition populations with a greater degree of common variation such as isolated populations can be used to identify rare variants in outbred populations. For example, the Finnish population descends from two waves of immigration, 200 years ago from the southern Indo-Europeans and 4000 years ago from eastern Uralic speakers. The population expanded from ~50,000 in the 12th century to the present day ~5,000,000. Relative homogeneity of culture and lifestyle has also been noted. Approximately 30 recessive diseases are enriched in Finland, whilst rare diseases found elsewhere in the world are absent. Both allelic and non-allelic heterogeneity are reduced which serve to increase association study power. Thus isolated populations share some of the advantages of inbred mouse lines and provide greater power in association studies to detect rare alleles (Lee *et al.*, 2001b).

1.5.3.5 Evolving resources for association studies in complex diseases

The association study data presented in this thesis serve as a reminder of the infancy of our knowledge of human genetic variation and ability to map complex traits. In the years since this work began, several aspects of study design, theory and the tools available to conduct these studies have matured. These advances are discussed in detail later and contrasted with our understanding at the outset of this work. Possibly the most significant difference however has been the availability of genomic variation and LD data, and advances in SNP genotyping technology.

An important consideration in association study design has been the construction of LD maps. Due to costs and feasibility issues, LD maps have historically been determined for candidate genes, as SNPs have had to be located, genotyped and LD assessed. From the year 2000, the volume of freely available SNP information in the database dbSNP has increased (Figure 1.7). dbSNP database now contains over 9.7 million SNPs (as of September 2006) obviating much of the need to ascertain SNPs in a candidate region.

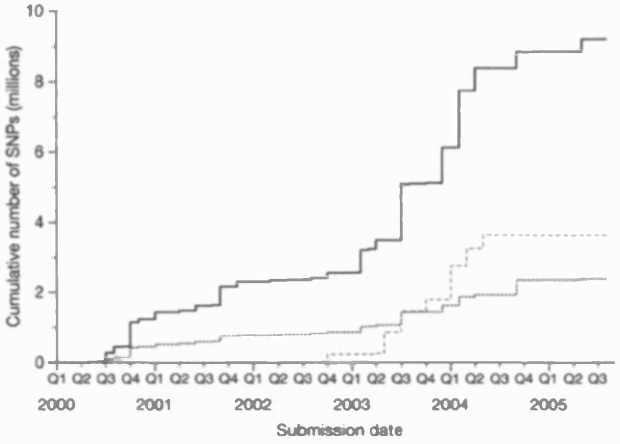

Figure 1.7 SNP submissions to dbSNP from over 5 years from 2000

Graph shows cumulative number of non-redundant SNPs, each mapping to a single location in the genome (solid line), the number of SNPs validated by genotyping (dotted line) and double-hit status (dashed line). Years are divided into quarters (Q1–Q4). (From The International HapMap Consortium, 2005)

Part of the exponential increase in SNP submissions since 2002 has been due to the launch of The International Haplotype Map project (HapMap) (International HapMap Consortium, 2003). This international collaboration undertook an extensive SNP discovery effort in 3 populations of African, Asian, and European ancestry to construct a dense 5kb SNP map and ascertain the underlying pattern of LD and therefore haplotype structure. This project has contributed vastly to our understanding of human genetic variation (The International HapMap Consortium, 2005) and has provided a resource for researchers choosing to undertake association studies. The availability of HapMap data (www.hapmap.org/) has obviated the need for investigators to have to ascertain SNPs and construct LD maps, saving considerable time and money. In addition, the advent of new genotyping technologies over the past seven years has seen genotyping costs reduced from $0.50 per genotype to $0.001 per genotype, which has had an effect on the number of SNPs and the number of samples that can be screened – ultimately increasing study power

1.6 Evolutionary analyses

The search for new methods to identify genes involved in complex diseases has led several authors to propose the use of natural selection to identify disease susceptibility loci (Jorde *et al.*, 2001; Nielsen, 2001). The rationale behind this approach is two fold: (i) The previous

identification of genes implicated in both Mendelian and complex diseases and other complex phenotypes, show patterns of genetic variation characteristic of selection (referred to from here as signatures of selection), see Table 1.2 – over 90 different loci have been proposed as possible targets for selection to date (Sabeti *et al.*, 2006). (ii) Genetic variants that may have been under evolutionary selection are by definition functional and thus maybe more likely to contribute to disease susceptibility today.

Disease or phenotype	Gene	Mode of selection	Reference
Malaria resistance	*G6PD* *TNFSF*	Positive	(Sabeti *et al.*, 2002)
Heart disease risk	*MMP3*	Positive	(Rockman *et al.*, 2004)
Speech	*FOXP2*	Positive	(Enard *et al.*, 2002; Zhang *et al.*, 2002)
Lactase deficiency	*LCT*	Positive	(Tishkoff *et al.*, 2007)
Autosomal dominant spinocerebella ataxia	*SCA2*	Positive	(Yu *et al.*, 2005)
Putative viral resistance	*CCR5*	Positive & balancing	(Bamshad *et al.*, 2002; Wooding *et al.*, 2005)
Sickle cell/malaria resistance	*HBB*	Positive & balancing	(Wood *et al.*, 2005)
Immune recognition	*HLA*	Balancing	(Meyer *et al.*, 2006)
Kuru	*PRNP*	Balancing	(Mead *et al.*, 2003)
Trichromatic colour	*OPN1LW*	Purifying	(Verrelli *et al.*, 2004)

Table 1.2 Reports of selection in the human lineage

Ten examples of genes with selection in the human lineage since the divergence of humans and chimpanzees. References given represent recent studies only and are not exhaustive. (Modified from Sabeti *et al.*, 2006).

1.6.1 Genetic variation is shaped by several forces

The genetic variation of human populations today, which may lead to disease susceptibility, comprises a composite of ancestral influences including mutation, natural selection and population history, also known as demography (i.e. migration, expansion, isolation etc).

1.6.2 Measuring genetic variation and disease mapping by natural selection

Our increased understanding of human genetic variation, largely due to the sequencing of the human genome and the completion of the HapMap project sequencing has augmented our ability to detect neutral variation and deviations from neutrality. The neutral theory of molecular evolution (Kimura, 1968), is perhaps the best place to begin this discussion as it is has been integral to recent studies of natural selection. The neutral theory posits that the majority of polymorphisms that arise through random mutation have no appreciable effect on fitness (i.e. are neutral) and that these polymorphisms vary randomly in frequency over time (genetic drift) and are eliminated or fixed in populations as a consequence of the stochastic effects genetic drift. Specifically, the neutral theory can be used to make explicit and quantitative predictions about the amount, structure, and patterns of sequence variation expected under neutrality, and serves as a null hypothesis by which to evaluate the evidence for or against selection in empirical data.

The pattern of neutral variation in the human genome can be summarised using the site frequency spectrum which represents the distribution of derived* allele frequencies in a population (see Figure 1.8C). Data from the Encyclopaedia Of DNA Elements (ENCODE)† regions of the HapMap project have illustrated the exponential decay in SNPs of increasing frequency, which illustrates that the human genome is composed of a majority of young alleles. The importance of this spectrum to population genetics is that several tests of selection are based on deviations from this expected allele frequency distribution including Tajimas's *D*, Fu and Li's *D* and Fu and Li's *F*. In addition, there are several selection statistics that are independent of the site frequency spectrum but which rely instead on comparisons of polymorphisms within and/or between species such as Macdonald-Kreitman, Hudson-Kreitman-Aguadé (HKA) test and d_N/d_s tests. A comprehensive description of these tests and their relative merits is beyond the scope of this thesis but several excellent reviews can be found (Bamshad *et al.*, 2003; Biswas *et al.*, 2006; Kreitman, 2000; Sabeti *et al.*, 2006).

1.6.2.1 Natural selection

Natural selection occurs when a new mutation results in differential reproductive success (fitness). In humans, it has been estimated that ~4 new amino-acid-altering mutations arise per diploid genome per generation (Eyre-Walker *et al.*, 1999); these mutations can be broadly categorized as positive (i.e. enhances fitness), negative (i.e. reduces fitness) and balancing (i.e. enhances fitness only in heterozygous state). Accordingly, each form of selection can characteristically increase, decrease or have an intermediate effect on the mutant allele frequency, under positive, negative and balancing pressure respectively, and produce a characteristic signature of selection in the surrounding neutral variation.

Negative selection is the most pervasive form of selection as most mutations that cause protein coding changes are deleterious. These mutations are selected against and are likely to be lost. As this type of selection conserves amino acid sequence it is often called purifying selection. In the presence of strong purifying selection, nucleotide diversity at tightly linked sites is also reduced (Charlesworth *et al.*, 1993), although this background selection is also dependent on local mutation and recombination rates.

Positive selection occurs when a new mutation enhances the fitness and is likely to become fixed within a population. The time taken for the new mutation to fixate is dependent on the mode of action of the new mutation: a dominant allele fixates faster than a recessive one. In addition, the type and the magnitude of the selective pressure influence time to fixation. If a

---

* New mutations create a polymorphic site – therefore derived alleles are younger than ancestral alleles
† ENCODE represents ten 500kb regions that have been fully resequenced in 48 unrelated samples to identify all variation sampled within the region

mutation increases in frequency, tightly linked neutral variation can be dragged along as well. This genetic hitchhiking can eliminate variation not linked to the advantageous mutation, resulting in a selective sweep.

Balancing selection occurs when the heterozygous phenotype has a greater fitness than either homozygote. The effect of balancing selection is to maintain both alleles at equilibrium frequency. There are few examples of balancing selection in human populations. Probably the most well known is sickle cell anaemia, in which the sickle cell mutation in the *HBB* gene offers resistance to malaria in the heterozygous state but causes severe and fatal anaemia in the homozygous state. The *G6PD* gene, which can cause haemolytic disease, has also been shown to have undergone balancing selection possibly as it is associated with protection against malaria in the heterozygous state. In addition, the Major Histocompatibility Complex (MHC) on chromosome 6 has been shown to have been under balancing selection which has been proposed to help maintain a wider repertoire for non-self-peptide recognition in an immune response. Most recently, the prion gene (*PRNP*), known to be associated with risk of human prion disease, has been shown to have undergone balancing selection worldwide. All three forms of selection have distinct effects on genetic variation surrounding a mutation.

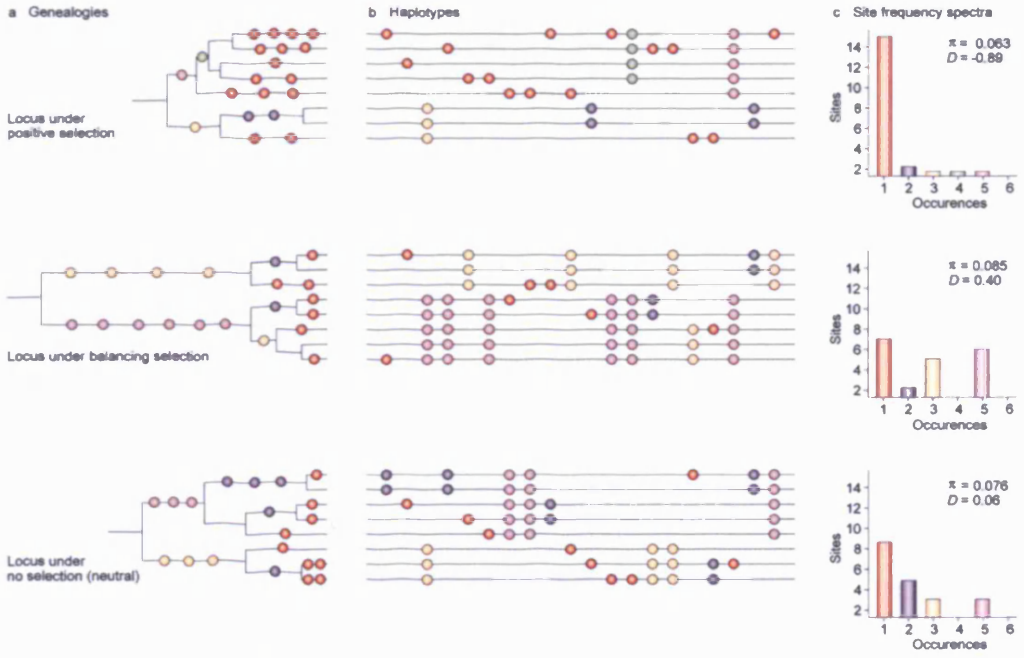

Figure 1.8 The effects of selection on the distribution of genetic variation

(**a**) The genealogies of three genes with 20 polymorphic sites that are typical of loci under positive selection (**top**), balancing selection (**middle**) and no selection (**bottom**) are shown. Each circle represents a mutation, and the colour shows the final frequency of each mutation.
(**b**) Each haplotype contains mutations that have accumulated on each lineage in the gene genealogy, assuming no recombination. (**c**) The site frequency spectrum of each gene. Positive selection (**top**) can result in a lower level of sequence diversity (π), an excess of low-frequency variants (red) and, consequently, a negative value of Tajima's *D*. Balancing selection (**middle**) can result in a higher level of sequence diversity (π), an excess of intermediate-frequency variants (purple) and, consequently, a positive value of Tajima's *D*. The diversity estimate and site frequency spectrum of a neutral locus (**bottom**) can be used for comparison. (From Bamshad *et al.*, 2003)

1.6.2.2 Testing for signatures of selection

Sabeti and colleagues have recently published a proposal of five signatures of selection, into which all specific tests can be categorised (Sabeti *et al.*, 2006), as summarised below:

(i) *High proportion of function-altering mutations*: genetic variants that alter protein function are usually deleterious and are thus less likely to become common or reach fixation (i.e. 100% frequency) than are mutations that have no functional effect on the protein (i.e. synonymous change). Positive selection over a prolonged period, however, can increase the fixation rate of beneficial function-altering mutations and such changes can be measured by comparison of DNA sequence between species. The increase can be detected by comparing the rate of non-synonymous changes with the rate of synonymous or other presumed neutral changes, by comparison with the rate in other lineages, or by comparison with intraspecies diversity. Statistical tests commonly used to detect this signature include the K_a/K_s, d_N/d_S and MKA tests.

(ii) *Reduction in genetic diversity*: As an allele increases in population frequency, genetic hitchhiking alters the typical pattern of genetic variation in the region – leading to a selective sweep. In a complete selective sweep, the selected allele rises to fixation, bringing with it closely linked variants; eliminating diversity in the immediate vicinity and decreasing it in a larger region. Although new mutations eventually restore diversity, these appear slowly (because mutation is rare) and are initially at low frequency. Positive selection thus creates a signature consisting of a region of low overall diversity, with an excess of rare alleles. The opposite is true (but has been observed less frequently) for balancing selection, such as that of the prion gene *PRNP* – an excess of high frequency is seen. Statistical tests commonly used to detect this signal include Tajima's *D*, the HKA test, and Fu and Li's *D**.

(iii) *High-frequency derived alleles*: Derived alleles arise by new mutation and typically have lower allele frequencies than ancestral alleles. In a selective sweep, however, derived alleles linked to the beneficial allele can hitchhike to high frequency. As a result of an incomplete sweep or recombination, many of these derived alleles will not reach complete fixation, thus positive selection creates a signature of a region containing many high-frequency derived alleles. For example, the 10-kb region around the Duffy red cell antigen (FY) has an excess of high-frequency derived alleles in Africans and is therefore, thought to be the result of selection for malaria resistance (Escalante *et al.*, 2005; Hamblin *et al.*, 2002). A commonly used statistical test to detect this signal is Fay and Wu's *H*.

(iv) *Differences between populations*: When geographically separate populations are subject to distinct environmental or cultural pressures, positive selection may change the frequency of an allele in one population but not in another. Large differences between populations in the selected allele frequency or in surrounding variation can therefore signal a locus that has

undergone positive selection. For example, the region surrounding the lactase (*LCT)* locus demonstrates large population differentiation between Europeans and non-Europeans, reflecting strong selection for the lactase persistence allele in Europeans (Bersaglieri *et al.,* 2004). A commonly used statistic for population differentiation includes F_{ST}.

(v*) Long haplotypes:* Under positive selection, a selected allele may rise in prevalence rapidly enough that recombination cannot substantially erode LD with hitchhiking alleles on the ancestral chromosome. In these circumstances alleles have both high frequency (typical of old alleles) and long-range LD with other alleles (typical of young alleles). Thus, selective sweeps can produce a distinctive signature that would not be expected under neutral genetic drift. Long-range LD manifests as a long haplotype that has not been broken down by recombination. For example, the lactase persistence allele at the *LCT* locus lies on a haplotype that is common (~77%) in Europeans but that extends undisrupted for more than 1 megabase (Mb) (Bersaglieri *et al.,* 2004), much farther than is typical for an allele of that frequency. This signature can be detected with the long-range haplotype (LRH) test.

1.6.2.3 Confounding factors – demography and ascertainment

Robust inferences of natural selection from DNA sequence data are difficult because of the confounding effects of population demographic history, such as population bottlenecks, expansions and subdivisions, and ascertainment bias within the study design. Ascertainment bias results from the fact that low frequency SNPs can go undetected if the genotyping sample size is too small. As the probability that a SNP is identified in a limited sample is a function of the allele frequency, rare SNPs are more likely to go undiscovered compared with common SNPs. As a consequence the site frequency spectrum obtained will be different from that obtained under complete sampling (e.g. by resequencing the entire study sample). As a result, statistical attributes that rely on the site frequency spectrum - including Tajima's *D*, F_{ST}, and LD - will be affected.

Confounding due to population demography can mimic signatures of selection. For example, both positive selection and increases in population size lead to an excess of low-frequency alleles in a population relative to that expected under a neutral model. In addition population subdivision can lead to spurious departures from Hardy-Weinberg equilibrium (discussed below). Whilst population demography affects genetic variation across the entire genome, selection is much more likely to act in a defined region only. Therefore, a true signature of selection can be distinguished from population demography by examining unlinked loci or by determining an empirical genome-wide distribution for test statistics used. As genome-wide genotyping has become more feasible, a greater number of authors have attempted to use

genome-wide scans for tests of selection (Akey *et al.*, 2002; Carlson *et al.*, 2005; Kelley *et al.*, 2006; Nielsen *et al.*, 2005).

1.6.3 Hardy-Weinberg equilibrium

Hardy-Weinberg equilibrium (HWE; otherwise known as Hardy-Weinberg law or principle) describes a mathematical model which has been routinely applied to population genetics and more recently, as a tool to identify disease loci. Independently discovered in 1908 by Wilhelm Weinberg, a German physician, and Godfrey Harold Hardy, a British mathematician, the Hardy-Weinberg principle states the frequencies of alleles in a population will remain the same regardless of the starting frequencies and that equilibrium genotypic frequencies will be established after one generation of random mating (i.e. genotype frequencies will be constant from generation to the next). HWE is found when the measured genotype frequencies match those predicted by allele frequencies using

Equation 1.4 $p^2 + 2pq + q^2 = 1$ (genotype frequency AA= p^2, Aa=$2pq$, aa=q^2)

The principle is based on assumptions of random mating, large population size, equal sex distribution and the absence of migration, mutation and selection. Expected and observed genotype frequencies can be tested for significance using a χ^2 test and departures from HWE can imply that one of the assumptions listed above is incorrect. Departures from HWE have therefore been used as a quality control measure for large-scale genotyping and as a method for localising disease genes and loci under selection (Feder *et al.*, 1996; Lee, 2003; Nielsen *et al.*, 1998).

1.7 Amyotrophic lateral sclerosis

1.7.1 Clinical and pathological features of ALS

Amyotrophic lateral sclerosis (ALS), first described by the French physician and neurologist Jean-Martin Charcot in 1869, is characterised by the progressive degeneration of motor neurons from the motor cortex and corticospinal tract. Disease onset usually occurs focally in either limb, presenting as muscle weakness, or with bulbar/corticobulbar ALS, generally presenting as affected speech or swallowing. As the disease advances, symptoms of progressive weakness, atrophy, paralysis, spasticity and emotional lability are seen. Death usually occurs 2 to 5 years after disease onset and is commonly due to respiratory failure as a consequence of denervation of the respiratory muscles and diaphragm.

Pathologically, ALS is characterised by the loss of upper motor neurons in the motor cortex, degeneration of the corticospinal tract and loss of lower motor neurons in the brain stem and spinal cord. The selective degeneration of motor neurons only, generally spares the patient's sensory and cognitive functions. Motor neurons involved in ocular, sphincter and urethral

function are spared and these signs are often used to exclude other diagnoses. Histopathology of surviving lower motor neurons shows ubiquinated inclusions and marked axonal swelling.

In the absence of a diagnostic test, the clinical diagnosis of ALS is primarily one of exclusion. The early symptoms of ALS are often indistinguishable from similar disorders that affect motor neurons, and these are often confused for ALS. In the United Kingdom (UK), these disorders are termed motor neuron diseases (MNDs) – a blanket term referring to a whole spectrum of diseases which differentially affect the upper and lower motor neurons or both. In the United States, the term ALS is commonly used interchangeably with MND, where it is also known as Lou Gehrig's[‡] disease, after the baseball player.

ALS is currently classified based on a set of diagnostic criteria set out by the World Federation of Neurology; the El Escorial Criteria (Brooks, 1994), and its recent revision, Airlie House Criteria (Miller *et al.*, 1999). Clinical diagnosis of ALS using these criteria, is based on the presence of upper and lower motor neuron impairment, the detection of symptom progression over a limited period of time, and the exclusion of other conditions that may mimic ALS.

1.7.2 Epidemiology

ALS is currently the third most common neurodegenerative disease after Alzheimer's and Parkinson's disease and is largely a disease of midlife (although rare juvenile onset forms are the exception) with an average age of onset between the 5th and 6th decade of life. A slight sex bias exists with males more likely to be affected than females in a ration of 1.3:1–1.6:1 (Nelson, 1995). Estimates of the lifetime risk currently vary between 1 per 800-2000 (Cleveland *et al.*, 2001; Shaw, 2005) and the annual incidence of ALS is ~1-2 per 100,000 which increases with age. Disease prevalence is ~2-4 per 100,000, which is kept low due to the rapid disease course. ALS incidence is uniform throughout the world with the exception of several high incidence foci, such as those in the Western Pacific (the Kii peninsular of Japan and Guam in the Marianas), where a variant of ALS seen with Parkinsonism and dementia has been observed at an increased frequency (Arnold *et al.*, 1953; Kimura, 1961). Although the vast majority of ALS cases are sporadic (known as sporadic ALS; SALS) with no apparent familial recurrence of the disease, ~10% of all ALS cases and ALS- related syndromes are inherited (known as familial ALS; FALS).

1.7.3 The Mendelian genetic basis of ALS

As with many other diseases, the greatest advance in our understanding of the genetics of ALS has come from familial forms of the disease, which show clear Mendelian inheritance. Given

[‡] Lou "The Iron Horse" Gehrig is still regarded today as one of the greatest baseball players of all time, Of his many records, Lou Gehrig played in the most number of consecutive games over 15 years from 1925 to 1939 – a streak which ended when he developed ALS and subsequently died two years later.

that until recently, gene identification strategies have largely relied on observing Mendelian inheritance, within large families with highly penetrant mutations, it is not surprising that these genetic loci are the most robustly replicated genetic causes of ALS to date. However, FALS accounts for only a small proportion of all ALS cases and to date at least 12 genetic loci have been identified (Table 1.3).

The first ALS-associated gene to be identified was *copper-zinc superoxide dismutase 1* (*SOD1*), on chromosome 21q22.1 (Rosen *et al.*, 1993) which accounts for the greatest number (~20%) of familial ALS cases. To date, over 100 disease causing point mutations in SOD1, spanning all five exons, have been identified (Andersen *et al.*, 2003) (see www.alsod.iop.kcl.ac.uk/als), the vast majority of which are heterozygous missense mutations (insertions and deletions are rarely seen). Almost all mutations are dominantly inherited with the exception of recessive inheritance such as the D90A mutation (Andersen *et al.*, 1995).

ALS disease type	Onset	Inheritance	Gene	Locus	References
Mendelian genes					
ALS1	Adult	AD, AR (D90A)	*SOD1*	21q22.1	(Al Chalabi *et al.*, 1998; Rosen *et al.*, 1993)
ALS2	Juvenile	AR	Alsin	2q33	(Hadano *et al.*, 2001; Yang *et al.*, 2001)
ALS4	Juvenile	AD	*SETX*	9q34	(Blair *et al.*, 2000; Chen *et al.*, 2004)
ALS8	Adult	AD	*VAPB*	20q13.33	(Nishimura *et al.*, 2004b; Nishimura *et al.*, 2004a)
Progressive LMN disease	Adult	AD	*DCTN1**	2p13	(Munch *et al.*, 2004; Munch *et al.*, 2005; Puls *et al.*, 2003)
ALS with dementia, Parkinsonism	Adult	AD	*MAPT*	17q21	(Clark *et al.*, 1998; Hutton *et al.*, 1998; Siddique *et al.*, 1995)
Mendelian loci					
ALS3	Adult	AD	?	18q21	(Hand *et al.*, 2002)
ALS5	Juvenile	AR	?	15q15.1-q21.1	(Hentati *et al.*, 1998)
ALS6	Adult	AD	?	16q12	(Abalkhail *et al.*, 2003; Ruddy *et al.*, 2003; Sapp *et al.*, 2003)
ALS7	Adult	AD	?	20ptel-p13	(Sapp *et al.*, 2003)
ALS-FTD	Adult	AD	*?*	9q21-22	(Hosler *et al.*, 2000)
	Adult	AD	?	9p13.2-21.3	(Morita *et al.*, 2006; Vance *et al.*, 2006)
	Adult	AD	?	17q	(Wilhelmsen *et al.*, 2004)
ALS X	Adult	AD	?	Xp11-q12	(Siddique *et al.*, 1998a)
Mitochondrial genes and misc.					
ALS-M		Maternal;	*Cox1*	mtDNA	Single case (Siddique *et al.*, 1998a)
ALS-M		Maternal	*IARS2*	mtDNA	Single case (Borthwick *et al.*, 2006)
ALS-M		Maternal	*CCO1*	mtDNA	Single case (Comi *et al.*, 1998)
		AD	*NFH*		Single case (Al Chalabi *et al.*, 1999)

Table 1.3 Familial ALS genes and loci

Autosomal dominant (AD);amyotrophic lateral sclerosis (ALS); autosomal recessive (AR); alsin (ALS2); cyclooxygenase 1 (COX1); frontotemporal dementia (FTD); mitochondrial isoleucine tRNA synthetase (IARS2); mitochondrial DNA (mtDNA); senataxin (SETX); superoxide dismutase 1 (SOD1); vesicle-associated membrane protein-associated protein B (VAPB); and unknown gene (?)

The pathogenesis of *SOD1* mutations is unclear. The normal 153–amino acid SOD1 protein functions as a copper and zinc containing homodimer, which detoxifies superoxide (produced during oxidative phosphorylation by mitochondria) to oxygen and hydrogen peroxide, thus preventing oxidative damage. SOD1 is ubiquitously expressed and predominantly located in the cell cytoplasm. Most *SOD1* mutations affect correct subunit folding and dimerisation, although the resulting effect on SOD1 activity varies (e.g. G93A mutations have almost no effect on activity whilse H46R mutations inactivate SOD1). No clear correlation has yet been identified between mutant SOD1 activity, including copper affinity, protein half-life and ability to scavenge superoxide, and disease onset or duration. Patients with SOD1 mutations have normal protein levels suggesting that pathogenesis is not due to haploinsufficiency, however, SOD1 may exert a dominant negative effect or toxic gain of function.

Clinically, SOD1 FALS is indistinguishable from SALS although onset is ~10 years earlier and there is 90% penetrance by age 70. The mean age of onset is consistently 46 to 47 years regardless of the underlying SOD1 mutation. Mean duration is 3-6 years, however, exceptions such as the aggressive A4V mutation which has a short disease duration of 1.4 years (Cudkowicz *et al.*, 1997) and G37R or G41D which have longer survival prognoses (Orrell *et al.*, 1997b). Initially, SOD1 FALS cases present with predominantly lower motor neuron signs. Bulbar onset is unusual and is usually associated with a later-onset cases.

There are few common pathological features of SOD1-mediated ALS such as corticospinal and anterior horn cell loss but generally pathology varies with different mutations. SOD1-mediated FALS clinical phenotype including age of onset, severity and survival all vary and the wide range of mutations in SOD1 cannot account for this variability. In addition clinical variation can be observed in members of the same family (Andersen *et al.*, 1995), suggesting that additional environmental or genetic factors may modify phenotype. That some SOD1 FALS mutations may appear more complex than previously thought is illustrated by the incomplete penetrance of the D90A mutation (discussed below) which is recessive on some genetic backgrounds and dominant on others (Al Chalabi *et al.*, 1998).

1.7.4 The complex genetic basis of ALS

The biggest challenge for ALS research is currently dissecting the aetiology of sporadic ALS which accounts for ~90% of all ALS cases. As Simpson and Al-Chalabi have noted, the assumption that sporadic disease implies a disease with no genetic cause is no longer valid

(Simpson *et al.*, 2006). Indeed, clinical, epidemiological and genetic studies of SALS cases have all revealed a genetic component.

1.7.4.1 A genetic component to sporadic ALS

Perhaps the simplest example of a genetic component to SALS is the discovery of SOD1 mutations in 2 to 7% of SALS cases (Andersen *et al.*, 1995; Jackson *et al.*, 1997; Jones *et al.*, 1994a; Jones *et al.*, 1994b), indicating that at least some sporadic cases of ALS are genetic, although it is unclear how many are *de novo* mutations. Several lines of evidence implicate a genetic component to SALS:

Heritability A UK twin study, investigating concordance between mono- and dizygotic twins, has provided additional support for a genetic component to SALS. The authors demonstrated heritability of ALS risk to be between 38 and 85% - essentially that between 38% and 85% of variation in ALS is attributable to inherited (i.e. genetic) factors (Graham *et al.*, 1997). In addition estimated sibling relative risk (λs), under a set of assumptions regarding family history and inheritance patterns, is between 20 and 50 (i.e. the sibling of an affected individual is 20 to 50 times more likely to develop disease) (Simpson *et al.*, 2006).

Ethnic differences It is widely recognized that there is variation within and between human populations with respect to their susceptibility to many diseases (Burchard *et al.*, 2003). Investigation of variation in ALS incidence by ethnicity has been a source of much epidemiological research and controversy. In these studies, ethnicity can be regarded as a proxy to describe population genetic variation or variation in genetic background. Epidemiological data from worldwide populations analysing rates of ALS incidence and prevalence, migration and mortality have shown that the rates are consistently lower in African, Asian and Hispanic ethnicities that in Caucasians see for example (Dean *et al.*, 1993; Elian *et al.*, 1993; Noonan *et al.*, 2005). However these studies often suffer from ascertainment and reporting bias. Cronin and colleagues have recently reviewed 61 published articles examining ethnic variation in the incidence of ALS and based on standardised measures of incidence, they concluded that African, Asian and Hispanic ethnicities did show a lower overall incidence of ALS compared to Caucasians (Cronin *et al.*, 2007). It is entirely plausible that these differences may be due to differential environmental exposures too.

Genetic background has been postulated to influence several familial forms of ALS. For example, the D90A mutation of SOD1 is responsible for a recessively inherited form of ALS in families from the Torne Valley, in Sweden and Finland (Andersen *et al.*, 1995; Andersen *et al.*, 1996; Andersen *et al.*, 1997). In addition, families from southern Sweden, UK, France and Belgium, heterozygous for the D90A mutation have also been reported with a more aggressive and variable ALS phenotype, and a few individuals with no family history of ALS have also been described (Andersen *et al.*, 1995; Robberecht *et al.*, 1996, Jackson *et al.*, 1997; Khoris *et al.*, 1997). Remarkably, all families carrying the D90A mutation have been shown to have descended from a single ancient founder ~895 generations ago, with the recessive allele becoming established in Torne Valley during the settlement and isolation of the area ~63 generations ago (Al Chalabi *et al.*, 1998; Parton *et al.*, 2002). Importantly, a region of up to 265kb around *SOD1* is shared by the recessive Torne Valley kindreds which is postulated to contain a tightly linked *cis*-acting protective factor, such that two copies of D90A are required for ALS to develop. No such linked protective factor has yet been identified.

In addition the failure of replication of ALS association studies conducted in different worldwide populations may be due to differences in genetic background, they may also be due to different environmental factors, e.g. *VEGF* (Van Vught *et al.*, 2005).

1.7.5 Susceptibility genes in sporadic ALS

Based on the liability threshold model, susceptibility to ALS can be considered to be a spectrum of genetic and environmental risk: (i) at one end of the spectrum are the well studied single genes, with large effect size, that cause fully penetrant, autosomal dominant FALS and (ii) at the opposite end are the multiple genes of small effect that may interact with the environment to cause apparently SALS. Until recently, linkage studies have only been able to illuminate the genes of large effect responsible for one side of the liability spectrum but have lacked power in elucidating those genes of small effect. Genes of small effect have, until recently, been investigated in ALS using candidate gene association studies, often informed by those genes identified from linkage studies. However, the availability of cheaper genotyping and denser marker sets is changing how these susceptibility genes will be discovered. Table 1.2 summarises the candidate genes which have been investigated in ALS as modifiers of risk or phenotype. Rather than list every single one of these in the text, I will discuss some of the most studied.

Gene	Description	Reason for Investigation	Significance	References
ALAD	d-Aminolevulinic Acid Dehydratase	Lead exposure associated with ALS ALAD is involved in haem synthesis in erythrocytes	No association	(Kamel *et al.*, 2002; Kamel *et al.*, 2003)
ALS2	Alsin	Causes autosomal recessive juvenile ALS (ALS2).	No association	(Hadano *et al.*, 2001; Hand *et al.*, 2003; Hentati *et al.*, 1994; Hosler *et al.*, 1998; Yang *et al.*, 2001)
ANG	Angiogenin	ANG is functionally similar to VEGF	Association found in Scottish and Irish populations	(Greenway *et al.*, 2004; Hayward *et al.*, 1999)
APEX	Apurinic endonuclease	Defective DNA repair hypothesis of ALS etiology	May have small role but not major factor	(Hayward *et al.*, 1999)
APOE	Apolipoprotein E	Implicated in several other neurodegenerative disorders	Not associated with susceptibility. May be associated with age of onset, presentation and survival	(Al Chalabi *et al.*, 1996; Drory *et al.*, 2001; Moulard *et al.*, 1996; Mui *et al.*, 1995; Siddique *et al.*, 1998b)
AR	Androgen receptor	Causes Kennedy spinal and bulbar muscular atrophy.	No association	(Garofalo *et al.*, 1993)
CCS	Copper chaperone for superoxide dismutase	Gene responsible for copper insertion into SOD1	No association	(Silahtaroglu *et al.*, 2002)
CNTF	Ciliary neurotrophic factor	Mice lacking CNTF develop mild, progressive motor neuron loss	Contradictory results	(Al Chalabi *et al.*, 2003; DeChiara *et al.*, 1995; Giess *et al.*, 2002; Masu *et al.*, 1993; Orrell *et al.*, 1995; Takahashi *et al.*, 1994)
CYP2D6	Cytochrome p450, subfamily IID, polypeptide 6	Hypothesized poor metabolism of xenobiotics as risk factor	One reported association, not replicable	(Nicholl *et al.*, 1999; Siddons *et al.*, 1996)
DCTN1	Dynactin	Disruption of dynein/dynactin complex produces motor neuron disease phenotype in mice	One reported association, not yet replicated	(Munch *et al.*, 2005)
DYNC1H1	Dynein heavy chain	Mutations in Dnch1 result in progressive motor neuron degeneration in heterozygous mice, homozygotes also have Lewy-like inclusion bodies,	No association	(Ahmad-Annuar *et al.*, 2003; Hafezparast *et al.*, 2003; Munch *et al.*, 2004; Shah *et al.*, 2006)
EAAT2	Excitatory amino acid transporter 2	Excitotoxicity hypothesized to result in motor neuron degeneration	No association	(Aoki *et al.*, 1998; Flowers *et al.*, 2001; Honig *et al.*, 2000; Jackson *et al.*, 1999; Lin *et al.*, 1998; Meyer *et al.*, 1998; Meyer *et al.*, 1999)
HexA	Hexosaminidase A	HexA deficiency causes accumulation of ganglioside GM2 leads to neurodegeneration causing wide spectrum of neurological diseases	Occasionally causes rare ALS-like syndrome	(Drory *et al.*, 2003)
HFE	Haemochromatosis	Oxidative stress is hypothesized to be implicated in neurodegeneration and misregulation of iron induces oxidative stress. Also, abnormal iron levels found in spinal cords of ALS patients	Contradictory results	(Wang *et al.*, 2004; Yen *et al.*, 2004)
LIF	Leukaemia inhibitory factor	LIF is same cytokine family as CNTF, involved in motor neuron survival	One reported association, not yet replicated	(Giess *et al.*, 2000; Meyer *et al.*, 1995)
LOX	Lysyl oxidase	LOX is a copper containing enzyme and copper-induced cytotoxicity is a hypothetical mechanism of motor neuron degeneration	No association	(Chioza *et al.*, 2001)
MAO-B	Monoamine oxidase B	MAO-B generates free radicals and these are implicated in neuronal damage	Association with age at onset, not yet replicated	(Orru *et al.*, 1999)
MAPT	Microtubule-associated protein tau	*MAPT* involved in other neurodegenerative diseases Guam variant of ALS has containing tau aggregates	Association reported but *p*-values were weak	(Kowalska *et al.*, 2003; Poorkaj *et al.*, 2001)

Gene	Description	Reason for Investigation	Significance	References
Mito	Mitochondrial DNA deletions	Accumulation of mitochondrial DNA mutations associated with aging development of degenerative diseases. In ALS, abnormal mitochondria are often found in spinal motor neurons	Associations reported, but all studies very small	(Dhaliwal *et al.*, 2000; Gajewski *et al.*, 2003; Mawrin *et al.*, 2003; Swerdlow *et al.*, 1998; Wiedemann *et al.*, 2002) (Mawrin *et al.*, 2004; Ro *et al.*, 2003)
NAIP	Neuronal apoptosis inhibitory protein	NAIP involved in related disease, spinal muscular atrophy	No association. Mutations in NAIP now considered specific for SMA	(Jackson *et al.*, 1996; Kunst *et al.*, 2000; Orrell *et al.*, 1997a; Parboosingh *et al.*, 1999)
ND2	Subunit 2 of mitochondrial NADH dehydrogenase	Expression of ND2 found in Alzheimer's brains	No association	(Lin *et al.*, 1992)
NEFH	Neurofilament, heavy chain	Neurofilament accumulation is a hallmark of ALS	Significant association, tail domain deletions present in 1% ALS patients, not in controls. Findings have replicated in several studies	(Al Chalabi *et al.*, 1999; Julien *et al.*, 1995; Meyer *et al.*, 1995; Rooke *et al.*, 1996; Tomkins *et al.*, 1998; Vechio *et al.*, 1996)
PRPH	Peripherin	Transgenic mice over-expressing peripherin develop motor neuron degeneration	Few mutations found, not a common cause of ALS	(Gros-Louis *et al.*, 2004; Leung *et al.*, 2004)
PSEN1	Presenilin-1	PSEN1 involved in apoptosis, a postulated mechanism for neuronal death	Weak association found, small study, not replicated	(Panas *et al.*, 2000)
PVR	Poliovirus receptor	Poliovirus attacks motor neurons selectively, enteroviral nucleic acids found in spinal cord of ALS patients	Association with lower motor neuron disease found in one small study, not yet replicated	(Saunderson *et al.*, 2004)
SETX	Senataxin	Mutations in SETX cause autosomal dominant juvenile ALS (ALS4)	New familial gene, not yet tested in sporadics	(Chen *et al.*, 2004)
SMN1/2	Survival of motor neuron 1/2	Deletions and mutations of SMN genes cause spinal muscular atrophy	SMN genotypes which reduce SMN protein levels associated with sporadic ALS	(Corcia *et al.*, 2002b; Corcia *et al.*, 2002a; Veldink *et al.*, 2001; Veldink *et al.*, 2005)
Spastin and paraplegin	Hereditary spastic paraparesis	Mutations in spastin and paraplegin are the most common causes of hereditary spastic paraparesis	One case reported of young onset, slowly progressive upper and lower motor neuron syndrome with spastin mutation. No association with paraplegin	(McDermott *et al.*, 2003; Meyer *et al.*, 2005)
SNCG	Persyn	Persyn is a member of the synuclein family, γ-synuclein. Mutations in α-synuclein found in Parkinson's disease	No association	(Flowers *et al.*, 1999)
SOD1	Cu/Zn superoxide dismutase 1	Mutations in SOD1 account for 20% of familial ALS.	2–7% sporadic cases	(Andersen *et al.*, 1997; Johnston *et al.*, 2006; Jones *et al.*, 1994b; Rosen *et al.*, 1993; Siddique *et al.*, 1991)
SOD2	Manganese superoxide dismutase	SOD2 is a related protein of SOD1, found in mitochondria	No association	(Tomkins *et al.*, 2001)
VAPB	Vesicle-associated membrane protein-associated protein B	Mutations in VAPB cause an autosomal dominant, slowly progressive ALS (ALS8)	New familial gene, not yet tested in sporadics	(Nishimura *et al.*, 2004b)
VDR	Vitamin D receptor	Lead exposure associated with ALS. Vitamin D can affect lead absorption and distribution	Not significant	(Kamel *et al.*, 2002; Kamel *et al.*, 2003)
VEGF	Vascular endothelial growth factor	Susceptibility	Association in some populations	(Lambrechts *et al.*, 2003; Oosthuyse *et al.*, 2001; Terry *et al.*, 2004; Van Vught *et al.*, 2005)

Table 1.4 ALS susceptibility loci

(Modified from Simpson *et al.*, 2006)

1.7.6 *DYNC1H1* as a candidate susceptibility locus

The *cytoplasmic 1 dynein heavy chain 1* (*DYNC1H1*) has been implicated as a potential causative gene for motor neuron degeneration and possibly for ALS. The first evidence implicating *DYNC1H1* as a locus for investigation in ALS came from mouse models of motor neuron degeneration generated by mutagenesis screen. The heterozygous '*Legs at odd angles*' (*Loa*) mouse and allelic '*Cramping 1*' (*Cra1*) mouse both displayed progressive locomotor defects. Although this did not affect lifespan, homozygous mice died within 24 hours of birth (Hafezparast *et al.*, 2003). Histopathology, of the *Loa* mice showed significant anterior horn cell loss and deposition of ubiquitin, SOD1 and neurofilament in the remaining cells which also contained Lewy-like bodies.

1.7.6.1 The cytoplasmic dyneins and dynactin

The dyneins are large multi-subunit protein complexes that undertake a wide range of roles within the cell. They are microtubule minus-end-directed molecular motors that can be divided into two classes based on function: axonemal and cytoplasmic dyneins (reviewed in Gibbons, 1995; Vallee *et al.*, 2004). Axonemal dyneins are responsible for the movement of cilia and flagella and cytoplasmic dyneins are involved in a range of microtubule-associated functions within the cell. Two cytoplasmic dynein complexes with distinct cellular functions exist, termed cytoplasmic dynein 1 and cytoplasmic dynein 2. Cytoplasmic dynein 2 is involved in intraflagellar transport (IFT), a process required for the assembly of cilia and flagella (reviewed in Cole, 2003). Cytoplasmic dynein 1 is the more abundant complex and is involved in a greater number of functions such as diverse as spindle-pole organization and nuclear migration during mitosis and the positioning and functioning of cellular organelles and compartments, including the endoplasmic reticulum (ER), Golgi apparatus and the nucleus. In addition cytoplasmic dynein 1 also provides the minus-end-directed transport of vesicles along microtubules, including endosomes and lysosomes, and retrograde axonal transport in neurons.

The cytoplasmic dynein 1 complex also interacts with other proteins such as LIS1, which is thought to modulate the enzymatic activity of DYNC1H1 (Mesngon *et al.*, 2006), and a second multimer, dynactin, which is itself comprised of at least seven different proteins including p22, p50 and p150 and possesses three functional domains: microtubule-binding, dynein-binding, and cargo binding (reviewed in Schroer, 2004). These domains allow dynactin to function both as an adaptor, associating the dynein motor with different cargoes (Holleran *et al.*, 1998; Karki *et al.*,

1998; Karki *et al.*, 1999), and as an enhancer of dynein motor processivity is enhanced two- to four-fold over the distance travelled by a single dynein molecule alone (Culver-Hanlon *et al.*, 2006; King *et al.*, 2000).

1.7.6.2 Cytoplasmic dynein 1 heavy chain subunit and function in neurons

The cytoplasmic dynein 1 complex comprises several subunits: two large heavy chain polypeptides (~530 kDa each) which homodimerise to form the core of the complex and associated intermediate (~74 kDa), light intermediate (~33-59 kDa), and light chain polypeptides (~10-14 kDa) (see Figure 4.1). In the interest of brevity and as this thesis is largely focused on the dynein heavy chain, only the heavy chain will be discussed however several excellent reviews exist for the interested reader (see for example Pfister *et al.*, 2005b).

The cytoplasmic dynein-dynactin complex performs multiple cellular roles and are essential protein complexes in higher eukaryotes; both fly and mouse knockouts are lethal in embryogenesis (Gepner *et al.*, 1996; Harada *et al.*, 1998). Within post-mitotic neurons cytoplasmic dynein is responsible for several essential functions including maintaining ER to Golgi traffic, vesicle transport, mRNA localisation and retrograde axonal transport. In motor neurons in particular, which possess axons that can exceed 1m in length and which form multiple synapses with other neurons and muscle cells, correct and efficient retrograde transport is essential. Cytoplasmic dynein utilises the axonal cytoskeleton within motor neurons to transport cargo such as organelles and structural and signalling proteins and neurotrophic factors from the axon termini to the perikaryon. Indeed, defects in the machinery that drives retrograde transport may inhibit neurotrophic factor signalling, and therefore lead to neuronal degeneration (Holzbaur, 2004). In support of this hypothesis, inhibition of retrograde transport in postnatal motor neurons by over-expression of a dynactin subunit results in motor neuron loss and muscle atrophy (LaMonte *et al.*, 2002).

1.7.6.3 Cytoplasmic dynein and human motor neuron degeneration

The cytoplasmic dynein-dynactin complex has been implicated in several instances of human motor neuron degeneration. Puls and colleagues identified a G59S mutation in the p150^{Glued} subunit of dynactin (*DCTN1*) in a family with a slowly progressive autosomal dominant form of motor neuron disease (Puls *et al.*, 2003; Puls *et al.*, 2005). Affected individuals with this mutation developed symptoms in early adulthood including: vocal fold paralysis causing breathing difficulty; progressive facial weakness, and weakness and atrophy in distal-limb muscles. The

G59S mutation resides in a highly conserved domain that interacts directly with microtubules and the microtubule plus end protein EB1 (Ligon *et al.*, 2005) leading to decreased microtubule binding and enhanced dynein and dynactin aggregation (Levy *et al.*, 2006), thus contributing to the degeneration of motor neurons.

Mutations in *DCTN1* have also been identified in three FALS cases and one SALS case in a study of 250 ALS patients and 150 unrelated controls (Munch *et al.*, 2004). In this study Munch and colleagues investigated all *DCTN1* exons and identified a T1249I change in the SALS case and a M571T change in one of the FALS cases. The two remaining FALS cases were related, from the same kindred and possessed an autosomal dominant R785W mutation. Interestingly, two unaffected individuals from the same kindred also possessed the R785W mutation, suggesting that this mutation may display incomplete penetrance or that this mutation may not be responsible for disease and it is instead an unknown autosomal recessive gene defect or that *DCTN1* represents a genetic risk factor, rather than a causative factor for ALS.

1.8 Human prion diseases

Prion diseases are a group of human and animal neurodegenerative conditions that have in common a key role for the prion protein in their pathogenesis. The archetypal prion disease, sheep scrapie, was first reported in the 18th century (McGowan, 1922) (the name is derived from the scratching of fence posts by diseased, ataxic animals), and since then several additional animal and human prion diseases have been identified. There are three aetiological categories of human prion disease: inherited, acquired (transmitted between humans or animals) and sporadic. Inherited prion diseases include Gerstmann-Sträussler-Scheinker (GSS) disease, fatal familial insomnia (FFI) and familial Creutzfeldt-Jakob disease (fCJD); acquired prion diseases include iatrogenic CJD, variant CJD (vCJD) and kuru; and sporadic disease is sporadic CJD (sCJD).

1.8.1 Aetiology of prion diseases

A key feature of the prion diseases is their transmissibility amongst and between species (Chandler.L, 1961; Cuillé *et al.*, 1936; Gajdusek *et al.*, 1967). The discovery of the aetiology of prion diseases is a fascinating story (Collinge, 2005) and is based largely on the observations of disease transmissibility and the search for, and identification of, the transmissible species. A single protein, the prion protein (PrP), seen to copurify with infectivity has led to the development of a 'protein-only' hypothesis of prion disease. Under this hypothesis, the infectious agent of prion diseases is comprised of abnormal isoforms of PrP and these disease associated isoforms act as templates to promote the conversion of normal cellular PrP (PrP^C) to the pathological state PrP^{Sc} (Prusiner, 1982).

1.8.1.1 PrP and *PRNP*

The normal prion protein is a large protein 33-35 kDa whose sequence is highly conserved in most mammals (Wopfner *et al.*, 1999). PrP^C is widely expressed in most adult tissues (Manson *et al.*, 1992) however highest expression levels are seen in the central nervous system. The precise cellular function of PrP^C is still not known, however, as a glycosyl phosphatidyl inositol-anchored cell-surface glycoprotein, it has been speculated that PrP^C may have a role in cell adhesion or signalling processes.

Human and mouse genetics have made major contributions to prion disease research. Following the identification of PrP as the transmissible agent, partial sequencing of the protein allowed for the prediction of coding nucleotides and eventually to the cloning of the cognate human (*PRNP*) the and mouse (*Prnp*) prion protein genes on chromosomes 20 and 2 respectively (Chesebro *et*

al., 1985; Oesch *et al.*, 1985; Robakis *et al.*, 1986). Strong supportive evidence for the central role of PrP in prion disease has been provided by (i) the linkage of scrapie incubation time loci in the mouse to *Prnp* (Carlson *et al.*, 1986) and (ii) the identification of mutations in *PRNP* linked to the inherited human prion diseases fCJD (Owen *et al.*, 1989) and GSS (Hsiao *et al.*, 1989).

The human *PRNP* gene on chromosome 20 comprises two exons (Puckett *et al.*, 1991) and spans ~16kb. The open reading frame (ORF) of 759 nucleotides is entirely contained within the larger second exon. In the mouse, *Prnp* is located in the syntenic region of chromosome 2 and comprises three exons (with an additional short second exon compared to *PRNP*), with the ORF located in exon 3. The ORFs of mammalian prion genes are well conserved, generally exhibiting ~90% similarity. Several regions of human PrP are relevant to disease. The N-terminal domain (codons 51–91) encodes a 5-mer repeat region consisting of a nonapeptide followed by four identical octapeptides. Alterations in the number of repeats are found as polymorphisms and pathogenic mutations, but no point mutations or common SNPs have been found in this region. The C-terminal domain of PrP contains known point mutations, causing inherited prion disease ,and a common coding polymorphism at codon 129 of *PRNP* (A385G) between methionine and valine has a critical role in susceptibility and modification of prion disease (discussed later).

1.8.2 Inherited prion diseases

Approximately 15% of all human prion diseases are inherited as autosomal dominant disorders and all can be accounted for by mutation of *PRNP*, of which over 30 different mutations have been described to date (Mead, 2006). Three types of pathogenic *PRNP* mutation exist in inherited prion disease: (i) point mutations leading to an amino-acid substitution or leading to (ii) a premature stop codon and (iii) insertion of additional octapeptide repeats (OPRI). With the exception of some OPRI cases and C-terminal point mutations, all mutations are fully penetrant.

Inherited prion disease is generally associated with an earlier age of onset and longer duration of illness than sporadic forms. However, the phenotype is highly variable ranging from prolonged slowly progressive dementia over 20 years to an aggressive disease indistinguishable from sporadic CJD. The spectrum of inherited prion diseases has been historically encapsulated by three clinical categories: GSS, FFI and fCJD, with features including slow progression of ataxia followed by later onset dementia in GSS; refractory insomnia, hallucinations, dysautonomia and motor signs in FFI; and rapidly progressive dementia, with myoclonus in fCJD. The phenotypic variability of inherited prion diseases is clearly illustrated by a large British 6-OPRI mutation

family, where affected individuals show a range of pathological phenotypes from CJD to a slowly progressive dementia without characteristic neuropathology (Collinge *et al.*, 1992). Due to this clinical variability, it has been difficult to estimate the incidence of inherited prion disease and *PRNP* mutation is usually sought as confirmation of disease.

1.8.3 Sporadic prion disease

Over 85% of human prion disease cases worldwide are sporadic. In the UK, approximately 50 cases of sporadic CJD are seen annually (which equates to ~1 per million of the population), however this may be underestimated as autopsy studies have shown that 40% of all pathological cases of CJD go clinically undiagnosed (Bruton *et al.*, 1995). Disease incidence is approximately equal worldwide between the sexes and with an apparently random distribution. Age is a dominant risk factor for sCJD. The incidence of sCJD in younger adults aged <40 years is low, but above this age incidence increases and is seen to peak in the sixth decade. At older ages however, incidence appears to decline (Will *et al.*, 1998). There are several lines of evidence which indicate that the epidemiology of sCJD is inconsistent with a single major environmental influence, such as animal to human transmission. For example, cases of sCJD are well recognised in countries that have never reported sheep scrapie (Masters *et al.*, 1979).

In general, CJD is characterised by the rapid onset of neurological degeneration. This initially presents as dementia, followed by the development of movement disorders such as tremor, spasticity and rigidity. A common feature in almost all people with CJD is myoclonus, and most also display abnormal electroencephalogram recordings. Once symptoms are detected, the disease course is extremely aggressive (especially when compared to other neurodegenerative diseases such as Alzheimer's and Parkinson's), with average disease duration of 7.6 months, and the vast majority of patients (70%) die within 6 months (Collinge, 2001). At disease end stage, patients sink into akinetic mutism, with death usually occurring due to systemic or pulmonary infection. In terms of neuropathology, CJD displays extensive spongiform degeneration and neuronal loss, coupled with gliosis and deposits of the prion protein within the brain.

1.8.4 Acquired CJD

The most recent human prion disease to have been identified emerged in 1996 following an epidemic of the bovine prion disease, bovine spongiform encephalopathy (BSE), and was recognised as a novel clinico-pathological variant of CJD (Will *et al.*, 1998). To date there have been 161 deaths from definite or probable vCJD (Department of Health CJD statistics, 2 July

2007; www.cjd.ed.ac.uk/figures.htm). Several lines of evidence, including geographical and temporal coincidence and molecular studies, support a causative link between vCJD and exposure to BSE-infected bovine tissue (Bruce *et al.*, 1997; Collinge *et al.*, 1996; Hill *et al.*, 1997).

vCJD exhibits marked differences in disease profile to those associated with classical CJD or the other human prion diseases. The age at onset ranges from 16 to 51 years (mean 29 years), and the clinical course is unusually prolonged (9–35 months, median 14 months) (Collinge, 2001). The initial symptoms are behavioural, with disorders of movement such as ataxia occurring weeks to months later. Dementia and myoclonus (usually the initial symptoms in classical CJD) occur towards the later stages of the disease. The neuropathology of vCJD is also in marked contrast to most other human prion diseases, with spongiform degeneration concentrated in the basal ganglia and thalamus, and the presence of so called florid plaques, similar to other transmitted prion diseases including kuru and scrapie.

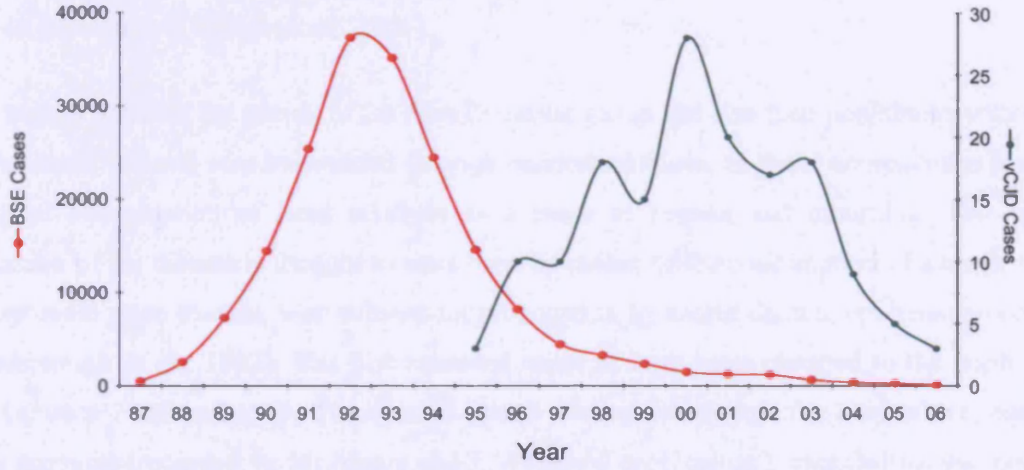

Figure 1.9 BSE and vCJD cases in the UK

Cases are based on monthly totals. Data from www.cjd.ed.ac.uk/figures.htm

Following the BSE epidemic, there has been widespread concern over an associated vCJD epidemic. Estimates based on current vCJD figures (see Figure 1.9) suggest that the total epidemic may be small (Ghani *et al.*, 2003). However, dietary exposure of the UK population to BSE prions is known to have been widespread and the precise disease incubation period of vCJD is not yet known. Estimates of incubation period based on evidence from the acquired prion disease epidemic kuru, where incubation times in excess of 50 years have been recorded in the absence of a species barrier, suggest that additional vCJD cases may be seen in the future (Collinge *et al.*, 2006). Additionally, as evidence from mouse studies have shown (discussed later) disease incubation may be under the control of multiple genetic loci and the vCJD patients

identified could represent a distinct genetic subpopulation possessing short incubation alleles to BSE prions, with the susceptibility *PRNP* genotype. Therefore, a human BSE epidemic may be multiphasic, and recent estimates of the size of the vCJD epidemic based on uniform genetic susceptibility could be substantial underestimations (Collinge *et al.*, 2006). Until such human modifier loci are identified and their gene frequencies in the population can be measured the size of a potential epidemic will be difficult to model.

1.8.5 Kuru

Kuru first came to the attention of Western medicine in 1957, after it reached epidemic proportions in a defined population of Eastern Highlands of Papua New Guinea (PNG), and provides our largest experience of an acquired prion disease for epidemiological study. At its peak, kuru was responsible for 200 deaths per year and the disease predominantly affected women (it was the main cause of female mortality) and children of both sexes, with only 2% of cases in adult men (Collinge *et al.*, 2006)

Kuru mainly affected the people of the Fore linguistic group and also their neighbours with whom they intermarried and was transmitted through endocannibalism, as these communities practised the ritual consumption of dead relatives as a mark of respect and mourning. The original acquisition of the disease is thought to have been by means of the consumption of a single person with sporadic prion disease, with subsequent propagation by cannibalism to epidemic proportions (Attenborough *et al.*, 1992). The first recorded cases of kuru were reported to the north of the Fore between 1920 and 1925. The disease spread southwards though the Fore where, based on living accounts (recorded by M. Alpers and J. Whitfield pers. comm.), cannibalism was common although practices varied. Different body parts were consumed by specific participants – the brain and other high prion titre organs were consumed by women and children. However, boys older than 6–8 years participated little in mortuary feasting as they ceased residing with their mothers and instead lived with male members of the group. Men rarely participated in mortuary feasts as traditionally this was considered emasculating and was considered to weaken a male's power. This is likely to explain the differential age and sex incidence. During the peak of the kuru epidemic, Papua New Guinea and the Eastern Highlands came under Australian administrative control and cannibalism was effectively prohibited. With the abrupt cessation of cannibalism, children born after the late 1950s have been free of kuru, indicating that maternal transmission was unlikely to have occurred.

1.8.5.1 Clinical and pathological characteristics

Clinically, kuru presents initially as progressive ataxia (kuru is the Fore word for shaking or trembling) until the patient is incapacitated, and cognitive impairment is also a feature. Towards the final stages of the disease, dementia is common and incontinence is frequently present. Death usually occurs within 3 years, often through starvation, infection or through falling into cooking fires. At autopsy, the neuropathological hallmarks have many similarities to those of CJD, including spongiform degeneration, vacuolated neurons and astrocytosis.

1.8.5.2 Genetics of kuru

Since 1967 when Gajdusek, Gibbs and Alpers demonstrated that kuru could be transmitted to chimpanzee - the first transmission of a human prion disease which confirmed that these human diseases belonged within the same category as the animal prion disease- kuru has continued to illuminate our understanding of prion disease (Gajdusek *et al.*, 1967). As with other human prion diseases, the major genetic determinant of kuru susceptibility is *PRNP*. As discussed in detail in Chapter 6, heterozygosity at codon 129 is a major susceptibility factor for kuru incubation time. Other loci have also been investigated for association with kuru incubation time but no associations have yet been seen (Collinge *et al.*, 2006). These include: the *PRNP* haplotype, which has previously been associated with sCJD (Mead *et al.*, 2001); the prion-like gene *Dopple* (*PRND*) to which no association to prion disease has yet been seen (Mead *et al.*, 2000); *APOE* and *HLA-DQB7* (see below). In addition, Mead and colleagues have shown, based initially on work with kuru exposed PNG samples, that the prion gene has undergone significant balancing selection both within PNG and possibly even worldwide (Mead *et al.*, 2003) – this is also discussed further in Chapter 6.

1.8.6 Evidence for human genetic susceptibility to prion disease

1.8.6.1 Information from animal studies - inbred mouse lines

Inbred mouse lines are an established model for prion disease genetics and have been useful in determining the genetic contribution to disease such as incubation time[•]. Following inoculation with a particular prion strain, mean incubation times can vary from 100 to over 500 days in different inbred mouse lines. There are many factors that can influence incubation time including prion strain type, level of host PrP^C, dose of infectious material and route of administration

[•] In experimental transmissions to mice this is measured in days from the time of prion inoculation to the onset of clinical signs.

(incubation times are shorter when inoculation is administered directly into the brain compared to peripheral or oral routes). When experimental conditions are kept constant, incubation times are highly reproducible with small standard deviations. Between mouse lines however, incubation times can vary substantially: incubation times in SM/J and MAI/Pas mice, inoculated with Chandler/RML mouse adapted scrapie, vary from 133±1 to 360±11 days respectively (Lloyd *et al.*, 2004). The major determinant of incubation time is the inbred mouse line used which implies a strong genetic effect.

Inbred mouse lines can be separated into two characteristic incubation groups: short incubation time (100-200 days) and long incubation time (>255 days). Over a period of a decade from 1988, several authors used classical genetic studies to link the genetic determinant of prion incubation time in different mouse strains to loci on chromosome 2 tightly linked to *PRNP*, which were eventually shown to be *PRNP* alleles (for review see Lloyd *et al.*, 2005). In all, three *PRNP* alleles have been identified which differ at amino acid 108 and 189 of the protein product: $PRNP^a$ (108-Leu, 189-Thr) and $PRNP^b$ (108-Phe, 189-Val) are the short and long incubation alleles respectively (Westaway *et al.*, 1987) and $PRNP^c$ (108-Phe, 189-Thr) is an intermediate incubation time allele (255±12 days) found only in MAI/Pas mice (Lloyd *et al.*, 2004). However, within a given *PRNP* genotype a range of incubation times are still seen (Table 1.5) suggesting that many genes, other than *PRNP*, also have a role in determining prion disease incubation time.

Strain	Incubation time (days) + SEM
***a* allele mice**	
NZW/OlaHsd	108 ± 1 (n=38)
SJL/OlaHsd	122 ± 1 (n=37)
FVB/NHsd	131 ± 1 (n=33)
SM/J	133 ± 1 (n=47)
SWR/OlaHsd	135 ± 1 (n=36)
RIIIS/J	135 ± 1 (n=34)
C57BL6/JOlaHsd	143 ± 1 (n=42)
***b* allele mice**	
JU/FaCt	313 ± 3 (n=24)
VM/Dk	300 ± 3
I/Ln	255 ± 14
***c* allele mice**	
MAI/Pas	360 ± 11 (n=20)
C57 MAI-*PRNP*	255 ± 12 (n=9)

Table 1.5 Incubation times following intracerebral inoculation

Mice inoculated with Chandler/RML mouse adapted scrapie (Modified from Lloyd *et al.*, 2005)

The first non-*PRNP* susceptibility locus was identified using congenic mice by Kingsbury and colleagues in 1983 (Kingsbury *et al.*, 1983) within the MHC on chromosome 17. The MHC was

specifically targeted because the lymphoid system is known to have a role in the peripheral early replication of prions. The locus was designated prion incubation determinant-1 (*Pid-1*).

Incubation time is a continuous or quantitative trait which can be used as a measurable phenotype in linkage studies. Several whole-genome linkage studies of F2-intercrosses† and backcrosses‡ to map prion disease QTLs have been conducted. Of the five studies conducted to date, over 20 loci have been mapped on eight mouse chromosomes (Lloyd *et al.*, 2001; Lloyd *et al.*, 2002; Manolakou *et al.*, 2001; Moreno *et al.*, 2003; Stephenson *et al.*, 2000). In the largest such study by Lloyd and colleagues, an F1 intercross between CAST/Ei and NZW/OlaHSd mice was challenged with RML prion strain. Consistent with the segregation of multiple prion incubation genes, the resulting F2 generation showed a larger standard deviation in incubation time than the F1 generation (26 days and 7 days, respectively). Three highly significant regions were mapped to chromosomes 2 (including *PRNP*), 11 and 12, with suggestive linkage on chromosomes 6 and 7. It is difficult to directly compare data from all five QTL studies, especially as they all involve different experimental conditions, however some loci are represented in more than one study such as the loci on chromosome 11 which are seen in two studies (Lloyd *et al.*, 2001; Stephenson *et al.*, 2000). Loci on chromosome 2 have also been identified in more than one study, which used identical CAST x NZW F2 intercrosses but innoculated with different prion strains (Lloyd *et al.*, 2001; Lloyd *et al.*, 2002). These two regions show considerable overlap and may represent the same underlying genes. The incubation times seen in the F2 mice were opposite to those observed in the parental lines, suggesting that a *PRNP* independent locus on chromosome 2 (or other loci) exists. Such discordance between incubation times and *PRNP* genotypes has been noted previously by Carlson and colleagues' whose work investigating *Prni* (a locus tightly linked to *PRNP* and which was at the time thought to be the major determinant of prion incubation time) identified a long incubation mouse with a short incubation time *PRNP* allele (Carlson *et al.*, 1986). Carlson speculated that this mouse was a rare recombinant between *Prni* and *PRNP*, which could not be verified as the animal died before it could be progeny tested. Together these results raise the possibility that a susceptibility locus tightly linked but separate from *PRNP* may exist.

In summary, studies of inbred mouse lines have identified *PRNP* as the major determinant of prion incubation time. Other genes are also involved and although QTL studies have identified

† Two heterozygous mice from the first filial generation (F1) are mated to produce offspring with genotypes in Mendelian ratios

‡ A heterozygous mouse is mated with a homozygous mouse of a parental line

several large regions of linkage, including a QTL linked to *PRNP* but independent of its coding sequence. The quantitative trait nucleotide (QTN) responsible has yet to be characterised.

1.8.6.2 HLA

The human leukocyte antigen (HLA) locus has been investigated as a susceptibility locus in several neurodegenerative diseases including idiopathic Parkinson's disease (Lampe *et al.*, 2003) and Alzheimer's (Lehmann *et al.*, 2006; Zareparsi *et al.*, 2002). In mouse, the HLA locus *Pid-1* has been associated with prion disease incubation time (Kingsbury *et al.*, 1983). In human prion disease, the HLA allele *HLA-DQ7,* has been shown to be associated with resistance to vCJD but not sCJD by Jackson and colleagues (Jackson *et al.*, 2001). In their study, Jackson *et al.* had access to a small sample set, analysing just 50 vCJD and 26 sporadic CJD cases. Subsequent studies by other investigators failed to reproduce this association but were also limited by available sample size (Laplanche *et al.*, 2003; Pepys *et al.*, 2003). The *HLA-DQ7* allele has been shown to vary significantly in different worldwide populations (Galvani *et al.*, 2005) may have confounded these previous studies.

Despite the lack of replication, the potential association of *HLA-DQ7* with vCJD is informative with respect to the distinct mechanism of pathogenesis compared to sporadic CJD. In vCJD peripheral prion replication, which occurs in the lymphoreticular system and is where the product of the HLA locus is likely to act, may be the greatest determinant of susceptibility (i.e. incubation time, progression etc.).

1.8.6.3 *PRNP* codon 129 polymorphism

A common polymorphism at codon 129 of the *PRNP*, encoding either a methionine or valine, is a strong susceptibility factor for all three aetiological categories of human prion disease. Methionine homozygotes comprise 37% of the UK population whereas valine homozygotes comprise 12% (Owen *et al.*, 1989). In sCJD, patients are largely methionine or valine homozygotes (Laplanche *et al.*, 1994; Palmer *et al.*, 1991; Windl *et al.*, 1996; Windl *et al.*, 1999), however an excess of methionine homozygotes over valine has been seen in sCJD (Salvatore *et al.*, 1994). In addition, codon 129 genotype has also been shown to correlate directly with phenotype. Windl and colleagues found that 90.5% of patients diagnosed with definite CJD were methionine homozygous compared to 1.9% valine homozygous. In addition an atypical sCJD cohort comprised 41.4% methionine and 14.8% valine homozygotes.

Susceptibility to iatrogenic growth hormone associated prion disease is mediated by valine homozygosity at codon 129 (Collinge *et al.*, 1991). In familial 6-OPRI cases, the age of onset for methionine homozygotes is approximately a decade earlier than that for heterozygotes (Poulter *et al.*, 1992). Incubation time in kuru is shortened for homozygotes of either allele (Cervenakova *et al.*, 1998) and all cases of variant CJD to date have been methionine homozygotes (Collinge, 2005).

The only non-codon 129 *PRNP* susceptibility allele identified to date has been a rare lysine to glutamine polymorphism at condon 219 (E219K) in Japan (Shibuya *et al.*, 1998). In this population, where both the codon 129 and 219 polymorphisms are rare, all sCJD patients have been found to be homozygous for either allele at codon 129 but lack the 219 polymorphism, suggesting a protective effect.

1.8.6.4 *PRNP* regulatory elements, *PRNP* expression and prion disease

PRNP mediated disease susceptibility is likely to extend beyond the coding sequence of the gene and also involve proximal *cis*-acting regulatory elements including the *PRNP* promoter and upstream enhancers but also long range elements such as locus control regions. The evidence for prion disease susceptibility influenced by variation in *PRNP* regulatory regions and thus affecting expression, is reviewed in Chapter 7.

1.9 Aims of this thesis

The aims of this thesis are to apply the techniques and analyses available to investigate complex diseases, towards identifying susceptibility loci for two neurodegenerative diseases, ALS and prion disease. More specifically, this thesis aims:

- to characterise the genomic arrangement of *DYNC1H1*, a candidate gene for human ALS supported by multiple lines of evidence
- to conduct a mutational screen of human *DYNC1H1* exons, homologous to those harbouring mutations in two mouse models of progressive neurodegeneration similar to ALS, in an attempt to determine if this gene explains cases of FALS or other motor neuron diseases
- to conduct a candidate gene association study of *DYNC1H1* with sporadic ALS, ascertaining SNPs for investigation, determining the LD and haplotype structure to define a minimum set of tSNPs which would allow an economic and effective means to test known and unknown genetic variation in the gene for an association with disease
- to clarify the nomenclature and genetic relationships of the cytoplasmic dynein subunits, to assist future studies and help devise a standardised nomenclature system. Investigating the genetic relationships of the subunit families in humans and mouse will also ensure that all homologous members of the cytoplasmic dyneins have been identified.
- to undertake a comprehensive analysis of kuru and Papua New Guinea codon 129 polymorphism data.
- to identify signatures of selection imposed by the kuru epidemic, experienced by the people of the Eastern Highlands of PNG, at codon 129 of *PRNP* as a paradigm for additional candidate gene or whole genome studies. These candidate genes may be identified from mice models of prion incubation time or cell-based studies of prion incubation.
- to develop a PNG sample set that will facilitate future investigations of candidate genes for signatures of selection.
- to assess the feasibility of conducting genome-wide genotyping on archived kuru DNA samples and identify optimal analysis parameters
- to assess if copy number variation of *PRNP* is a pathogenic or protective mechanism in both sporadic CJD and kuru.

2 Materials and methods

2.1 Materials

2.1.1 General chemicals and reagents

10x TBE	Life Technologies
Absolute ethanol (100%)	Sigma-Aldrich
Agarose (electrophoresis grade)	Invitrogen
Biotinylated anti-streptavidin antibody	Vector Laboratories
Bromophenol blue	Sigma-Aldrich
Denhardt's solution (50x)	Sigma-Aldrich
Dimethyl sulphoxide (DMSO)	Sigma-Aldrich
dNTPs	Promega
EDTA (0.5M, pH 8.0)	Ambion
Ethanol (96-100%)	BDH Chemicals
Ethidium bromide	Sigma
Glycerol	Sigma-Aldrich
H_2O (molecular biology grade)	Cambrex
Herring sperm DNA	Promega
Human Cot-1 DNA	Invitrogen
Hyperladder (I, IV and V)	Bioline
MES hydrate SigmaUltra	Sigma-Aldrich
MES sodium salt	Sigma-Aldrich
MGB probes	Applied Biosystems
Primers	Sigma-Genosys
Sodium acetate (NaAce)	Sigma-Aldrich
Sodium dodecyl sulphate (SDS)	Sigma-Aldrich
SSPE (20x)	Cambrex
Streptavidin, R-phycoerythrin conjugate (SAPE)	Invitrogen
TE buffer, reduced EDTA (10mM Tris HCl, 0.1mM EDTA, pH 8.0)	TEKnova
TMACL (5M)	Sigma-Aldrich
Tween-20 (10%)	Pierce

2.1.2 Prepared solutions

Loading Buffer	*Sodium Dodecyl Sulphate (SDS), 10%*
0.5ml 1M Tris-HCl pH7.6	100g SDS per 1ml autoclaved water
25ml glycerol	Stored at room temperature
0.5ml 10% SDS	
0.05g bromophenol blue	
Made up to 50ml with ddH_2O	
Stored at room temperature	

2.1.3 Commercial kits

Affymetrix DNA Amplification Clean-Up Kit	Affymetrix
Affymetrix GeneChip 500K Assay	Affymetrix
Better Buffer	Microzone
BigDye Terminator Ready Reaction kit	Applied Biosystems
Clontech TITANIUM Taq buffer	Clontech
Clontech TITANIUM Taq DNA polymerase	Clontech
DYEnamic ET Dye Terminator kit	Amersham Pharmacia Biotech
G-C Melt	Clontech
GeneScan 2500 TAMRA Red	Applied Biosystems
HotStartTaq DNA Polymerase	Qiagen
MegaBACE ET400-R Size Standard	Amersham Pharmacia Biotech
MegaBACE Loading Solution	Amersham Pharmacia Biotech
MegaBACE Long Read Matrix	Amersham Pharmacia Biotech
MegaBACE LPA Buffer	Amersham Pharmacia Biotech
MegaMix Blue	Microzone
MicroClean PCR purification kit	Microzone
QIAamp 96 DNA Blood Mini kit	Qiagen
QIAamp DNA Blood Mini kit	Qiagen
QuantiTect Probe PCR Master Mix	Qiagen

2.1.4 Restriction enzymes and ligases

*Enzyme**	*Buffer/conditions*	*Company*
DNaseI	-	New England Biolabs (NEB)
HinfI	2	New England Biolabs (NEB)
NspI	2 + BSA	New England Biolabs (NEB)
PvuII	2	New England Biolabs (NEB)
T4 DNA Ligase	T4 DNA Ligase Buffer	New England Biolabs (NEB)

2.1.5 Equipment

8 Strip PCR tubes and caps, thin-walled	Scientific Specialities Inc
96-well PCR plates	ABgene
ABI Prism 377 DNA Sequencer	Applied Biosystems
Allegra 25R centrifuge for 96-well plates	Beckman Coulter
Aluminium adhesive PCR foil roll	ABgene
DNA Engine Tetrad PTT-225 Peltier Thermal Cycler	MJ Research
Electrophoresis power packs	Amersham Pharmacia Biotech
Electrophoresis tanks (Horizon 11.14)	Life Technologies
Eppendorf 5415R Microcentrifuge	Eppendorf
Eppendorf Comfort Thermomixer 1.5ml	Fisher Scientific
GeneChip Hybridization Fluidics Station 450	Affymetrix
GeneChip Hybridization Oven 640	Affymetrix
GeneChip Scanner 3000 7G	Affymetrix
Gilson pipettes	Anachem
Grant JB5 waterbath	Wolf Laboratories
MegaBACE 1000 DNA Analysis System	Amersham Pharmacia Biotech
MicroAmp Fast Optical 96-well Reaction Plates	Applied Biosystems
MicroAmp Optical 96-well Reaction Plates	Applied Biosystems
MicroAmp Optical Adhesive Film	Applied Biosystems
Microtubes, hyrdophobic 0.65ml	Scientific Specialities Inc
PCR seal film	ABgene
Pipette tips	Anachem
QIAvac 96 vacuum manifold	Qiagen
Raven incubator	CTE Scientific
Sigma 6K 15 plate rotor 2 x 96-well plate	Qiagen

* updated nomenclature used, see (Roberts *et al.*, 2003).

Sigma 6K 15 refrigerated centrifuge	Sigma Laborzentrifugen GmbH
Ultrospec 2000 UV visible spectrophotometer	Pharmacia Biotech
Vacuum pump	KNF Neuberger

2.1.6 Photography

Gel Doc EQ UV-transilluminator	Bio-Rad Laboratories
Thermal paper for Mitsubishi video printer	Bio-Rad Laboratories

2.1.7 Software and websites

Bioinformatic-Harvester	http://harvester.embl.de/
BLAST	http://www.ncbi.nlm.nih.gov/BLAST (Altschul *et al.*, 1990)
ClustalW	http://www.ebi.ac.uk/clustalw (Thompson *et al.*, 1994)
Ensembl Fugu Genome Browser	http://www.ensembl.org/Fugu_rubripes
Entrez	http://www.ncbi.nlm.nih.gov/Entrez/index.html
GDAS	GeneChip DNA Analysis Software (Affymetrix)
HapMap	www.hapmap.org
HGNC	http://www.gene.ucl.ac.uk/nomenclature/
MGI	http://www.informatics.jax.org/
MultiPipmaker	http://pipmaker.bx.psu.edu/cgi-bin/multipipmaker
NCBI	http://www.ncbi.nlm.nih.gov
NEBcutter	http://tools.neb.com/NEBcutter2/index.php
NspI library files	GeneChip Human Mapping 500K Set library files (Affymetrix)
PHASE	http://www.stat.washington.edu/stephens/software.html (Stephens *et al.*, 2003)
PHYLIP	http://evolution.gs.washington.edu/phylip.html
PL-EM	http://www.people.fas.harvard.edu/~junliu/plem (Qin *et al.*, 2002)
PLINK	http://pngu.mgh.harvard.edu/~purcell/plink/
Power Calculator	http://pngu.mgh.harvard.edu/~purcell/gpc/ (Purcell *et al.*, 2003)
Primer Express v2.0	Applied Biosystems
Primer3	http://frodo.wi.mit.edu/cgi-bin/primer3/primer3_www.cgi
PubMed	http://www.ncbi.nlm.nih.gov/entrez/query.fcgi?db=PubMed
RepeatMasker	http://www.repeatmasker.org/cgi-bin/WEBRepeatMasker
Sequence Analyzer	Molecular Dynamics (Wu and King, 2003)

SNPHAP	http://archimedes.well.ox.ac.uk/pise/snphap-simple.html (Clayton, 2004)
TagIT	http://popgen.biol.ucl.ac.uk/software.html (Goldstein *et al.*, 2003b; Weale *et al.*, 2003)
Translate	http://us.expasy.org/tools/dna.html
UCSC	http://genome.ucsc.edu
WebCutter	http://www.firstmarket.com/cutter/cut2.html

2.2 Samples

2.2.1 Healthy population DNA samples

DNA samples from healthy individuals were obtained from the following sources: 33 European trios were obtained from the Centre d'Etude du Polymorphisme Humain (CEPH) and 48 unrelated Japanese and 49 unrelated West African (Cameroonian) individuals, were obtained from the laboratory of Professor David B. Goldstein, Institute for Genome Sciences and Policy, Centre for Population Genomics and Pharmacogenetics, Duke University, North Carolina, USA. DNA samples were collected by the Goldstein laboratory with signed consent or were anonymous legacy collections provided by collaborators from other academic institutions.

480 UK White Caucasian control samples (plates HRC-1 to 5), were obtained from the European Collection of Cell Cultures (ECACC). A further 90 UK Caucasian control samples used for whole genome SNP genotyping were collected by Dr. Simon Mead, MRC Prion Unit, London, UK from the West End Blood Donor Centre, c/o Dr Jean Harrison, London, UK. North American control samples comprising of both unaffected spouses from Caucasian familial ALS pedigrees and other Caucasian individuals were collected with signed consent by Professor Robert H. Brown Jr., Day Neuromuscular Research Laboratory, Massachusetts General Hospital, Massachusetts, USA or provided to R.H. Brown by collaborators from other North American academic and clinical institutions.

Chimpanzee DNA was extracted from blood provided by the Institute of Zoology, London Zoo, Regents Park.

2.2.2 Patient/case DNA samples

Sporadic ALS DNA samples were obtained from patients seen by Professor R.H. Brown at Massachusetts General Hospital or provided, to R.H. Brown by collaborators from various academic and clinical institutions across North America. All sporadic ALS patient samples were obtained with informed consent. Patients were diagnosed by El Escorial criteria and had not been

screened for *SOD1* mutations. The patient cohort comprised of 134 females and 147 males with an average age at diagnosis of 46 years (range 24 to 79 years). 34% of patients were diagnosed with early onset in the lower extremities, 35% with upper onset, 30% with bulbar onset and site of onset in the remaining 2% was unknown.

Motor neuron disease samples screened for *DYNC1H1* mutations were index cases from pedigrees with familial history of disease. ALS samples were collected by Professors Pamela Shaw, Sheffield University, Sheffield, UK and Karen Morrison, Department of Neurology, University of Birmingham, Birmingham, UK and Dr Richard Orrell, Department of Clinical Neuroscience, University College London, London, UK. All ALS samples were Caucasian adults with definite or probable ALS, without detectable *SOD1* mutation. Spinal muscular atrophy (SMA) samples were adult and juvenile onset cases without *SMN* deletions provided by Professor Morrison. All SMA cases were Caucasian, except 2 Indian and 1 Arab case (K. Morrison pers. comm.). Hereditary Spastic Paraplegia (HSP) samples were British Caucasian index cases from 32 different families (20 recessive inheritance families and 12 dominant inheritance families).

Sporadic CJD samples were obtained from patients seen at the Institute of Neurology, Queen Square, London, UK, with signed consent. Prion disease was confirmed post-mortem by the histological identification of spongiform change, astrocytosis, neuronal loss and proteinase-resistant PrP^{Sc} deposition in the brain. Of prion disease cases, sporadic CJD is a diagnosis of exclusion and diagnosis was made in the absence of histopathological and PrP^{Sc} strain-type features of variant CJD, the absence of mutation of the *PRNP* open reading frame seen in inherited prion disease and the absence of obvious exposure to infectious human prion material.

2.2.3 Papua New Guinea Samples

Papua New Guinean samples were obtained as frozen DNA and/or blood archives from the MRC Prion Unit, London, UK, or from the Papua New Guinea Institute of Medical Research (PNGIMR), Goroka, PNG. All studies were approved by the Papua New Guinea Medical Research Advisory Committee and by the local UK research ethics committees. The full participation in the project from the communities, which was critical with respect to the ethics and operation of the study, was established and maintained through discussions of the joint MRC-PNGIMR field team with village leaders, communities, families, and individuals. Field studies followed the principles and practice of the Papua New Guinea Institute of Medical Research.

2.3 Methods

2.3.1 DNA isolation from chimpanzee blood

DNA was extracted from whole blood using QIAamp DNA Blood Mini Kit (Qiagen) following its associated protocol. The basis of the procedure is salt deproteinisation and is summarised as follows: 200μl whole blood was added to 20μl QIAGEN Protease in a 1.5ml microcentrifuge tube – all centrifugation steps were carried out in a microcentrifuge (Eppendorf). The tube was gently agitated to ensure the proper mixing of the blood and enzyme. 200μl Buffer AL was added and the sample pulse-vortexed for 15 seconds to ensure efficient lysis of all cells. The protease and buffer mixture is required to lyse cells in the sample and degrade all proteins, including those bound to DNA. The buffer has a high salt content and optimum pH to precipitate protein out of solution and away from the DNA. The mixture was incubated in a waterbath at 56°C for 10 minutes and tube centrifuged briefly to remove liquid condensed on the lid. 200μl ethanol (96-100%) (BDH Chemicals) was added and the sample was again pulse-vortexed for 15 seconds and centrifuged briefly.

The sample was transferred into a QIAamp Spin Column placed in a 2ml collection tube, sealed and centrifuged at 6000 relative centrifugal force* (rcf), for 1 minute. The silica gel membrane within the spin column absorbs DNA but does not retain protein or other contaminants within the lysate. The addition of ethanol to the lysate optimises DNA binding to the membrane. The filtrate was discarded and the QIAamp Spin Column was placed in a clean 2ml collection tube and 500μl Buffer AW1 was added. Buffers AW1 and AW2 are both ethanol based wash buffers used to remove residual contaminants without affecting DNA binding to the spin column membrane. The QIAamp Spin Column was again centrifuged at 6000 rcf for 1 minute and the collection tube containing the filtrate was again discarded. The QIAamp Spin Column was placed in a clean 2ml centrifuge tube and 500μl Buffer AW2 was added. The column was centrifuged at 20,000 rcf for 3 minutes and then placed in a clean 1.5ml microcentrifuge tube and the collection tube containing filtrate was discarded. 200μl Buffer AE was added to the column to elute the DNA. The column was incubated at room temperature for 5 minutes and then centrifuged at 6000 rcf for 1 minute and the primary eluate containing the DNA was collected and stored at -20°C. The QIAamp Spin Column was again placed in a clean 1.5ml centrifuge tube for a second elution to increase the total DNA yield. Again, 200μl Buffer AE was added, incubated at room temperature for 5 minutes and centrifuged at 6000 rcf for 1 minute. The second elute was also stored at -20°C.

---

* rcf to rpm conversion: $\mathbf{rcf} = 1.12 \times \mathbf{r} \times (\mathbf{rpm}/1000)^2$, where **r** is rotor radius and **rpm** revolutions per minute.

2.3.2 DNA isolation from human blood

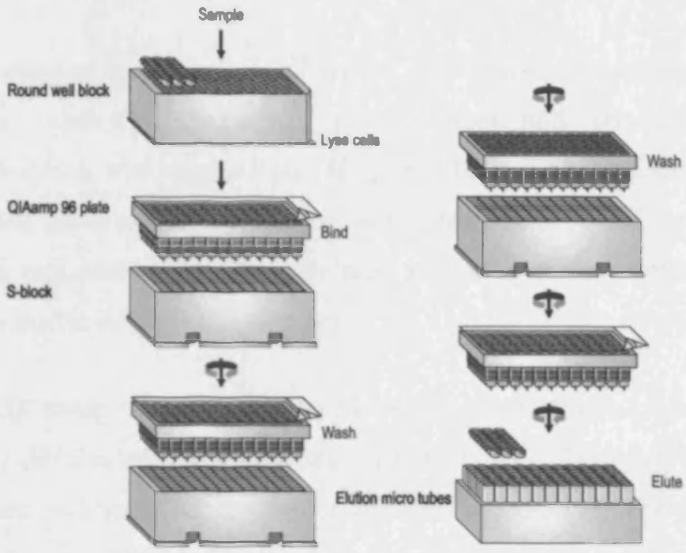

Figure 2.1 Overview of the QIAamp 96 DNA Blood Mini kit procedure
Adapted from the QIAamp DNA Blood Mini Kit protocol (Qiagen)

DNA was extracted from whole blood using QIAamp 96 DNA Blood Mini Kit (Qiagen) following its associated protocol. The kit is identical to the QIAamp DNA Blood Mini Kit but spin columns are in a 96-well plate format for increased throughput and a modified protocol summarised as follows: 20µl QIAGEN Protease was aliquoted to each well of a 96-round-well block (Figure 2.1) and 200µl whole blood was then added. 200µl Buffer AL was added to each sample and the wells were sealed using caps for blocks and tubes. Care was taken not to wet the well-rims at this stage to prevent caps from loosening in later steps. The sample was then mixed thoroughly by holding the round-well block with both hands and shaking up and down vigorously for 15 seconds. The block was centrifuged briefly at 2200 rcf (all centrifugation steps were carried out using the Sigma 6K 15 refrigerated centrifuge set at 40°C, unless otherwise stated) and then incubated at 70°C in a dry incubator for 10 minutes. A large heat-resistant weight was placed on top of the block to prevent the caps from popping off during the incubation and the contents evaporating. After incubation, the round-well block was briefly centrifuged again at 2200 rcf. 200µl ethanol (96–100%) was then added to each well of the block and the wells sealed with new caps for blocks and tubes. The block was again vigorously mixed by shaking for 15 seconds, and briefly centrifuged at 2200 rcf.

A QIAamp 96 plate was placed on top of an S-Block (Figure 2.1) and both were marked for later identification. The contents of the round-well block (620µl per well) was added to the QIAamp 96 plate. Care was taken not to wet the rims of the wells to avoid aerosol formation during

centrifugation. The QIAamp 96 plate was sealed with an AirPore Tape sheet and was placed with the S-Block into the centrifuge rotor bucket and centrifuged at 5796 rcf for 4 minutes.

The S-block was emptied of lysate and 500µl Buffer AW1 added to each well of the QIAamp 96 plate. The plate was sealed with a new AirPore Tape sheet and centrifuged at 5796 rcf for 2 minutes. Again the S-Block was emptied and 500µl Buffer AW2 was added to each well of the QIAamp 96 plate. The plate and S-Block were centrifuged at 5796 rcf for 15 minutes, without AirPore Tape (which was omitted to allow the heat generated during centrifugation to evaporate residual ethanol from Buffer AW2 in the sample).

To elute the DNA a QIAamp 96 plate was placed on top of a rack of elution MicroTubes (Figure 2.1) and 200µl Buffer AE was added using a multichannel pipette. The plate was sealed with a new AirPore tape sheet and incubated for 5 minutes at room temperature. The plate and MicroTubes rack were then centrifuged at 5796 rcf for 4 minutes. A further 200µl Buffer AE was added and the plate centrifuged at 5796 rcf for another 4 minutes to obtain an extra 20% yield.

2.3.3 Determination of DNA concentration and purity

DNA concentration and purity was determined using spectrophotometric analysis, where necessary. An appropriate dilution of DNA was prepared and absorption readings were taken at 260nm and 280nm, using either a Ultrospec 2000 Ultra Violet (UV) visible spectrophotometer (Pharmacia Biotech) or a NanoDrop 1000 spectrophotometric analyser (NanoDrop Technologies). The following equations were used:

DNA purity = A_{260}/A_{280} (an ideal A_{260}/A_{280} ratio was between 1.8 to 2.0)

DNA concentration (µg/µl) = A_{260} x dilution factor x 50µg/ml

2.3.4 Primer design

Primers were designed for Polymerase Chain Reaction (PCR) amplification, genotyping and sequencing reactions. Genomic sequence for the region of interest was obtained from National Center for Biotechnology Information (NCBI) (www.ncbi.nlm.nih.gov). Amplicon sequence and flanking primer binding sequence was examined for DNA repeats using RepeatMasker (www.repeatmasker.org/cgi-bin/WEBRepeatMasker) and potential primer sequences were designed to avoid annealing to repetitive DNA. Primers for PCR and sequencing were designed using Primer 3 software (http://frodo.wi.mit.edu/cgi-bin/primer3/primer3_www.cgi) or designed by eye. All primers were made by Sigma-Genosys.

2.3.4.1 Real-time PCR primers and probe design

Real-time primers and probes were designed using Primer Express v2.0 (Applied Biosystems) and all real-time probes were designed as Minor Groove Binder (MGB)* Primers and probes were designed based on the following principles:

- The template strand was selected to increase the cysteine (C) content of the probe rather than the guanine (G) content.
- Primers were designed to be as close to the probe as possible with an overall amplicon length of ~50-150bp.
- Minimum probe length was 13 nucleotides.
- Probe/primer G-C content was maintained at a 30–80% range.
- Probes with a guanine nucleotide on the 5′ end were avoided.
- Primers were limited to no more than two G and C residues within the last five nucleotides at 3' end.
- Probes/primers containing runs of an identical nucleotides were avoided (especially four or more guanine's)
- Probe melting temperatures (T_m) were between 65–67 °C.
- Primer T_m's were between 58–60 °C.

Primers were made by Sigma-Genosys and probes by Applied Biosystems. Probes were divided into 100μl aliquots upon receipt and care was taken to avoid excessive freeze-thawing and exposure to ultra violet (UV) light – which promotes aberrant cleavage of the end-labelled fluorescent reporter dyes.

2.3.5 Polymerase chain reaction

All PCRs were carried out using the following protocol in 0.65ml microtubes (Scientific Specialities Inc), 8 well PCR strips (Scientific Specialities Inc) or 96-well plates, unless otherwise stated: A PCR master mix was prepared containing 1 x PCR Buffer (supplied with HotStarTaq kit), 200μM dNTPs, 1μM forward primer, 1μM reverse primer, 0.2U/μl HotStarTaq DNA Polymerase (Qiagen) and distilled water, made up to a final reaction volume of 20μl. The master mix was then divided into 18μl aliquots using a Gilson Distriman repeater-pipette and 1μl DNA (~100ng/μl concentration) was added to each tube/well with one well assigned as a non-template, water control.

Thermal cycling conditions on the DNA Engine Tetrad Thermal Cycler (MJ Research) were as follows: HotStarTaq polymerase activation at 95°C for 1 min and then 35 cycles of: DNA template

* MGB probes use non-fluorescent quenchers, which allow a more precise measurement of reporter dye compared to conventional probes, They also bind the DNA minor groove, increasing their melting temperature (T_m) and allowing the use of shorter probes, with better allele discrimination properties.

denaturation at 94°C for 30 seconds, primer annealing at 60°C (or relevant temperature listed in table 3.1) for 30 seconds, extension 72°C for 1 minute, and a final extension step at 72°C for 5 minutes. After amplification, 4μl PCR product was mixed with 4μl loading buffer and electrophoresed on a 2% agarose gel; 2 grammes (g) agarose (Invitrogen) dissolved in 100ml 1x TBE (Life Technologies), containing 0.1μg/ml ethidium bromide (Sigma) and visualised by UV-transillumination. All agarose gels were 2% unless otherwise stated. 4μl of the appropriately sized DNA ladder of was used to estimate the specificity of PCR amplicons.

PCRs for genotyping microsatellites, a54000*, a108990*, D20S889, D20S482 and D20S97 were carried out in 15μl reactions containing 13.7μl MegaMix Blue (Microzone), 0.15μl forward primer (50pm/μl), 0.15μl reverse primer (50pm/μl) and 1μl template DNA (~50ng/μl). Cycling conditions on the Tetrad thermal cycler were polymerase activation step of 95°C for 3 minutes and then 34 cycles of: DNA template denaturation at 95°C for 30 seconds, primer annealing at 55°C (or relevant temperature) for 40 seconds, 72°C extension step for 45 seconds, and a final extension step of 72°C for 5 minutes and 15°C for 2 minutes. PCR products were electrophoresed as described above but without addition of loading buffer.

2.3.6 Purification of PCR amplicons for sequencing

PCR products were purified using *micro*CLEAN (Microzone), to remove reaction buffers, enzymes, primer dimers and unincorporated primers and dNTPs, following the manufacturer's protocol. Briefly, an equal volume of *micro*CLEAN was added to a 96-well plate containing PCR products and incubated at room temperature for 5 minutes. The plate was centrifuged at 3000 rcf for 40 minutes and then inverted onto absorbent paper and pulsed at 100 rcf to discard the supernatant. The purified DNA pellet was then resuspended in 20μl sterile distilled water.

2.3.7 Sequencing of purified templates

Automated fluorescent sequencing was carried out with the BigDye Terminator Ready Reaction Kit (Applied Biosystems), DYEnamic ET Dye Terminator Kit (Amersham Pharmacia) and 1μM PCR primers. For the BigDye Terminator Ready Reaction Kit, a sequencing master-mix was made containing (per reaction) 1μl BigDye terminators, 5μl BetterBuffer (Microzone), 0.5μl forward/reverse primer (1μM), and 7μl sterile distilled water. A Gilson Distriman repeater-pipette was used to aliquot 13.5μl BigDye master-mix into wells of a skirted 96-well plate, to which 1.5μl purified PCR products were added, for a total reaction volume of 15μl. Cycling conditions were 96°C for 30 seconds, followed by 30 cycles of 50°C for 15 seconds and 60°C for 3 minutes and a final hold step of 15°C for 5 minutes.

* From (Mead, 2002)

The DYEnamic ET Dye Terminator Kit sequencing master-mix contained, per reaction, 2μl ET terminators, 6μl BetterBuffer and 4μl forward/reverse primer (1μM). 12μl ET terminators master-mix was aliquoted into wells of a skirted 96-well plate, to which 8μl purified PCR products were added, for a total reaction volume of 20μl. Cycling conditions were 25 cycles of 95°C for 20 seconds, 50°C for 15 seconds and 60°C for 1 minute, with a final hold step of 10°C for 10 minutes.

2.3.8 Post-reaction clean-up with ethanol/salt precipitation

Sequencing products were precipitated to remove reaction buffers and unincorporated terminators to avoid tall early peaks, often termed "terminator blobs". 55μl 100% absolute ethanol (Sigma-Aldrich) and 1μl 3M sodium acetate (Sigma-Aldrich) was added to 20μl reaction and the mixture was chilled on ice for 15 minutes. The plate was centrifuged at 3000 rcf for 45 minutes to pellet the DNA and the supernatant discarded by inverting onto absorbent tissue paper and pulse-centrifuging at 100 rcf for 1 minute. 150μl 70% ethanol was added to wash the pellets and the plate was centrifuged at 3000 rcf for 10 minutes. Again, the plate was inverted onto absorbent tissue paper, pulse-centrifuged at 100 rcf for 1 minute to remove the supernatant and the pellet was allowed to air dry for 10 minutes.

2.3.9 DNA sequencing on the MegaBACE 1000 DNA Analysis System

The automated MegaBACE 1000 DNA Analysis System (Amersham Pharmacia) was used to sequence DNA. The MegaBACE uses capillary array electrophoresis to perform fragment size separation of fluorescently labelled DNA samples with a confocal optical system to collect data. The manufacturer's guidelines and protocols were followed unless otherwise stated. Precipitated DNA with fluorescently labelled terminators, was resuspended in 10μl MegaBACE Loading Buffer (Amersham Pharmacia), vortexed thoroughly to ensure the complete solublization of the DNA and then pulse-centrifuged to return the liquid to the bottom of the 96-plate wells.

MegaBACE Long Read Sequencing Matrix (Amersham Pharmacia) was used to pressure-fill the capillary array with sieving matrix to separate DNA fragments of varying sizes. Sequencing products were electrokinetically injected into the capillary array by a potential difference of 3kV for 40 seconds and electrophoresis was carried out in 1x LPA Buffer (Amersham Pharmacia) at 9kV for 100 minutes. Laser excitation of the fluorescently labelled samples yielded data as an electropherogram for each capillary/sample which were analyzed in forward and reverse directions using the Sequence Analyser v3.0 package (Molecular Dynamics), and inspected by eye.

2.3.10 SNP genotyping by restriction digestion

SNPs within *DYNC1H1* were tested for alteration of restriction enzyme recognition site using WebCutter (http://www.firstmarket.com/cutter/cut2.html) and NEBcutter (http://tools.neb.com/NEBcutter2/index.php). For SNPs that modified restriction enzyme recognition sites, PCR primers were designed to amplify a region of approximately 500bp around the polymorphism. PCR was performed as previously described in a 20μl reaction volume of which 4μl was electrophoresed on 2% agarose gel to check quality.

Restriction digestion was performed in 0.65ml microtubes in a total 20μl reaction volume, using 16μl un-purified PCR product and a 4μl restriction master-mix based on 1μl buffer recommended by manufacturer and 1-10 units of restriction enzyme per well. The amount of restriction enzyme required per SNP was estimated by initially performing a restriction digest on a subset of samples with only 1 unit of enzyme per sample. If this led to partial digestion of the amplicon after 3 hours, the experiment was repeated by adding additional enzyme until complete digestion was achieved. Digested amplicons were electrophoresed on 2% agarose and visualised as described previously.

The efficacy of SNP genotyping by restriction digest was tested by assaying a panel 25 CEPH samples, with *a priori* genotypes distinguished by DNA sequencing, in a blind test randomised by a second operator. Genotyping results from the blind test were then matched to sequence verified genotypes by the second operator and an efficacy score as a percentage was calculated.

2.3.11 Microsatellite genotyping

PCRs for microsatellites D20S482, D20S97, D20S889 and 108991 were initially multiplexed (each forward primer was tagged with 6-FAM, HEX, TET, 6-FAM fluorophores respectively; Sigma-Genosys) for the same DNA sample by mixing PCR products in the ratio 1:2:2:6 respectively, in a separate 96-well plate. Multiplexed PCRs comprised a total volume of 22μl and were made up to a total volume of 90μl with dd.H_2O. 45μl aliquots were stored at -20°C and the remaining 45μl were carried forward for clean-up. D20S97-HEX forward primer was eventually replaced by D20S97-6-FAM due to a low signal affected by spectral overlap* with microsatellite 108991 which had a similar sized PCR product. PCR clean-up was carried using ethanol/salt precipitation as describe above for post-sequencing reactions, with the following amendments: 45μl of ethanol was mixed with 1μl NaAce and aliquoted into 45μl multiplexed PCR sample. Pellets were resuspended in 10μl dd.H_2O.

* spectral overlap refers to the emission spectrum of one fluorophore overlapping with that of another, The excitation of one fluorophore therefore causes an erroneous recording of both fluorophores.

Microsatellites were genotyped using the MegaBACE 1000 DNA Analysis System. A loading solution of 5.6μl MegaBACE Loading Solution, 0.4μl MegaBACE ET400-R size standard and 2μl dd.H_2O was aliquoted into a new 96-well plate and 2μl resuspended PCR product added. The plate was vortexed briefly at medium speed and centrifuged briefly at 3000 rcf. The MegaBACE 1000 DNA Analysis System was set up following the manufacturer's guidelines and as described above. Multiplexed PCR products were electrokinetically injected into the capillary array by a potential difference of 3kV for 60 seconds and electrophoresis was carried out in 1 x LPA Buffer at 9kV for 70 minutes. Results were analysed using the Genetic Profiler v1.5 package (Molecular Dynamics).

2.3.12 Affymetrix GeneChip 250k NspI Assay

Whole-genome SNP genotyping was achieved using the NspI array of an Affymetrix GeneChip 500k kit. The manufacturer's protocol for the Affymetrix GeneChip 250k NspI assay was followed and is summarised in Figure 2.2. A designated pre- and post- PCR clean area was defined for the following steps, to avoid cross-contamination of pre-PCR steps with PCR amplicons. Genomic DNA samples were diluted to a 50ng/μl working dilution with reduced EDTA TE buffer (0.1mM EDTA) (TEKnova).

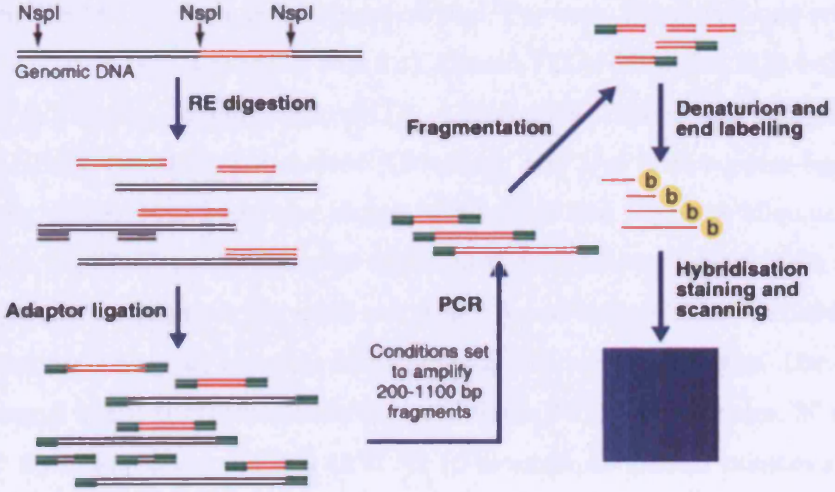

Figure 2.2 An overview of the Affymetrix GeneChip 250k NspI protocol

2.3.12.1 NspI digestion

The DNA Engine Tetrad thermal cycler was preheated to 37°C in preparation for genomic DNA digestion. A genomic DNA digestion master mix was prepared on ice with 1x NE Buffer 2 (NEB), 1x BSA (NEB) and 0.5 Units NspI (NEB), made up to a total volume of 14.75μl per sample, with molecular biology grade H_2O (Cambrex). 5μl genomic DNA (50ng/μl) was added to each well of a 96-well plate with a Gilson Distriman repeater-pipette and 14.75μl of the digestion master mix was added to each sample. The plate was then covered with a plate seal (Applied Biosystems), vortexed

at medium speed for 2 seconds and then centrifuged at 716 rcf for 1 minute. The plate was then placed on the thermal cycler on the following program: 37°C for 120 minutes, 65°C for 20 minutes and then held at 4°C. The digested DNA plate was stored in a -20°C freezer until required.

2.3.12.2 NspI adaptor ligation

The Tetrad thermal cycler was heated to 16°C in preparation for NspI adaptor ligation. A DNA ligation master mix of total volume 5.25μl per sample, was prepared on ice containing 1.5mM Affymetrix NspI adaptor (50mM), 1x T4 DNA ligase buffer (NEB), T4 DNA ligase (400U/μl) (NEB). 5.25μl ligation master mix was aliquoted into each digested DNA sample. The 96-well plate was covered with a new plate seal, vortexed at medium speed for 2 seconds and then centrifuged at 716 rcf for 1 minute. The plate was run in the thermal cycler at 16°C for 180 minutes, 70°C for 20 minutes and then held at 4°C. The adaptor ligated samples were stored in a -20°C freezer until required.

2.3.12.3 Adaptor-ligated fragment PCR and clean-up

The PCR master mix was prepared on ice to a final total volume of 270μl per sample, where each sample was amplified in triplicate in a volume of 90μl. For each 270μl triplicate reaction, 118.5μl molecular biology grade H_2O was added with 1x Clontech TITANIUM Taq PCR buffer (Clontech), 1M G-C Melt (Clontech), 350μM each dNTP, 4.5μM PCR Primer 002 (Affymetrix) and 1x Clontech TITANIUM Taq DNA Polymerase (Clontech). The 25μl NspI adaptor-ligated DNA was diluted 1 in 4 by adding 75μl molecular biology grade H_2O and 10μl was aliquoted to a 96-well plate in triplicate. 90μl PCR master mix was aliquoted to each adaptor-ligated DNA sample using a Gilson Distriman repeater-pipette. The plate was then covered with an adhesive plate seal, vortexed at medium speed for 2 seconds and then centrifuged at 716 rcf for 1 minute. The plate was then placed on a thermal cycler under the following conditions: 94°C for 3 minutes, 30 cycles of 94°C for 30 seconds, 60°C for 30 seconds and 68°C for 15 seconds, 68°C for 7 minutes and finally held at 4°C.

PCR clean-up was carried out using a Clean-Up Plate (Affymetrix) placed on a QIAvac 96 vacuum manifold (Qiagen) and attached to a vacuum pump (KNF Neuberger). 8μl 0.1M EDTA (Ambion) was added using a Gilson Distriman repeater-pipette to each PCR and the plate covered with a plate seal, vortexed at medium speed for 2 seconds and centrifuged at 716 rcf for 1 minute. The three PCRs for each sample were consolidated into a single well of the Clean-Up Plate and ~600mbar vacuum applied until the wells were completely dry. The PCR products were washed by adding 50μl of molecular biology grade H_2O and dried by applying a ~600mbar vacuum. Two additional washes were applied. The Clean-Up Plate was removed from the vacuum manifold and any excess

liquid on the bottom of the plate removed using absorbent paper. 45μl RB Buffer (supplied with Affymetrix Clean-Up Kit) was added to each well and the plate covered with a PCR plate seal. The Clean-Up Plate was agitated at a moderate speed on a plate shaker (the plate was secured by strong adhesive tape to an Eppendorf Thermomixer usually used for mixing 1.5ml Eppendorf tubes), for 10 minutes at room temperature, to recover the PCR product. Recovered PCR products were pipetted to a new 96-well plate and yield quantified using spectrophotometric analysis of a 50-fold diluted sample. Approximately 90μg of purified DNA was transferred to a new 96-well plate and the total volume of each sample brought up to 45μl with RB Buffer (supplied with GeneChip kit).

2.3.12.4 Fragmentation

For the fragmentation step, the thermal cycler was pre-heated to 37°C. 5μl 10x Fragmentation Buffer was added to each sample on ice. The Fragmentation Reagent was diluted to 0.05U/μl in a total volume of 120μl (12μl Fragmentation Buffer and the remainder molecular biology grade H_2O up to 120μl), on ice. 5μl of diluted Fragmentation Reagent was added to the sample plate containing Fragmentation Buffer. A plate seal was used to cover the plate and it was vortexed at medium speed for 2 seconds and then centrifuged briefly at 716 rcf at 4°C. The fragmentation plate was placed immediately in the pre-heated thermal cycler and the following cycling conditions were applied: 37°C for 35 minutes, 95°C for 15 minutes and finally the plate held at 4°C. 4μl fragmented PCR product was mixed with 4μl loading buffer and run on 4% agarose gel (made as described previously) at 120V for 45 minutes.

2.3.12.5 Labelling and target hybridisation

A labelling master mix was prepared on ice containing 1x Terminal deoxynucleotidyl Transferase (TdT) Buffer, 0.857mM GeneChip DNA Labelling Reagent, 1.5U/μl TdT, at a total volume of 19.5μl per sample, and vortexed at medium speed for 2 seconds. 19.5μl of the labelling master-mix was aliquoted into the fragmentation plate containing 50.5μl of product from the fragmentation step. The plate was vortexed at medium speed for 2 seconds and then centrifuged at 716 rcf for 1 minute. The plate was then cycled at 37°C for 4 hours, 95°C for 15 minutes and held at 4°C indefinitely. The plate was again centrifuged briefly at 1500 rcf.

All procedures carried out from this point forward were undertaken at the Institute of Child Health Gene-Array Centre, Institute of Child Health (ICH), London, UK, using solutions specified in Affymetrix protocol, prepared by staff at the centre (consult the Affymetrix manual for details on making up these solutions). A hybridisation cocktail master mix was prepared to a total volume of 190ul containing 0.056M 2-(N-Morpholino) ethanesulfonic acid (MES) (1.25M), 5% dimethyl sulphoxide (DMSO) (100%), 2.5x Denhardt's Solution (50x), 5.77mM EDTA (0.5M), 0.115mg/ul

Herring sperm DNA (10mg/ul), 1x Oligo Control Reagent, 11.5ug/ml Human Cot-1 DNA (1mg/ml), 0.0155% Tween-20 (3%) and 2.69M TMACL (5M).

Each 70μl labelled DNA sample was transferred from the plate to a 1.5ml Eppendorf tube and 190μl of hybridization cocktail master mix aliquoted into the same tube. The 260μl mixture was heated at 99°C in a pre-heated heat block (a stationary Eppendorf Thermomixer was used) for 10 minutes to denature the DNA and cooled on ice for a maximum of 10 seconds. The tubes were centrifuged at 400 rcf in a microcentrifuge and placed at 49°C for a minute. The solution was mixed by pipetting to ensure any precipitate was properly dissolved and then 200μl injected into each GeneChip array. Arrays were hybridised in Affymetrix Hybridisation Oven 640 at 49°C for 16 hours at 60 rpm.

2.3.12.6 Washing, staining and scanning

The Fluidics Station 450 was set-up according to manufacturer's guidelines to run the GeneChip arrays. Buffers Wash A (non-stringent wash buffer), Wash B (stringent was buffer), Stain Buffer and 1x Array Holding Buffer were prepared by staff at the ICH Gene-Array Centre according to the Affymetrix protocol. Each array was filled with 250μl Array Holding Buffer. For each Fluidics module, 495μl Stain Buffer was mixed with 5μl Streptavidin Phycoerythrin (SAPE) (1mg/ml) in an Eppendorf tube and placed in sample holder 1; 495μl Stain Buffer mixed with 5μl biotinylated antibody (0.5mg/ml) was placed in sample holder 2 and 800μl Array Holding Buffer was placed in sample holder 3. The Fluidics wash/stain/scan protocol was run as described in the Affymetrix protocol. Briefly, the protocol involved two post hybridisation washes of the arrays, with non-stringent Wash Buffer A and stringent Wash Buffer B to remove excess labelling and hybridisation reagents. The arrays were then stained with SAPE solution. SAPE contains streptavidin molecules, which bind with high affinity to biotin and therefore will bind biotinylated DNA hybridised to the array, conjugated to the fluorophore phycoerythrin. A post-stain wash with Wash Buffer A removed excess SAPE and a second staining with the biotinylated anti-streptavidin antibody, followed by SAPE solution, was used to amplify the fluorescent signal. A final wash with Wash Buffer A removed any unbound SAPE and the arrays were then filled and held in Array Holding Buffer. Arrays were scanned on a GeneChip Scanner 3000 7G (Affymetrix) and the data stored for analysis using GeneChip DNA Analysis Software (Affymetrix).

2.3.12.7 Array data analysis

GeneChip array intensities were converted into genotype calls and call rates assessed using the Affymetrix GeneChip DNA Analysis Software (GDAS) at various rank score thresholds (see Chapter 6). Concordance/discordance data for replicate or pseudo-replicate chips were generated

using HelixTree (Golden Helix). Pairwise LD comparisons were conducted by importing data from Affymetrix Genotyping Analysis Software (GTYPE) into Haploview.

2.3.13 Quantitative real-time PCR

Allele discrimination reactions for SNP genotyping were performed as follows. Initially 15μl volume reactions were used. A quantitative real-time PCR (qPCR) master-mix was prepared on ice consisting of 8μl QuantiTect Probe PCR Master Mix (2x) (Qiagen), 0.3μl forward primer (50pmol/μl), 0.3μl reverse primer (50pmol/μl), 0.65μl SNP probe allele A (5pmol/μl), 0.65μl SNP probe allele B (5pmol/μl) and 4.1μl dd.H_2O. 14μl qPCR master-mix was aliquoted using a Gilson Distriman repeater-pipette into a MicroAmp Optical 96-well Reaction Plate on ice and 1μl genomic DNA (~50ng/μl) added. Work by colleagues within the MRC Prion Unit had suggested that efficient allelic discrimination could be achieved with total reaction volumes of 5μl and therefore in the latter part of my work the following small-volume qPCR master-mix was used, on ice: 2.5μl QuantiTect Probe PCR Master Mix (2x), 0.09μl forward primer (50pmol/μl), 0.09μl reverse primer (50pmol/μl), 0.2μl SNP probe allele A (5pmol/μl), 0.2μl SNP probe allele B (5pmol/μl) and 0.92μl dd.H_2O. 4μl the qPCR master-mix was aliquoted into a MicroAmp Optical 96-well Reaction Plate on ice and 1μl genomic DNA (~50ng/μl) added.

Plates were sealed using MicroAmp Optical Adhesive Seals with particular attention paid to sealing around the edges of the plate to prevent evaporation. Plates were then vortexed briefly at medium speed for 2 seconds and pulse centrifuged at 3000 rcf. Plates were run on an ABI 7000 Sequence Detection System (Applied Biosystems), following the manufacturers protocol. A rubber evaporation mat supplied with the machine was used to prevent evaporation. Cycling conditions were: 95°C for 10 minutes, 40 cycles of 94°C for 15 seconds and 60°c for 1 minute.

Copy number assays were conducted in a similar manner to allelic discrimination assays but run in triplicate in 25μl reaction volumes, unless otherwise stated. The major differences in protocol are as follows: A qPCR master-mix was prepared containing 12.5μl QuantiTect Probe PCR Master Mix (2x), 1μl SNP *PRNP* probe (5pmol/μl), 1μl SNP *βActin* probe allele B (5pmol/μl), 0.45μl *PRNP* forward primer (50pmol/μl), 0.45μl *PRNP* reverse primer, 0.1μl *βActin* forward primer (50pmol/μl), 0.1μl *βActin* reverse primer (50pmol/μl), and 7.4μl dd.H_2O. The master-mix was aliquoted into a MicroAmp Optical 96-well Reaction Plate or a MicroAmp Fast Optical 96-well Reaction Plate as previously described, and run following manufacturers guidelines on an ABI 7000 Sequence Detection System or ABI 7500 Sequence Detection System, respectively. Data was analysed using ABI Sequence Detection Software v1.3.1 (Applied Biosystems).

2.3.14 Linkage disequilibrium analysis and "tagging" SNP selection

Linkage disequilibrium between SNPs was calculated and visualised using the freely available program, TagIT (Goldstein *et al.*, 2003a; Weale *et al.*, 2003) (http://popgen.biol.ucl.ac.uk/software.html). Methods outlined in the associated User's Guide were followed and the supplied matrix converter was used to convert SNP genotypes into a binary matrix. Briefly, SNP genotypes were imported into the TagIT matrix converter and modified using the convention 1=major allele and 2=minor allele for each locus in the CEPH population and 0 for missing genotypes. All subsequent allele assignments in additional populations were identical to those in the CEPH to ensure that each allele was represented by the same binary number in all populations. For trio data, TagIT was used to identify deviations from Mendelian inheritance using the "*checkM(M)*" command, as a safeguard against genotyping errors. Genotypes at each locus were checked for deviations from HWE which, although may often be caused by gene mutation, gene migration, genetic drift, non-random mating or natural selection (Hosking *et al.*, 2004), may also be caused by sampling or genotyping errors. Non-significant χ^2 values (χ^2 >3.841, p>0.05) indicated consistency with HWE.

Haplotypes were inferred directly for trio data using the "*EMtrio*" function, with EM algorithm parameters as default: haplotypes returned with an estimated minimum frequency ("*limit*" parameter) of 0.5% and with a frequency difference of less than 10^{-6} for any haplotype between one EM iteration and the next. Haplotypes were cropped to those with an estimated frequency ≥1% and the remaining haplotype frequencies were summed to one. Linkage disequilibrium patterns were detected and presented using the TagIT graphical output for D' and r^2. The Fisher's Exact test *P*-values for 2x2 tables was invoked using the "*EMpairP*" command specific for EM estimated haplotypes and visualised in a graphical format to statistically correlate non-random association between SNPs.

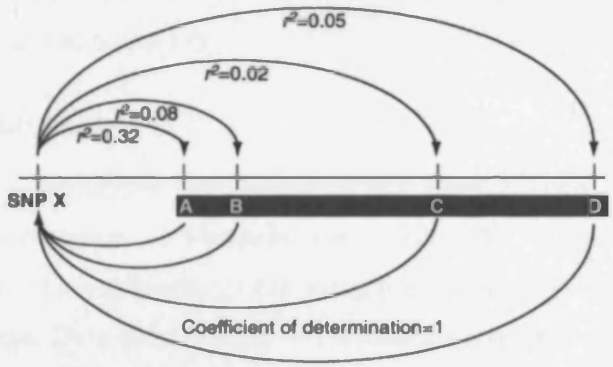

Figure 2.3 The principle of haplotype tagging

SNPs A,B,C and D are tSNPs for a genomic region. As shown none of the tSNPs has a pairwise r^2 against SNP X, however SNP X is perfectly predicted by the haplotype r^2 criterion or coefficient of determination. (Modified from Goldstein *et al.*, 2003a).

A minimal set of SNPs, or "tagging" SNPs (tSNPs), sufficient to represent a level total genetic diversity in a gene region was identified using the following TagIT routine: Criterion 5 was used to assess the performance of tSNP sets as this criterion was recommended by the authors as the best to use to identify tSNP sets to be used in future association studies (see TagIT User's Guide). TagIT uses a direct approach to identify a set of tSNPs which maintain high r^2 values directly with other (Goldstein *et al.*, 2003a) SNPs or a set of haplotypes that do so, however selecting tSNPs based on their pairwise r^2 values with the tagged SNPs (Carlson *et al.*, 2003) has well-documented limitations in that to achieve high r^2 values, the frequencies of the variants must be matched. Using haplotype r^2, or the coefficient of determination resolved by a linear regression of tSNP haplotypes which predict the state of tagged SNPs, can overcome the limitation of pairwise analysis (Figure 2.3). This method also has shortcomings and has reportedly failed to represent SNPs even though the coefficient of determination with tSNPs (or the haplotypes they define) was 1 (Goldstein *et al.*, 2003a). A minimum r^2 threshold was chosen at the 0.85 level, allowing any tSNP chosen to represent 85% of the detected and undetected variation.

Using crit=5 and an r^2 threshold of 0.85, the "best" set size *H* SNPs was determined so that the set *H*+1 did not greatly increase the performance of the "best" against excluded loci, as described in (Goldstein *et al.*, 2003a). Briefly, the performance of a set of tSNPs against excluded loci can assess how well the set represent as yet undetected SNPs. If **K** is the total number of SNPs identified in the region of interest, **H** the tSNPs identified from **K** and **A** the set of all common SNPs in the region, the issue is how well **H** represents **A.** The "*excludes*" function in TagIT invoked a sub-sampling procedure to determine this: SNPs are sequentially dropped out from the set **K** (to give **K'**) and the performance of tSNPs derived from **K'** is tested for ability to predict the state of each dropped SNP in turn. For large data sets, the "*excludes*" function was too computationally expensive and so alternatively, the "*forward2Bx*" function was used. tSNP sets were also evaluated for performance against known loci without excluding loci.

2.3.15 Haplotype inference

For unrelated individuals, haplotypes were identified in a phase unknown manner using either: (i) Partition Ligation–Expectation Maximisation (PLEM) (Qin *et al.*, 2002) (www.people.fas.harvard.edu/~junliu/plem/) run using parameters top=0, parsize=2 (Japanese data only) and 1 (West African Data only), buffer=n (population size) and number of rounds=20 and input data file prepared according to published documentation. (ii) SNPHAP (Clayton, 2004) via the online GENEPISE interface at the Archimedes/Wellcome Trust server

(http://archimedes.well.ox.ac.uk/pise/snphap-simple.html), with input data file prepared according to published documentation.

PHASE (version 2.1) (Stephens *et al.*, 2003) (www.stat.washington.edu/stephens/software.html) was used with the following command line parameters: -n, -f1, -S (random seed) and default values for number of iterations (100), thinning interval (1) and burn-in* (100). The random seed was required to initiate the random number generator and was changed for each subsequent run. Adhering to the author's recommendation, each data set was run a minimum of five times to ensure that results were consistent. For obtaining more reliable recombination data the x100 flag was also added, which multiplied the number of iterations, thinning intervals and burn-ins by 100 fold.

Comparison of haplotype inference simulations using PL-EM, PHASE and SNPHAP has been shown to demonstrate a good concordance (Adkins, 2004) although PL-EM performs slightly better under certain circumstances (Goldstein, pers. comm.). Unless otherwise stated, haplotype inference was achieved using PL-EM data and using SNPHAP and PHASE to assign allelic states to loci unspecified by PL-EM.

2.3.16 Human and mouse cytoplasmic dyneins nomenclature, map positions and sequences

Cytoplasmic dynein nomenclature was collated using literature searches of the Human Genome Nomenclature Committee (HGNC) database (www.gene.ucl.ac.uk/nomenclature/), the National Library of Medicine database, PubMed (www.ncbi.nlm.nih.gov/entrez/query.fcgi?db=PubMed); searching the Mouse Genome Informatics (MGI) database (www.informatics.jax.org/), the single-query interface Locus-Link available at NCBI (www.ncbi.nlm.nih.gov/) and all aliases recorded in sequence submissions to the GenBank and Entrez sequence databases (Wheeler *et al.*, 2003).

Human and mouse chromosomal locations were obtained from the literature and from the MGI and LocusLink databases. Nucleotide and protein sequences (prefix NM_ and NP_ respectively) were NCBI Reference Sequence (RefSeq) and UniProt/Swiss-Prot accession numbers (Wheeler *et al.*, 2003) drawn from the primary sequence database GenBank using the Entrez query interface (www.ncbi.nlm.nih.gov/Entrez/index.html).

2.3.17 Human/mouse homology searches

Homology searches of human and mouse genes for paralogy and orthology were conducted using Position Specific Iterative BLAST (Altschul *et al.*, 1997) at NCBI (www.ncbi.nlm.nih.gov/BLAST.

* A burn-in is the portion of the Markov Chain algorithm (implemented in the PHASE software) that is discarded before a stationary distribution is reached.

The PSI-BLAST program identifies families of related proteins using an iterative BLAST procedure (Altschul *et al.*, 1997). In an initial search, a position specific scoring matrix (PSSM) is constructed from a multiple sequence alignment of the highest scoring hits. Subsequent iterations using the PSSM are performed in a new BLAST query to refine the profile and find additional related sequences. Nucleotide and protein sequences of known genes were used through PSI-BLAST to query the human and mouse non-redundant (nr) sequence databases at GenBank, using default parameters and the BLOSUM-62 substitution matrix, the most effective substitution matrix to identify new members of a protein family (Henikoff *et al.*, 1993). Where protein isoforms were present, the longest sequence was used to search the databases. Homology searches to identify conserved non-coding sequences were conducted using MultiPipmaker (http://pipmaker.bx.psu.edu/cgi-bin/multipipmaker) (Schwartz *et al.*, 2000).

2.3.18 Phylogenetic analyses of the cytoplasmic dynein genes

Homologous sequences were identified by searching the GenBank non-redundant protein database, with the human protein using PSI-BLAST with default parameters and the BLOSUM-62 substitution matrix. Searches of pufferfish sequence *Takifugu rubripes* were performed using the BLAST (TBLASTN) feature at the Ensembl Fugu Genome Browser (version release 2.0; www.ensembl.org/Fugu_rubripes), searching with human protein sequence against a translated nucleotide database.

Protein sequences were aligned for comparison across their full-lengths using the multiple sequence alignment program CLUSTALW (Thompson *et al.*, 1994) (www.ebi.ac.uk/clustalw/) applying the GONNET250 matrix as default, allowing 250 accepted point mutations per 100 amino acids using scoring tables based on the PAM250 matrix (Gonnet *et al.*, 1992).

Two different phylogenetic methods were used to analyse the dynein gene family alignments. Maximum-likelihood trees were inferred under the Jones, Taylor, and Thornton (JTT) empirical model of amino-acid substitution using PHYML (Version 2.4.3;(Guindon *et al.*, 2003)), as was non-parametric bootstrapping* using 100 resampled alignments for each gene family. Bayesian analyses were performed using MrBayes (Version 3.0) (Ronquist *et al.*, 2003), using the default Bayesian priors on tree topologies and branch lengths. Two different sets of analyses were performed for each gene family, the first allowing the Markov-chain Monte-Carlo algorithm to move between the 11 different amino-acid substitution models available in MrBayes, and another specifying the JTT

* Bootstrapping is a method for testing the reliability of a dataset. It involves the creation of pseudoreplicate datasets by resampling of the original. The frequency with which a given branch is found is recorded as the bootstrap proportion and can be used as a measure of the reliability of branches in the optimal tree.

model. The first analysis allowed the chain to take into account uncertainty in the substitution process. For all analyses performed, the posterior probability of the JTT model was at least 99%, confirming that this model best describes the evolution of the dynein sequences. Only results from the fixed-JTT model analyses were used.

For each analysis, three chains of 1,000,000 generations each were run, sampling parameters every 100 generations and discarding the first 100,000 generations as a burn-in period. Running these multiple independent chains allowed visual confirmation that the chains had reached a stationary state by ensuring that all three chains were moving around a region of similar likelihood. In all cases, the majority rule consensus of the posterior sample of tree topologies from all three Markov chains was used and trees drawn using TREEVIEW (Page, 1996) with posterior clade probabilities and maximum-likelihood bootstrap values shown for each clade on these trees.

2.3.19 *PRNP* codon 127 statistical analysis

Analysis of F_{ST} was performed with SPAGeDi. The age of the G127 polymorphism was estimated using the formula in (Risch *et al.*, 1995), as corrected by (Colombo, 2000): for a given marker, the age in generations (g) is estimated from g = log(delta) / log(1 - theta) where, if p_D is the frequency of a specified allele on V carrying chromosomes and p_D the frequency on G carrying chromosomes, delta = (p_D - p_N)/ (1 - p_N). 13 micro-satellites were genotyped for this analysis: of these 4 were uninformative and one was excluded because of doubt over the genetic distance between this marker and *PRNP*. The median results for the remaining 8 markers was used as the point estimate of age, and provide confidence intervals based on 10000 bootstraps of the data (Efron, 1993).

2.3.20 Miscellaneous software

DNA sequence was translated into protein sequence in all six reading frames using the program Translate (http://us.expasy.org/tools/dna.html) at the online proteomics server, ExPASy. Genomic DNA, mRNA and protein sequences were retrieved from NCBI (www.ncbi.nlm.nih.gov/). HapMap data was downloaded from www.hapmap.org. Power calculations were calculated using Genetic Power Calculator at http://pngu.mgh.harvard.edu/~purcell/gpc/.

3 Mutation screening of *DYNC1H1*

3.1 Introduction

The research detailed in this chapter investigates the candidate gene *DYNC1H1* for motor neuron disease associated variation. The paucity of information available on human *DYNC1H1* and the recent publication of high quality human genome sequence, dictated that the initial work required for identifying disease associated variants was to elucidate the genomic architecture of *DYNC1H1*, using *in silico* methods. The localisation of *DYNC1H1* to chromosome 14q32.32 on human genome contig AL118558 and identification of a 78-exon structure is the first work presented in this chapter, and these data informed much of the later work in this chapter and subsequent chapters. The 86.6kb locus of *DYNC1H1* would have been too costly to resequence in its entirety and so, this chapter concludes with a screen of candidate exons 8 and 13, homologous to those causally mutated in the *Loa* and *Cra1* mouse models of late-onset neurodegeneration, and also intron 13 and exon 14. No variants were identified as significantly associated with motor neuron disease in the regions screened and so this chapter closes with a discussion on the significance of this result and shortcomings of this technique.

3.2 Determining the genomic structure of the *DYNC1H1* locus in silico

When this study was undertaken in April 2003, little or no published information was available on the genomic architecture of human *DYNC1H1*. With emerging evidence for the importance of this gene as candidate for ALS and other motor neuron diseases, determining the genomic organisation of the gene was paramount. Following the publication of high-quality genomic sequence of human chromosome 14 in February 2003 (Heilig *et al.*, 2003), it became possible to accurately determine the genetic architecture of *DYNC1H1* by *in silico* means: essentially, transcribed *DYNC1H1* sequences collated in sequence databases could be aligned back on to a genomic reference sequence to identify protein-coding sequences (Figure 3.1). The results of this otherwise straightforward experiment were extremely important, primarily for formulating a cost-effective strategy for screening the gene for an association with disease.

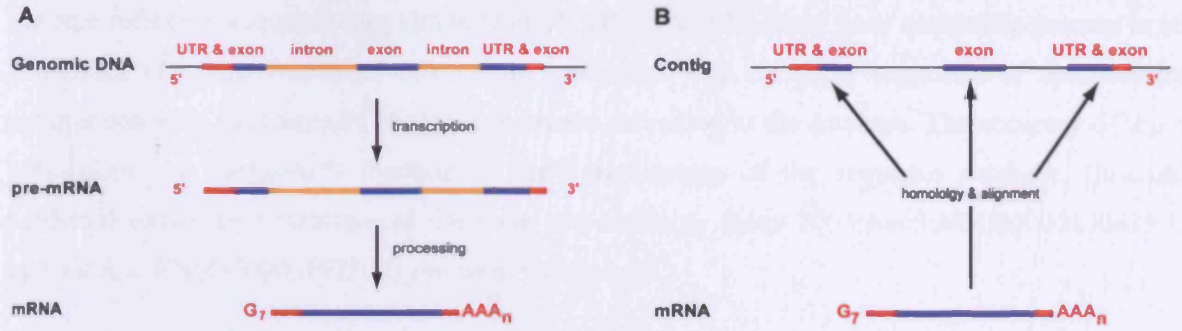

Figure 3.1 Scheme representing the reverse mapping of transcribed sequences onto genomic sequence

A. Transcription and intron splicing of protein coding genes. **B**. In silico identification of exonic sequence using cDNA homology and alignment to a human genome contig.

3.2.1 Information available on the genomic organisation of *DYNC1H1* in 2003

The chromosomal location of human *DYNC1H1* had been known since the publication of work from Narayan and colleagues in 1994, who used fluorescence *in situ* hybridisation (FISH) to locate the gene to the long arm of chromosome 14 (Narayan *et al.*, 1994). Refinement of the chromosomal position to the cytogenetic band 14q32 was published in 2002 (Witherden *et al.*, 2002), but further refinement of gene location, to the resolution of human genome assembly contig and exact sequence, would be needed before elucidating the genomic architecture of *DYNC1H1* could even be attempted.

Cursory information was available however, on the genomic organisation of *DYNC1H1* at two public sequence repositories and genome browsers, NCBI and Ensembl, but the data available were neither comprehensive nor conclusive. For example, comparing NCBI RefSeq* entries for *DYNC1H1* coding sequence (Acc: NM_001376), between April 2003 (GI† 29788997) and May 2006 (GI 94557306) illustrates the paucity of sequence information available in 2003, as compared to the current state of the database: A 443% increase in coding sequence length is seen between the two *DYNC1H1* RefSeq entries, increasing the available cDNA sequence from 3210 bp to 14229 bp (full-length).

The Ensembl database and genome browser (release 16; May 2003) did provide some useful information on predicted *DYNC1H1* genomic organisation. Ensembl is a stable genome database with the capability of annotating known genes and predicting novel genes against the human

---

* RefSeq or **Ref**erence **Seq**uence, is a database that provides a biologically non-redundant collection of DNA, RNA, and protein sequences. Each RefSeq represents a single, naturally occurring molecule from a particular organism is a synthesis of information, not a piece of a primary research data in itself.

† GI or GeneInfo **I**dentifier is a unique sequence identification number for a nucleotide sequence. Every time a change is made to a sequence, a new version of the sequence is produced and a new GI number is assigned. GI numbers are not changed after changes to sequence annotation)

genome reference sequence (see Hubbard *et al.*, 2002). The Ensembl gene annotation process is an automated one, based upon *ab initio* gene predictions that are either supported or modified by comparison with experimental sequence evidence submitted to the database. The accuracy of these predictions are therefore a function of the completeness of the sequence database. Ensembl predicted exon/intron structure of the gene was available (May 2003;Acc:ENSG00000100839.1, current Acc:ENSG00000197102) and used for analysis.

3.2.2 Fine-scale localisation of *DYNC1H1* to the human genome, chromosome 14 assembly

The initial step in determining the genomic architecture of *DYNC1H1* was to localise the gene at the resolution of DNA sequence, on the Human Genome Project assembly (human genome build 33; April 2003). The genome assembly DNA sequence would provide a reference to compare transcribed sequences against and allow annotation of the genomic architecture of the gene.

At the time, no full-length human cDNA or overlapping cDNA clones had been published for *DYNC1H1* but full-length mouse cDNA (*Dync1h1* Acc: AY004877) and human protein sequence (DYNC1H1 Acc: NP_001367) were both available to conservatively estimate the size of the human gene. The length of the mouse cDNA and reverse translation of the 4646 amino acid human protein both suggested that the size of the human gene was at least ~14 kb. Assuming the human gene contained introns, the gene size was likely to be greater than 14 kb. The mouse *Dync1h1* cDNA sequence was aligned against the human genome using the sequence alignment tool WU-BLAST v2.0, interfaced through Ensembl genome database and browser. The sequence aligned with an average of 92% homology to human bacterial artificial chromosome (BAC) clone AL118558, contained within the chromosome 14 'golden tile path' BAC RP11-1017G21 and RefSeq contig NT_026437, and the cytogenetic location of the gene was found to be 14q32.32 (Figure 3.2).

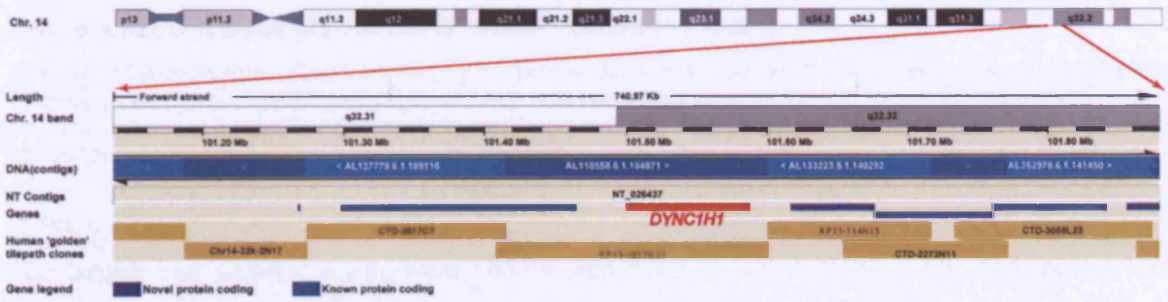

Figure 3.2 Fine-scale localisation of *DYNC1H1* on chromosome 14 (Builds 33 to 36.1)

DYNC1H1 was localised to clone AL118558, within the 'golden' tile path BAC RP11-1017G21, and contig NT_026437at the margin of 14q32.31 and 14q32.32. Adapted from www.ensembl.org/Homo_sapiens.

3.2.3 Identifying *DYNC1H1* exons and introns

DYNC1H1 exons were identified by aligning transcribed gene sequences against human genome contig AL118558 and identifying regions of homology, which were then annotated against the genomic reference (Figure 3.1). In the absence of available full-length human cDNA sequence, full-length cDNA sequences from mouse (Acc: AY004877) and rat (Acc: D13896) were used. The mouse and rat transcribed sequences were specifically chosen as (i) both species are closely related to humans reducing the omission of exonic sequences due to species/sequence divergence and (ii) full-length sequences were available. Sequences were aligned against AL118558 using the web-based alignment program 'BLAST 2 Sequences'. In addition, a number of partial human cDNA sequences (Acc: AB002323, AF234785, LOC196863 and U53530) and expressed sequence tags (ESTs) (Acc: AI418688, AI457261 AI478488, AI497769, AI652200, AI971265, AI991665, AW292121, BE673985, BE701697, BE701780, BE811371, BF062339, BF511560, BF511676, BF515276, BF940018) were aligned against AL118558 (not shown).

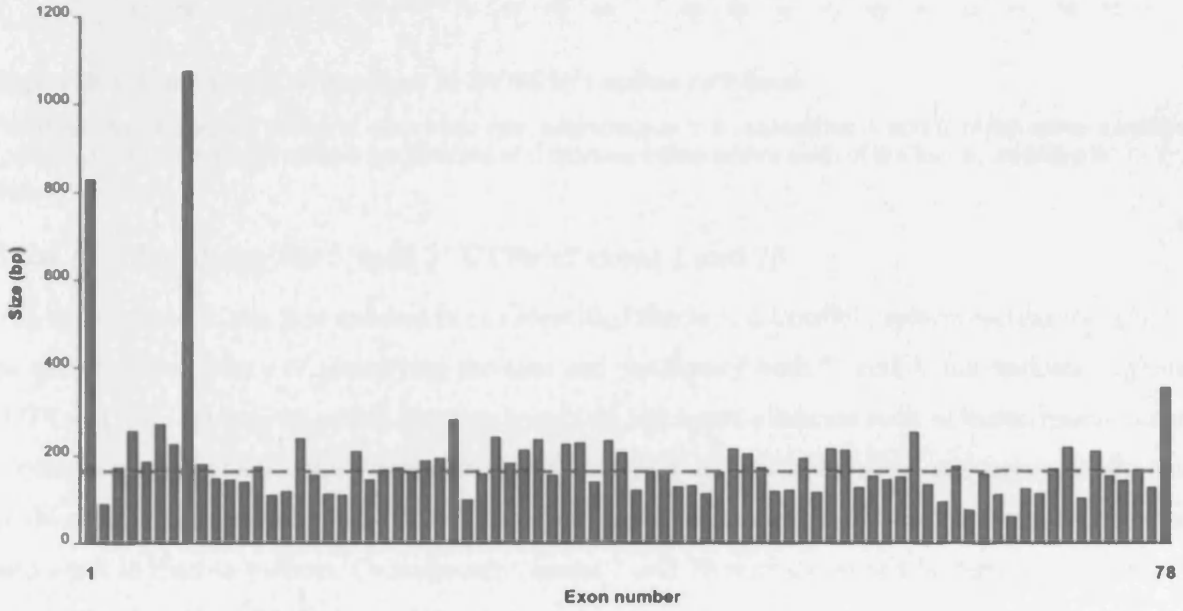

Figure 3.3 Exon sizes across the *DYNC1H1* genomic locus

78 exons of varying sizes were identified by sequence alignment of transcribed human, mouse and rat dynein 1 heavy chain 1 sequences, against human chromosome 14 genome clone, AL118558. Exons are shown in genomic order and exons 1 and 78 include the 5' and 3' UTR sequences respectively. Median exon size was 165bp (broken red line).

In total, 78 putative exons were observed with an average 90% identity between the three species. The largest and smallest exons were 1077bp and 61bp in length (Figure 3.3) and median exon length was 165bp (mean 188bp), which conforms well with the mean exon size observed in the human genome of <200bp (excluding non-coding UTR sequences) (Sakharkar *et al.*, 2004). All 78 exons had near identical alignments between the three species, which provided a high degree of confidence for the result. However, discordance between alignments were repeatedly observed at

intron/exon boundaries, which were easily resolved by inspecting boundary sequences for conserved splice junction motifs* (Figure 3.4).

The *in silico* delineated gene architecture was compared to the predicted exon/intron structure available on Ensembl (accessed April 2003; search term "DNCH1") and all exons corresponded extremely well (data not shown), except exons 1 and 78

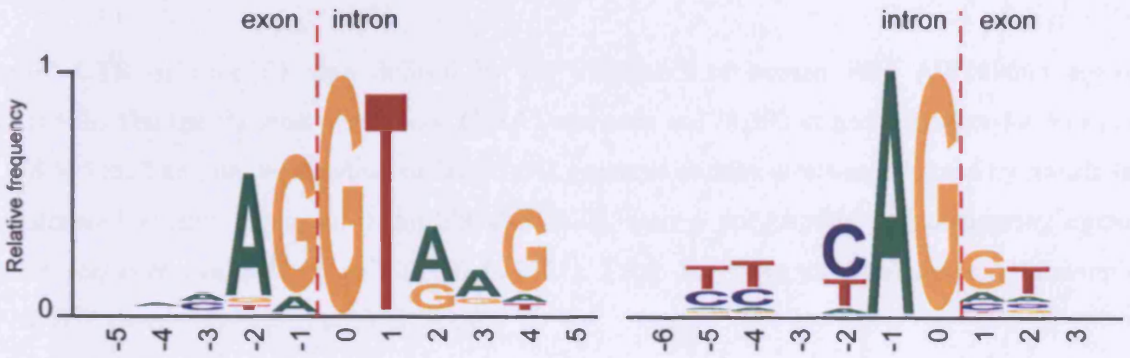

Figure 3.4 Consensus sequences at *DYNC1H1* splice junctions

Relative frequencies are shown at each base pair, extending up to 6 nucleotides 5' and 3' of the splice junction (position 0). Positions with relative frequencies of 0 represent sites where each of the four nucleotides is equally frequent.

3.2.4 Identifying the 5' and 3' UTRs of exons 1 and 78

The discordance of the first and last exons identified above and Ensmbl predictions was thought to be due to the accuracy of identifying the size and position of both 5' and 3' untranslated regions (UTRs). UTRs are regions which commonly encode functional elements such as transcription factor binding sites and cDNA stabilisation sites, and are essential for correct gene expression. Mutations in these regions (especially the 5'UTR) can affect gene dosage and therefore these regions may be important in disease process. Consequently, exons 1 and 78 were examined in detail to ensure that the UTRs were identified in their entirety.

Exon 1 contains the common **ATG** translational start site (TSS) at nucleotide 92,523 of the cDNA, which encodes the first amino acid – a methionine – of the DYNC1H1 protein. The methionine TSS is well represented within a conserved ribosomal binding motif, known as a Kozak consensus sequence (Figure 3.5), named after Marilyn Kozak who first described the sequence (Kozak, 1981; Kozak, 1984; Kozak, 1986). The 5' UTR of exon 1 was delimited to position 91,948 by aligning human EST BF511676 against the genomic sequence. The placement of the 5' UTR was supported by the identification of several common eukaryotic RNA polymerase II elements within the

* consensus sequences of up to 9 nucleotides in which AG/GT is commonly conserved at exon-intron boundaries and AG/G is commonly conserved at intron-exon boundaries; see (Mount, 1982).

sequence: a conserved transcriptional start site or transcriptional initiator (Inr) element was found at position 91,948 and a well conserved downstream promoter element (DPE) was seen at 91,971 nt. In addition two promoter elements, a TATA box motif and CAAT box motif, were seen at positions approximately 30 nt and 80 nt respectively, upstream of the transcription initiation site. The software UTRscan identified two cis-acting elements further upstream of the Inr, including an internal ribosome entry site (IRES), both of which are involved in cDNA stabilisation and translational control.

The 3' UTR of exon 78 was defined by the alignment of human EST AW249663 against AL118558. The translational stop codon (TAA) was seen at 178,392 nt and polyadenylation signal at 178,605 nt. The final verification of *DYNC1H1* genomic architecture was achieved by translating concatenated exonic sequence, using TRANSLATE, into a polypeptide and comparing against protein sequence available on NCBI (NP_001367). Table 3.1 gives the final genomic location of *DYNC1H1* exons and introns on AL118558.

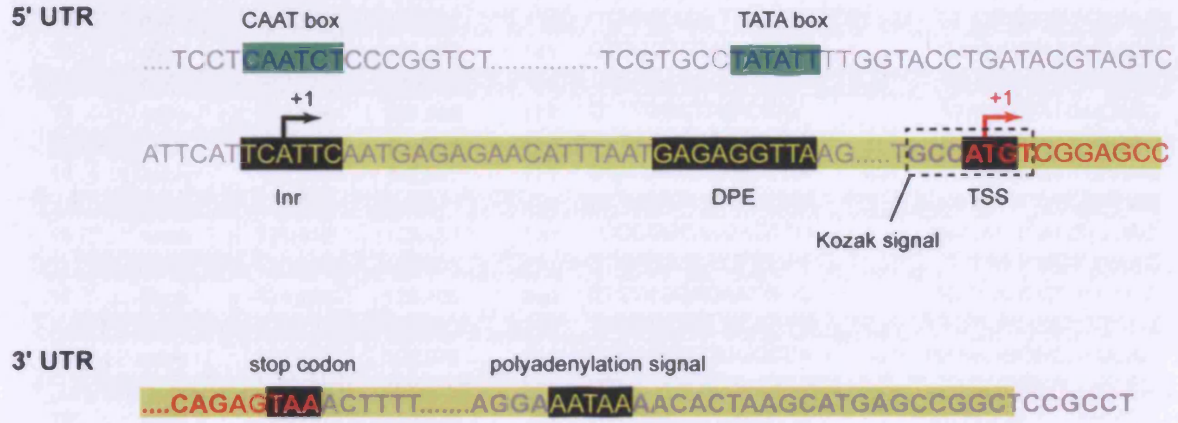

Figure 3.5 *DYNC1H1* UTR sequences and conserved motifs

Coding sequence shown in red and UTRs highlighted in yellow. 5' UTR extends to the transcription initiator (Inr; +1 position), position 91,948 on AL118558, encompassing the downstream promoter element (DPE) at 91,971 and translational start site (TSS) at 92,523.

Exon/intron number		AL118558 pos* (bp)		Size	Sequence		
		Start	End	(bp)	5'		3'
1	5' UTR	91,948	92,778	830	TTCAATGAGAGAACA	...	GCTCCACGCTCAAAG
	intron	92,779	103,542	10764	GTGCGGGGCCGCGGA	...	TATTATGATTTGTAG
2	exon	103,543	103,630	88	AGGACGTCGGTGATG	...	GGTTAAATCCAATAG
	intron	103,631	107,149	3,519	GTGAGTAGTACAAAT	...	TATTTTTCTTTTTAG
3	exon	107,150	107,323	174	CTTGGCATTCATTAA	...	TGGCAAGGCAGACAG
	intron	107,324	107,549	226	GTAAAAACTGTGGTT	...	GAAATCTGTTTTTAG
4	exon	107,549	107,805	256	GGATGGTGATAAAAT	...	CGAGAAATTCAAAAA
	intron	107,806	108,194	389	GTAAGAGCACAGGAT	...	ATTTTATTTTCAAAG
5	exon	108,195	108,381	187	GTGACCAAACTGGAT	...	TTGACACTGACACAG
	intron	108,382	110,849	2,468	GTAACAACTAGAACT	...	TCTCTGTTAATATAG
6	exon	110,850	111,121	272	GTCTAAAACAGGCTT	...	GAAGAATTTGAAAAA
	intron	111,122	111,212	91	GTAAGTTTGAATATA	...	GAAATTATATCCTAG
7	exon	111,213	111,440	228	GTTATGGTAGCATGC	...	GTCCTGAGGCCACAG
	intron	111,441	113,517	2,077	GTAAGATTTGCATTC	...	ATCTTTCTCCTTTAG
8	exon	113,518	114,594	1,077	GTCACGGCAGTTGCA	...	AACTTCCAAGAAAAG
	intron	114,595	115,283	689	GTATGCTCTCATGTA	...	TATTTCTTCCTTCAG
9	exon	115,284	115,463	180	GTGGATGATCTGCTG	...	AAGCTTGACATGGAG
	intron	115,464	116,533	1,070	GTAAGGGATAGAATT	...	TAACGTTGTCTGTAG
10	exon	116,534	116,683	150	ATTGAAAGAATATTG	...	GAGCCAAAGATCAAA
	intron	116,684	119,357	2,674	GTGAGTGCTTCTGTG	...	ACCTTTCTTTCACAG
11	exon	119,358	119,504	147	AATGTCGTTCATGAG	...	AGTCAGAGGTACCAG
	intron	119,505	122,014	2,510	GTAAGCCTTTGGTGA	...	GCTTTGGTTGGCTAG
12	exon	122,015	122,155	141	GTGGGTGTACATTAC	...	GAACAGTATGTCAAG
	intron	122,156	122,503	348	GTAAGAAACTCCTAA	...	GTTCTTCATTTGCAG
13	exon	122,504	122,680	177	GTTTGGCTTCAGTAT	...	ATAGATTATGGCAAG
	intron	122,681	122,816	136	GTGAGCCCTGCTGTC	...	CTATTTCACCCTCAG
14	exon	122,817	122,927	111	GTACAATCTAAGGTG	...	TCCCAGATCTCAAAG
	intron	122,928	123,011	84	GTGAGGACATAGGAT	...	CCTCTCTCTGAACAG
15	exon	123,012	123,131	120	TCCCGCCAAGAGTTG	...	GAGAAGCAAGTTGAG
	intron	123,132	124,865	1,734	GTGAGCTCTGTGCAT	...	TTTTAACTCTCAAAG
16	exon	124,866	125,105	240	CTCTACCGCAATGGC	...	ACCAAGCCTGTCACG
	intron	125,106	127,819	2,714	GTGAGTCCCGCCAGG	...	TCTGACTGCTTTCAG
17	exon	127,820	127,975	156	GGCAACCTTCGCCCA	...	GAAGAGCGCGTGCAG
	intron	127,976	128,116	141	GTATGAACCACTGGG	...	TATTCTCAATCGCAG
18	exon	128,117	128,230	114	GTGGCCTTAGAAGAA	...	GTACAGCCTCGAAAG
	intron	128,231	128,784	554	GTATATCATGAAATC	...	TGTTTCTCTCGACAG
19	exon	128,785	128,895	111	CTTCGACAAAATTTG	...	AAAGGTTACATGAAG
	intron	128,896	128,975	80	GTAGGTGGCCAGTAT	...	TTACTTTCTCCACAG
20	exon	128,976	129,185	210	ATAAATATGCTGGTG	...	GAATTTTTGAAGCAG
	intron	129,186	129,365	180	GCGAGTAATAGGACT	...	CTGGTTTGAATTCAG
21	exon	129,366	129,512	147	ATAAGAGAAGTGTGG	...	TCTCCGTATTACAAG
	intron	129,513	130,367	855	GTGCTGTTGCTGGGG	...	CTGTCTGCCCACCAG
22	exon	130,368	130,534	167	GTTTTTGAAGAGGAT	...	CCAGCGGTTTCAGAG
	intron	130,535	130,622	88	GTATGGCCTCCAGCC	...	TAATTTCATTTGTAG
23	exon	130,623	130,796	174	CATCAGCACTGAGTT	...	GTCATCTTTCCCCAG
	intron	130,797	132,348	1,552	GTAAGATCCTTGCTT	...	TTATTTTAATTTTAG
24	exon	132,349	132,514	166	GTTCTATTTTGTGGG	...	CGGGAAGGAGAGGAG
	intron	132,515	132,592	78	GTAAATTTATGTTCG	...	TTGTATTTATTTCAG
25	exon	132,593	132,781	189	GTTATGTTTAAAACT	...	ATTGATAAATACCAG
	intron	132,782	132,872	91	GTAATCTATAGTAGA	...	TTCTGTGTCTTTCAG
26	exon	132,873	133,067	195	GCCCAGCTTGTGGTT	...	AAGCTAGAACACTTG
	intron	133,068	133,718	651	GTTAGTCTCACACCT	...	ACTCTCTTTCTTCAG
27	exon	133,719	134,001	283	ATTACAGAGTTGGTT	...	GGGGTTCCCCATTTG
	intron	134,002	134,838	837	GTAAGTTCTTCCACA	...	CTTTTCTTTAAACAG
28	exon	134,839	134,939	101	GACCTGCTGGAACTG	...	ACCTTTGATTTCCAG

Exon/intron number		AL118558 pos* (bp)		Size	Sequence		
		Start	End	(bp)	5'		3'
	intron	134,940	136,008	1,069	GTGAGACACTTTATG	...	TCCTCTCCTTTCCAG
29	exon	136,009	136,168	160	GCAATGGGCCGGATC	...	CCAACTACGACAAGA
	intron	136,169	137,673	1,505	GTAAGACACCTCTTC	...	TCATCTCATTCTCAG
30	exon	137,674	137,917	244	CCTCTGCCCCCATTA	...	CGTCCCGTTTTTTAA
	intron	137,918	138,106	189	GTAAGTAGCCTAGAA	...	TTTCTTCTTTTCTAG
31	exon	138,107	138,290	184	ACTATGCGATGAGCA	...	CTCCCTGAACAAGAG
	intron	138,291	138,570	280	GTTCGTTACAAACGT	...	GCCCTCTCCCCGTAG
32	exon	138,571	138,783	213	ATTCTGATACAGAGC	...	ATGTGGGTTGAAAAG
	intron	138,784	139,705	922	GTAACTTGGATTGTT	...	TGTTGGGCCCTGCAG
33	exon	139,706	139,944	239	GTTCTCCAGCTCTAT	...	ACACGTGCTGAGAAA
	intron	139,945	140,144	200	GTACGTCTTCTTTGA	...	ATCCTTCCCAACCAG
34	exon	140,145	140,301	157	GATCATCGACAGCGT	...	AGTCTTCCACCCAAT
	intron	140,302	142,935	2,634	GTAAGTAGCCTTTTG	...	ATGTTTTCTTTCAAG
35	exon	142,936	143,163	228	GTGAGAATAATGTTT	...	TCCCCCATGCTGCAG
	intron	143,164	143,686	523	GTACGCCCAGGTGGG	...	CCTTCCACTTTCTAG
36	exon	143,687	143,917	231	ATCCAAAGAGATGCA	...	GAGCGCTACATTCAG
	intron	143,918	144,179	262	GTCAGGGGGCATCAG	...	TTCCCTTTTTAATAG
37	exon	144,180	144,320	141	CGATATCTGGTTTAT	...	ATTATCGATTATGAG
	intron	144,321	144,596	276	GTGAGCATGCAGCTA	...	CATCTCCGTGTGTAG
38	exon	144,597	144,830	234	GTGTCCATCAGCGGA	...	TTGCCTGACATGGAG
	intron	144,831	144,918	88	GTAAAGAGGCCAGGA	...	GTCTTCCCTCCAAAG
39	exon	144,919	145,125	207	GTGGTGGGTCTCAAC	...	TCCTTCATCAGACAG
	intron	145,126	145,213	88	GTTTGTTTCTATCCA	...	TGTCCCTTCCTTCAG
40	exon	145,214	145,335	122	ATGGTGGAGCACGGA	...	GCCCCTCTCACACAG
	intron	145,336	146,281	946	GTAAAACAGCTCGGT	...	GCTATCTGTGCACAG
41	exon	146,282	146,447	166	GTTCCTGCGCCACGT	...	TACACCATGTCTCAG
	intron	146,448	147,723	1,276	GTACGCAGAGTTTCT	...	TTCTCATTGCCATAG
42	exon	147,724	147,887	164	GAGAGATTCACCCAG	...	TCTCTTCCAAGATAG
	intron	147,888	150,581	2,694	GTAAGGGAAGCCGAG	...	CTGCTCTCCCCACAG
43	exon	150,582	150,711	130	ACTCGTAGAGGATGA	...	AACTGGCTGTCAAAG
	intron	150,712	154,404	3,693	GTAGCAAACTCGCAT	...	CCTTTTTTTCTATAG
44	exon	154,405	154,538	134	GATTACATCCCAGTA	...	GCTGAGGATTGACAG
	intron	154,539	155,004	466	GTGGGCTTTTTTGTT	...	CTCGTAATGTTTCAG
45	exon	155,005	155,119	115	AATATTCCGTCAACC	...	GTGTACCAGATTAAG
	intron	155,120	155,213	94	GTGCGTCTGGTCGGT	...	CCTCTGCTTCTGTAG
46	exon	155,214	155,375	162	GTCCATAGGAAGTAC	...	CTGGCCAATGGAGAG
	intron	155,376	155,449	74	GTAATTAGGTGACGT	...	TGTGCTGTTTCCCAG
47	exon	155,450	155,664	215	GTGCCTGGTCTCTTT	...	AGCACTTTTCAACAG
	intron	155,665	155,767	103	GTACGTGGGCCTTTA	...	GGGCCTCTTTCTCAG
48	exon	155,767	155,972	205	GTGTGTGTTGAATTG	...	CAGACTCTTCACCAG
	intron	155,973	157,369	1,397	GTGGGTTCAGTTTTG	...	ACTATTTTCTGAAAG
49	exon	157,370	157,543	174	GCGAATGCTCGGCTA	...	GAGACAGTCGACCAG
	intron	157,544	157,649	106	GTGCGTCACAGGCAC	...	GGCTTTGCTCTTTAG
50	exon	157,650	157,769	120	GTAGAAGAACTGCGT	...	GCTGAAAAGAAGAAG
	intron	157,770	157,992	223	GTATGGTGTCAGGGA	...	ATCCCTCCTTTCTAG
51	exon	157,993	158,113	121	GTTATGAGCCAAGAA	...	TTGAGGCCCAGAATG
	intron	158,114	160,102	1,989	GTATGTAAAGACTGT	...	CCTGCTGCCACTCAG
52	exon	160,103	160,298	196	CTGTGAAGTCGATCA	...	TGCAGAGGAGATCAG
	intron	160,299	160,895	597	GTGAGAAAGTGGAAG	...	ATTCGTCTTTTACAG
53	exon	160,896	161,013	118	TGACGCCATAAGGGA	...	TGGGCAATTGCACAG
	intron	161,014	161,099	86	GTGATTAACACAGCC	...	ATTGGTTCTTCCCAG
54	exon	161,100	161,315	216	CTTAACTATGCAGAC	...	GCTGTCGAGGCAAAA
	intron	161,316	161,806	491	GTAAGATTATCATCA	...	CGGTTTTCCTTTTAG
55	exon	161,807	162,019	213	GTAAACCGGAGCACT	...	CAAGCCAACATCCAG
	intron	162,020	162,155	136	GTGAGAATCACGGGG	...	GGCCTTGCCTTTCAG
56	exon	162,156	162,283	128	TTCCGTACAGATATT	...	GAAACGATTCAATAG

Exon/intron number		AL118558 pos" (bp)		Size	Sequence		
		Start	End	(bp)	5'		3'
	intron	162,284	164,319	2,036	GTATGAGCTCGGGTG	...	TGGCCTCATCCTCAG
57	exon	164,320	164,473	154	GTATCCGCTGATCAT	...	CCCCTTCTGGTCCAG
	intron	164,474	166,290	1,817	GTTGGTGTTGGCCTT	...	CCGTGTGGAATGCAG
58	exon	166,291	166,437	147	GATGTGGAAAGCTAC	...	ACCCGGGATCCAACT
	intron	166,438	166,528	91	GTAAGGAATGGGACC	...	TACCTATTTTGGCAG
59	exon	166,529	166,679	151	GTCGAGTTCCCACCA	...	TTCTTAAACTTCAAG
	intron	166,680	166,831	152	GTAGGATCTGGACCT	...	TTTTATTCATTTAAG
60	exon	166,832	167,085	254	GGGAATTTCAGCTCC	...	GAGTCCCTCAAGCAG
	intron	167,086	167,242	157	GTGGGTGCCTTGGCC	...	ACTGCTTCCTTTCAG
61	exon	167,243	167,377	135	ATACACTTCTTGTAC	...	AAGGACCTCTTCCAG
	intron	167,378	167,468	91	GTAGAGTGAGGTCCT	...	CTGCTCTTGTCCCAG
62	exon	167,469	167,563	95	GTGGCGTTTAACCGA	...	GAAGGGCACCGTGGG
	intron	167,564	168,066	503	GTAAGAGCACTCACG	...	TTGCACCCTTCGCAG
63	exon	168,067	168,241	175	GGAGCCCACCTACGA	...	GTTCAGGCAGACGAG
	intron	168,242	168,428	187	GTGATTGTTCTCTTG	...	CTATTGTCTCCACAG
64	exon	168,429	168,504	76	CAATTTGGCATCTGG	...	AAGAAACACCTGCAA
	intron	168,505	169,404	900	GTAAGCCCCACTGTG	...	CTGTACCTGTTTCAG
65	exon	169,405	169,565	161	CACCCATTGGCCAGG	...	ATTGTGGGCACAGAG
	intron	169,566	169,843	278	GTAATGTCCTGGTAC	...	CTTCTTTGTTTGCAG
66	exon	169,844	169,955	112	GTGAAGCCCAACACT	...	CTTCAATTGCAATCG
	intron	169,956	170,058	103	GTAAGGATGCTTGAG	...	GTTTCCCTGCACCAG
67	exon	170,059	170,119	61	GCTCTGCAGAAGGCT	...	TGTAAAGTCGGGCAG
	intron	170,120	170,214	95	GTAGGCCTGTTCTCT	...	ACTTTGTGTGTGCAG
68	exon	170,215	170,338	124	GTGGGTGATGCTGAA	...	GAGATCAACCCCAAG
	intron	170,339	170,465	127	GTGGGTGGTTGAAGG	...	GGCGCTCTCCCTTAG
69	exon	170,466	170,579	114	GTGCCTGTGAATCTG	...	TCACGGATATGCAAG
	intron	170,580	171,705	1,126	GTAAGTACCTTGTCC	...	CACTTTCCTCACCAG
70	exon	171,706	171,876	171	TCTCCCAACGAGCGT	...	GATGACACGGCCAAG
	intron	171,877	172,104	228	GCAAGTGTGGGCCAT	...	CTTTTCCTCCCCCAG
71	exon	172,105	172,322	218	GGCAGGCAGAACATC	...	GCCAGATGGCATCAG
	intron	172,323	172,425	103	GTATGCTGCTGCCTG	...	GCACTGGTTTTCTAG
72	exon	172,426	172,529	104	GCGAGAGGAGTTTGT	...	TCCTTACCACACAGG
	intron	172,530	175,647	3,118	GTAGGCAACAAGGAT	...	GGGACTGTGGCCCAG
73	exon	175,648	175,859	212	GTGTGGACATGATCA	...	GTGGAGAATATCAAG
	intron	175,860	176,346	487	GTAGCTGGGAGGGTG	...	TTTGAACGATTTTAG
74	exon	176,347	176,500	154	GATCCTTTGTTCAGG	...	ACGAGCTAGTGAAAG
	intron	176,501	177,270	770	GTGCGTGAGAGGCCG	...	GTGCCTTGGCTGCAG
75	exon	177,271	177,413	143	GGATCTTGCCTCGGA	...	GCCAAGGAGCTAAAG
	intron	177,414	177,544	131	GTGAAGGCGCTCCTG	...	TGCTGCTTTCCACAG
76	exon	177,545	177,713	169	AACATCCACGTGTGC	...	GCTTCGGAGTCACGG
	intron	177,714	177,901	188	GTGAGTGGAGTCTCA	...	GCTTCCGCCTCACAG
77	exon	177,902	178,029	128	GTTTGAAACTTCAAG	...	AAGAAGGCCAGTGTG
	intron	178,030	178,265	236	GTAAGGAGGCACTGC	...	CCTCTGCTTCTGCAG
78	exon	178,266	178,628	363	GTAACCTTACCTGTC	...	CTAAGCATGAGCCGG

Table 3.1 *DYNC1H1* genomic organisation

78 exons of *DYNC1H1* were identified. Exon/intron positions given relative to position on genome contig AL118558. First and last 15 nt of exon/inton sequence is shown. (From Ahmad-Annuar *et al.*, 2003).

3.3 Mutation screening of *DYNC1H1* exons 8, 13 and 14, and intron 13

After determining the genomic architecture of the human *DYNC1H1*, the next step was to screen the gene for variants associated with disease. Detecting mutations by resequencing the entire 86.6 kb genomic locus was cost-prohibitive and therefore regions of the gene had to be prioritised.

3.3.1 Prioritising regions of *DYNC1H1* to screen

Screening a single gene in an association study leaves two further variables that can influence the cost and outcome of the study: the number of samples and the number of amplicons screened. With the effect size of a disease associated mutation in *DYNC1H1* unknown, as many samples as were available were required for screening. Therefore, the number of amplicons had to be minimised to ensure that the study did not exceed that available budget for its completion. This required careful prioritization of regions of the gene that were considered *a priori* to be of importance to disease pathogenesis. It was not feasible to screen all 78 exons of coding sequence for functionally relevant coding changes and conserved domains such as the motor domain were too large to screen in their entirety. The 5' and 3' UTR were considered for screening but the regions that were screened were those which carried mutations in mouse models of motor neuron disease.

Exons 8 and 13, homologous to those harbouring the mouse *Loa* and *Cra1* mutations respectively, were to be screened as a priority. Aligning mouse and human protein sequences AAF91078 and Q14204 using BLAST, indicated that the regions corresponding to mouse and human exon 8 and 13 share 99% and 100% homology respectively. The conservation of amino acids between the two species suggested that mutation of either human exon may also yield a deleterious phenotype similar to that seen in the mouse.

3.3.2 Primer design and sequencing of exons 8 and 13

Primers for PCR amplification and sequencing were designed to incorporate coding sequence, splice junctions and flanking sequence to ensure that potential mutations producing aberrant amino acid sequence or splicing would be detected. Due to the small size of exon 13 (177 bp) it was possible to include exon 14 and the intervening intron 13, within a single PCR amplicon and sequencing reaction. Exons were sequenced in both forward and reverse orientation and sequences were checked for mutations by eye.

3.3.3 Patient samples screened for *DYNC1H1* mutations

DNA from the FALS, HSP and SMA patients screened in this study was collected with informed consent by Professors Karen Morrison and Pamela Shaw and Dr Richard Orrell. All samples collected were of UK residents although for the majority of samples, ethnicity was not known. In

order to eliminate the possibility that a potential mutation in the case samples was actually a polymorphism found at low frequency in the Caucasian population, 100 unrelated CEPH individuals were screened as controls. Prior to the screening of any samples, ethical approval for research was obtained from the Central Office for Research Committee Ethics, London, UK.

3.3.4 Mutation screening of exon 8

Exon 8 coding sequence, splice junctions and flanking sequence were sequenced in a panel of 170 FALS, 31 HSP and 26 SMA patient samples, and 100 CEPH control samples. One synonymous A/G variant was found at the third base pair of codon 836, encoding alanine (A836) (Figure 3.6). The SNP was found in a heterozygous state in two FALS samples and also in a single control sample, with minor allele frequencies (MAF) 0.6% in cases and 0.5% in controls.

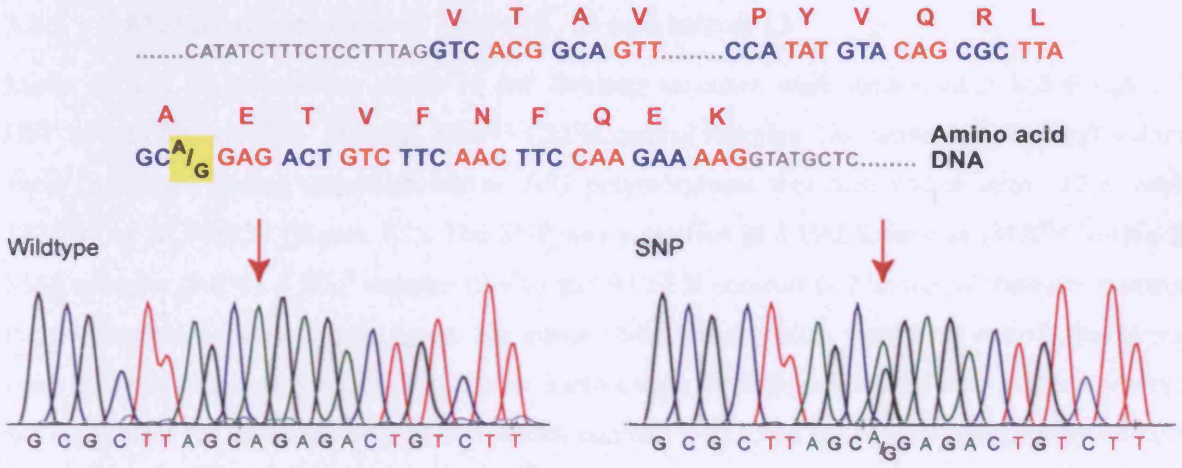

Figure 3.6 Exon 8 A/G synonymous SNP

Top. Exon 8 genomic sequence was screened for mutations including flanking intronic sequence (grey) and coding sequence (blue and orange). Position of the A/G SNP is indicated and amino acid translation of the exonic sequence shown above each codon (red).
Lower. Electropherograms of the exon 8 wildtype forward sequence (left) and A/G transition (right) seen in both cases and controls. The A/G SNP was a synonymous change at codon 836, encoding an alanine residue.

Genotypes were observed to be in HWE `in both cases and controls and a Fisher's exact test for the independence of SNP frequency in cases compared to controls was not significant (Fisher's exact; p=0.1) when all cases were considered together and also, when FALS samples only were tested against controls (Table 3.2).

Samples				Genotype			Allele frequency (%)		HWE	Fisher's exact test
Types		Number (N)	Chromosomes (2N)	A/A	A/G	G/G	A	G		
Cases	FALS	170	340	168	2	0	99.4	0.6	ns	
	HSP	31	62	31	0	0	100	0	-	
	SMA	26	52	26	0	0	100	0	-	
										p=0.10
Controls	CEPH	100	200	99	1	0	99.5	0.5	ns	

Table 3.2 Summary of *DYNC1H1* exon 8 mutation screen, in motor neuron disease patients and controls

The mutation screen was undertaken in a cohort of familial ALS (FALS), familial hereditary spastic paraplegia (HSP) and spinal muscular atrophy (SMA) patients, and CEPH controls. Deviations of genotype proportions from Hardy-Weinberg equilibrium (HWE) and Fisher's exact test between cases and controls were not significant (ns).

3.3.5 Mutation screening of exons 13, 14 and intron 13

Exons 13 and 14, intervening intron 13 and flanking sequence were sequenced in 165 FALS, 32 HSP and 26 SMA patient samples, and 93 CEPH control samples. No variants were found within exon 13 and 14 coding sequences but an A/G polymorphism was seen within intron 13 at base 122,704 of AL118558 (Figure 3.7). The SNP was identified in 8 FALS patients (MAF= 2.4%), 5 SMA samples (9.6%), 6 HSP samples (9.4%) and 9 CEPH controls (4.8%) and all samples bearing the polymorphism were heterozygous. No minor allele homozygotes were seen and all genotypes were in Hardy-Weinberg equilibrium. Fisher's exact tests for independence of SNP frequency were not significant for the entire case cohort versus controls p=0.83 or for cohorts analysed by disease type (ALS p=0.20; SMA p=0.19; HSP p=0.22 (Table 3.3).

Figure 3.7 Intron 13 A/G SNP

Top. Exons 13 and 14 coding sequence (blue and orange) and intron 13 sequence (grey) were screened for mutations. Position of the A/G SNP identified is indicated and the amino acid translation of the exonic sequence shown above each codon (red).
Lower. Electropherograms of the intron 13 wildtype forward sequence (left) and A/G transition (right) seen in both cases and controls.

Samples				Genotype			Allele frequency (%)		HWE	Fisher's exact test
Types		Number (N)	Chromosomes (2N)	A/A	A/G	G/G	A	G		
Cases	FALS	165	330	157	8	0	97.6	2.4	ns	
	HSP	32	64	26	6	0	90.6	9.4	ns	
	SMA	26	52	21	5	0	90.4	9.6	ns	
										p=0.83
Controls	CEPH	93	186	84	9	0	95.2	4.8	ns	

Table 3.3 Summary of *DYNC1H1* mutation screening of exons 13, 14 and intron 14 in motor neuron disease patients and controls

The mutation screen was undertaken in a cohort of familial ALS (FALS), familial hereditary spastic paraplegia (HSP) and spinal muscular atrophy (SMA) patients, and CEPH controls. Deviations of genotype proportions from Hardy-Weinberg equilibrium (HWE) and Fisher's exact test between cases and controls were not significant (ns).

3.4 Discussion

The results detailed in this chapter describe work to assess the significance of the candidate gene *DYNC1H1* as a causal or susceptibility factor for ALS and/or other motor neuron diseases. At the time that this research began in April 2003, little information was available on the genomic organisation of *DYNC1H1*. The nature of research carried out in the cytoplasmic dynein community has historically focused on examining proteins and expressed sequences of non-human species and so, there existed a paucity of sequence information on the human cytoplasmic dyneins. This consequently impeded initiatives by genome databases such as Ensembl to identify the genomic architecture of predicted and known genes by automated methods. Elucidating the genomic structure of a candidate gene is a problem seldom faced by researchers today, with high quality *in silico* and sequence data readily available in public databases, but establishing the size and structure of a candidate gene to be screened for an association with disease is paramount.

Through comparative sequence techniques (comparing against mouse and rat sequences) *DYNC1H1* was localised to chromosome 14q32.32 and to the human genome assembly on contig AL118558. The gene was found to comprise 78 exons and span 86.6kb. The use of homology to related species allowed the complete gene structure to be elucidated where only a partial structure was seen at on browsers such as Ensembl. A similar technique called "gene builds" has since been implemented by Ensembl as an automated method for identifying and describing genes from 2004 (Curwen *et al.*, 2004). In addition, the availability of additional eukaryotic genome sequences and sequence comparison tools, such as MultiPipmaker (Schwartz *et al.*, 2003), have facilitated the identification of functionally conserved sequences, including putative coding sequences (Morgenstern *et al.*, 2002), and confirm the genomic structure predicted in this chapter was correct.

The final results in this chapter detail the screening of exons 8, 13 and 14 and intron 14 of *DYNC1H1* for mutations associated with various forms of motor neuron disease. Two variants were identified; one in exon 8 and one within intron 13. The exon 8 variant was an A/G transition at low frequency (~0.5%) in both cases and controls and constituted the third base position of an alanine codon (A837). Due to the redundancy of the human genetic code, the SNP does not alter the amino acid composition of the protein - GCA and GCG both code for an alanine - and so a deleterious phenotype in individuals possessing the SNP is unlikely. There was no significant difference in allele frequency of the SNP between cases and controls, and therefore it is likely that this SNP is simply a neutral polymorphism.

The intron 13 SNP was identified in all three disease types and controls, at varying frequencies, which is likely to reflect an ascertainment bias due to sample size. The SNP was an A/G transition which bears no obvious functional relevance as it does not occur at the splice junctions. There was no significant difference in allele frequencies between cases and controls, when cases were compared by disease type or when combined, and genotypes were seen in HWE, suggesting that this SNP is not associated with disease.

3.4.1 Updated SNP information

Since this screen was carried out, information on SNP content of *DYNC1H1* and SNP frequencies has become available at dbSNP. The SNPs discovered in this screen have been identified by other investigators and have been submitted to dbSNP in 2004, with SNP IDs: rs17512054 and rs4900529 for exon 8 and intron 13 respectively. Both SNPs have been validated and frequency information is available. No other SNPs have been discovered in the regions screened in this study except for rs17540908, which is 9bp downstream from rs4900529. This SNP, with a MAF of 0.6%, has not yet been validated and so may be an artefact.

Frequency data available for rs17512054 gives a MAF of 1.4% which is in contrast to the 0.6% and 0.5% we identified in cases and controls. This discrepancy is almost certainly due to differences in populations used as the dbSNP data are generated using a multi-ethnic polymorphism discovery resource panel of 90 samples (PDR90) and a Caucasian population was used in this screen (Collins *et al.*, 1998). Population differences accounting for frequency discrepancies seen for SNP rs4900529, for which a MAF of 4.8% was found for Caucasian controls in this screen compared to a MAF of 14.7% on dbSNP using PDR90. As rs4900529 was genotyped in the HapMap project, population specific frequencies are available and it is clear that in European samples the MAF is 5.8% and in Asian and Sub-Saharan African samples the MAF varies from 27.5% to 19.3%.

Therefore the minor allele frequencies experimentally derived for both SNPs in this screen were similar to the frequencies known for these SNPs in Caucasian populations.

3.4.2 Implications and explanations of a negative screen

The lack of association between the SNPs in exon 8 and intron 13 and FALS, HSP and SMA suggests that these specific SNPs may not be relevant to disease pathogenesis but does not preclude the significance of mutations in *DYNC1H1* to ALS pathogenesis and other motor neuron diseases. There are several caveats to this screen: (i) although the FALS cohort was of a reasonable size, the HSP and SMA cohorts were small, with 32 and 26 individuals respectively. It is possible therefore, that these variants may account for a rare minority of familial SMA and HSP which would not be detected with such a limited sample size. (ii) all three diseases are known to demonstrate genetic heterogeneity and although *SOD1*, *SMN* and *Spastin* mutations had been ruled out in the FALS, SMA and HSP cases respectively, several additional loci which are known to be mutated in familial forms of these disorders, had not been screened. (iii) the study only screened a discrete region of *DYNC1H1* for association with disease. Without an understanding of the extent of LD surrounding these SNPs, this screen can only be considered a direct association study and therefore, regions of the gene not investigated may still harbour disease associated mutations. To investigate the gene in its entirety, the LD pattern spanning the gene was elucidated and an association study conducted.

4 *Cytoplasmic dynein 1 heavy chain 1* association study

4.1 Introduction

Despite screening *DYNC1H1* candidate exons 8 and 13 in a number of familial motor neuron disease cases and controls, no variants associated with disease were found. This chapter extends those previous analyses by using a linkage disequilibrium based association study to investigate the entire *DYNC1H1* genomic locus in an attempt to identify an association with sporadic ALS in a northern European-derived population. 16 SNPs were examined, of which two (rs2251644 and rs941793) were found to be sufficient to tag the majority of haplotypic variation ($r^2 \geq 0.85$). These tSNPs were tested in 261 North American sporadic ALS patients and 225 matched controls but no association with the disease was found. In addition, the genetic diversity of *DYNC1H1* was examined in Japanese and Cameroonian populations to establish the evolutionary history for this gene. This chapter finishes with a brief discussion of the caveats associated with this work and how association studies have changed since this study was initiated.

4.1.1 Mutation screening of large genes can be problematic

As previously described, the genomic locus of *DYNC1H1* spans over 86.6 kb and contains 78 exons. Screening genes of this size for disease associated mutations can be prohibitively expensive and the cost of such a strategy is further multiplied for complex diseases, where mutations are likely to have a small effect size and require, therefore, a large sample size to have an appreciable power to detect a disease-associated mutation. One method for overcoming the limitations associated with mutation screening of large genes is to screen a limited part of the gene instead of screening for all possible mutants, which leads to the question: which region of the gene should be screened? As previously discussed, prior hypotheses based on experimental or bioinformatic data can narrow down a candidate region for screening; for example, the screening of exons 8 and 13 of *DYNC1H1* was based upon known mutations in of the mouse homolog of the gene. No mutations were discovered in this gene and therefore to investigate the entire *DYNC1H1* genomic locus for an association with sporadic ALS, a linkage disequilibrium-based association study was conducted.

4.2 *DYNC1H1* association study design

4.2.1 Evolving resources and methodologies in LD-based association studies influence study design

The *DYNC1H1* association study was designed based on the understanding of case-control association studies and LD mapping available at the time the study was undertaken in 2002. The

paucity of genetic variation data available for *DYNC1H1* in 2002 as compared to today greatly influenced the study design, with much of the preliminary work directed towards describing variation within the gene. Contemporary LD-based association studies are able to exploit large amounts of publicly available data on SNP position and frequency, LD patterns, genotypes in various worldwide populations and even tagging performance – almost none of which was available when this study was initiated. Today, the first stop for the majority of researchers interested in the genetics of complex neurodegenerative diseases are data resources such as The International HapMap Project which, although initiated in 2002, has come to fruition too late to influence the design of this study. The majority of work presented in this chapter was designed and completed before changes in this field had become common place, so many of the techniques and analyses are redundant for today's investigators. In later sections of this chapter, the differences in study design and their effect on success are discussed.

4.2.2 Three phased study design

The *DYNC1H1* study design encompassed three broad phases; discovery, tagging and testing. The goal of the SNP discovery phase was to construct both SNP and LD maps spanning *DYNC1H1* at a density of approximately 1 SNP every 10kb. This SNP density was, at the time, shown to be highly effective for identifying regions of elevated LD whilst representing the true pattern of genomic variation in a region (Dawson *et al.*, 2002; Gabriel *et al.*, 2002; Goldstein *et al.*, 2003a; Reich *et al.*, 2001a). The discovery phase was necessary due to a general deficit of available marker information assigned to SNPs present in the public databases: SNPs lacked (i) validation data, essential for authenticating SNPs, (ii) data on their physical locations and (iii) information on their allele frequencies. The tagging phase was used to identify tSNPs which could efficiently represent variation across the gene. These tSNPs were then taken forward to the test phase, where they were assayed in case and control samples and analysed for association with disease status.

4.2.3 Estimating LD to assess tagging approach feasibility

The absence of *a priori* information on the pattern of LD across *DYNC1H1* at 14q32.32, made it initially difficult to assess how powerful a tagging SNP strategy would be and the level of economy this approach could afford. However, as there is a general relationship of inverse proportionality between LD and recombination distance (Huttley *et al.*, 1999), putative LD across *DYNC1H1* was estimated by considering recombination rates between markers flanking the gene.

The recombination rate was estimated by comparison of genetic and physical maps for the region. Sequence tagged sites (STSs)* flanking *DYNC1H1* were identified using the Genome Database (http://www.gdb.org/gdb; accessed November 2002) and two STS loci, *D14S1051* and *D14S293*, were found approximately 0.2Mb and 0.9Mb upstream and downstream, respectively. Both STS loci had physical map coordinates on the NCBI sequence contig Hs14_10185 and genetic map coordinates on the Généthon chromosome 14 map, which allowed a ratio (i.e. the recombination rate) to be calculated (Table 4.1).

Marker	Map	Coordinate	Units
D14S1051	NCBI contig Hs14_10185	5.2	Mb
	Généthon chromosome 14	137	Kosambi cM
D14S293	NCBI contig Hs14_10185	3.9	Mb
	Généthon chromosome 14	133	Kosambi cM
	Genetic / physical ratio	**3.08**	**cM/Mb**

Table 4.1 Marker information for sequence tagged sites flanking *DYNC1H1*

Physical map coordinates are given in Megabases (Mb) and genetic map coordinates given in Kosambi centiMorgans (cM).

The recombination rate was 3.08 cM/Mb, approximately twice the sex averaged recombination rate for chromosome 14 (1.36 cM/Mb) and almost 3 times greater than genome-wide sex averaged recombination rate (1.13 cM/Mb) (Kong *et al.*, 2002). The high recombination rate did not preclude however, the existence of elevated LD at shorter distances than the 1.3Mb physical distance between the two STS markers – i.e. fine-scale LD (Reich *et al.*, 2001a). Indeed, by considering the STS marker information available in 2006, this estimate is reduced to 2.15 cM/Mb (using *D14S1051* and *D14S272* genetic positions from the Marshfield map; *D14S272* is 0.17 Mb closer to *DYNC1H1* than *D14S293*). Without typing markers at a greater proximity to the gene and across the gene, it was difficult to accurately estimate the extent of LD across the region. Therefore, a SNP map of the region spanning the gene needed to be constructed.

4.2.4 Study power and estimating required sample size

Despite the absence of accurate LD estimates across the gene, power and sample size calculations were conducted using the genetic power calculator of Purcell, Cherny and Sham (http://pngu.mgh.harvard.edu/~purcell/gpc) (Purcell *et al.*, 2003). Calculations were performed with helpful advice from Professor David Goldstein and using the conventional power threshold ≥80%. Without prior knowledge of LD across the gene, *D'* values between 0.8 and 1.0 were used which

* STSs serve as landmarks on the physical map of the human genome, Each is a short DNA segment that occurs only once in the human genome and whose exact location and order of bases are known. Because each is unique, STS markers are helpful for chromosome placement of mapping and sequencing data from many different laboratories.

related to samples sizes varying from 982 to 647 respectively, to achieve 80% power of detection (Figure 4.1).

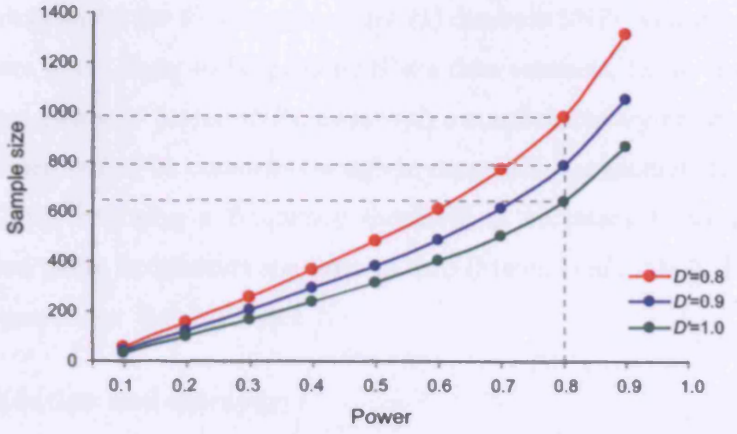

Figure 4.1 *DYNC1H1* association study power and related sample size for varying *D'* values

Expected power was calculated by considering a causal variant under a multiplicative risk model, with genotypic relative risks of 2.0 for homozygotes and 1.41 for heterozygotes, and an allele frequency of 0.1. Alpha (type I error rate) was set to 0.05 and marker allele frequency was set at 0.1. Dashed grey lines indicate sample sizes with 80% power of detection.

4.3 Phase I - SNP discovery

4.3.1 *In silico* SNP ascertainment

Several public SNP databases were used to identify the physical locations of SNPs across *DYNC1H1,* to construct a SNP map. The primary database interrogated was dbSNP (www.ncbi.nlm.nih.gov/projects/SNP/), a central repository for human and mouse SNP data held at the National Cancer for Biotechnology Information (NCBI) as, dbSNP (Smigielski *et al.,* 2000). Although by September 2000 dbSNP contained SNPs at a frequency of one SNP every 2.03kb, the number of SNPs found in and around *DYNC1H1* were few and with little or no information on heterozygosity or validation status. A second database, Human Genome Variation Database (HGVBASE, formerly HGBASE; http://hgvbase.cgb.ki.se), independent of dbSNP was also used (Brookes *et al.,* 2000).

Compounding the paucity of SNP information was the absence of validation, which left the possibility that potential SNPs could be errors due to sequencing artefacts, the presence of paralogous sequences elsewhere in the genome or due to inaccurate laboratory assays. Initially to overcome the problem of verification, overlapping detection of SNPs by multiple independent databases was used to validate genuine polymorphisms. However this method proved impractical as only a small percentage of SNPs were seen in both databases and only 40% of final SNPs were seen in 3 databases. SNPs therefore had to be validated experimentally.

Data on SNP MAF was also unavailable. The minimum acceptable SNP MAF was selected to be 10%. Although commonly set at 5% (for later statistical chi-squared analysis to be valid), the MAF was set at a 10% threshold for the following reasons: (1) database SNPs with minor allele frequency annotation ≥10% are more likely to be genuine SNPs than artefacts, (2) to ensure that the study would have sufficient power to detect SNPs, even with a small discovery sample (3) to ensure that haplotypes later defined would be common enough to represent an ancestral state rather than more recent "singletons", (4) imposing a frequency threshold is necessary to avoid spuriously high estimates of LD when allele frequencies are close to zero (Mateu *et al.*, 2001). The impact of using a MAF >5% is discussed later in this chapter.

4.3.2 SNP validation and discovery

SNPs identified from the databases were validated by genotyping in a discovery sample of 32 chromosomes from 16 unrelated CEPH individuals, obtained from Dr. Howard M. Cann at the Foundation Jean Dausset (Dausset *et al.*, 1990). Individuals from the CEPH reference families were chosen as their northern European ancestry is similar to that of the North American case and control samples which were to be tested for association (discussed later), serving as a proxy for genetic variation in the limited North American samples. Initially, the process was to be expedited by genotyping SNPs which altered endonuclease restriction sites; however these were found to be vanishingly rare, comprising less than 4% of the total number investigated. SNPs were therefore, genotyped by automated dideoxy sequencing in both DNA strand directions. Primers were designed as described in Chapter 2.3.4 to maximise amplicon size, exploiting maximum sequence length to identify novel SNPs.

4.3.3 Minor allele frequencies

In addition to validating each SNP, resequencing 32 chromosomes from unrelated individuals allowed an assessment of MAF for each SNP. Invariant loci, or where SNP MAF<10%, were disregarded and instead a neighbouring SNP was chosen from the databases and validated until at least one SNP approximately every 10 kb was identified. If no neighbouring SNPs were listed within the databases, SNPs were identified by resequencing sequential 500kb amplicons either side of the original SNP until a polymorphic site with MAF ≥10% was found.

In total, 60 SNP loci were examined through resequencing approximately 16.7kb DNA: 36 SNPs were found to be invariant when assayed in 32 chromosomes and a further 8 SNPs were seen to have MAF below the threshold value (Table 4.2). Additionally, 6 new SNPs were identified

(rs3742426*, rs941792, rs10135238, bp183293†, rs11849604 and rs1190618) not previously reported in any database. Anecdotally, fewer SNPs, and at lower frequencies, were seen in the 5' region of the gene (between SNPs 1 and 44). Approximately 13kb of resequencing (75% of total) was undertaken in the region between SNPs 1 to 44, with only one novel SNP found. In contrast, 3.7kb resequencing between SNPs 45 and 60 yielded 5 novel SNPs, suggesting possible reduced genetic diversity in the 5' region of the gene compared to the 3' region.

In total, 16 SNPs were identified with MAF ≥10%, which were all unremarkable in their locations: 8 SNPs were located within intronic sequence but not at splice junctions and 7 SNPs were outside the transcribed region. A single SNP (rs13749) was identified within coding sequence as a synonymous change (Figure 4.2), located at the fully redundant third position of the 4360 threonine amino acid codon (ACC), and therefore did not alter the amino (T4360T). The SNP density, averaged across the gene, was approximately one SNP every 6.9kb, with the largest inter-SNP gap of 21kb between rs2180510 and rs941793.

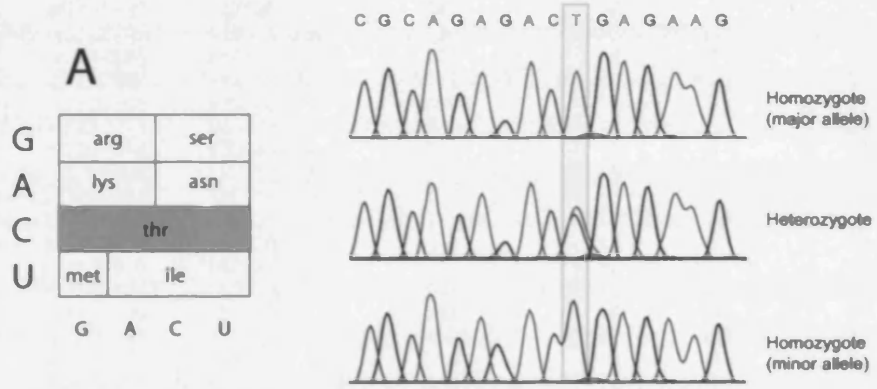

Figure 4.2 SNP rs13749 electropherograms and the redundancy of the threonine codon

Right. A single synonymous T/C coding SNP rs13749 was identified. **Left**. The minor SNP allele was located at the fully redundant third position of the ACT threonine codon, so no corresponding coding change was seen.

* rs12895291 was merged into rs3742426 on dbSNP in May 2006

† bp183293 is not present in any database. The SNP ID is given by its position on the AL118558

SNP				Amplicon	Genotype[c]			Frequency
Number	ID[a]	Position (bp)[b]	Alleles	Size (bp)	AA	AB	BB	(%)
1	rs2180511	27670	A/T	535	14	2	0	6.0
2	rs1678034	30289	A/C	566	14	2	0	6.3
3	rs2180513	61497	C/T	622	16	0	0	0
4	rs1956297	74179	C/T	453	16	0	0	0
5	rs2474677	75613	C/T	360	16	0	0	0
6	rs2474678	75617	A/G		16	0	0	0
7	rs2448241	76261	C/T	500	16	0	0	0
8	rs2093025	76319	C/T		16	0	0	0
9	rs2474679	76323	C/T		16	0	0	0
10	rs1044838	76846	A/C		16	0	0	0
11	rs2281539	76858	C/T	510	16	0	0	0
12	rs2273434	76920	C/G		16	0	0	0
13	rs2273435	77049	A/G		15	1	0	3.1
14	rs2448240	77419	C/G	360	16	0	0	0
15	rs2448239	79006	A/G	520	16	0	0	0
16	rs1741151	81081	C/T	320	14	2	0	6.3
17	rs2403015	89054	A/G	591	16	0	0	0
18	rs1622886	89874	A/G	420	16	0	0	0
19	**rs1741155**	89892	A/G		12	3	1	**15.6**
20	rs2749911	90216	C/T	460	16	0	0	0
21	**rs2720193**	90225	A/G		12	4	0	**12.5**
22	**rs2720194**	90295	A/G		12	4	0	**12.5**
23	rs2448242	91338	A/G	440	16	0	0	0
24	**rs2273438**	107101	C/T	390	12	4	0	**12.5**
25	rs2273439	107195	C/T	380	16	0	0	0
26	rs2720218	109449	A/C	190	16	0	0	0
27	**rs2749890**	114824	A/G	200	12	4	0	**12.5**
28	rs2749894	119522	A/C	211	16	0	0	0
29	rs2720206	119787	C/T	260	16	0	0	0
30	rs2720213	126498	C/G	160	15	1	0	3.1
31	**rs2251644**	129341	A/G	280	12	4	0	**12.5**
32	rs2749896	132256	A/G	380	16	0	0	0
33	rs2749897	138855	A/G		16	0	0	0
34	rs2720197	139455	A/G		16	0	0	0
35	**rs3742426***	147536	A/G	600	12	4	0	**12.5**
36	**rs2180510**	147694	A/G		12	4	0	**12.5**
37	rs2749899	150639	A/G	453	16	0	0	0
38	rs2749900	151540	C/G	365	16	0	0	0
39	rs2720198	151863	A/C	440	16	0	0	0
40	rs2403016	153341	C/T	359	16	0	0	0
41	rs2295445	157537	C/G	367	16	0	0	0
42	rs754598	160726	A/G	498	16	0	0	0
43	rs941632	163482	A/G	275	16	0	0	0
44	rs2093024	167571	A/C	530	16	0	0	0
45	**rs941793**	168955	C/T	260	12	4	1	**17.6**
46	rs1190605	171447	C/G	420	16	0	0	0
47	rs1043455	172220	C/T	327	16	0	0	0
48	**rs13749**	175721	C/T	430	12	4	0	**12.5**
49	rs2273656	175929	A/C		16	0	0	0
50	**rs941792***	176207	C/T	380	12	3	1	**15.6**
51	rs1127284	176475	C/T		16	0	0	0
52	**rs1004903**	176509	A/G		12	3	1	**15.6**
53	**rs10135238**	180364	C/T	530	12	4	1	**17.6**
54	**rs1190610**	180468	A/G		12	3	1	**15.6**
55	**rs1190613**	183028	C/T	440	12	4	1	**17.6**
56	bp183293*‡	183293	A/T		15	1	0	3.1
57	rs1190614	185042	A/T	570	13	3	0	9.4
58	rs11849604	185073	A/T		13	3	0	9.4
59	rs1203482	193407	C/T	360	16	0	0	0
60	**rs1190618***	193460	C/G		12	4	1	**17.6**

Table 4.2 SNPs identified and validated in a discovery panel of 16 CEPH individuals

SNPs were initially identified from databases and genotyped by bi-directional resequencing in 16 unrelated CEPH individuals to validate their presence and determine minor allele frequency. Relative location of *DYNC1H1* represented by the yellow box; SNPs within the yellow box are intergenic. *novel SNPs identified in 2004, have since been added to dbSNP. † rs12895291 was merged into rs3742426 on dbSNP in May 2006. ‡ bp183293 not present in any SNP database. SNP ID given by position on AL118558

4.4 Genotyping validated SNPs

The 16 validated SNPs were genotyped in 32 mother, father and child CEPH trios*, to identify haplotypes and construct a detailed LD map across the region (Figure 4.3). Comprehensive genotype information was obtained by bidirectional dideoxy sequencing for all individuals using the same primers/conditions applied to the discovery panel (full genotyping results are given in Appendix 1), however, genotypes for rs3742426 and rs2180510 continually failed for the child in trio 6 (id:34603). These SNPs displayed weak PCR products and their sequencing reactions continually failed. Both of these SNPs reside in the same PCR amplicon and therefore, the genotyping failure may have been due to a polymorphism in the primer binding sequence which can reduce the affinity of a primer for the DNA template. However, as both parents were homozygous for the major allele at each locus, the child's genotype could be easily inferred and therefore, genotyping this SNP was not pursued (although this did not rule out a potential deletion in this region).

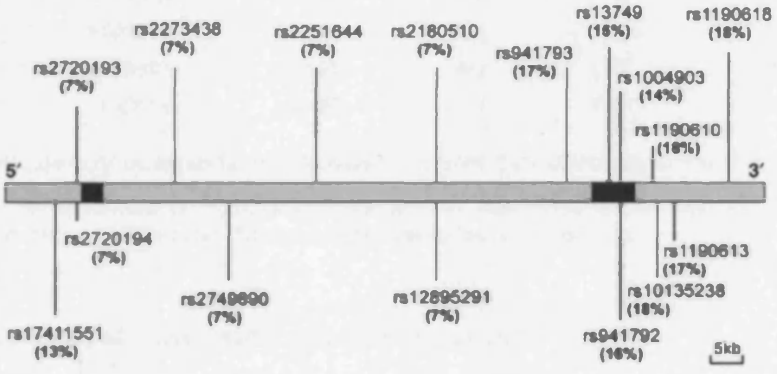

Figure 4.3 *DYNC1H1* SNP map

A schematic of the *DYNC1H1* genomic locus shown positioned 5' to 3', with dbSNP accession numbers and minor allele frequencies (in parentheses). Black boxes represent first and last exons.

There was good concordance between allele frequencies of the 32 chromosome validation panel and the full CEPH panel of 64 unrelated parents (Table 4.3), especially where MAF ≥10% in the full panel. However, several SNPs were seen to decrease their MAF from 12.5% in the discovery panel to 7% in the LD panel. These SNPs were syntenic, occurring in the 5' region of the gene whilst SNPs in the 3' region of the gene maintained their MAF of approximately 18%. This may have been due to a sampling anomaly whilst randomly selecting CEPH individuals for the discovery panel which may not have been representative of the full CEPH panel.

* Trios were used to provide information on SNP phase and aid accurate haplotype inference

SNP				Frequency (%)	
Number	ID [rs]	Position [bp]	Alleles	n=32	n=128
1	1741155	89892	A/g	15.6	13.2
2	2720193	90225	A/g	12.5	7.0
3	2720194	90295	A/g	12.5	7.0
4	2273438	107101	T/c	12.5	7.0
5	2749890	114824	A/g	12.5	7.0
6	2251644	129341	A/g	12.5	7.0
7	3742426	147536	G/a	12.5	7.0
8	2180510	147694	G/a	12.5	7.0
9	941793	168955	A/g	17.6	17.2
10	13749	175721	T/c	12.5	14.8
11	941792	176207	G/a	15.6	16.4
12	1004903	176509	G/a	15.6	14
13	10135238	180364	T/c	17.6	18
14	1190610	180468	A/g	15.6	18
15	1190613	183028	A/g	17.6	17.2
16	1190618	193460	C/g	17.6	18

Table 4.3 SNP frequency comparison between 32 and 128 chromosome discovery panels

SNP ID refers to dbSNP identification numbers with rs- prefixs. Alleles are shown with the common allele in uppercase. SNP with frequencies in red changed significantly between panels.

4.4.1 Quality control - assessing genotyping accuracy

An estimate of genotyping accuracy was empirically determined, to identify assays bias and to prevent errors affecting later association tests. This work was carried out with the help of Dr. Azlina Ahmad-Annuar. SNPs rs2251644 and rs1004903 were chosen at random and resequenced in 40 individuals, with the operator blind to all sample identifiers. A second operator coded the samples and when decoded, the genotyping error rate was ~1%. This error rate demonstrated that a high fidelity of the genotyping assay was achieved.

4.4.2 Quality control – Mendelian inheritance and Hardy-Weinberg equilibrium

Genotype data was prepared for analysis using the tagging SNP selection software TagIT (Goldstein *et al.*, 2003b) as described in Chapter 2.3.14. As an additional genotyping quality control measure and to ensure that no errors had been introduced during manual input of data, the "check matrix" command ('*checkM(M)*') in TagIT was used to identify inconsistencies in Mendelian inheritance within trios. A single case of non-Mendelian transmission was seen in which a heterozygous parent (AC genotype) and homozygous major parent (AA genotype) resulted in a homozygous minor child (CC genotype). Upon investigation of the original sequencing data, this

was found to be due to a data inputting error and was rectified. The data were also tested for deviations from Hardy-Weinberg equilibrium using TagIT, a conventional practice in assessing the quality of genotype data. Although there are a number of circumstances including mutation and demographic changes that could lead to the perturbation of HWE, deviations from HWE proportions may also arise from genotyping errors. Non-significant χ^2 values for all 16 loci (χ^2 <3.841, p<0.05; 1 d.f.), indicated consistency with HWE.

4.5 The haplotype structure of *DYNC1H1*

The utility of using CEPH trio genotype data is apparent when identifying haplotypes across *DYNC1H1*. Although a number of frequently occurring haplotypes were visible by manual inspection of the genotype data, TagIT was used to comprehensively identify transmitted haplotypes from parent to child within each trio using the '*knownhap*' function. In this manner, TagIT resolved a total of 116 transmitted haplotypes from a possible 128, or 90% of the total haplotypes possible.

ID[a]	Haplotypes[b]	Transmitted[c]		EM[d]	
		Count	Freq (%)	Count	Freq (%)
1 A	1 1 1 1 1 1 1 1 1 1 1 1 1 1 1 1	89	76.72	95	74.20
2 B	1 1 1 1 1 1 1 1 1 1 1 1 1 1 1 2	7	6.30	8	6.20
3 G	1 1 1 1 1 1 1 1 2 2 2 2 2 2 2 1	3	2.59	3	2.30
4 C	2 2 2 2 2 2 2 2 2 2 2 2 2 2 2 1	3	2.59	3	2.30
5 E	2 1 1 1 1 1 1 1 2 2 2 2 2 2 2 2	3	2.59	3	2.30
6 F	2 2 2 2 2 2 2 2 2 2 2 2 2 2 2 2	2	1.72	2	1.56
7 D	2 1 1 1 1 1 1 1 2 1 2 2 2 2 2 2	1	0.86	3	2.30
8 H	2 2 2 2 2 2 2 2 2 2 2 1 2 2 2 2	1	0.86	2	1.56
9 I	1 1 1 1 1 1 1 1 2 2 2 2 2 2 2 2	1	0.86	2	1.56
10 J	2 2 2 2 2 2 2 2 2 1 2 2 2 2 2 2	1	0.86	1	0.78
11 K	2 1 1 1 1 1 2 2 2 1 2 2 2 2 2 2	1	0.86	1	0.78
12 L	1 1 1 1 1 1 1 1 1 1 2 1 1 1 1 1	1	0.86	1	0.78
13 M	1 1 1 1 1 1 1 1 1 2 1 1 1 1 1 1	1	0.86	1	0.78
14 N	2 1 1 1 1 1 1 1 2 2 2 1 2 2 2 2	1	0.86	1	0.78
15 O	2 1 1 1 1 1 1 1 2 2 2 2 2 2 2 1	1	0.86	1	0.78
16 P	2 2 2 2 2 2 2 2 2 2 1 1 2 2 2 1	-	-	1	0.78
17 Q	1 1 1 1 1 1 1 1 1 1 1 1 2 2 1 2	-	-	1	0.72
	Total	116	100	128	100

Table 4.4 The haplotype structure of *DYNC1H1* in CEPH

[a] Haplotype designation
[b] Loci are arranged in the order snp1–snp16 (as in Table 4.3). A haplotype is reported if observed in resolved chromosomes or if EM frequency is ≥1% (1 = major allele; 2 = minor allele)
[c] Frequencies and counts estimated from resolved parental chromosomes only
[d] Frequencies and counts estimated by the EM algorithm for trio data

The 12 haplotypes not observed were attributable to ambiguous SNP phase in trios 9, 17 and 30; each possessing one or more SNP locus heterozygous in **all three** trio members (Figure 4.4). Proceeding with the readily identifiable, transmitted haplotypes to discern the pattern of LD across

DYNC1H1 would have omitted information from approximately 10% of the total genotyping dataset due to ambiguous phase, therefore the phase-ambiguous haplotypes needed to be identified.

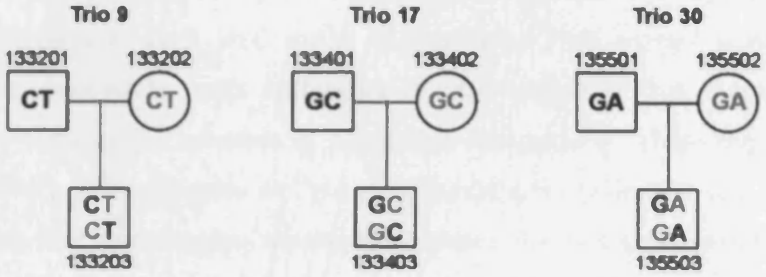

Figure 4.4 Phase-ambiguous SNPs in CEPH trios

In CEPH trio 9, both parents and child are heterozygous at all loci except SNPs 11, 12 and 16; SNP 4 is shown. In CEPH trio 17, both parents and child are heterozygous at SNP locus 16. In CEPH trio 30 both parents and child are heterozygous at SNP loci 13, 14 and 16; SNP 13 is shown. Paternal SNP alleles are in black, maternal SNP alleles in red and the two possible alleles inherited by the children are shown. CEPH identification numbers are given above/below the pedigree symbols.

The SNP/haplotype ambiguity was resolved by applying an Expectation Maximisation (EM) algorithm to infer the missing haplotypes. The EM algorithm, first proposed by Clark in 1990, determines resolved haplotypes from individuals with no haplotype ambiguity and sequentially applies these to phase-ambiguous individuals, to resolve their haplotypes (Clark, 1990). The algorithm uses maximum likelihood estimates of haplotype frequencies in the sample using an initial set of haplotype frequency estimates to calculate the conditional distribution for haplotype pairs that each individual carries (the Expectation step). The initial set of haplotype frequencies were restricted to those phased haplotypes identified from the CEPH trios. Based on these conditional distributions, haplotype frequency estimates can be updated (Maximization- step) and the algorithm iterates between the two steps until the haplotype frequency estimates converge. Haplotypes were inferred using the EM algorithm implemented within TagIT, with a minimum frequency threshold of ≥1%.

The EM analysis identified a total of 17 different haplotypes ≥1% frequency, 15 of which were previously seen transmitted amongst the trios (Table 4.4). The EM estimated frequencies agreed well with the transmitted haplotype frequencies and both data sets show that haplotype A predominates, present at approximately 75% on average. Two new haplotypes P and Q were identified through the EM procedure, although these were present at low frequency (1%) and a greater number of haplotypes were seen at 3% frequency, which most likely represent those haplotypes that were previously unresolved.

Interestingly, several pairs of haplotypes were seen with completely mismatching alleles (i.e. nucleotides differing at every SNP position in a haplotype pair) which, at the time they were identified, had not previously been reported by any other groups. The high frequency of these mismatching haplotype pairs: A+F, B+C and to a lesser extent J+M, seemed an odd occurrence and through successive discussions with colleagues it was suggested that these haplotypes may represent a genetic signature of selection or population demography. These haplotypes have since been termed by Zhang and colleagues as "yin yang haplotypes" (Zhang *et al.*, 2003). Finally, the haplotype data provided encouraging anecdotal evidence for linkage disequilibrium across the region: the A haplotype comprised approximately 75% of the total haplotype diversity, with the remaining 25% comprised of haplotypes at much lower frequencies many of which are variants of haplotype A.

4.6 Linkage disequilibrium patterns

The empirical assessment of linkage disequilibrium across the gene was a crucial measure to determine the magnitude of economy, if any, available in using tagging SNPs to represent variation across *DYNC1H1* and also in selecting the tSNPs.

The extent of LD across *DYNC1H1* was calculated by assessing the frequency of 2-locus haplotypes (i.e. pairwise comparisons) within the total pool of phased chromosomes and then calculating D' and r^2 measures from these values. In view of the haplotype frequencies discussed above and considering how the D' measure is calculated (D' is maximal when two of the four possible haplotypes, in a two-locus situation for example, are absent – see D' derivation from Chapter 1) high D' scores between the majority of pairwise SNP comparisons were predicted.

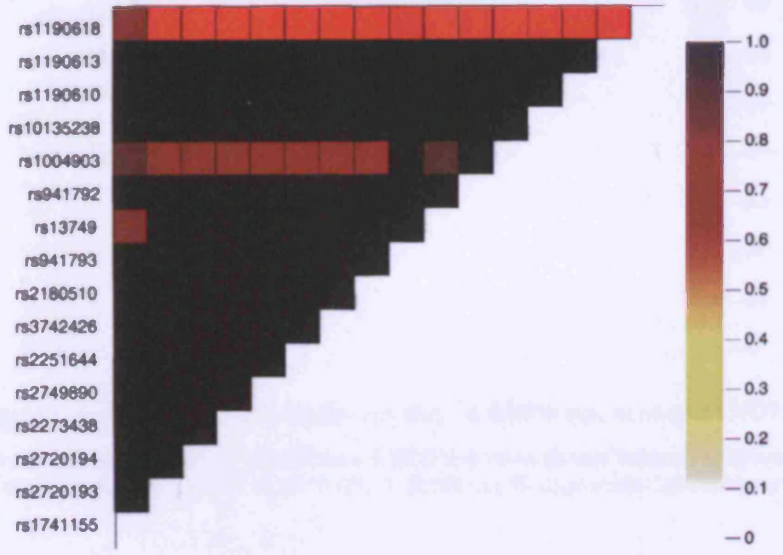

Figure 4.5 Linkage disequilibrium (*D'*) between the 16 SNPs spanning *DYNC1H1*

Assessing pairwise LD between the 16 SNPs across *DYNC1H1* reveals two regions of elevated LD. SNP ID numbers arranged on the left from most 5' (top) to the 3' (bottom). Colour scale bar represents *D'* values from 0 (white) to 1 (black).

Figure 4.5 provides a graphical illustration of pairwise *D'* between the 16 *DYNC1H1* SNPs calculated using TagIT and substantiated the high *D'* prediction. Average *D'* across the gene was 0.98 and although it is presented here as mainly a descriptive statistic, it supports the original power calculation made (where *D'*~1). *D'* also informs on recombination across the region, which appears to be absent except for at the 3' most SNP.

As previously discussed, a more useful measure of LD for association studies is r^2. Although r^2 is sensitive to marker allele frequencies it does provide a simple linear relationship to sample size, as the reciprocal of r^2 (that is, $^n/_{r^2}$) relates to the proportional increase in sample size required to obtain the same power as testing the functional variant itself (Pritchard *et al.*, 2001). With this linear relationship in mind, a minimum working threshold of $r^2 \geq 0.85$ was used, requiring an increase in sample size of ~18% to have equivalent power of typing the causal SNP itself. Figure 4.6 provides a graphical illustration of pairwise r^2 values between the 16 *DYNC1H1* SNPs. The r^2 data clearly show two defined regions of elevated LD: the first region bounded by SNPs rs2720193 to rs3742426 and the second region by SNPs rs941793 to rs1190613. Although the average LD across the gene was r^2=0.61, within the two regions LD was r^2=1 and r^2=0.91 on average.

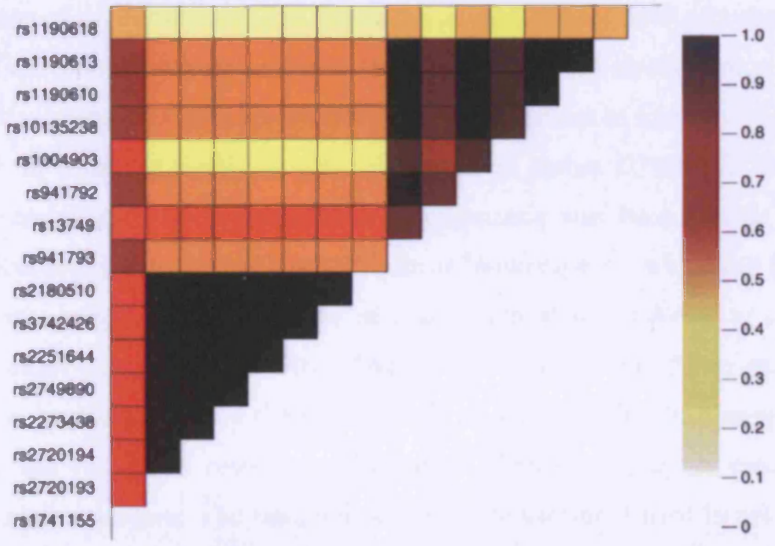

Figure 4.6 Linkage disequilibrium (r^2) between the 16 SNPs spanning *DYNC1H1*

Assessing pairwise LD between the 16 SNPs across *DYNC1H1* reveals two regions of elevated LD. SNP ID numbers arranged on the left from most 5' (top) to the 3' (bottom). Colour scale bar represents r^2 values from 0 (white) to 1 (black).

4.7 Phase II - SNP tagging

Subsequent to identifying and phasing the CEPH *DYNC1H1* haplotypes and calculating pairwise LD amongst the 16 SNPs, the investigation converged to identifying tagging SNPs. Tagging SNP selection was performed using Goldstein and Weale's TagIT software. Goldstein and Weale's method uses a direct approach to identify a set of tSNPs that maintain high r^2 values with the other SNPs (thus tagging them), or that define a set of haplotypes that do so. In general, there are two approaches in which a reduced set of tSNPs can be selected to represent a larger set of known SNPs. The first approach is based on capturing as much of the original haplotype diversity present in a set of known SNPs when condensed to a smaller set of tSNPs, as exemplified by Johnson and colleagues 2001 paper (Johnson *et al.*, 2001). The second approach involves establishing a maximal association between the reduced tSNP set and the original set of known SNPs from which they are derived, as described in Chapman's 2003 paper (Chapman *et al.*, 2003). Although TagIT incorporates both of these approaches to identify tSNP sets, the association based approach is a more directly relevant approach to SNP prediction in the context of an association study (Weale *et al.*, 2003), and therefore all tSNPs in this study were selected on association based performance.

The size of a tSNP set may be determined empirically or predefined. Identifying tSNP sets of a predefined size can be useful if tSNP set size is constrained by cost (for example, if a large number of genes are being tested in a single study); however, this method can underpower studies, especially in regions of low or variable LD. Instead, minimal tagging SNP sets can be chosen based on their ability to exceed a minimum performance threshold. In this circumstance the tSNP set size varies to provide a minimum level of association with the larger set of known SNPs from which the tSNP are derived. In selecting tSNPs to represent variation across *DYNC1H1* the latter approach was used. The measure used to evaluate tSNP performance was based on an "average locus" association criterion, termed by Goldstein and Weale as '*haplotype* r^2', which has been suggested to be an optimal performance measure for use in association studies (Weale *et al.*, 2003) and in estimating associations between SNPs with MAF of 6% or more (Goldstein pers. comm.). This measure reduces the performance of a tSNP set against all known SNPs, to a single value by taking the weighted average (weighted relative to the minor allele frequency at each locus) of each individual performance measure. The minimal performance threshold used in selecting a tSNP set was set at $r^2 \geq 0.85$.

All tSNP sets of varying size H were identified for which the average locus performance criterion for each tSNP set was $r^2 \geq 0.85$ against the 16 dynein SNPs (Figure 4.7).

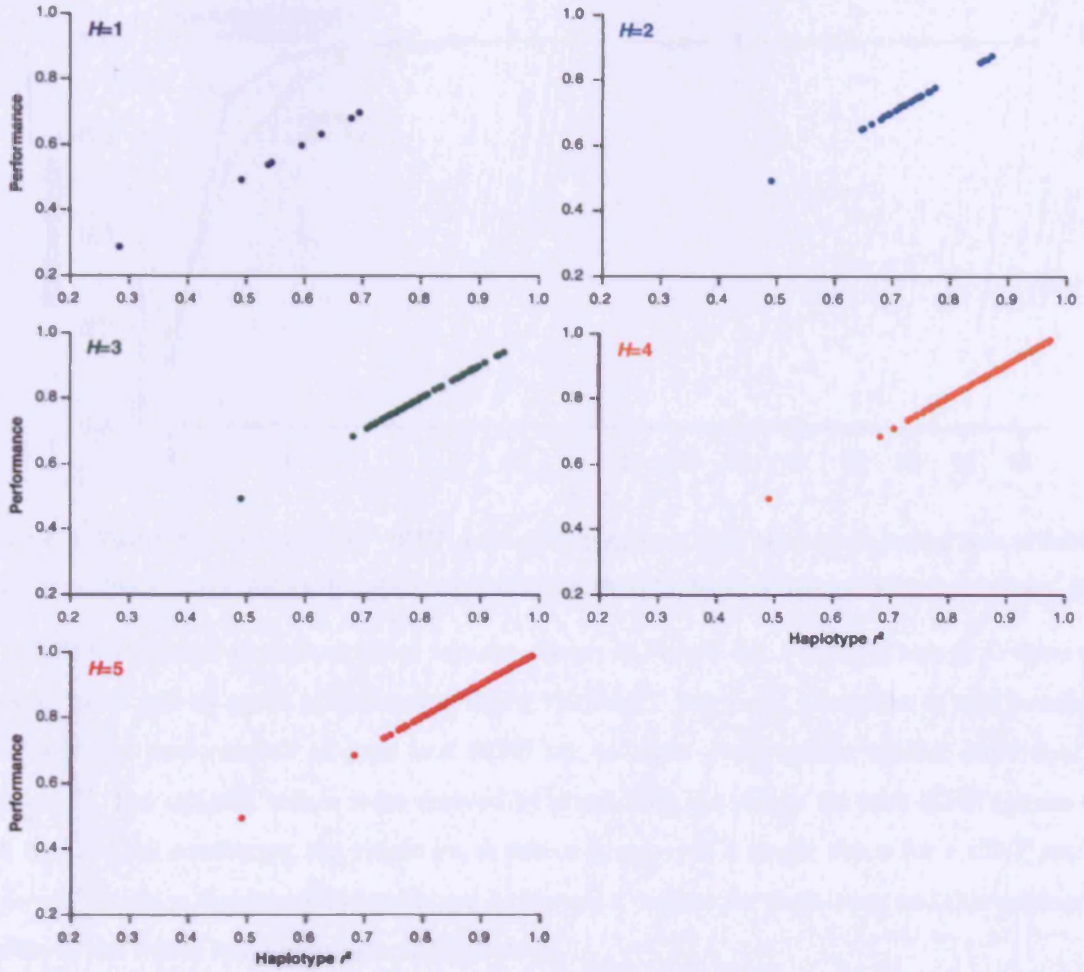

Figure 4.7 Average locus haplotype r^2 performance of all tSNP sets sizes from *H*=1 to *H*=5

H=1 there are 16 possible tSNP sets, *H*=2 there are 120 possible tSNP sets, *H*=3 there are 560 possible tSNP sets, *H*=4 there are 1820 possible tSNP sets and *H*=5 there are 4368 possible tSNP sets.

The highest performing tSNP sets were identified for different tSNP sizes. As *H* increased, the performance of all tSNP sets approached 1, as a greater number of variants were tagged. But which value of *H* is optimal? As Figure 4.8 illustrates, the minimum tSNP set size to achieve an average locus association performance threshold $r^2 \geq 0.85$ is *H*=2. The data shown in Figure 4.8 are the "best", or highest scoring, tSNP sets taken from the average locus analysis, although more than one tSNP set of a given size can be "best"). There were diminishing returns in increasing *H*>4, with no appreciable increase in performance, and increasing tSNP set size beyond *H*=7 yields no additional benefit and therefore, in an average locus analysis, all haplotypes can be tagged by a minimum of 7 tSNPs. A two tSNP set exceeded the 0.85 threshold and also performed well in representing the diversity of haplotypes available – capturing 94% of the total haplotype diversity.

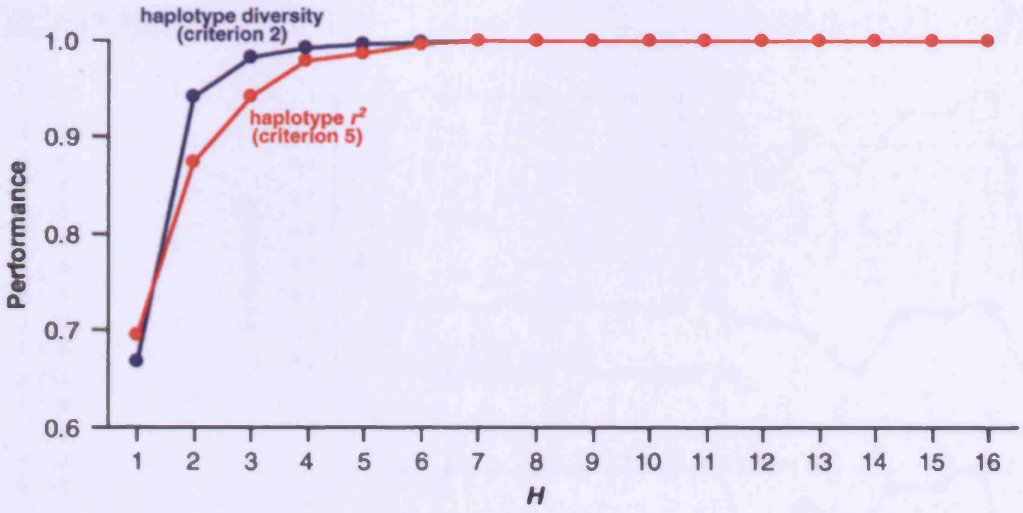

Figure 4.8 Performance of "best" tSNP sets of increasing size *H* chosen using two criteria

Performance measure is given as average locus haplotype diversity (blue) or average locus haplotype r^2 (red).

The tSNPs that related to these optimal sets are shown in Figure 4.9. For tSNP sets $H>2$ there were multiple 'best' sets of equal performance. Using the TagIT '*performL*' function, it was possible to decompose the performance of each best tSNP set, to show performance against individual loci (Figure 4.9). The optimal values were derived by combining the values for each tSNP against each locus and further combining the single locus scores to provide a single value for a tSNP set. The '*performL*' function displayed the combined *haplotype* r^2 values for each locus and this manner it is possible to see which loci are influencing the result.

The results indicated that a solo tSNP set (SNP 5 or 9) was insufficient to capture the variation of the entire region - each single tSNP tags the region of elevated linkage disequilibrium it resides in. In concordance with the LD data and the haplotype data, the SNP tagging data confirmed that two "sub-regions" with different properties exist across the gene and that these regions could not be summarised by a single tSNP. A two tSNP set overcame this problem and although a weighted average of the performance values was greater than 0.85, it was clear that there were four SNPs that could not be tagged well (SNPs 1, 10, 12 and 16). These SNPs could only be reliably tagged by increasing the tSNP set size to $H=3$ and $H=4$ and only if they themselves were chosen as tSNPs (i.e., they are tagging nothing but themselves).

H	tSNPsets				
1	9				
	15				
2	2	9			
	2	15			
	3	9			
	3	15			
	4	9			
	4	15			
	5	9			
	5	15			
	6	9			
	6	15			
	7	9			
	7	15			
	8	9			
	8	15			
3	2	9	16		
	2	15	16		
	3	9	16		
	3	15	16		
	4	9	16		
	4	15	16		
	5	9	16		
	5	15	16		
	6	9	16		
	6	15	16		
	7	9	16		
	7	15	16		
	8	9	16		
	8	15	16		
4	2	10	12	16	
	3	10	12	16	
	4	10	12	16	
	5	10	12	16	
	6	10	12	16	
	7	10	12	16	
	8	10	12	16	
5	1	2	10	12	16
	1	3	10	12	16
	1	4	10	12	16
	1	5	10	12	16
	1	6	10	12	16
	1	7	10	12	16
	1	8	10	12	16

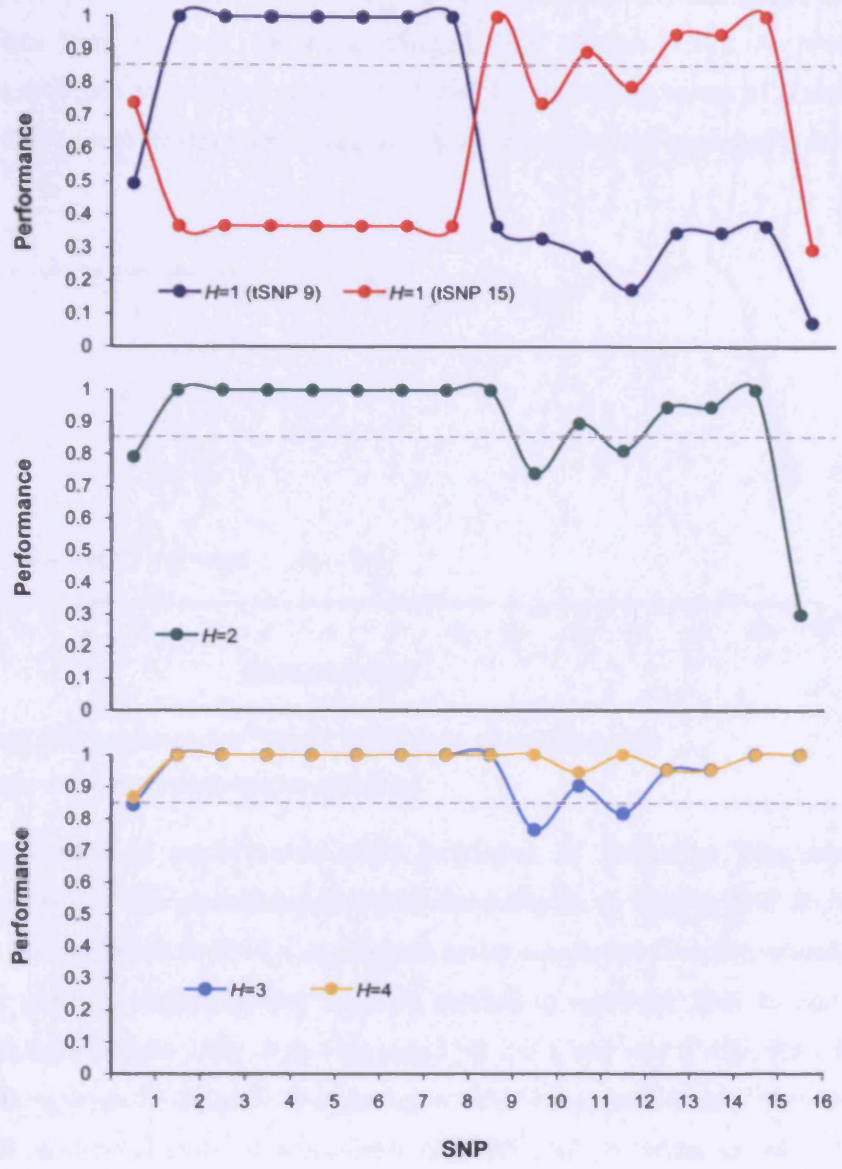

Figure 4.9 Optimal tSNP sets of size *H* and their performance against all loci

Left. Table gives "best" tSNP sets for varying set size *H*. SNPs 1 to 16 are rs1741155, rs2720193, rs2720194, rs2273438, rs2749890, rs2251644, rs3742426, rs2180510, rs941793, rs13749, rs941792, rs1004903, rs10135238, rs1190610, rs1190613 and rs1190618 respectively. **Right**. Performance of "best" tSNP sets for each locus. All performance tested using association criterion 5. Broken grey line represents 0.85 performance threshold.

4.7.1 Assessing tSNPs – "SNP-dropping"

Of paramount importance in selecting tagging SNPs is the performance of a chosen tag set to capture unknown variation. This was tested using the TagIT SNP-dropping routine "*excludes*", to sequentially drop each SNP from the full SNP set, to simulate an "unknown" polymorphism, and

assess the performance of tSNPs selected from the remaining reduced SNP set to tag the dropped SNP. The SNP-dropping routine was carried out for varying tSNP set sizes (*H*) and single-locus performance criteria values were returned for each dropped SNP (Figure 4.10). As shown previously, more than one tSNP set was defined as equally "best" for increasing values of *H* and in these circumstances the single-locus performance criteria values returned were averaged over all "best" tSNP sets.

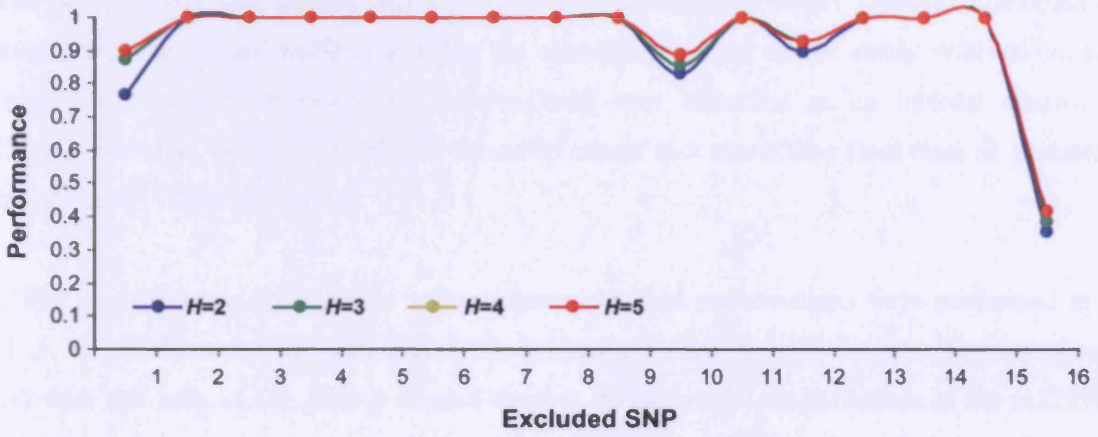

Figure 4.10 SNP dropping performance for "best" tSNP sets of varying size

Performance relates to average single locus performance criterion 5.

Very little difference was seen in performance with increasing *H* indicating diminishing performance returns (Figure 4.10). The procedure confirmed the difficulty in tagging SNP 16, and to a lesser extent, SNP 10 and 12. When SNP 16 was dropped, no tag set chosen from the remaining 15 SNPs was able act as a proxy, indicating that the only method to represent SNP 16 and its associated variation would be to include SNP 16 as a tagging SNP itself. But was it imperative that this SNP and its associated variation be tagged? The position of SNP 16, approximately 15kb from the last exon of *DYNC1H1*, and the absence of appreciable LD with SNP 15 (which is only 4.5kb from exon 78) suggested that it probably did not tag any functional variants in the 3'UTR and so, tagging this SNP was not a priority.

Taken together, these analyses suggested that a two tSNP set could provide the optimal performance. It was unlikely that any appreciable gain would have been seen in adding extra tSNPs to this set, apart from tagging low frequency clades of the haplotype genealogy, however the occurrence of a functional variant in a low frequency clade cannot be ruled out. Of the 14 possible two tSNP combinations shown in Figure 4.9, tSNPs 6 (rs2251644) and 9 (rs941793) were chosen to genotype in cases and controls. As all 14 tSNP sets performed equally well, the only discriminating criteria was the ease of genotyping - both rs2251644 and rs941793 modify restriction endonuclease recognition sequences and therefore these SNPs were pursued.

4.7.2 Restriction endonuclease assays for rs2251644 and rs941793

The major allele of tSNP rs2251644 was found to destroy an NsiI endonuclease recognition site within the 270bp PCR amplicon originally used for genotyping in the CEPH trios, and the minor allele of tSNP rs941793 created a SacI recognition sequence within its the 300bp amplicon. To control for partial and complete digestion failures, additional invariant restriction endonuclease recognition sites were investigated as internal controls. These internal control endonucleases were chosen on the basis that double digestions* could be performed under identical conditions (at identical temperatures and buffers) and that the cleavage products can be easily resolved on 2.5% agarose gels. No suitable restriction endonuclease was identified as an internal control for rs2251644 cleavage, however, NheI was found to cleave at a site 100bp from SacI as an internal control for rs941793 (Figure 4.11).

All tSNP genotyping and restriction endonuclease cleavage optimisations were performed at the Cecil B. Day Laboratory for Neuromuscular Research, Massachusetts General Hospital, Boston (USA) with the help of Dr. Azlina Ahmad-Annuar. Non-specific amplification of the rs2251644 SNP PCR product was sporadically seen despite identical primer sequences being used to those used for genotyping of CEPH trios, which had previously worked well in London. Inconsistency of the rs2251644 PCR product may have been due to differences in the reagents and thermalcyclers used between the two laboratories and dictated the design of new primers for genotyping the tSNP. The new primers (rs2251644CBDay, shown in Appendix 2 Primer Table) provided a repeatable and robust PCR product, approximately 392bp in length.

Due to the absence of an internal control for tSNP rs2251644 and a change of genotyping reagents, protocol and location from those previously used, the restriction endonuclease assays were checked for genotyping fidelity. Genotypes of 96 randomly selected control individuals (from a panel later used in the sporadic ALS association study) for both tSNPs, were determined by double digest and sequencing on a Beckman Coulter Genetic Analysis system (Figure 4.11). The operator was blinded to all sample identifiers to ensure impartiality. Genotypes from both assays were compared for consistency and acceptable error rates of approximately 1% were seen (<1% for rs2251644 and 1.09% for rs941793).

* A double digest is the cleavage of a single DNA moiety by two restriction endonucleases

tSNP			Enzyme		PCR conditions	Fragment size (bp)		
ID	Major allele	Minor allele	Primary	Internal control		AA	Aa	aa
rs2251644	A	G	NsiI ↓ atgca	n/a	37°C	230 162	392 230	392
rs941793	A	G	SacI ↓ ga gct	NheI ↓ g ctagc	37°C	212 88	212 112	112 100

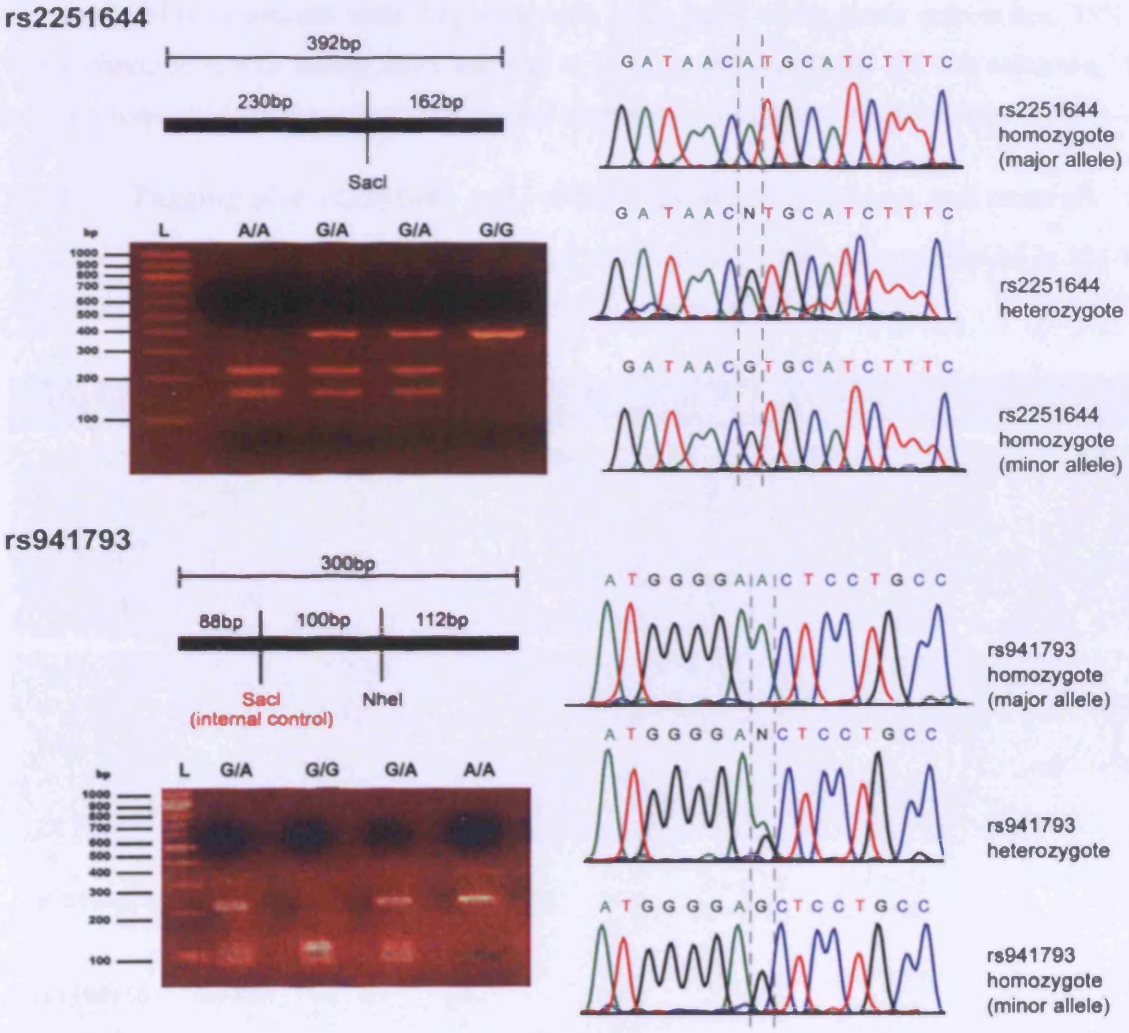

Figure 4.11 Restriction digests for tSNPs rs2251644 and rs941793

Top. Table summarising tSNP restriction endonuclease properties and expected product sizes. No internal control was identified for rs2251644. Fragment sizes are given in base pairs after complete digestion of AA (major allele homozygotes), Aa (heterozygotes) and aa (minor allele homozygotes) by the respective enzymes. **Middle**. rs2251644 PCR amplicon schematic, gel electrophoresis results and sequence verification. **Bottom**. rs941793 PCR amplicon schematic, gel electrophoresis results and sequence verification.

4.8 Phase III - Testing in sporadic ALS cases and controls

4.8.1 Association study samples

Sporadic ALS case samples were generously provided by R.H. Brown at Massachusetts General Hospital or collaborators from various academic and clinical institutions across North America. All sporadic ALS patient samples were obtained with accompanying signed consent. Patients were diagnosed by El Escorial criteria and had not been screened for *SOD1* mutations. The patient cohort comprised of 134 females and 147 males with an average age at diagnosis of 46 years (range 24 to 79 years). 34% of patients were diagnosed with early onset in the lower extremities, 35% with upper onset, 30% with bulbar onset and site of onset in the remaining 2% was unknown. As all samples were obtained retrospectively, limited phenotypic information was available.

4.8.2 Tagging SNP rs2251644 and rs941973 genotyping in cases and controls

With the endonuclease assay functioning well, the *DYNC1H1* tSNPs were genotyped in 281 North American sporadic ALS cases and 225 age matched controls (Table 4.5).

tSNP ID	Sample		Genotype count observed	Expected	Allele frequencies	HWE Analysis	Association test
rs2251644	SALS	AA	171	173.4	A = 0.88	χ^2= 2.15;	
		GA	53	48.3	G = 0.12	*p*=0.357	
		GG	1	3.4			χ^2= 1.40
	control	AA	202	202.4	A = 0.87	χ^2= 0.04;	*P*= 0.76
		GA	60	59.3	G = 0.13	*p*= 0.850	
		GG	4	4.4			
rs941793	SALS	AA	141	140.8	A = 0.75	χ^2=0.004;	
		GA	94	94.4	G = 0.25	*p*= 0.100	
		GG	16	15.8			χ^2= 3.20
	control	AA	120	126.9	A = 0.75	χ^2= 6.12;	*p*= 0.93
		GA	98	84.1	G = 0.25	***p*= 0.01**	
		GG	7	13.9			
rs10135238	control	TT	69	74.3	T = 0.77	χ^2= 7.48;	
		TC	54	43.4	C = 0.23	***p*= 0.05**	
		CC	1	6.3			
rs1190610	control	AA	70	75.3	A = 0.78	χ^2= 7.36;	
		GA	54	43.5	G = 0.22	***p*= 0.05**	
		GG	1	6.3			

Table 4.5 Genotype frequencies of tSNPs rs2251644 and rs941793 in sporadic ALS cases and matched controls

Observed and expected tSNP genotype frequencies are shown for sporadic ALS (dark grey panels) and controls (light grey panels). No significant differences were seen in genotype or allele frequencies between cases and controls. Deviation from Hardy-Weinberg equilibrium was seen based on χ^2 distribution at tSNP rs941793 in the controls and at two additional SNP loci rs10135238 and rs1190610 (cream panels).

4.8.2.1 Association study genotyping accuracy

The genotype data was tested for deviations from Hardy-Weinberg proportions using the software HWSIM (http://krunch.med.yale.edu/hwsim) to assure the quality of the data and prevent errors or cryptic genetic factors leading to a spurious association. HWSIM calculated expected genotype frequencies and performed a Pearson χ^2-test for accordance between the observed and expected genotypes. As χ^2-tests are a poor approximation when one or more genotype class has a value less than 5, HWSIM was used to implement a Monte-Carlo permutation test with 10,000 iterations for rs2251644 case and control data. A two-tailed test was used (obtained by counting how many times, across iterations, the original data and all other distributions that are **more** deviant from Hardy-Weinberg were observed) which, compared to a one-tailed test, did not require a judgement to be made on whether greater or fewer heterozygotes are to be expected. Two-tailed values for rs2251644 and rs941793, in cases were p=0.3574 p=1.000. All other genotypes were tested using HWSIM based on the χ^2 distribution and were seen to be in HWE (i.e. $\chi^2 \leq 3.84$, with 1 degree of freedom; d.f.) except for rs941793 in the control panel (p=0.01), which showed an excess of GA heterozygotes and deficit of GG homozygotes. The relevance of which is discussed further below.

4.8.2.2 Hardy-Weinberg disequilibrium in control samples

There are several possible explanations to account for the deviation of rs941793 from HWE in control samples. The first could have been due to a poorly functioning genotyping assay. As the SacI restriction endonuclease assay for rs941793 cleaves the minor (G) allele, it was initially thought that the deficit of GG homozygotes could be due to suboptimal or incomplete digestion of PCR products. However, on closer inspection of the agarose gel images of the cleavage products, the internal control enzyme had cleaved correctly. In addition, due to the nature of this assay, suboptimal/incomplete digestion of the PCR products would have resulted in a reduction of heterozygotes rather than an excess, which is contrary to the observed data. Alternatively a polymorphism within the rs941793 primer binding region, could have caused the biased amplification of the major allele, although this is unlikely as both the case panel and the discovery CEPH panel would be similarly affected. In addition, no polymorphisms in the rs941793 primer biding regions have been identified in any SNP database to date.

As a number of 2 tSNP sets were identified as "best", a number of additional SNPs were available to replace rs941793. Two such SNPs were rs10135238 and rs1190610, present on the same amplicon. These were both genotyped in the control cohort by sequencing using the Beckman Coulter Sequencer – this deliberate move to use a different genotyping platform was to avoid any assay-related errors that may have lead to the deviation from HWE (and it allows both SNPs to be genotyped simultaneously). Both SNPs were found to deviate significantly (p=0.01) from the chi-

squared distribution, however, simulated *p*-values showed that the results were marginally significant Monte-Carlo *p*-values rs10135238 p=0.0495 and rs1190610 p=0.0466. Analysis of SNP rs941793, using Monte-Carlo permutation tests reduces the significance of deviation to p=0.07, suggesting that based on the genotypes seen, the probability of obtaining equally deviant data sets with a paucity of heterozygotes is highly likely. Taken together, these SNPs show a trend to significance which is not entirely unexpected, given the high LD between rs941793, rs10135238 and rs1190610 and suggests that the result may be a genuine property of the control cohort and not an assay-related error.

4.8.2.3 A sampling bias?

To identify if the HWE deviation was due to an intrinsic property of the control cohort generated through a sampling bias, the details of all control samples were reviewed with Diane McKenna-Yasek, coordinator of the Day Lab DNA collection. Samples from the control panel were checked to identify related individuals, which could result in a skewing of allele frequencies by over-representing one genotype compared to another. The review confirmed that the majority of the cohort was comprised of spousal controls, precluding relatedness between the individuals.

4.8.2.4 Hardy-Weinberg equilibrium at genes independent of *DYNC1H1*

Several different factors can lead to perturbations of HWE, such as demographic processes, selection and genotyping error. Although demographic processes, such as population admixture, can lead to deviations in HWE, these effects are observed genome-wide. Could the deviation from HWE seen in the control samples be due to a demographic or sampling error? This question was answered by assaying for deviations from HWE at sites independent of *DYNC1H1*. Data were available from two additional studies which used the same control panel to that used in the heavy chain study: 8 SNPs from a study of the cytoplasmic dynein intermediate chain 1 (*DYNC1I1*) gene on chromosome 7 (Azlina Ahmad-Annuar, pers. comm.) and 3 SNPs in the vascular endothelial growth factor (*VEGF*) gene on chromosome 6 (Carsten Russ, pers. comm.) were all in HWE (Table 4.6). This suggests that the HWE perturbations seen at *DYNC1H1* may be a locus-specific artefact in the controls rather than genome-wide effect due to demographic processes. Genotyping errors may also result in significant deviations from HWE and although the majority of HWE deviations are due to problematic and non-specific assays, there remain a number of instances where no root cause for genotype error is detectable (Hosking *et al.*, 2004).

4.8.3 A comparison of tSNP genotype frequencies between cases and controls

Despite the deviation from HWE, genotypes of the two tSNPs were analysed for significant differences between cases and controls, using the software. The null hypothesis was that there was

no significant difference between the two samples and this was tested using a Fisher's exact test of the tSNP genotypes and χ^2-test of the tSNP allele frequencies. The tSNPs showed no significant differences in genotype proportions between sporadic ALS cases and age matched controls (Table 4.5).

tSNP ID	Gene		Genotype count Observed	Expected	Allele frequency	HWE analysis
rs940424	*DYNC1I1*	AA AT TT	10 51 95	8.08 54.84 93.08	A = 0.17 T = 0.83	χ^2= 0.77; *p*= 0.59
rs2690289	*DYNC1I1*	AA AG GG	46 88 25	50.94 78.11 29.94	A = 0.59 G = 0.41	χ^2= 2.55; *p*=0.21
rs3129314	*DYNC1I1*	AA AG GG	63 76 35	58.63 84.75 30.63	A = 0.58 G = 0.42	χ^2= 1.85; *p*=0.30
rs1488513	*DYNC1I1*	AA AG GG	32 80 47	32.60 78.79 47.60	A = 0.48 G = 0.52	χ^2= 0.04 *p*= 0.89
rs1685818	*DYNC1I1*	GG GT TT	28 83 55	29.10 80.80 56.10	G = 0.42 T = 0.58	χ^2= 0.13 *p*= 0.77
rs81018	*DYNC1I1*	AA AG GG	40 85 25	45.38 74.25 30.37	A = 0.46 G = 0.54	χ^2= 3.14 *p*= 0.16
rs720780	*DYNC1I1*	AA AG GG	62 61 22	59.01 66.98 19.01	A = 0.65 G = 0.35	χ^2= 1.16 *p*= 0.45
rs2299282	*DYNC1I1*	GG GT TT	9 51 105	7.21 54.57 103.21	G = 0.21 T = 0.79	χ^2= 0.71 *p*= 0.59
rs6966540	*DYNC1I1*	CC CT TT	13 61 52	15.02 56.96 54.02	C = 0.37 T = 0.63	χ^2= 0.63 *p*= 0.49
2578	*VEGF*	CC CA AA	45 104 63	44.9 105.3 61.8	C = 0.46 A = 0.54	χ^2= 0.0292 *p*= 0.86
1154	*VEGF*	GG GA AA	81 98 33	78.9 100.9 32.2	G = 0.61 A = 0.25	χ^2= 0.1380 *p*=0.71
634	*VEGF*	GG GC CC	103 90 19	100.9 90.7 20.4	G = 0.69 C = 0.31	χ^2= 0.0109; *p*=0.92

Table 4.6 *DYNC1I1* and *VEGF* control genotypes in Hardy-Weinberg equilibrium

SNPs 2578, 1154 and 634 are *VEGF* promoter polymorphisms

4.8.4 Comparison of tSNP haplotypes between cases and controls

As the tSNPs were originally selected based on their individual tagging performance and as haplotypes, two marker haplotype frequencies were next compared between cases and controls. The software FASTEHPLUS (Zhao *et al.*, 2002) was used to perform the haplotype association analysis based on the case control genotype data. FASTEHPLUS was used to estimate two locus haplotype frequencies from the entirety of the genotype data and haplotypes were then compared between cases and controls. From the total dataset of 472 individuals, 64 records were discarded due to missing data.

tSNP haplotype		Frequency (%)		χ^2 test
rs2251644	rs941793	Cases	controls	
A	A	0.75	0.74	χ^2= 0.32
A	G	0.13	0.12	p= 0.956
G	A	0.09	0.00	
G	G	0.03	0.13	

Table 4.7 *DYNC1H1* tSNP haplotype frequencies in sporadic ALS cases and matched controls

Two-marker haplotype frequencies calculated by FASTEHPLUS based on 408 unrelated individuals. No significant association was seen based on a χ^2 test.

Based on comparing the two-marker haplotype frequencies in sporadic ALS cases and matched controls a heterogeneity statistic is outputted based on a χ^2 distribution (χ^2= 0.32; p= 0.956). Taken together, the individual tSNP loci, rs2251644 and rs941793 and their two-marker haplotypes show no significant association with sporadic ALS (Table 4.7).

4.9 Evolutionary analysis of the *DYNC1H1* locus

Despite the absence of association between *DYNC1H1* variants and SALS, the pattern of variation, more specifically the apparent reduction in diversity at the sequence level, was interesting and it was thought that analysis of this characteristic might hold potential clues as to the genes' role in ALS. To identify differences in genetic diversity and test for selection at *DYNC1H1*, the 16 SNP loci were genotyped in additional Japanese and Cameroonian populations. However, since this study began it has been shown that the hierarchal sampling method commonly used to ascertain SNPs, and the exportation of these SNPs for investigation in other populations, can introduce bias to the data which can distort tests of genetic diversity and selection (Akey *et al.*, 2003; Weiss *et al.*, 2002). Due to this SNP ascertainment bias, we were unable to exploit many of the indices commonly used to infer selection or deviations from neutrality. Many of the properties of these three populations presented here are affected by ascertainment bias and therefore they are provided as descriptive.

4.9.1 SNP ascertainment bias and impact on measurements of selection

To date, the most common strategy for discovering SNPs has been by full resequencing of a small number of samples, followed by targeted genotyping of these discovered SNPs in larger clinical samples. The initial appeal of this strategy is obvious – it makes sound economic sense - but it has since been shown to introduce bias which can confound subsequently population genetic analyses. The problem of this ascertainment bias has affected almost every large-scale polymorphism discovery project to some extent, including The SNP Consortium and HapMap projects (Clark *et*

al., 2005) and affects the *DYNC1H1* study too. Ascertainment bias results from the fact that SNP discovery panels are often small, so that the probability that a SNP is identified in this sample, and later genotyped in a larger sample, is a function of the allele frequency (the probability of witnessing a rare allele is the same as its frequency). This conditional sampling of genetic variation imposes a bias, in that rare variants are likely to be missed in the larger sample. This frequency-specific distortion in SNP discovery consequently means that the SNP frequency spectrum obtained from a two-tier sampling will be different from that obtained under complete sampling (for example, by resequencing the entire study sample). As a result, statistical attributes that rely on the site frequency spectrum will be affected.

4.9.2 *DYNC1H1* chimpanzee genotyping

Before further analysis was undertaken, the ancestral allelic states of the 16 *DYNC1H1* SNP loci were assessed. Knowing the ancestral status of human polymorphisms can provide valuable evidence of evolutionary forces acting on the region. The 16 loci were genotyped, in 8 chimpanzees (*Pan troglodytes*) permitting alleles with MAF>6.25% be identified. DNA was extracted from chimpanzee blood (provided by the Institute of Zoology, London Zoo, Regents Park, UK) and genotyping conducted by bidirectional resequencing using identical primers and cycling conditions as those previously used on human samples.

	SNP number															
	1	2	3	4	5	6	7	8	9	10	11	12	13	14	15	16
Chimpanzee	G	A	A	T	A	A	G	A	G	C	G	G	T	G	G	G
Human	A	A	A	T	A	A	G	G	A	T	G	G	T	A	A	C

Table 4.8 Ancestral chimpanzee and common human *DYNC1H1* haplotypes

Ancestral alleles are shown in red and derived alleles in white. SNPs are indicated by position 5' to 3' along the gene

In the chimpanzee, all loci corresponding to the human SNPs were either monomorphic or polymorphic at an undetectable frequency (MAF<6.25%) in this small sample. There was concordance between the ancestral chimpanzee and the common human SNP allele at only 9 loci (Table 4.8). There is a direct relationship of a derived* allele with age (Kimura *et al.*, 1973) and it has been shown that (generally) for major SNP alleles with frequencies greater-than 80%, the major allele usually represents the ancestral allelic state (Hacia *et al.*, 1999). This implies there should be a preponderance of *DYNC1H1* major SNP alleles identical to the chimpanzee alleles, as they are all present in the CEPH at frequencies >>80% - however there is concordance between the two species

* A derived allele is the term given to a new allele produced by mutation

at only 9 of the 16 loci. Moreover, the ancestral chimpanzee haplotype is completely absent from the CEPH haplotype pool.

These relationships between allele frequencies and their age are generally true under conditions of neutrality. So, does this evidence suggest that neutrality may have been perturbed at this locus? An excess of high-frequency-derived mutations can be a signature of positive selection, or of genetic hitchhiking* with linked alleles driven rapidly to fixation (Smith *et al.*, 1974). However it may be a pronounced feature of a population bottleneck, so to discriminate between the two, additional populations could be useful.

4.9.3 Genetic variation of *DYNC1H1* in additional populations

To determine if the pattern of variation seen at the *DYNC1H1* locus in the European-derived CEPH samples was confined to northern Europe or common across populations, the 16 *DYNC1H1* SNPs were genotyped in 48 unrelated individuals from east Asia (Japan) and 49 unrelated individuals from West Africa, namely Bantu speaking Cameroonians. These samples were obtained from the laboratory of Professor David Goldstein, with full and appropriate consent for research. With the exception of SNP 16 in the Cameroonian samples (χ^2=10.8717; p<0.001), all SNPs were in HWE. There was no obvious reason why SNP 16 was not in HWE.

4.9.3.1 Allele frequency comparisons

Comparison of SNP frequencies, standardised by the derived CEPH allele, in each population, showed a clear reduction in allele frequency in the northern European-derived samples as compared to the other two populations (Figure 4.12).

Average gene diversity or expected allelic heterozygosity (H), which assesses the genetic diversity in a population and may be characteristically altered by natural selection, was calculated under the assumptions of HWE for each population, using Nei's measure of heterozygosity. Generally the average gene diversity was expected to be higher in the West African population than the Japanese or CEPH, as African populations are more diverse. Average gene diversity ($H \pm$ S.E.M) across the *DYNC1H1* locus was: northern Europeans 0.211±0.019, Japanese 0.317±0.016 and Cameroon 0.440±0.011. A clear gradient in allelic heterozygosity was observed from the northern Europeans, to the Cameroonians. This result is not unexpected as African populations generally display greater diversity and populations which have later migrated out of Africa possess a part of that diversity.

* Genetic hitchhiking occurs when alleles linked to a selected mutation, which is driven rapidly to fixation, are also dragged along to high frequency

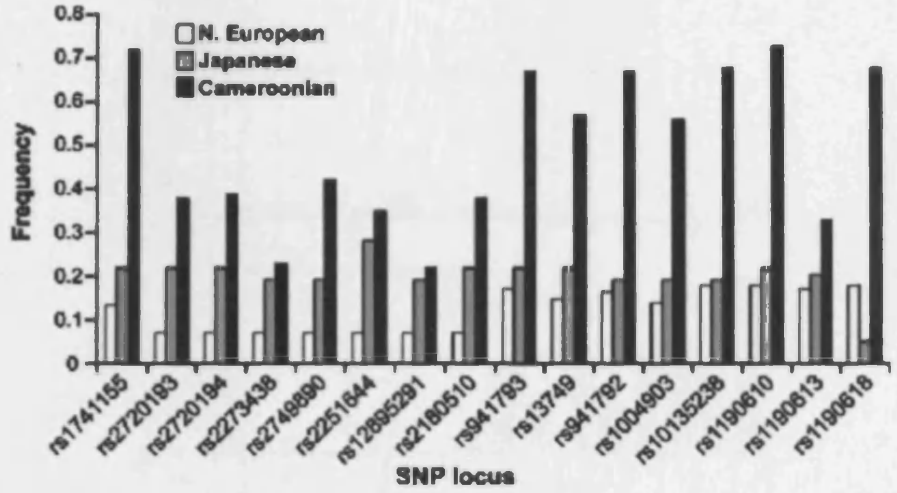

Figure 4.12 A comparison of *DYNC1H1* SNP allele frequencies between 3 populations

Minor allele frequencies are shown, standardized by allelic state in northern European, Japanese and Cameroonian populations.

4.9.3.2 Genetic differentiation

Interpopulation differences in gene diversity can be attributed to genetic differentiation due to causes including natural selection, population sub-division and admixture. To assess the possible role of selection in shaping population differentiation, Wright's F_{ST} is often calculated. This statistic allows allelic diversity of sub-populations to be measured against a global average to quantify genetic differentiation (varies between 0 and 1 with 1 being complete genetic differentiation). A modification of Wright's measure is Weir's weighted F_{ST}, which is used here to calculate total (global) and population pairwise comparisons of F_{ST} at each locus (Figure 4.13). Global F_{ST} (± SEM) averaged across the entire locus is 0.25±0.04 and pairwise comparisons of northern European against Japanese is 0.04±0.05; against Cameroonian is 0.37±0.056 and Japanese against Cameroonian is 0.29±0.065.

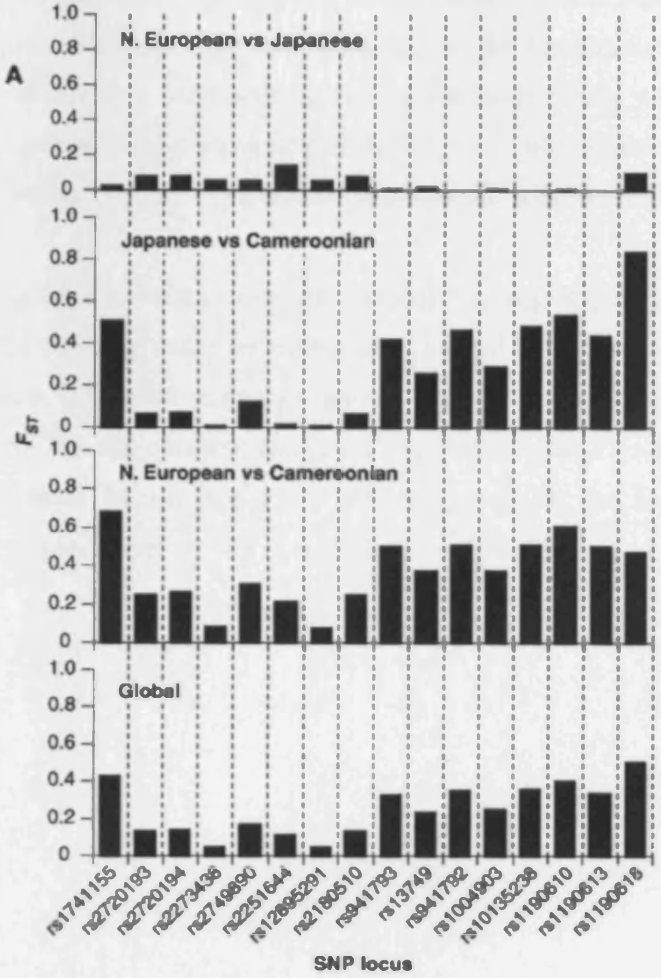

Figure 4.13 Global and pairwise F_{ST} comparisons

Weir's FST is shown for global and population comparisons at each SNP locus. The region bounded by SNPs rs2720193 and rs2180510 demonstrated less differentiation than other SNPs tested.

4.9.4 Haplotype and LD comparisons between three worldwide populations

The software PLEM was used to infer haplotypes for the unrelated Cameroonian and Japanese samples. Inferring haplotypes using unrelated samples can occasionally lead to spurious results and therefore haplotype frequencies were verified by reseeding the EM algorithm applied within PLEM with varying integers and also by using a second EM based program, SNPHAP, for conformation. No appreciable differences were seen in the results from varied seeds and either program. EM inference of Japanese haplotypes yields 9 haplotypes >1% frequency, suggesting a simple haplotypic structure of *DYNC1H1*. In contrast with both the northern European and Japanese haplotypes, there are 28 haplotypes exceeding an estimated population frequency of 1% in the Cameroonian samples. Generally, greater allelic and haplotypic diversity was seen in the Cameroonian population compared to the Japanese and European-derived, which is consistent with

other reports (Stephens *et al.*, 2001). Haplotype A, the most frequent haplotype in the CEPH at 74.2%, was found to be the highest frequency haplotype in all 3 populations: with frequencies of 67.9% and 21.4% in the Japanese and Cameroonians respectively (Table 4.9). Haplotype C is also common to all three populations and conversely to haplotype A which increases in frequency from the Cameroonian to northern European population, haplotype C is decreases in frequency.

A Ewens-Watterson test (F) was used to evaluate the observed haplotype frequency-distribution for goodness of fit with that expected under neutrality using the infinite alleles model of mutation (i.e. a model with no selection, where all mutations are selectively neutral) (Ewens, 1972; Watterson, 1978; Watterson, 1986). For the northern European population only, F is positive and significant (p=0.976) at the 0.05 level in this two-tailed test, implying that the haplotype distribution is inconsistent with neutral conditions devoid of selection.

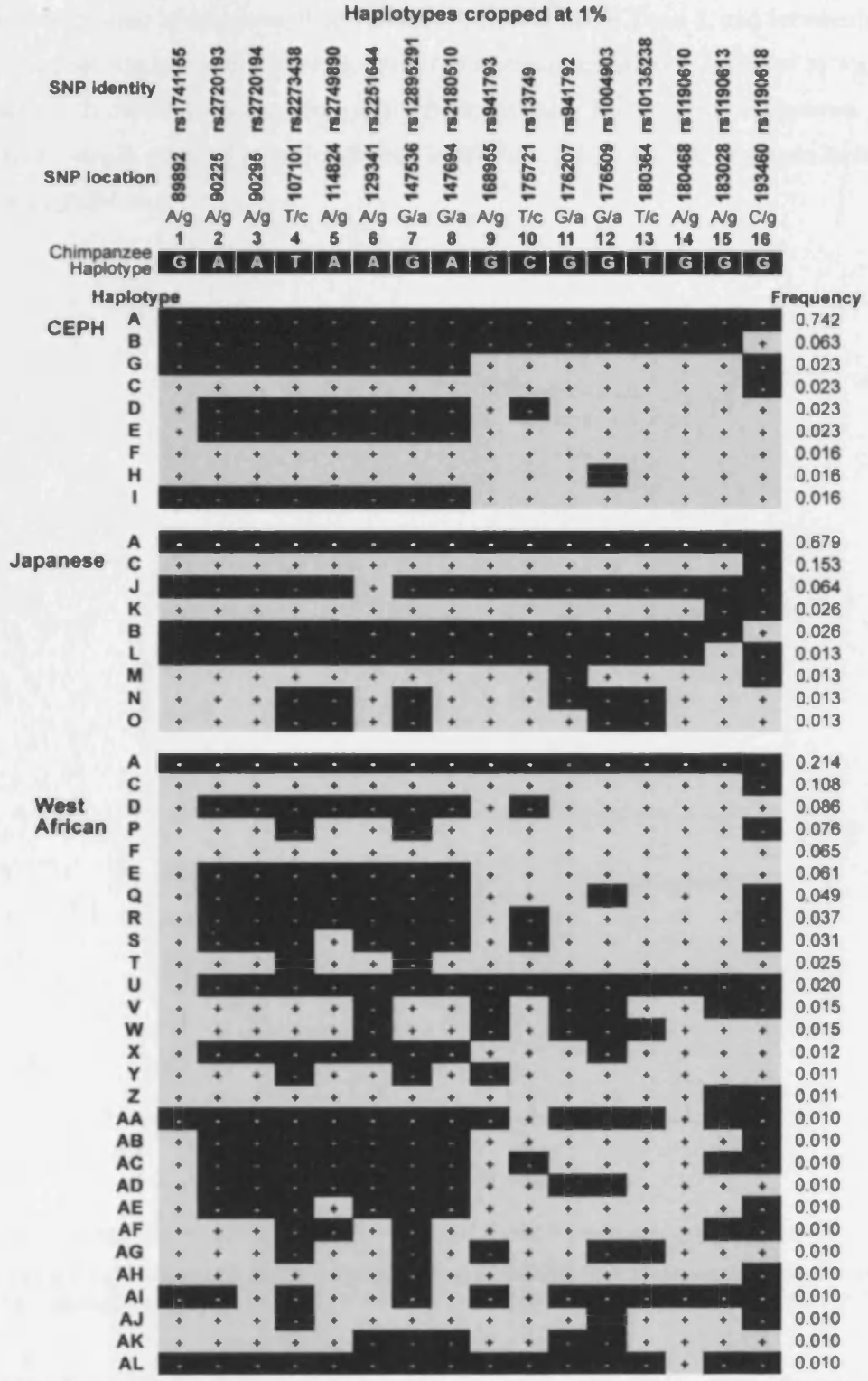

Table 4.9 Northern European, Japanese, Cameroonian and chimpanzee *DYNC1H1* haplotypes

Haplotypes >2% frequency shown with corresponding single letter identifiers. SNPs coded as major allele (-) and minor allele (+). Major SNP allele shown as uppercase.

The general pattern of pairwise LD in the Cameroonians was similar to that seen in the northern Europeans, comprising two regions of elevated LD between SNPs 2 and 8, and between 10 and 15. However, the pairwise LD values were the lowest of all three populations, reflected by a greater rate of LD decay with physical distance compared to the northern Europeans and Japanese. LD in the Japanese was a single elevated region delimited by SNPs 1 and 16 and LD was seen to decay at the lowest rate over distance.

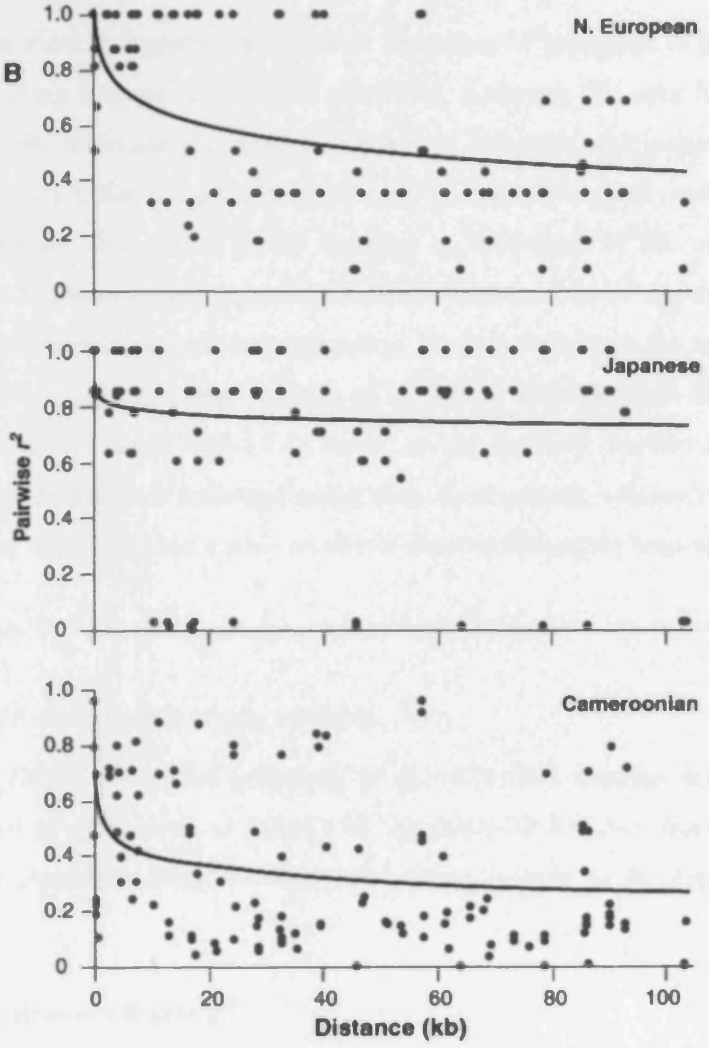

Figure 4.14 Linkage disequilibrium decay across *DYNC1H1* in 3 populations

Plotting pairwise r^2 values amongst the 16 SNPs spanning *DYNC1H1* in N. European, Japanese and Cameroonian populations against distance between each comparison illustrates three very different patterns of LD decay.

Pairwise haplotypic F_{ST} between populations was also calculated and F_{ST} comparisons were highly significant for both the northern Europeans and the Japanese against the Cameroonians (F_{ST}=0.228, p<<0.000001 and F_{ST}=0.1375, p<<0.000001) and just significant for the CEPH versus Japanese (F_{ST}=0.0348, p<0.02).

These results showed a general reducing cline in average gene diversity at *DYNC1H1* from the northern European to the Cameroonians. This reduction in variation was further illustrated by an elevated global F_{ST} value for all three populations combined, compared to the empirical genome-wide average of 0.123 (Akey *et al.*, 2002), largely due to the extent of differentiation between the northern Europeans and Japanese against the Cameroonians.

4.9.5 Natural selection at *DYNC1H1*?

The haplotype results show an approximate cline in frequency of haplotype A from West Africa, to East Asia and to northern Europe (21%, 68% and 74%). Although this may be due to population demography which can confound the genetic signals of selection, the concomitant decrease in frequency of haplotype C in these populations (11%, 15% and 2%) suggests mechanisms other than demography may operate. We asked if the increase in frequency of the common haplotypes, reduction in diversity and to some extent genetic differentiation, could be signals of selection at this locus rather than demographic or neutral processes. Positive selection for an allele can reduce genetic diversity, elevate LD and lower the rate of LD decay with physical distance (Bamshad *et al.*, 2003 see for review). The elevated LD levels in the northern Europeans compared to the Cameroonians may be a feature of selection rather than demography, although due to confounding by ascertainment bias, our results are unable to conclusively differentiate between the two.

4.10 Discussion

4.10.1 *DYNC1H1* association study caveats

The involvement of *DYNC1H1* in the pathology of sporadic ALS remains unclear. Although this study has not detected an association of *DYNC1H1* variants with SALS, it does not preclude a role of the gene as a susceptibility factor as there are several caveats to the approach that must be acknowledged.

4.10.1.1 An under-powered study?

The numbers of case and control samples used are likely to have not been amenable to detecting associated variants. As described previously, under optimistic allelic association conditions where $D'=1$, a sample size of 647 case individuals are required to achieve 80% power. In this study, although D' was approximately equal to 1, a maximum of only 281 cases were available for screening, giving 51% power to detect an association (at a marker/disease allele frequency of 12%). This relative power of detection could be improved by supplementing this analysis with additional cases and controls, collected since this study was undertaken.

4.10.1.2 Changes in study design?

Since this work began in 2002, there have been a number advances in our understanding of the problems and pitfalls associated with association studies and their design. There are countless variables that can be potentially altered in any LD-based association study, including: SNP ascertainment strategies, densities, minor allele frequencies, haplotype inference, tagging SNP selection which have all come under recent scrutiny. Many of the changes proposed were introduced too late to influence this study but mark essential considerations for future association studies:

4.10.1.2.1 Two-stage SNP ascertainment

SNP discovery and validation are two issues that many contemporary association studies will not have to face, having access to *a priori* information on LD patterns and tSNPs in many different populations from sources such as the HapMap project. SNP discovery and validation was essential in this study to identify the underlying pattern of LD across *DYNC1H1* and to select tSNPs, however, this may have introduced a source of potential bias that reduced the overall power of the association study. Identifying or validating SNPs in a smaller sub-sample of individuals, although a common sense approach for any investigator with limited resources, biases the distribution of variants detected towards high frequency common variation. The deficit of SNPs of low frequency in this two-stage* approach to SNP ascertainment means that the power to detect associations is reduced when the variants that actually cause disease are rare. Therefore, ascertainment bias may have eroded the power of this study to detect and tag rare variants associated with disease, when applied to a larger case/control sample. Conversely, the power to detect associations when the causal SNP is common is actually thought to be increased (Clark *et al.*, 2005).

* Two-stage SNP ascertainment describes the identification of SNPs in a limited sub-sample of individuals from which tagging SNPs are derived (stage one) and applied to test a larger sample of cases and controls (stage two). N.B. two-stage is not referred to here in terms of replication of a tSNP association in a larger sample set, as described in (Hirschhorn *et al.*, 2005).

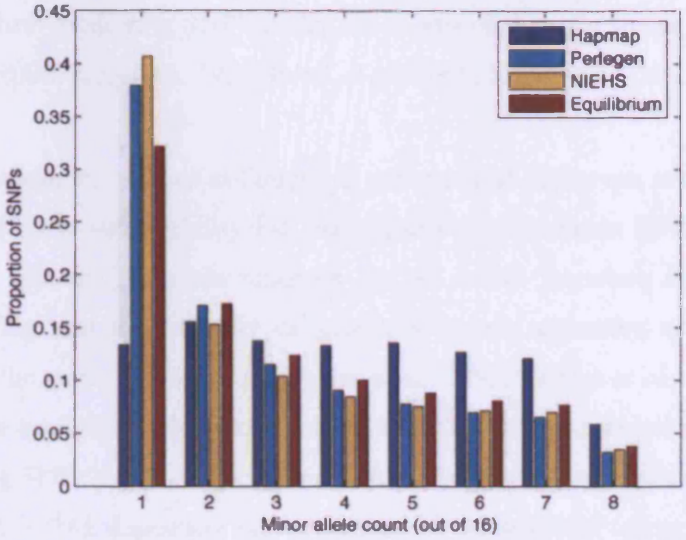

Figure 4.15 Site frequency spectra for empirical data with varying ascertainment bias

Site frequency spectra for the fully resequenced NIEHS gene set, for the Perlegen sequencing-by-hybridization SNP ascertainment set, and for the set of SNPs that the International HapMap consortium genotyped, all contrasted to the neutral expectation. Note the marked absence of rare SNPs and oversampling of SNPs of intermediate frequency in the HapMap sample. (From Clark *et al.*, 2005)

Ascertainment bias is a common issue, known to also have affected large polymorphism discovery projects including the Human Genome Project and the HapMap and to date few robust methods exist to avoid introducing this type of bias or for correcting biased data (Clark *et al.*, 2005).

4.10.1.2.2 What is the "right" SNP density and allele frequency?

Over the last five years, the most appropriate SNP density for association studies has been under considerable debate. Early studies using marker densities varying from SNP per kb to one SNP per 15kb (Dawson *et al.*, 2002; Jeffreys *et al.*, 2001; Patil *et al.*, 2001) demonstrated that the extent of linkage disequilibrium is inversely related to marker density. Although this holds true for fine-scale LD, broader patterns of LD remain relatively insensitive to SNP (Ke *et al.*, 2004). Gabriel and colleagues suggested that as a trade-off, using a SNP density of one common SNP every 7.8kb would be sufficient to capture the majority of common haplotype variation throughout the genome (Gabriel *et al.*, 2002). However, Wang and Todd showed in 2003 using simulated data, that incomplete SNP maps of 1 SNP per 2.5kb, 5kb and 10kb ascertained approximately 75%, 50% and 40% of the total underlying common SNP variation, respectively, implying that only dense SNP maps would be useful for indirect association mapping (Wang *et al.*, 2003). Choosing an appropriate marker density for an association study SNP map relies on a number of factors including SNP ascertainment criteria, SNP frequency, LD and tagging methods used (Wang *et al.*, 2003). The HapMap has settled on map densities of 5kb (Phase I) and 1kb (Phase II) to provide researchers with data on fine-scale variation in LD and it is this information that will most likely

influence future studies: modifying SNP density for an association study according to the extent of LD (Dunning *et al.*, 2000; Kruglyak, 1999; Pardi *et al.*, 2005; Reich *et al.*, 2001a)

Almost all recent association studies utilising LD patterns and haplotype structures in the human genome to identify disease susceptibility loci, have focused on common SNPs with a minor allele frequency of 5% or greater. The main rationale for this is the "common allele-common disease hypothesis" suggesting that the majority of common genetic disorders are caused by genetic variants common in the general population (Bueler *et al.*, 1993; Collins *et al.*, 1997; Lander, 1996). However, despite the limitations stipulated by the CDCV hypothesis, several authors have recently demonstrated that tag SNPs chosen from common (MAF ≥5%) variants can capture a proportion of rare alleles (1%<MAF<5%), dependent on the method of tag selection (using an exhaustive allelic transmission disequilibrium test, or EATDT, approach) (de Bakker *et al.*, 2005; Lin *et al.*, 2004). An interesting development of the influence of allele frequencies to the outcome of association studies comes from the frequency matching of SNPs. It was recently empirically shown that using the r^2 LD measure, if SNPs of equal or near equal frequency are compared, the correlation between them more accurately represents the true correlation than of SNPs of unmatched frequencies (Eberle *et al.*, 2006) (an intuitive result considering the derivation of the r^2 equation). Although the resulting impact of this finding on the power of tag SNPs selected from these frequency matched variants has not yet been investigated, this information taken together with the EATDT data, may mean that future studies will not be worried so much about minimum MAF of each SNP, but more so about ensuring that MAFs are approximately equal.

4.10.1.2.3 Tag SNP selection

There are myriad algorithms implemented in software currently available to select tagging SNPs from genotype data (see Table 1 from (Halldorsson *et al.*, 2004) for example and see (de Bakker *et al.*, 2005; De La Vega *et al.*, 2006; Howie *et al.*, 2006; Liu *et al.*, 2006)). It is beyond the scope of this thesis to review the relative merits of these algorithms against the TagIT method implemented in this study however, the TagIT routine (i.e. not the algorithm, but the way it is implemented) has been updated since its use in this study by Ahmadi *et al.* (Ahmadi *et al.*, 2005) and can be assessed.

If an identical data analysis was undertaken today, the criterion used in the TagIT routine would be based on a 'worst locus' (TagIT criterion 11) rather than 'average locus' (TagIT criterion 5) which describes how the tSNP set of any size is described in terms of its performance against all of the original SNPs it was derived from (Ahmadi *et al.*, 2005). The 'worst locus' approach returns a single value based on the minimum performance of any tSNP set, where as the 'average locus'

approach returns a weighted average value. In this respect, the 'worst locus' approach is more conservative and provides a minimum performance for a tSNP set. Based on the original data and analysed with criterion 11, a minimum of 3 tSNPs would be needed to provide a minimum haplotype r^2 performance >0.85 (data not shown), implying that some regions of the gene may not have been sufficiently represented in the original study, thus reducing power to detect an association.

4.10.2 Case sample heterogeneity

As previously described in this chapter, the 281 sporadic ALS samples used in this study were obtained retrospectively with little accompanying phenotypic information. There was some variation in the pattern of onset amongst patients, with approximately a third of all patients presenting with either (i) early onset in the lower extremities, (ii) upper onset and (iii) with bulbar onset. Although these patients were screened by the El Escorial criteria, it is not known what proportion of patients were possible, probable or definite ALS and what proportion were diagnosed later with primary lateral sclerosis or primary muscular atrophy. These variations of ALS may have slightly different pathogenesis and therefore it is conceivable that different genes may be involved. Such phenotypic (and potentially genetic) heterogeneity can reduce the power of a candidate gene association study to identify a true association. In addition, genetic heterogeneity may have been introduced by the unknown *SOD1* status of the case samples, which may have again reduced study power.

4.10.3 The availability of HapMap data

With SNP and HapMap data now available, the extent of power lost in using the study design adopted here could be cursorily examined. At the beginning of 2007, information on 42 coding SNPs within *DYNC1H1* was available from dbSNP (which contrasts starkly to the single coding SNP discovered in this study) and 95 SNPs were identified from HapMap in the ~121kb sequence surrounding the *DYNC1H1* locus. After trimming of SNPs with MAF<1%, 56 SNPs remained, giving an average SNP density of 1 SNP per ~2.1kb – over three-times the density empirically determined in this study. The HapMap data was analysed using Tagger, with MAF set to 0.01, 0.05 and 0.07, HWE p-value cut-off at 0.001, and minimum percentage genotype at 75%. At all MAF thresholds, strong LD was identified.

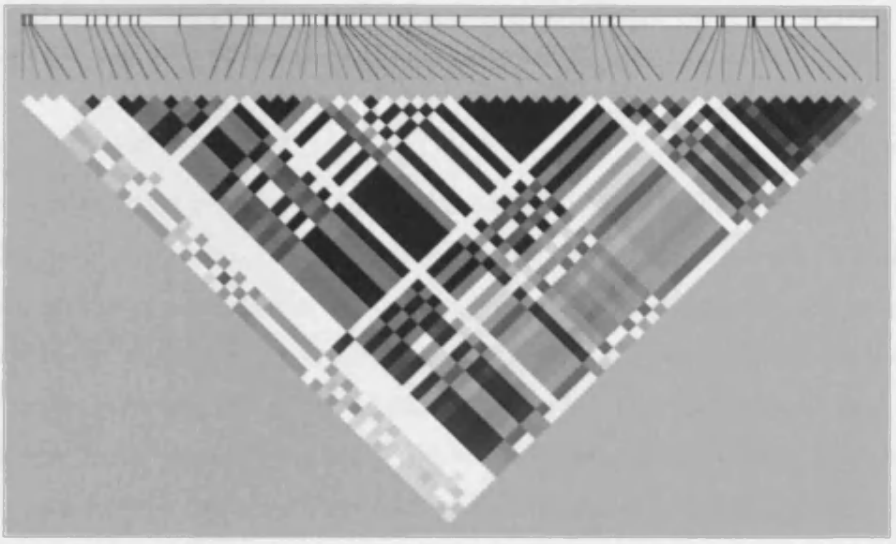

Figure 4.16 Linkage disequilibrium (r^2) across DYNC1H1 identified using HapMap data

SNPs from 121kb region centring on *DYNC1H1* were analysed using Haploview. Only SNPs with MAF ≥1% were included in the analysis.

It is difficult to directly compare the experimentally derived data with that from the HapMap as they are composed of different SNP sets, obtained in different ways and analysed by different methods. Using the aggressive tagging approach implemented in Haploview (pairwise tagging and by 2 and 3 SNP haplotypes), only 63% of SNPs with MAF ≥1% could be tagged by two tSNPs r^2>0.8 (mean r^2=0.97). Both of these tSNPs (rs10135238 and rs2251644) were identified in the *DYNC1H1* study and one, tSNPs (rs2251644), was used to interrogate case and controls. It could be extrapolated therefore, that the original tSNPs from the association study may have only tagged ~63% of SNPs ≥ 1% frequency.

5 Genetic analysis of the cytoplasmic dynein subunit families

5.1 Introduction

The absence of association between *DYNC1H1* and sporadic ALS and the propensity for ALS and other neurodegenerative disorders to demonstrate genetic heterogeneity provides a compelling case to investigate additional components of the cytoplasmic dynein complex for association with disease. The work presented in this chapter was born through a necessity for clarification of the mouse and human cytoplasmic dynein subunit data presented in the literature and in databases including nomenclature, genetic mapping positions and family relationships. The chapter begins with a justification for why this work was considered necessary and the results of an effort to collate the varied aliases historically applied to the subunits. Clarifying the cytoplasmic dynein subunit mapping positions is presented next, describing an *in silico* methodology which also provided an excellent opportunity to survey both mouse and human genomes for novel cytoplasmic dynein paralogs. This chapter concludes with an *in silico* experiment to identify cytoplasmic dynein subunit orthologs, a description of how these data have aided the implementation of a new system of nomenclature and the direction in which these results may lead a future dynein and ALS association study.

5.1.1 Beyond the cytoplasmic dynein heavy chain – the need to consider pathways

Despite the evidence implicating *DYNC1H1* as both a causal locus and susceptibility factor for ALS and other motor neuron disorders, no association with disease has yet been found. As discussed previously, one potential explanation may be the confounding effect of non-allelic genetic heterogeneity (mutations in different genes resulting in identical phenotypes) reducing the power to detect a disease-associated variant. The propensity for familial ALS cases to demonstrate genetic heterogeneity and the precedence of genetic heterogeneity within single pathways in other neurodegenerative diseases (such as the APP pathway in Alzheimer's), it is plausible that genetic heterogeneity within the dynein pathway may elicit an ALS phenotype. In addition, tantalising evidence for dynein associated non-allelic genetic heterogeneity has come from the investigation of the dynein-associated complex dynactin, a subunit of which is mutated in familial forms of motor neuron disease (Munch *et al.*, 2005; Puls *et al.*, 2003). The next line of enquiry of the role of the cytoplasmic dyneins in ALS and other motor neuron disorders should consider subunits additional to the heavy chains of the dynein complex.

5.1.2 The cytoplasmic dynein subunits and a need for clarity

Cytoplasmic dynein is a large multi-subunit complex which, at its core, consists of a heavy chain homodimer bound by various intermediate, light intermediate and light chain polypeptides (Figure 5.1A, right panel).

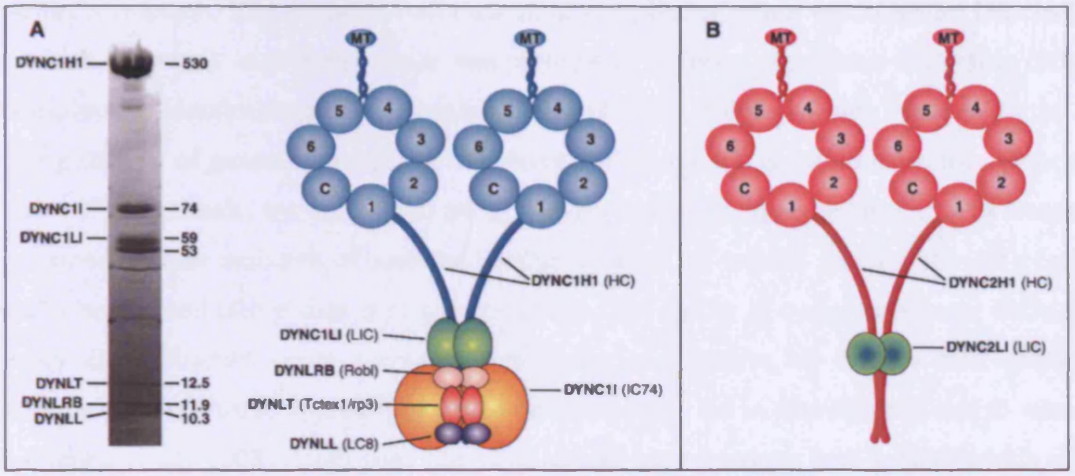

Figure 5.1 The mammalian cytoplasmic dynein complexes

A. (left panel) Polypeptides of immunoaffinity purified rat brain cytoplasmic dynein. Polypeptide mass (kDa) and consensus family names are indicated. (right panel) Structural model of the cytoplasmic dynein complex: comprising a DYNC1H1 homodimer core and intermediate, light-intermediate and light chain subunits. **B**. Structural model of the cytoplasmic dynein 2 complex. DYNC2H1 is predicted to be similar to that of the cytoplasmic dyneins. DYNC2LI1 is the only known subunit of this complex. (Pfister *et al.*, 2005b)

Investigation of these subunits as potential candidate loci for ALS and other motor neuron diseases exposed confusion associated with their nomenclature and the mapping positions of their genes in the literature and within databases. Before further study could be undertaken to investigate the dynein complex as a candidate in ALS, it was necessary to clarify the number of dynein subunits, their names, mapping positions and other information relevant for further study.

5.1.3 Standardising nomenclature – why agreeing a name for each gene is important.

The need to standardise human gene nomenclature was recognised as early as the 1970s when the first guidelines for human gene nomenclature were presented at the Edinburgh Human Genome Meeting (Shows *et al.*, 1979) and is based largely on the fact that many genes share a common origin. The accepted dogma is that all present-day genes are likely to be derived from a 'core' of between 7,000 and 12,000 ancestral genes that existed more than 500 million years ago (Nebert *et al.*, 2003). Therefore present-day genes, which exhibit homology within and between species, can be clustered together as families, and as such, should be identified as being related by being designated with a similar symbol.

However, in practice scientific communities working on diverse organisms have regularly named genes and proteins in an uncoordinated manner (see for example names such as 'daughterless', 'groucho' and 'saxophone' used by fruit-fly geneticists). These genes often have homologs in other species that may be given names based on a different nomenclature system specific to that community's research. The situation becomes more complicated when you consider bias in letter usage which can result in different genes and proteins of different organisms, with quite different functions, having identical names and symbols (Nebert *et al.*, 2004) - or vice versa. With the ever expanding number of genome sequencing initiatives (409 eukaryote genomes have been sequenced, of which 107 are animals; www.ncbi.nlm.nih.gov/entrez/query.fcgi?db=genomeprj, as of November 2006), providing vast amounts of gene and sequence data for myriad species, the only feasible method to handle and utilize data is to use computers. The ability of current computer software to accurately and efficiently cross-reference, cross-index and analyse all of thse data, requires a systematic and co-ordinated approach to gene nomenclature to aid in data retrieval and to minimise errors (Nebert *et al.*, 2003). Each gene therefore should have a unique core symbol which can be applied and amended to other members of a gene family (Wain *et al.*, 2002).

One well utilised method for identifying members of a gene family prior to standardising their nomenclature is to use evolutionary trees– a phylogenetic approach –which has already been used for over 124 families/superfamilies (Nebert *et al.*, 2004).

5.2 Clarifying mouse and human cytoplasmic dynein subunit nomenclature, genomic locations and accession numbers

Research on the cytoplasmic dynein subunits has historically been undertaken in myriad organisms from yeast (*Saccharomyces cerevisiae*) to humans (*Homo sapiens*). The nomenclature of mammalian genes encoding these proteins has drawn on homologs in other organisms, which in turn have often been defined and named by criteria such as their molecular mass and mobility on sodium dodecyl sulphate–polyacrylamide electrophoresis (SDS-PAGE) gels (Figure 5.1A, left panel) (Pfister *et al.*, 2005b). Consequently a number of synonyms can be found for any given human or mouse cytoplasmic dynein subunit. Much of the early research into the cytoplasmic dyneins was conducted in the biflagellate green alga *Chlamydomonas,* on the dyneins found in the flagellar axoneme, and therefore some mammalian cytoplasmic dynein nomenclature derives from these studies. For example, mammalian members of the cytoplasmic light chain families DYNLRB and DYNLL have commonly been referred to as LC7 and LC8 respectively, which are the names of homologous *Chlamydomonas* axonemal dynein subunits.

The lack of consistency and coordination of dynein nomenclature has also led to the erroneous cross-indexing of gene names and other data on databases. Consequently, this has introduced errors in nomenclature, mapping position and in the sequence accession numbers into the databases, which are propagated onto additional databases and even into the literature (the opposite is also true; errors in the literature are propagated onto database entries). For example, searching NCBI LocusLink for human and mouse gene entries with the root symbol 'dhc', often prefixed to the cytoplasmic dynein gene names, gives 17 results which include cytoplasmic and axonemal dyneins, several different enzymes and transmembrane proteins (Table 5.1).

Gene name	Organism	Gene symbol	LocusLink*
Cytoplasmic dynein heavy chain 1	*Homo sapiens*	*DHC1*	1778
Dynein heavy chain domain 1	*Homo sapiens*	*DHCD1*	144132
Axonemal dynein heavy chain 12	*Homo sapiens*	*DHC3*	8679
Transmembrane 7 superfamily member 2	*Homo sapiens*	*DHCR14*	1717
Lamin B receptor	*Homo sapiens*	*DHCR14B*	3930
7-dehydrocholesterol reductase	*Mus musculus*	*Dhcr7*	13360
3-beta-hydroxysterol delta-24 reductase	*Mus musculus*	*Dhcr24*	116932

Table 5.1 NCBI LocusLink human and mouse genes containing the root symbol 'dhc'
Search limited to records created between 1995 and 2004. *LocusLink accession number

5.2.1 Collating human and mouse cytoplasmic dynein subunit synonyms

To identify the extent and variety of synonyms in use, literature searches were conducted using PubMed and the online databases MGI, NCBI (including LocusLink/Entrez Gene) and Ensembl (all searches were carried out between January and July 2004). For fast interrogation of online bioinformatics resources, the bioinformatics meta-search engine Bioinformatic-Harvester was also used. Table 5.2 lists aliases, map position and protein/DNA sequence accession data identified for each known mouse and human cytoplasmic dynein gene. More synonyms were observed in online databases than cited in the literature, which most likely reflects both the automated collection/annotation approach of database records and the lack of curation/review of these entries. The origins of each cytoplasmic dynein subunit synonym were traced to verify their validity ensuring for example, that the synonym did not simply represent a typographical error.

Many of the synonyms identified were named in accordance with their method of detection – projects responsible for originally identifying a gene or gene product, or projects detecting previously identified genes or gene product. For example (from Table 5.2), the 'MGC' prefixes are from the National Institutes of Health Mammalian Gene Collection (MGC) as part of an initiative to identify and sequence cDNA clones containing a full-length open reading frame for human, mouse and rat (Strausberg *et al.*, 2002). 'CGI' prefixes are assigned by the Comparative Gene

Identification study, which use the *Caenorhabditis elegans* (*C. elegans*) proteome as an alignment template to assist in novel human gene identification from human EST nucleotide databases (Lai *et al.*, 2000). 'Rik' suffixes are aliases assigned by the Riken Genomic Sciences Centre (http://genome.gsc.riken.jp).

5.2.2 The many names of *cytoplasmic dynein 1 heavy chain 1*

Amongst the cytoplasmic dynein subunits, *DYNC1H1* had the greatest number of synonyms published in the literature and online, with 15 aliases published for the human heavy chain and 9 for the mouse. Some alternative cytoplasmic dynein gene names were from large-scale gene and transcript identification efforts such as the partial *DYNC1H1* clone KIAA0325 and its mouse homolog 'mKIA00325', generated by the Kazusa cDNA project (Ohara *et al.*, 1997). A small number of gene names were derived from DNA markers and cDNA clones used to identify the genes, for example, *DYNC2LI1* was named DKFZp564A033 after the cDNA sequence and clone of the same name and *DYNC1H1* referred to as Hp22 after a marker generated from its human cDNA sequence, as well as the rat-derived marker Rk3-8 and a cDNA clone named HL-3.

Two synonyms for mouse and human *DYNC1H1* that were investigated and ultimately rejected were 'cell division cycle 22' (CDC22) and 'cell division cycle 23' (CDC23), respectively. The mouse CDC22 alias was annotated on to the NCBI entry for *Dync1h1* full-length mRNA (Acc. NM_030238; sequence revision history 21 December 2003) and partial mRNA (Acc. BC004751; sequence revision history 16 April 2003), and was also found at the MGI database (Figure 5.2). The human CDC23 alias was annotated on to the NCBI entry for *DYNC1H1* full-length mRNA (Acc. NM_001376; sequence revision history 23 December 2003) and partial mRNA mRNA (Acc. BC021297; sequence revision history 9 December 2003) (Figure 5.2). The validity of these aliases were investigated by first conducting literature searches using the search terms 'CDC22', 'CDC23' and 'cell division cycle' and identifying any papers citing these terms in association with cytoplasmic dynein. No citations of these terms were found or with the name 'cytoplasmic dynein chain' with the suffixes '22' and '23'. This suggested that the error was most probably generated and propagated solely on the database.

Figure 5.2 Mouse and human *DYNC1H1* synonyms from the Entrez database at NBCI

Screen-shot of the NCBI sequence database entry for human *DYNC1H1* mRNA sequence, accession number NM_001376 (A) and mouse *Dync1h1* mRNA sequence, accession number NM_030238 (B). Synonyms listed within the entry are indicated by the red arrow and CDC22 and "cytoplasmic dynein complex" are boxed in red. Database accessed April 2004.

To test the validity of these synonyms and to identify if they had been assigned based on sequence homology to other known proteins, homology searches were conducted. Human and mouse CDC23 and CDC22 cDNAs and protein sequences were obtained by searching GenBank using the terms 'CDC23' and 'CDC22'. The GenBank entries for CDC23 were listed as "cell division cycle protein..... homologous to *Saccharomyces cerevisiae* cdc23", however no entries were seen for CDC22. The yeast cdc23 protein, a component of anaphase-promoting complex (APC), is essential for cell cycle progression through the G2/M transition and highly conserved in eukaryotic cells, was also included for comparison. The human and mouse dynein heavy chains were compared against the human and mouse cell division cycle subunits and against two different yeast cell division cycle subunits using BLAST. The *Schizosaccharomyces pombe* cdc22 protein, which shows no significant homology to *S. cerevisiae* cdc23 was included as a possible homolog of the mouse CDC22. Both cDNA and protein alignments were conducted using ClustalW. No significant similarity was seen between the dynein heavy chains and the cell division cycle proteins at both the nucleotide of protein level (data not shown).

Cytoplasmic dynein gene family	Official gene name HUGO[a] (human)	Aliases	Location Human (Hsa) NCBI[b] Mouse (Mmu) MGI[c]	Entrez Gene ID[d] (human and mouse) *MGI ID (mouse)*	mRNA (NCBI RefSeq accession numbers)	Protein (NCBI and SwissProt[e] accession numbers)
Cytoplasmic dynein 1 heavy chain	DYNC1H1	**Human** DNCHC1 (Ahmad-Annuar *et al.*, 2003) DNECL (Narayan *et al.*, 1994) Hp22 (Vaisberg *et al.*, 1993) pM7 (Vaughan *et al.*, 1996) Rk3-8 (Vaughan *et al.*, 1996) DHC1 (Vaisberg *et al.*, 1996a) DHC1a (Gibbons *et al.*, 1994) MAP1C (Paschal *et al.*, 1987) DNCL (HGNC, 2004) HL-3 (Vaughan *et al.*, 1996) KIAA0325 (Ohara *et al.*, 1997) AB002323 (Nagase *et al.*, 1997) Dyh1 (Byers *et al.*, 2000) cDHC (Harada *et al.*, 1998) DYHC_HUMAN[e]	Hsa14q32	1778	NM_001376	NP_001367 Q14204
	Dync1h1	**Mouse** Dnchc1 (Vaughan *et al.*, 1996) cDHC (Harada *et al.*, 1998) Loa (Witherden *et al.*, 2002) Rk9-32 (Vaughan *et al.*, 1996) Dnec1 (HGNC, 2004) DNCL (Fridolfsson *et al.*, 1997) MAP1C (Mikami *et al.*, 1993) mKIAA0325 (MGI, 2004; Okazaki *et al.*, 2003) DYHC_MOUSE[e]	Mmu12 (55cM)	13424 *103147*	NM_030238	NP_084514 Q9JHU4
Cytoplasmic dynein 2 heavy chain	DYNC2H1	**Human** DHC2 (Criswell *et al.*, 1996; Vaisberg *et al.*, 1996a) DHC1b (Criswell *et al.*, 1996) DLP4 (Tanaka *et al.*, 1995) DYH1B (Gibbons, 1995) Dyh2 (Byers *et al.*, 2000) hdhc11 (Neesen *et al.*, 1997) FLJ11756 (Ota *et al.*, 2004)	Hsa11q21-q22.1	79659	XM_370652	XP_370652 O00432
	Dync2h1	**Mouse** Dnchc2 (Mouse Genome Informatics, 2004) Mdhc11 (Neesen *et al.*, 1997)	Mmu9 (1cM)	110350 *107736*	XM_358380	XP_358380 O08822
Cytoplasmic dynein 1 intermediate chain	DYNC1I1	**Human** IC1 (Vaughan *et al.*, 1995) IC74 (Paschal *et al.*, 1992b) IC74-1 (Susalka *et al.*, 2002) D1 IC74 (Grissom *et al.*, 2002) DH IC-1 (Online Citation assigned by submitter, 1998) DNCI1 (Crackower *et al.*, 1999) DYI1_HUMAN[e]	Hsa7q21.3-q22.1	1780	NM_004411	NP_004402 O14576
	Dync1i1	**Mouse** Dncic1 (Mouse Genome Informatics, 2004) Dnci1 (Crackower *et al.*, 1999) DYI1_MOUSE[e]	Mmu6 (4cM)	13426 *107743*	NM_010063	NP_034193 O88485
	DYNC1I2	**Human** IC2 (Vaughan *et al.*, 1995) IC74-2 (Susalka *et al.*, 2002) DH IC-2 (NCBI: Online Citation assigned by submitter, 1998) DYI2_HUMAN[e]	Hsa2q31.1	1781	NM_001378	NP_001369 Q13409

	Dync1i2	**Mouse** Dncic2 (Mouse Genome Informatics, 2004) Dnci2 (Crackower *et al.*, 1999) DYI2_MOUSE*	Mmu2 (41cM)	13427 *107750*	NM_010064	NP_034194 O88487
Cytoplasmic dynein 1 light intermediate chain	**DYNC1LI1**	**Human** Light chain A (NCBI, 2004e) D1LIC (Grissom *et al.*, 2002) LIC57/59 (Hughes *et al.*, 1995) LIC-1 (Hughes *et al.*, 1995) DYJ1_HUMAN*	Hsa3p22.3	51143	NM_016141	NP_057225
	Dync1li1	**Mouse** Dnclic1 (Mouse Genome Informatics, 2004) MGC32416 (NCBI, 2004f)	Mmu9 F3	235661 *2135610*	NM_146229	NP_666341
	DYNC1LI2	**Human** LIC53/55 (Hughes *et al.*, 1995) LIC-2 (Hughes *et al.*, 1995) DYJ2_HUMAN*	Hsa16q22.1	1783	NM_006141	NP_006132 O43237
	Dync1li2	**Mouse** Dnclic2 (Mouse Genome Informatics, 2004)	Mmu8 (50cM)	110801 and see 234663 *107738*	XM_134573	XP_134573
Cytoplasmic dynein 2 light intermediate chain	**DYNC2LI1**	**Human** D2LIC (Grissom *et al.*, 2002) LIC3 (Mikami *et al.*, 2002b) CGI-60 (Mikami *et al.*, 2002a; NCBI, 2004a) DKFZP564A033 (NCBI, 2004a)	Hsa2p25.1-p24.1	51626	NM_016008 (isoform 1) NM_015522 (isoform 2)	NP_057092 (isoform 1) NP_056337 (isoform 2)
	Dync2li1	**Mouse** 4933404O11Rik (NCBI, 2004g) D2LIC (NCBI, 2004g) mD2LIC (NCBI, 2004g) MGC7211 (NCBI, 2004g) MGC40646 (NCBI, 2004g)	Mmu17 E4	213575 *1913996*	NM_172256	NP_758460
Cytoplasmic dynein Tctex1 light chain	**DYNLT1**	**Human** TCTEL1 (Watanabe *et al.*, 1996) Tctex1 (King *et al.*, 1996c; Lader *et al.*, 1989) Protein CW-1 (Mueller *et al.*, 2002) DYLX_HUMAN*	Hsa6q25.3	6993	NM_006519	NP_006510 Q15763
	Dynlt1	**Mouse** Tctex1 (King *et al.*, 1996c) Tcd1 (King *et al.*, 1996c; Lader *et al.*, 1989) DYLX_MOUSE*	Mmu17 (4cM)	21648 *98643*	NM_009342	NP_033368 P51807
	DYNLT3	**Human** TCTE1L (Roux *et al.*, 1994) rp3 (Roux *et al.*, 1994) TCTEX1-L (Roux *et al.*, 1994) TCTL_HUMAN*	HsaXp21	6990	NM_006520	NP_006511 P51808
	Dynlt3	**Mouse** Tcte1l (Mouse Genome Informatics, 2004) 2310075M16Rik (Shibata *et al.*, 2000) TCTL_MOUSE*	MmuX A1.1	67117 *1914367*	NM_025975	NP_080251 P56387
Cytoplasmic dynein light chain Roadblock	**DYNLRB1**	**Human** MGC15113 (NCBI, 2004d) DNCL2A (Jiang *et al.*, 2001) bithoraxoid-like protein (BLP) (Bowman *et al.*, 1999; Dole *et al.*, 2000) BITH (Fracchiolla *et al.*, 1999) hkm23/mLC7-1 (Tang *et al.*, 2002b) Robl1 (Nikulina *et al.*, 2004) Roadblock(robl)/LC7 (Bowman *et al.*, 1999) HSPC162 (Quackenbush *et al.*, 2001; Zhang *et al.*, 2000) DL2A_HUMAN*	Hsa20q11.21	83658	NM_014183 (isoform a) NM_177953 (isoform b) NM_177954 (isoform c)	NP_054902 Q9NP97 (isoform a) NP_808852 (isoform b) NP_808853 (isoform c)

	Dynlrb1	**Mouse** Dncl2a (Mouse Genome Informatics, 2004) Dnclc2A km23/mLC7-1 (Tang *et al.*, 2002b) 2010012N15Rik (Shibata *et al.*, 2000) 2010320M17Rik (Shibata *et al.*, 2000) **DL2A_MOUSE***	Mmu2 H1	67068 *1914318*	NM_025947	NP_080223 Q88567
	DYNLRB2	**Human** DNCL2B (Jiang *et al.*, 2001) bithoraxoid-like protein (BLP) (Bowman *et al.*, 1999; Dole *et al.*, 2000) Robl2 (Nikulina *et al.*, 2004) LC7-like (Jiang *et al.*, 2001) mLC7-2 (Tang *et al.*, 2002b) DL2B_HUMAN*	Hsa16q23.3	83657	NM_130897	NP_570967 Q8TF09
	Dynlrb2	**Mouse** Dncl2b (Mouse Genome Informatics, 2004) DL2B_MOUSE*	Mmu8 E1	75465 *1922715*	NM_029297	NP_083573 Q9DAJ5 AAH48623
Cytoplasmic dynein light chain LC8	**DYNLL1**	**Human** DCL1 (Naisbitt *et al.*, 2000a) DNLC1 DNCL1 (Cras-Meneur *et al.*, 2004) Mr 8000 LC (King *et al.*, 1996b) Mr 8000 DLC (King *et al.*, 1995) DLC8 (Espindola *et al.*, 2000) LC8 (Pazour *et al.*, 1998) LC8a (Wilson *et al.*, 2001) PIN (Jaffrey *et al.*, 1996) hdlc1 (Dick *et al.*, 1996b) Dlc-1 (Crepieux *et al.*, 1997) DYL1_HUMAN*	Hsa12q24.31	8655	NM_003746	NP_003737 Q15701
	Dynll1	**Mouse** Dnclc1 (Mouse Genome Informatics, 2004)	Mmu5 F	56455 *1861457*	NM_019682	NP_062656 Q9D6F6
	DYNLL2	**Human** DLC2 (Naisbitt *et al.*, 2000a) LC8b (Wilson *et al.*, 2001) MGC17810 (NCBI, 2004c)	Hsa17q23.2	140735	NM_080677	NP_542408
	Dynll2	**Mouse** Dlc2 (Mouse Genome Informatics, 2004) 1700064A15Rik (NCBI, 2004b) 6720463E02Rik (NCBI, 2004b)	Mmu11 C	68097 *1915347*	NM_026556	NP_080832

Table 5.2 Human and mouse cytoplasmic dynein genes and map positions

Mapping prefixes are Hsa (*Homo sapiens*) and Mmu (*Mus musculus*) followed by the chromosomal localisation. All databases were accessed November 2005.
[a] HUGO: www.gene.ucl.ac.uk/nomenclature/
[b] NCBI: www.ncbi.nlm.nih.gov
[c] MGI: www.informatics.jax.org/; mapping position shown in cM or cytogenetic band
[d] NCBI Entrez Gene: www.ncbi.nih.gov/entrez/query.fcgi?db=gene
[e] SwissProt: http://ca.expasy.org/sprot/
* name as given by SwissProt

5.2.3 Clarifying subunit mapping positions and identifying paralogs

Mapping positions of mouse and human cytoplasmic dynein subunits were clarified by identifying regions of sequence homology between the dynein subunit sequences, available from the sequence databases, and the mouse or human genome assembly. The elegance of this method was that it provided an assumption-free approach to identifying cognate genetic loci as it did not rely on *a priori* data from the literature or databases. However, published data obtained through PubMed

literature searches and from the online databases MGI, NCBI (including LocusLink and OMIM) and Ensembl, was also used, but only when corroborated by the sequence alignment results. Genome alignments were conducted using megaBLAST, with default settings and restricted to human and mouse genomes only. To designate the alignment of a query sequence against the genome as a cognate dynein subunit genetic locus, the following specified criteria had to be met:

1. the entire query sequence must align to discrete region of the genome
2. the alignment must demonstrate a rational genomic architecture – conservation of splice junctions, promoter sequences etc.
3. *in silico* splicing and translation of the putative cognate locus results in a known protein product of that subunit
4. supporting evidence from the literature, if available

The mapping results are shown in Table 5.2. This approach also provided a valuable secondary analysis by identifying potential unknown dynein subunit paralogs*.

The dynamic nature of mouse and human genome evolution can generate paralogous sequences through mechanisms of duplication at the level of entire genomes, chromosomes, chromosomal segments and retrotransposition events (see for example, (Koonin, 2005; Sankoff, 2001; Taylor *et al.*, 2004)). Each distinct mechanism of gene duplication and subsequent functional or non-functional sequence divergence generates a specific signature of evolution; from intron containing paralogs created by duplication to intron-less pseudogenes created by retrotransposition. However, as with many bioinformatics techniques, the limitation of this approach was anticipated to be the quality and completeness of the query sequences and the genome assembly. Therefore homology searches were also made against the nucleotide and protein sequence databases (GenBank) to identify potentially expressed and translated paralogs. Although low homology sequence was seen frequently, no functional loci were identified (data not shown) except for *DYNLL1*. Although the *DYNLL1* locus appeared functional, no protein product was found. In the interest of brevity two examples of this work are given here, which are representative of the full work undertaken.

5.2.3.1 Example 1: C*ytoplasmic dynein light chain 1*

The *cytoplasmic dynein light chain 1* (*DYNLL1*) gene illustrates many of the methods used to clarify dynein subunit information. *DYNLL1* possessed two different loci, the cognate locus 12q24.21 and the incorrect locus at 14q24 which was reproduced and propagated on genome browsers. The origin of the discrepancy most likely stemmed from the work of Dick and colleagues

* Paralogs are genes related by duplication within a genome. Orthologs retain the same function in the course of evolution, whereas paralogs evolve new functions, even if these are related to the original one.

who took N and C terminal sequences of *Drosophila* and *C .elegans* and designed primers by reverse translation and used PCR to design 300bp probes and isolated 2 cDNAs (Dick *et al.*, 1996a). FISH probes constructed with this sequence mapped to 14q24. This error was also seen at the Human Genome Nomenclature Committee (HGNC) website at the Galton Laboratory, UCL, London, UK (www.gene.ucl.ac.uk/nomenclature) during a search of all loci containing the name "cytoplasmic dynein". The Galton Laboratory gave *DYNLL1* a 14q24 locus and two additional pseudogene loci, *DNCL1P1* and *DNCL1P2* on chromosome 14. In addition Online Mendelian Inheritance in Man (OMIM) website, used to collate information about human genetic diseases reported a 14q24 location but LocusLink (now EntrezGene) gave a 12q24.23. To resolve these differences the full-length *DYNLL1* cDNA was aligned against the human genome using megaBLAST (Table 5.3).

Genomic location			Alignments (nt)		% identity	ORF?	Protein	% identity	Ensembl Gene		NCBI Gene
Chromosome	Hsa	Contig	*DYNLL1*	Contig Position	NM_003746		(aa)	NP_003737	Name	Accession	Accession
1	1p36.13	NT_077921	2 – 371	456983 – 457323	91	Yes	89	87	DYLL_HUMAN	ENSG00000124854	XM_372768 XP_372768
1	1p36.11	NT_037485	307 – 550	2790937 – 2790695	93	No	—	—			
3	3q25.3	NT_005612	39 – 94 119 – 640	60870198 – 60870252 60870268 – 60870791	83	No	—	—			
4	4q23	NT_016354	23 – 546 570 – 628	25458035 – 25457518 25457506 – 25457440	83	No	—	—			
7	7q21.1	NT_007933	1 – 66 79 – 370	10245012 – 10244953 10244947 – 10244659	93	No	—	—	Hs_7_c1269	OTTHUMG00007007517	LOC392947 XM_374628 XP_374628
			377 – 640	10245024 – 10245285	93	No	—	—			LOC392067 XM_373171 XP_373171
12	12q24.13	NT_009775	87 – 456 472 – 578 560 – 640	4746361 – 4745993 4745993 – 4745887 4745587 – 4745506	89 89 82	No	—	—			
	12q24.31		1 – 89 8 – 226 224 – 640	11452675 – 11452763 11452960 – 11453099 11454616 – 11455032	98 100 99	Yes	89	100			
14*	14q31.1	NT_026437	1 – 640	61633039 – 61632401	94	Yes	89	91	K14_NN_963_1	ENSG00000183992 and OTTG00000002869	LOC246720 NG_001584
	14q31.1		38 – 635	61799299 – 61799896	94	No	—	—	K14_NN_968_1	OTTG00000002889	

Table 5.3 *DYNLL1* megaBLAST alignments against the human genome

An intact open reading frame (ORF) was seen on three chromosomes, with three potentially translated proteins 89 amino acids (aa) in length. Chromosome 12q24.31 was identified as the cognate genetic locus and loci on chromosome 1 and 14 as untranslated pseudogenes. Mapping prefix Hsa refers to Homo sapiens chromosomal location and all alignments are given by nucleotide (nt)

Alignments to chromosome 12q24.31 had the highest percentage identity, spanning the entire length of the cDNA sequence. To ensure this megaBLAST alignment was correct, the *DYNLL1* cDNA sequence was aligned against chromosome 12 contig only (Acc: NT_009775) using BLAST2Seq and the corresponding alignments checked for the presence of conserved sequence features indicative of an expressed gene. The sequence alignment was identical to that seen using megaBLAST (data not shown). The entire cDNA length was represented against the chromosome 12 contig in three distinct exonic regions and several conserved sequence motifs, such as Kozak consensus sequence, splice junctions and polyadenylation signals were identified which supported this chromosomal locus (Figure 5.3). The exonic sequences were artificially spliced and translated using TRANSLATE and resulting protein compared to DYNLL1 (Acc: NP_003737) using BLAST2seq - the two sequences were identical (Figure 5.4).

Figure 5.3 Schematic representation of the putative *DYNLL1* locus at 12q24.31

Exonic sequence shown in blue font and intronic in grey font. Translational start codon (methionine) is shown in red at +1 within Kozak conserved signal (grey box). Conserved splice junctions indicated within green lines, TAA stop codon and polyadenylation signal highlighted in yellow.

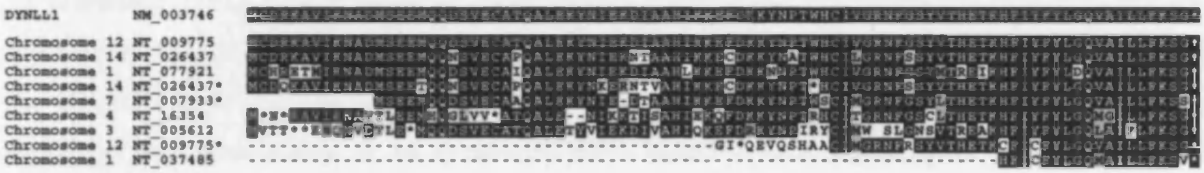

Figure 5.4 *In silico* translation of artificially spliced *DYNLL1* alignments

DYNLL1 alignments from various chromosomes were spliced and translated in silico and aligned to the known DYNLL1 protein NM_003746 using ClustalW. The alignment at chromosome 12q24.31 showed complete homology to *DYNLL1* and all other loci showed evidence of sequence degeneration associated with pseudogenes.

This method of analysis was carried out for all *DYNLL1* alignments shown in Table 5.3. Several loci including those on chromosomes 1, 7 and 14 were characteristic of processed pseudogenes; lacking introns, encompassing a poly(T) tail and comprised of degenerate sequence (i.e. possessing

stop codons in the ORF) (Vanin, 1985). The "processed" nature of these loci implied duplication of the cognate locus by retrotransposition. This hypothesis was confirmed by analysing the sequence context of each suspected locus using RepeatMasker (www.repeatmasker.org/) – all loci except chromosome 12q24.31, were seen to possess hallmark flanking sequences of non-long terminal repeats (LTR) Class I retrotransposable elements: chromosome 1 loci possessed short interspersed nuclear elements (SINEs) and chromosome 12 possessed long interspersed nuclear elements (LINEs). Corresponding sequences were seen in the mouse in regions syntenic to those in humans suggesting that duplication of the cognate locus occurred in the common ancestor of both human and mouse species. Locus 12q24.31 was proposed identified as the cognate locus, which was supported by the mapping of the mouse *Dynll1* to a region syntenic to 12q24.31 on Mmu5.

To ensure that no potential paralogs had been missed the cDNA and protein sequences of *DYNLL1* were used to search the sequence databases using nucleotide and protein BLAST. A match to "*Homo sapiens lung cancer oncogene 5*" (*HLC5*) was found with 99% identity over 85% of the length of *DYNLL1* cDNA. *In silico* translation of the antisense strand of HLC5 produced a 100% match to the full length DYNLL1. It is likely that the *HLC5* data, which remains unpublished and is based on a single observation from a study of mRNA species in cancerous tissue, is incorrect and most likely represents a detection of *DYNLL1*.

5.2.3.2 Example 2: *Cytoplasmic dynein 1 heavy chain 1*

A search for sequences paralogous to *DYNC1H1*, using BLAST to query the cDNA sequence against the nucleotide database, did not yield significant results however a BLAST search of the protein database yielded a sequence with 27% identity to DYNC1H1. The sequence (Acc. XP_085578, XM_085578) was the predicted product of a hypothetical gene, FLJ46675, located at chromosome 17p13.1. The existence of a second heavy chain species DYNC2H1 was already known and so this result suggested a possible third heavy chain existed. By aligning the sequences for DYNC1H1, DYNC2H1, FLJ46675 and DNAH9 used as an outgroup, it was shown that the sequence was more likely to be axonemal (33% identity, 51% similarity to DYNC1H1) than cytoplasmic (Figure 5.5).

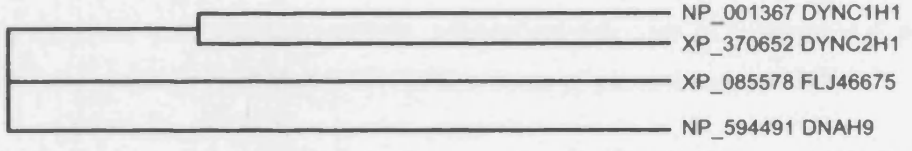

Figure 5.5 Cladogram of the relationships between human dynein heavy chains and the hypothesised heavy chain FLJ46675

Human cytoplasmic heavy chains DYNC1H1 and DYNC2H1 are more closely related to each other than the hypothetical protein FLJ46675. Axonemal heavy chain DNAH9 was used as an outgroup.

5.2.4 Cytoplasmic dynein subunit accession numbers

Cytoplasmic dynein subunit nucleotide and protein accession numbers were obtained from NCBI RefSeq. The majority of sequences were found through links from the central gene-based data resource LocusLink. Human *DYNC2H1* sequences XM_370652 and XP_370652 were predicted by analysis of genomic sequence (NT_033899) using the NCBI gene prediction method GNOMON, supported by mRNA and EST evidence. Mouse *Dyn1li2* sequences XM_134573 and XP_134573 were also predicted on genomic sequence (NT_078575) using a similar method.

5.3 Identifying cytoplasmic dynein orthologs

With the availability of sequence data from different organisms, cytoplasmic dynein orthologs were identified by searching the GenBank non-redundant protein database, with the human dynein proteins using PSI-BLAST with default parameters and the BLOSUM-62 substitution matrix. Searches of pufferfish sequence *Takifugu rubripes* were performed by using human protein sequence against the translated Fugu Genome nucleotide database (version release 2.0; www.ensembl.org/Fugu_rubripes). Where possible, outgroup sequences were identified from homologs in *Chlamydomonas reinhardtii* as these axonemal dynein proteins have been extensively studied in this species and many of the subunits in higher-order species are known to be related. The accession numbers of all protein sequences identified are given in the Appendix. Phylogenetic analyses were conducted using these sequences by Dr James Cotton at the Natural History Museum, London, UK; using the methods outlined in Chapter 2.3.18. For the Markov-chain approach, the consensus of three Markov-chain analyses was used to ensure that the algorithm had converged to a stationary state. For one of the cytoplasmic dynein heavy chain gene family, the three chains had reached different likelihood values after 1,000,000 generations, suggesting failure to converge. Running another three independent chains resulted in five out of six chains agreeing on the likelihood values, suggesting that only one chain had not converged properly. In all cases, the phylogeny presented is the majority rule consensus of the posterior sample of tree topologies from all three Markov chains. A positive control in the identification of homologous sequences to construct phylogenetic trees was the multiple independent detection of subunits: e.g. searching for human DYNC1H1 paralogs identified DYNC2H1 with an alignment score of 30%.

5.3.1 Cytoplasmic dynein heavy chain gene family (DYNC1H1, DYNC2H1)

Figure 5.6A illustrates the phylogenetic relationships amongst the sequences identified as orthologous to DYNC1H1 and DYNC2H1 from various organisms. The existence of several

axonemal dynein heavy chain proteins in the *Chlamydomonas* proteome made identifying an outgroup sequence difficult, however the outer arm heavy chain (ODA11) was arbitrarily chosen (all *C. reinhardtii* heavy chains had comparable sequence similarity to DYNC1H1). A partial fragment of a suggested third dynein heavy chain identified in the literature (Vaisberg *et al.*, 1996a) was included in the analysis (fragment was termed "DNAH12frag"). Only partial sequence (336aa) of the mouse DYNC2H1 (XP_35830) protein was available in the GenBank database. Adding this partial sequence to the analysis resulted in spurious clustering and therefore, an extended putative sequence was required. The extended sequence was obtained by aligning human and rat sequences XP_370652 and NP_075413 respectively, against the translated mouse genome (Build 32) using TBLASTN. Incomplete mouse genomic assembly at the DYNC2H1 locus yielded a truncated sequence 3455 amino acids in length, 85% the length of human DYNC2H1.

The heavy chain sequences fell into two distinct clades and the relationships within each clade were generally consistent with known evolutionary distances between the organisms shown*. The deep branching of the dynein 1 and dynein 2 clades, and the presence of myriad species on both branches, suggests that the origin of these two dynein heavy chain proteins is ancient, possibly predating the divergence of *C. reinherdtii* from a primordial species. The phylogeny complemented and extended, previous phylogenetic analyses of the heavy chain proteins (Porter *et al.*, 1999; Vaisberg *et al.*, 1996b). Importantly, the analysis indicated that the partial human sequence, suspected to be a third cytoplasmic heavy chain, was unlikely to be a cytoplasmic dynein; it possessed good homology to DNAH12 (Acc:AAB09729) and was termed "DNAH12frag".

5.3.2 Cytoplasmic dynein intermediate chain gene family (DYNC1I1, DYNC1I2)

Figure 5.6B shows the dynein intermediate chain protein phylogeny. The protein sequence data demonstrated an evolutionary distant relationship between axonemal and cytoplasmic dynein intermediate chains; for example, mammalian rat DYNC1I1 (NP_062107) has 48% similarity to the *Chlamydomonas* axonemal outer arm dynein intermediate chain encoded by the ODA6 locus and therefore ODA6 was used as an outgroup (Mitchell *et al.*, 1991; Paschal *et al.*, 1992a). The intermediate chain sequences fell into two clades, intermediate chain 1 and 2, which were comprised of vertebrate species only.

An alternative placement of a *Takifugu* sequence, as a member of the intermediate chain 1 clade was almost as well-supported by the data as the placement shown in Figure 5.6B (49% bootstrap

* Relationships amongst dynein sequences of different species do not necessarily reflect the evolutionary relationships amongst species as a gene tree does not always reflect a species tree; see (Tajima, 1983) and (Pamilo *et al.*, 1988) for further details.

support against 51% support). In view of this and with all non-vertebrate species falling outside these clades, the data suggest a recent evolutionary origin for an intermediate chain 1 and 2 gene split, perhaps as part of a '2R' event of genome duplication (see (Wolfe, 2001) for review). The absence of an amphibian intermediate chain 1 protein may have been due to the paucity of *Xenopus laevis* sequences in the GenBank sequence database at the time of analysis.

5.3.3 Cytoplasmic dynein light intermediate chain family (DYNC1LI1, DYNC1LI2, DYNC2LI1)

Figure 5.6C illustrates the phylogenetic relationships amongst the dynein light intermediate chain protein sequences from various organisms. The light intermediate chains separated into two deep clades, mirroring the dynein 1 and 2 heavy chain tree. The dynein 1 clade was further split the two intermediate chain components of cytoplasmic dynein 1 complexes, DYNC1LI1 and DYNC1LI2 (Entrez GeneID: 51143 and 1783, respectively) which are more closely related to each other than to the cytoplasmic dynein 2 light intermediate chain, DYNC2LI1. DYNC2LI1 homologs were only identified in species possessing DYNC2H1, emphasising the distinct cellular identities and roles of these separate dynein complexes (Figure 5.1B). *C .elegans* appeared to possess one light intermediate chain (dli-1) (Entrez GeneID: 178260) for cytoplasmic dynein (DYNC1H1-based complexes), and one (xbx-1) (Entrez GeneID: 184080) for cytoplasmic dynein 2 (DYNC2H1-based complexes) (Schafer *et al.*, 2003).

5.3.4 Cytoplasmic dynein light chain Tctex1-family (DYNLT1, DYNLT3)

Cytoplasmic dynein light chain Tctex1-family is one of three known dynein light chain gene families that are components of cytoplasmic dynein 1: (1) the *t*-complex associated family (DYNLT1, DYNLT3), (2) the Roadblock family (DYNLRB1, DYNLRB2), and (3) the LC8 family (DYNLL1, DYNLL2). These gene families are named according to their original discovery, through the effect of mutations in mouse (t-complex associated, Tctex1) and Drosophila (Roadblock) or according to the size of the protein in *Chlamydomonas* (LC8). The dynein light chain Tctex1-family protein phylogeny is shown in Figure 5.8A, and shows distinct clades for DYNLT1-like and DYNLT3-like sequences.

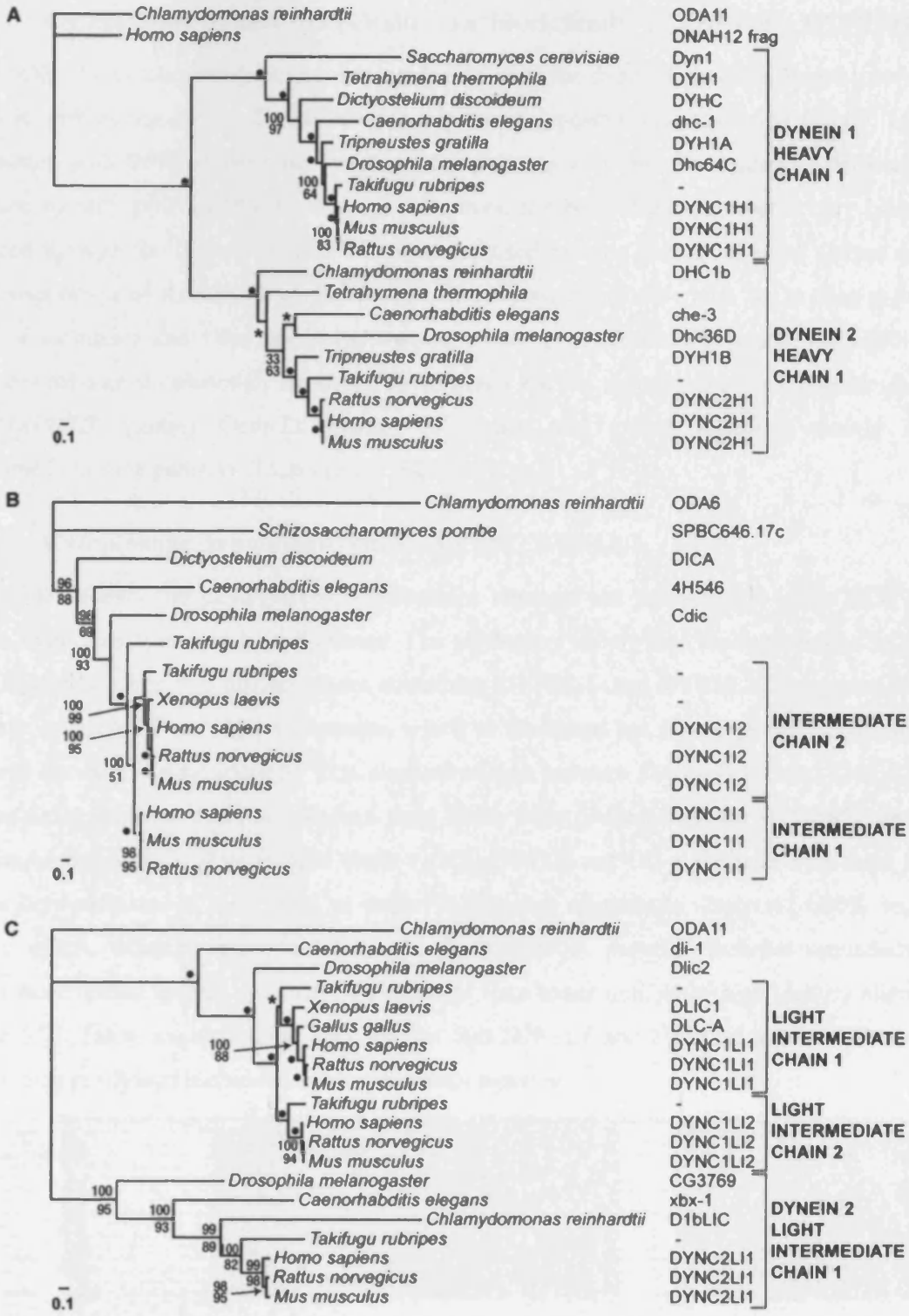

Figure 5.6 Protein-based phylogenies of the cytoplasmic dynein heavy chain, intermediate chain and light intermediate chain families

Species names for heavy chain (**A**), intermediate chain (**B**) and light intermediate chain (**C**) phylogenies are given with NCBI/GenBank gene/protein names (sequence accession numbers are given in Appendix). Orthologous human, mouse, and rat gene names use the revised systematized consensus nomenclature (Pfister *et al.*, 2005b). Named clades are indicated in the right margins. Bayesian and maximum-likelihood bootstrap values are shown as percentages adjacent to branch points. *bootstraps below 50%. •bootstraps at 100%. Scale-bar represents evolutionary distance (estimated numbers of amino-acid substitutions per site).

5.3.5 Cytoplasmic dynein light chain Roadblock family (DYNLRB1, DYNLRB2)

Figure 5.8B shows the phylogenetic relationships amongst the dynein light chain Roadblock protein family in various organisms. The Roadblock sequences appeared well-conserved from *T. rubripes* to humans, with 96% of pairwise sequence comparisons amongst all sequences demonstrating sequence identity >50% (data not shown). However, the high alignment scores may have been produced through the limited number of sequences used and the paucity of more distant species. The conservation of Roadblock sequences (i.e. Roadblock domains) within the coding regions of genes of mammals and other species (Bowman *et al.*, 1999; Koonin *et al.*, 2000) highlights a necessary functional constraint. However, these genes are not thought to be cytoplasmic dyneins; e.g. *MAPBPIP* (Entrez GeneID: 28956) in human and mouse functions mainly in the endosome/lysosome pathway (Lunin *et al.*, 2004).

5.3.6 Cytoplasmic dynein light chain (LC8) 1, DYNLL1

Figure 5.8C shows the phylogenetic relationships amongst the dynein light chain LC8 family protein sequences from various organisms. The phylogeny shows that the mammalian LC8 light chain family falls into two distinct clades containing DYNLL1- and DYNLL2-like genes. DYNLL is highly conserved from algae to humans, which is illustrated by: (i) a high degree of sequence similarity between distant species - 92% similarity exists between *Drosophila* Cdlc1 (NP_525075) and the 8kDa flagellar outer arm dynein light chain from *Chlamydomonas* (Q39580), and 91% between human and *C. elegans* light chain 1 (NP_498422) and (ii) a flat tree with short branch lengths between taxa. In total, 67% of pairwise sequence alignments illustrated >50% sequence identity which, although fewer that seen for the Roadblock proteins, includes sequences from several more distant species and therefore accounts for a lower number of high identity alignments (Figure 5.7). Taken together these data suggest that *DYNLL1* and *DYNLL2* are both likely to be under strong purifying selection to conserve protein function.

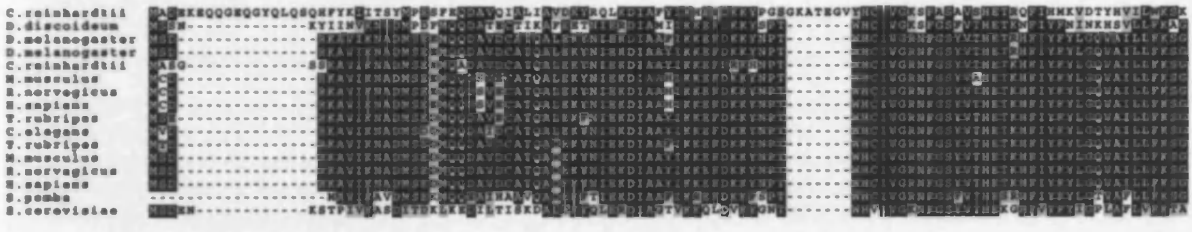

Figure 5.7 Cytoplasmic dynein light chain (LC8) family protein alignments

67% of all alignments were >50% sequence identity. Protein sequences are presented in the same order as the tree in Figure 5.8C. Alignments were conducted using ClustalW.

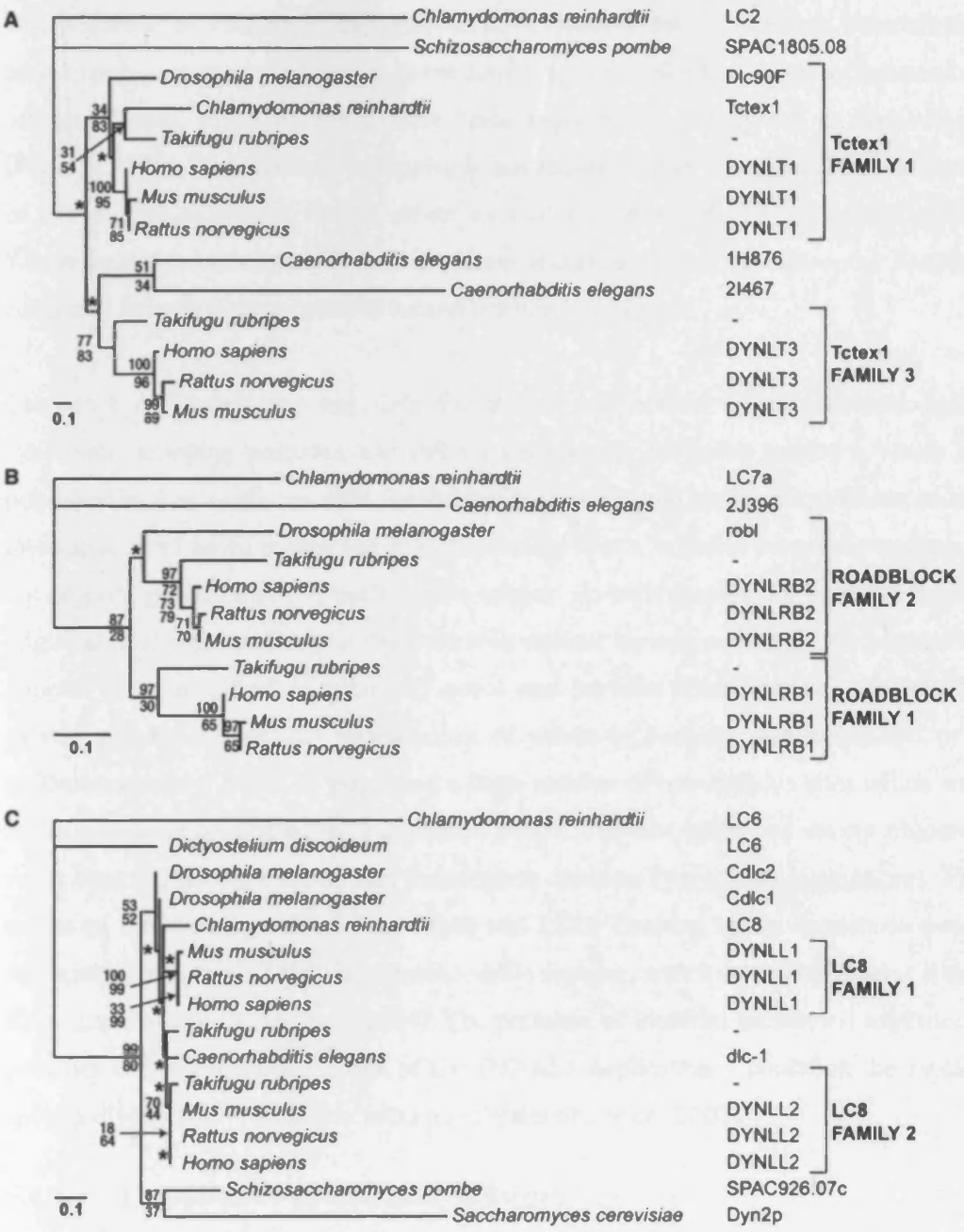

Figure 5.8 Protein-based phylogenies of the cytoplasmic dynein light chain family

Species names for Tctex1 (**A**), Roadblock (**B**) and LC8 (**C**) dynein light chain phylogenies are given with NCBI/GenBank gene/protein names (sequence accession numbers are given in Appendix). Orthologous human, mouse, and rat gene names use the revised systematized consensus nomenclature (Pfister *et al.*, 2005b). Named clades are indicated in the right margins. Bayesian and maximum-likelihood bootstrap values are shown as percentages adjacent to branch points. *bootstraps below 50%. •bootstraps at 100%. Scale-bar represents evolutionary distance (estimated numbers of amino-acid substitutions per site).

5.4 Discussion

In preparing to undertake a systematic analysis of the components of the cytoplasmic dynein pathway for a large scale association study, confusion and errors regarding the nomenclature, mapping positions and sequence accession numbers were observed in the literature and databases.

The accuracy of electronic data should be a concern for all research communities as it is an increasingly common problem; it is estimated, for example, that ~15% of annotation in GenBank contains errors, many of which have been found to be propagated in peer-reviewed literature (Pennisi, 1999). The dynein community is not exceptional in this respect and as the data presented in this chapter catalogue, several errors were identified in cytoplasmic dynein subunit annotation. Where mistakes were identified in databases and other online resources, the hosting institute was contacted to review their data and amend it where necessary.

Table 5.2 catalogues the key data for mouse and human dynein subunits including subunit synonyms, mapping positions and mRNA and protein accession numbers, which has since been published as a valuable resource for the cytoplasmic dynein community (Pfister *et al.*, 2005b). The investigation of novel mouse and human paralogs was a valuable secondary analysis in confirming the cognate genetic locus of each dynein subunit. In both species, for many of the subunits tested, alignments of expressed sequences were seen against various regions of the genome however, these regions were identified as either: (i) genes and proteins containing homologous domains to the dynein subunits tested, (ii) pseudogenes of whole or partially duplicated loci or (iii) incorrect genome assembly. *DYNLL1* possessed a large number of homologous sites which were determined to be pseudogenes created by duplication events. All loci identified except chromosome 1, have since been included on the human pseudogene database (www.pseudogenes.org). The "intronless" nature of the pseudogenes and the SINE and LINE flanking repeat sequences were indicative of duplication by a non-LTR Class 1 transposable element, which moves by reverse transcription of an RNA intermediate (Silva *et al.*, 2004). The presence of identical transposed sequences in the mouse provides an indication of the age of the *DYNLL1* duplication – predating the mouse and humans species divergence ~75 million years ago (Waterston *et al.*, 2002).

5.4.1 Cytoplasmic dynein nomenclature

Collation of the myriad names used to describe the cytoplasmic dynein subunits illustrated the extent of confusion in the cytoplasmic dynein field. All subunit synonyms were investigated to establish their accuracy and many, such as the "CDC23" synonym were proven to be incorrect (Chapter 5.2.2). The data presented in this chapter, including the phylogenetic analyses, were influential in facilitating a revision of the human and mouse dynein nomenclature to a standardised format. Standardising nomenclature of large gene families has been undertaken for many different proteins; see for example (Marenholz *et al.*, 2004; Miki *et al.*, 2005; Rodgers *et al.*, 2007; Wilson *et al.*, 2006) and have in common the use of phylogenetic analyses to establish inclusion/exclusion criteria for family members. The investigation of paralogous and orthologous cytoplasmic dynein

sequences allowed a complete investigation of known and unknown dynein subunit family members, which could then be named accordingly.

5.4.1.1 A new nomenclature system for the cytoplasmic dynein subunits

Revision of the mammalian cytoplasmic dynein nomenclature system was undertaken by Pfister and colleagues (Pfister *et al.*, 2005a) and was approved by the Human Genome Organisation Nomenclature Committee (HGNC, 2004) and the International Committee on Standardised Nomenclature for Mice (Maltais *et al.*, 1997). Phylogenetic analyses of the dynein proteins substantiated the existence of two distinct dynein complexes, cytoplasmic dynein 1 and cytoplasmic dynein 2 and the exclusive occurrence of DYNC2H1 and its binding protein DYNC2LI1. In accordance with HGNC policy, Pfister and colleagues designated each unique cytoplasmic dynein subunit with the root "DYNC" (for dynein, cytoplasmic), followed by the specific dynein complex subtype 1 or 2 (e.g. cytoplasmic dynein 2 was designated DYNC2). The shared light chains were rooted with "DYN" and other subunits were designated with a letter(s) for the size of the polypeptides: H for the Heavy Chain, I for the Intermediate chain, LI for the Light Intermediate Chain, and L for Light Chain. Additional letters (T, RB and L) were used to distinguish the three distinct light chain families and individual members of the gene families were assigned numbers. The revised nomenclature has been used throughout this thesis.

5.4.2 Changing databases and future studies

As with many *in silico* approaches, the results of an investigation are often correlated to the quality and completeness of the raw data used and as such, the data presented in this chapter reflect the state of the sequence and genome databases at the time they were accessed. Identifying paralogous dynein sequences in the mouse and human benefited from the availability of complete genome, nucleotide and protein data, however, the identification of orthologous sequences in newly or partially sequenced genomes may have suffered from incomplete sequence ascertainment. Therefore, the cytoplasmic dynein subunit phylogeny is currently accurate but with the publication of genome sequences from additional species, the phylogeny may be refined in the future and weak nodes provided with greater support.

5.4.2.1 Priority candidate genes: *DYNLL* family and *DYNLRB* family

The cytoplasmic dynein light chain LC8 phylogenetic tree suggests that human *DYNLL1* and *DYNLL2* may both be promising candidates for a future ALS candidate gene association study. The flat branch network illustrated the extent to which proteins of this family are conserved between distantly related species that diverged ~1717 million years ago (Nei *et al.*, 2001). More closely related species such as human, mouse, rat, pig, and cow show extraordinary sequence conservation;

between these species the amino acid sequences of both DYNLL1 and DYNLL2 are identical (Wilson *et al.*, 2001). The observed DYNLL amino acid sequence homogeneity between species can be explained by the action of purifying selection which serves to eliminate those mutations that have a deleterious effect on protein function. Purifying selection is generally a more pervasive mechanism of selection than other forms of directional selection (Hughes *et al.*, 2003; Kimura *et al.*, 1974) and has been shown to maintains stringent interspecies sequence homogeneity in proteins with essential functions, such as H4 histones (Piontkivska *et al.*, 2002). The conservation of the DYNLL protein family raises questions as to what essential function these proteins play and whether perturbation of this function may yield a neurodegenerative phenotype. As yet, no neuronal phenotypes are known.

The significance of DYNLL to neuronal function (and conversely, degeneration) is not known. However, DYNLL is known to be an integral part of brain cytoplasmic dynein, although it is ubiquitously expressed in all cells of the body and large amounts of brain DYNLL are not associated with the dynein complex (King *et al.*, 1996a). The functional role of these LC8 light chains is varied: DYNLL is a substrate of a p21-activating kinase (Vadlamudi *et al.*, 2004), a component of the actin-based motor myosin V (Naisbitt *et al.*, 2000b) and a component of the nNOS complex (Grissom *et al.*, 2002). DYNLL mutants display various developmental and fertility phenotypes (reviewed in (Pfister *et al.*, 2005b) and total loss-of-function *Drosophila* mutants are embryonic lethal (Dick *et al.*, 1996a).

Drosophila Roadblock mutants also result in a number of phenotypes including the accumulation of axonal cargoes, mitotic defects, female sterility, and larval/pupal lethality (Bowman *et al.*, 1999). The Roadblock proteins also demonstrated high sequence similarity of interspecies pairwise alignments which suggests that these proteins have also been conserved. Although, more distantly related species were not available for comparison during the original analyses (which may have inflated the apparent level of protein conservation), several new protein sequences have recently become available and continue to show high sequence identity: *Dictyostelium discoideum* hypothetical protein (XP_637964) displays 62% sequence similarity to human DYLRB1 (NP_054902). The Roadblock proteins are promising candidates for neurodegeneration with mutants affecting neuroblast proliferation, reducing dendritic complexity and causing defects in axonal transport (Reuter *et al.*, 2003).

The human *DYNLL* and *DYNLRB* genes should therefore make valuable candidates for future ALS and other motor neuron disease association studies.

6 Identifying kuru susceptibility loci

6.1 Introduction

Mapping disease susceptibility loci by identifying genes affected by natural selection imposed by the disease, is a novel approach to mapping complex traits. In this chapter such evolutionary analyses of the prion gene (*PRNP*) is undertaken as a paradigm for future studies of prion disease candidate loci and whole-genome analyses. This chapter begins with an updated analysis of the role of codon 129 as both a susceptibility locus and as a protective factor for kuru, in the kuru-exposed linguistic groups of the Eastern Highlands of Papua New Guinea. The resulting genetic impact of the kuru epidemic is investigated in the surviving populations, with codon 129 genotypes analysed stratified by age and sex. A large sample of elderly South Fore females and slightly younger South Fore males show significant Hardy-Weinberg disequilibrium at codon 129, driven by an excess of heterozygosity, an observation consistent with their participation in mortuary feasts. Examination of codon 129 valine allele frequency worldwide illustrates a significant West-East reducing cline, against which the PNG valine frequency contrasts starkly. An update and refinement of individual village exposure to kuru by establishment of an Exposure Index, allowed a more subtle analysis of valine allele frequency. A significant increasing cline was seen from non-Highland to Highland populations however no local cline within the Eastern Highlands was seen. Similarly, no increase in LD between microsatellites flanking *PRNP* is seen. This chapter concludes with a feasibility study on the whole-genome analysis of a small number of elderly Fore women and whole genome amplified kuru samples using 250,000 SNP arrays. Although the amplified kuru samples genotyped poorly, the remaining 7 samples from elderly Fore women are used to determine analysis criteria and examine cursory LD data.

6.1.1 Kuru and the evolution of human *PRNP*

The evolution of human *PRNP* is a contentious topic which has been investigated by several authors. In 2003, the work of Mead and colleagues investigated the *PRNP* locus in a number of worldwide populations including the people of the Eastern Highlands of Papua New Guinea who experienced the human prion disease epidemic of kuru (Mead *et al.*, 2003). Mead identified that the prion locus had undergone kuru imposed balancing selection in the Fore people of the Eastern Highlands by identifying a significant excess of heterozygotes in the surviving Fore population; a significant excess of human coding polymorphisms as tested by a McDonald-Kreitman test against both Old and New World monkeys; a significant positive Tajima's *D* for polymorphisms within 4.7kb sequence; a bifurcating haplotype genealogy characterised by two long deep branches with highly divergent clades (which were associated with each codon 129 allele) and extended linkage

disequilibrium with microsatellites flanking ~30 kb either side of *PRNP* with reduced diversity of alleles. In addition, several of these features were shared by other worldwide populations prompting the suggestion that the prion gene had undergone balancing selection throughout human history and speculation that (as one hypothesis) the selective pressure was provided by widespread cannibalistic practices in prehistoric humans. Several authors have challenged Mead's proposition with regards to balancing selection at *PRNP,* imposed by cannibalism-associated prion-like diseases during the evolution of modern humans, citing polymorphism ascertainment as a bias introducing factor (Brookfield, 2003; Soldevila *et al.,* 2003; Soldevila *et al.,* 2006).

Despite this, there is general agreement that the data presented for the Fore does illustrate the action of natural selection in this population and that the basis for this selection pressure is the marked survival advantage of *PRNP* codon 129 heterozygotes (Cervenakova *et al.,* 1998; Mead *et al.,* 2003). The strength of balancing selection in the Fore, within a single generation, has been identified as the strongest documented to-date in any human population (Hedrick, 2003) and surpasses the commonly quoted example of malaria on the *C* and *S* alleles of β-haemoglobin (Hedrick, 2004). Such great selection pressures could rapidly establish/eliminate mutations within the population and therefore by examining the evolutionary signatures of selection, kuru may provide a unique resource for the investigation of disease modifying loci in prion disease and possibly other neurodegenerative diseases. Therefore, the main aim of this chapter was not to resolve the debate regarding worldwide balancing selection but to investigate further the genetic signature of balancing selection on the Fore, how this can be utilised to identify other mediators of human prion disease and the applicability to this method of analysis to other neurodegenerative diseases. Further, this chapter aims to:

to update previous assessments of the role of codon 129 in kuru susceptibility and protection, by analysing larger data sets.

(i) to identify a correlation between the extent of kuru experienced by Eastern Highland linguistic groups and the pattern of genetic variation at *PRNP* (i.e. identify signatures of selection) as a precedent for performing larger candidate gene or whole-genome study

(ii) to establish a resource to identify novel susceptibility loci. By identifying a correlation of genetic variation at *PRNP* proportional to exposure to kuru, a panel of samples from different linguistic groups with differing exposure to kuru could be used to identify/support additional susceptibility loci

(iii) to pilot a whole genome hyper-case-control association study between kuru and multiple exposure samples.

6.2 Kuru susceptibility is mediated by *PRNP* codon 129 genotype

Cervenáková and colleagues originally illustrated the influence of codon 129 genotype on kuru susceptibility by examining genotype data from 92 kuru patients (Cervenakova *et al.*, 1998). They correlated homozygosity at codon 129 with an earlier age of kuru onset and shorter duration of illness, compared to heterozygosity. The MRC Prion Unit's collection of 161 kuru samples provided an opportunity to re-examine the effect of codon 129 on kuru susceptibility with a larger sample size and for a sex-specific genotype distribution.

Kuru samples were obtained as either DNA or blood/sera from which DNA was extracted by the MRC Prion Unit Human Genetics Group, using QIAmp mini DNA extraction kits and following safety procedures relevant to handling infectious material. *PRNP* codon 129 genotyping was performed by allelic discrimination on all samples (described in Materials and Methods Chapter 2.3.13) using a FAM-tagged *PRNP* codon 129M probe, VIC-tagged *PRNP* codon 129V probe and flanking forward and reverse primers taqmvf2 and taqmvr respectively (see Primer Table in Appendix). Data on age at sample collection and sex were obtained for all samples however, 18 samples lacked this information and were removed from further analysis. Deviations from HWE were calculated using PLINK.

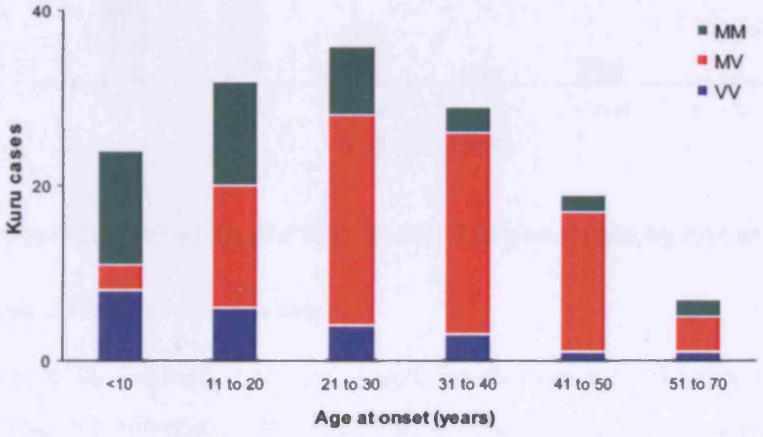

Figure 6.1 Distribution of *PRNP* codon 129 genotypes by age in 147 kuru cases
The proportion of kuru MV heterozygotes increases with age of onset.

Genotype proportions in early onset kuru cases were significantly distorted away from those estimated by HWE (Figure 6.1) with excess homozygosity (P_{exact} =0.0003, in patients ≤10 years old). Concomitant increase in heterozygosity was seen with age, with a significant excess of heterozygotes in the age groups 31 to 40 years (P_{exact} =0.003) and 41 to 50 years (P_{exact} =0.006). The 11 to 20 and 21 to 30 years age groups were both in HWE (P_{exact} =0.70 and 0.087 respectively), which represented the intersection of decreasing homozygosity and increasing heterozygosity with age and therefore the genotype proportions appeared normal. Comparison by Pearson χ^2 test of the

most (<20 years old) and least susceptible (>30 years old) kuru groups was highly significantly different ($P<<0.001$, 2 d.f.). These data illustrate the protective effect of heterozygosity at codon 129 which results in a later age of kuru onset.

When partitioned and analysed by sex (Figure 6.2) the data illustrated and was consistent with several epidemiological aspects of kuru including: (i) the extent to which kuru largely affected females as compared with males and (ii) the peak kuru incidence in males occurred between 11 to 20 years old, which supports the participation of only boys less than 8 years old at mortuary feasts (given a mean kuru incubation period of ~12 years).

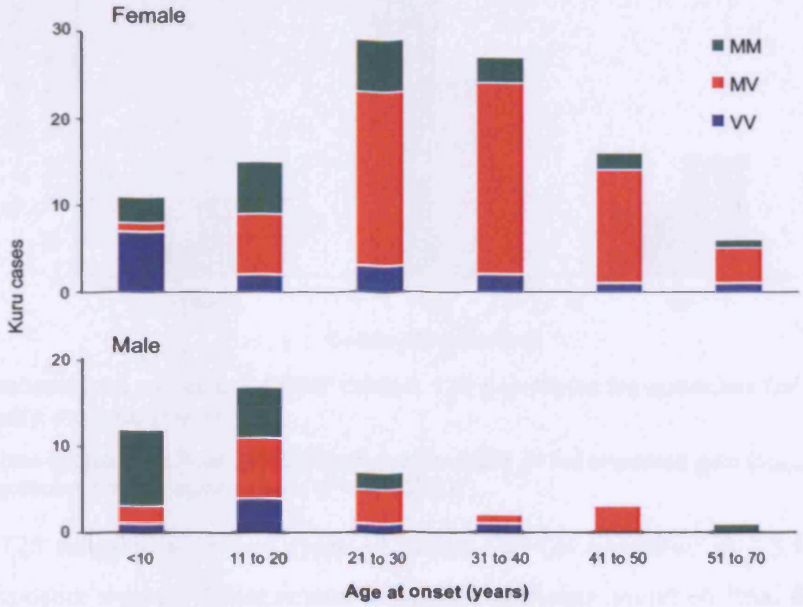

Figure 6.2 Sex specific distribution of *PRNP* codon 129 genotypes by age at collection in 146 kuru cases

Top. Female kuru cases. **Bottom**. Male kuru cases.

Detailed inspection of the earliest onset males and females cases (≤10 years old), identified an excess of female valine homozygotes and methionine homozygotes in males (two-tailed Fisher's exact, P=0.015). Lee and colleagues also noted this result in young Fore males ≤20 years and suggested that it reflected an increased susceptibility of methionine homozygotes to kuru (Lee *et al.*, 2001a) although their analysis may have been affected by small sample size. Taking this into account, the conflicting absence of MM and VV genotypes in males and females most likely reflects a sampling artefact.

6.3 *PRNP* codon 129 heterozygosity mediates protection against kuru

Expanding on the work of Mead and colleagues who examined codon 129 status in 30 elderly Fore women, blood was obtained from an additional 104 women (Mead, 2002). All women were aged 50

years or over in the year 2000, had a history of multiple exposures to kuru at mortuary feasts and resided in a village documented to have a moderate to high level of exposure. The 134 samples were obtained form the South Fore (n=68), North Fore (n=36), Gimi (n=27) and Keiagana (n=3) and ranging in age from 50 to 82 years old, with a mean age of 60 years. On closer inspection of village-specific kuru exposure (explained later in this chapter), 9 individuals were found to originate from an unexposed village and were removed from further study.

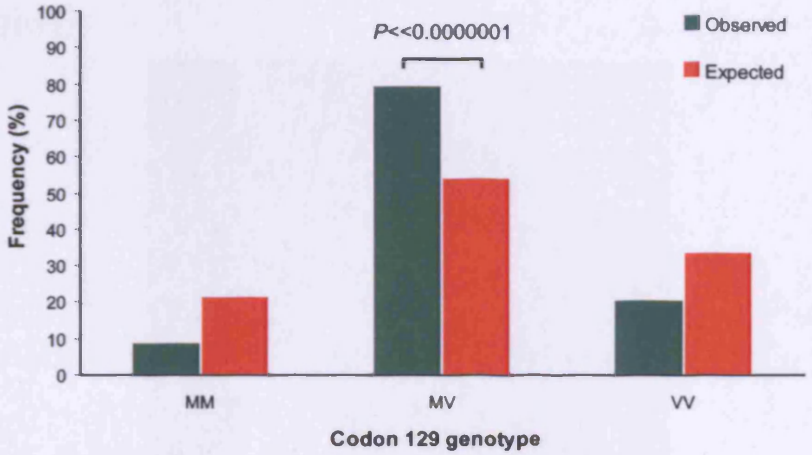

Figure 6.3 Observed and expected *PRNP* codon 129 genotype frequencies for elderly Fore women repeatedly exposed to kuru

Expected frequencies calculated under HWE. Significant deviation of the observed data (P_{exact}=3.1 x 10-5) from HWE and significant heterozygote excess (P<<0.000001).

The remaining 125 samples were genotyped at codon 129 (as described in 2.3.13). The elderly multiple-kuru exposure women demonstrated a highly significant deviation from Hardy-Weinberg equilibrium (P_{exact}=3.1 x 10^{-5}) with a significant excess of heterozygotes (P<<0.0000001) as tested using the Score test* implemented in the software GENEPOP (Figure 6.3).

The added data support the original analyses and illustrate the remarkable survival advantage proffered by heterozygosity at codon 129 to a cohort with acute and repeated exposure to kuru. An interesting question raised by these data relates to the "protection" afforded to homozygotes – in a cohort of women acutely exposed to kuru on multiple occasions, how have women with a "susceptible" codon 129 genotype managed to survive? These data suggest the possibility of codon 129 independent protection, which is examined later in this chapter.

* The Score test (or U test) as implemented in GENEPOP, is an exact HWE test which specifically tests for excess heterozygosity as an alternate to the null hypothesis, which is that the population examined is in HWE

6.4 Investigating *PRNP* for a kuru-mediated signatures of selection

6.4.1 Codon 129 genotypes in the surviving Eastern Highlands population

Codon 129 genotype proportions were used to examine the scale and the extent of the kuru epidemic in the surviving population of the Eastern Highlands. The reduced fitness of codon 129 homozygotes and their subsequent removal from the population should have produced a characteristic signature in the genotype proportions of the remaining population, detectable as deviation from HWE.

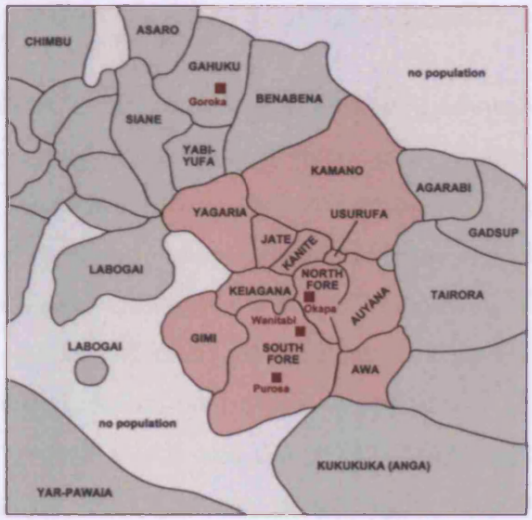

Figure 6.4 Schematic map of the Eastern Highlands of Papua New Guinea

Approximate localisation of neighbouring linguistic groups are shown. For simplicity, geographical and topographical features have been omitted. Linguistic groups with experience of kuru are shaded brown and groups unaffected by kuru are shaded green.

The extent of Hardy-Weinberg disequilibrium will be proportional to the extent of kuru experienced by each population examined, with the greatest deviations seen in the North and South Fore. To examine HWE by kuru exposure, an estimate of exposure level for each linguistic group was obtained based on an assessment of number of kuru cases recorded since records began in 1957 made by the MRC-PNGIMR field team. The Eastern Highlands were divided into kuru exposed and unexposed areas (Figure 6.4).

A total of 3200 DNA samples representing 12 linguistic groups of the Eastern Highlands were obtained, either as previously extracted DNA samples held at the MRC Prion Unit or extracted from whole blood. All samples were genotyped at codon 129 as described previously. For each sample the following data were collated and samples lacking these data were not retained for analysis: the individual's sex, age at collection, year of collection and village. Approximately 2350 samples from the South Fore (n=1279), North Fore (n=276), Keiagana (n=220), Yagaria (n=114), Agarabi (n=90),

Tairora (n=77), Siane (n=74), Awa (n=46), BenaBena (n=46), Jate (n=43), Morae (n=43) and Gadsup (n=42) were carried forward for further analysis.

6.4.1.1 The special case of heterozygote advantage

The availability of age at collection and date of collection data was imperative for accurate HWE analysis to be undertaken. These data allowed the analysis of individuals born during the period of the kuru epidemic, as opposed to individuals born after the cessation of cannibalism. To understand the importance of obtaining the effect of balancing selection on allele frequencies in generations subsequent to the removal of selective pressure should be considered:

Balancing selection establishes a unique condition in which although Hardy-Weinberg's law is disobeyed (i.e. the assumption of an absence of selection is violated), the allele and genotype frequencies in successive generations, after the selective pressure is removed, remain stable and in equilibrium. Consider the condition where complete heterozygote advantage is seen (i.e. homozygosity is lethal) in a single locus system with alleles A and B. Within a single generation all AA and BB homozygotes perish and only AB heterozygotes remain. Following mating of the surviving heterozygotes (frequencies of both alleles A and B are 50% each) all genotypes are represented at equilibrium frequency (AA and BB at 25% frequency and AB at 50%). With the removal of selective pressure, only a single generation is required to return genotypes to equilibrium conditions and any signal of selection that is based on allele frequency and genotype proportions is lost.

Therefore, the PNG samples were analysed stratified by age and exposure to kuru, calculated based on epidemiological information available. The enforced cessation of cannibalism in the mid-1950s was used as a watershed for age calculations. The majority of PNG samples were collected between 1997 and 2002 and individuals recorded as being >50 years old at sample collection were assumed to have lived during the kuru epidemic.

6.4.2 Hardy-Weinberg equilibrium in the surviving population

The surviving linguistic groups of the Eastern Highlands were tested for deviations from HWE, stratified by age. Linguistic groups were analysed (i) as a whole, (ii) stratified by age and (iii) for the North and South Fore only, stratified by age and sex, as these cohorts were sufficiently large enough to avoid small sample sizes. Significance was tested using the exact χ^2 test implemented in PLINK (Table 6.1). Significant Hardy-Weinberg disequilibrium was seen in the South Fore for the whole group (P_{exact}=0.005) and all South Fore individuals >50 years alive during the kuru epidemic (P_{exact}=0.003). By analysing the >50 years group by sex, it was seen that females >50 years were

driving this result (P_{exact} =0.0004) and no significance was seen for the corresponding male group. Significant deviation from HWE was also seen in South Fore males <50 years old. This group was further analysed by decade of birth (data not shown) and only those men born between 1950 and 1960, during the peak of the kuru epidemic, showed a significant deviation (P_{exact} =0.0287). These data support the epidemiological and cultural data suggesting that boys up to 8 years of age would have participated at feasts with their mothers.

HWE in the North Fore population and additional kuru exposed groups including Keiagana, Jate, Agarabi, Yagaria and Awa, was puzzling. Kuru cases have been recorded in all of these linguistic groups and the North Fore, in particular females >50 years old, are recorded to have experienced frequent kuru cases, second only to the South Fore. The absence of a significant deviation from HWE in these linguistic groups may relate to a sample ascertainment problem, with all linguistic groups sharing a paucity of individuals >50 years old.

	Linguistic Group (years old)	N=	Codon 129			P-value HWE
			MM	MV	VV	
Exposed	**S.Fore**	1279	248	687	344	**0.005**
	>50	122	16	77	29	**0.003**
	<50	1157	232	610	315	0.044
	S.Fore male	426	72	240	114	**0.006**
	>50	74	11	40	23	0.474
	<50	352	61	200	91	**0.007**
	S.Fore female	853	176	447	230	0.149
	>50	48	5	37	6	**0.0004**
	<50	805	171	410	224	0.571
	N.Fore	276	52	146	78	0.331
	>50	81	10	43	28	0.356
	<50	195	42	103	50	0.474
	N.Fore male	109	19	53	37	1.0
	>50	42	5	21	16	0.749
	<50	67	14	32	21	0.807
	N.Fore female	167	33	93	41	0.163
	>50	39	5	22	12	0.506
	<50	128	28	71	29	0.288
	Keiagana	220	42	106	72	0.784
	>50	4	2	1	1	0.429
	<50	216	40	105	71	0.890
	Jate	43	7	26	10	0.226
	>50	14	1	8	5	0.590
	<50	29	6	18	5	0.278
	Agarabi	90	17	37	36	0.190
	>50	13	1	8	4	0.566
	<50	77	16	29	32	0.061
	Yagaria	114	28	56	30	0.853
	>50	36	8	19	9	1.0
	<50	78	20	37	21	0.655
	Awa	46	5	26	15	0.351
	>50	4	1	1	2	0.429
	<50	42	4	25	13	0.194
Unexposed	**BenaBena**	46	11	23	12	1.0
	>50	8	1	5	2	1.0
	<50	38	10	18	10	0.752
	Gadsup	42	4	26	12	0.101
	>50	5	0	5	0	0.127
	<50	37	4	21	12	0.321
	Morae	43	10	19	14	0.540
	>50	0	0	0	0	n/a
	<50	43	10	19	14	0.540
	Siane	74	18	35	21	0.646
	>50	17	4	9	4	1.0
	<50	57	14	26	17	0.595
	Tairora	77	15	43	19	0.364
	>50	16	2	8	6	1.0
	<50	61	13	35	13	0.313

Table 6.1 Hardy-Weinberg analysis of the Eastern Highland linguistic groups

HWE *P*-value calculated using exact test – significant deviations from HWE are in bold

6.4.3 Heterozygosity at codon 129

The Hardy-Weinberg data in Table 6.1 clearly indicates that deviations from HWE are due to excess heterozygosity at codon 129. It has been proposed that reduced diversity at various loci can be used as a tool to identify genes undergoing directional selection (Hughes *et al.*, 2003) and so it was hypothesised that conversely, loci with greater-than-expected diversity may indicate genes undergoing balancing selection. To further refine the HWE data and develop a test to apply to other loci, heterozygosity (H) was examined at codon 129. Linguistic groups were grouped based on kuru exposure levels: 1668 high kuru exposure samples (North and South Fore), 333 low exposure samples (Awa, Gimi, Jate, Keiagana and Yagaria) and 487 unexposed samples (Agarabi, Asaro, BenaBena, Gadsup, Gahuku, Labogai, Morae, Siane, Tairora and Yabiyufa) were analysed.

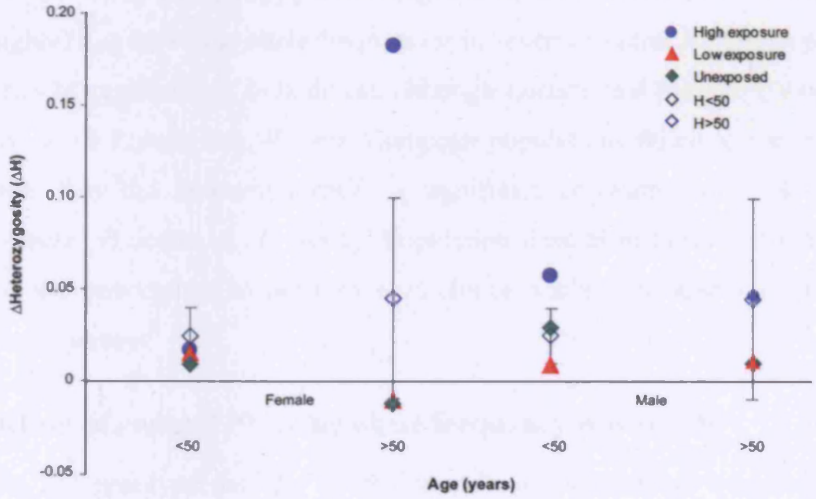

Figure 6.5 Heterozygosity at *PRNP* codon 129 stratified by sex and age
Mean heterozygosity (H) shown ± 1.96 SEM

The difference between expected and the observed heterozygosity (ΔH) was calculated and highly exposed women >50 years and men <50 years both differed significantly (P<0.001) from the global mean ΔH ± 1.96 SEM (Figure 6.5). In addition, all cohorts examined for HWE were tested using the Score test implemented in GENEPOP. All results were negative except highly exposed women >50 years, *P*=0.0002 and South Fore men between 40 and 50 years *P*=0.0049.

6.5 Variation of *PRNP* codon 129 valine allele frequency

The geographical co-variation of allele frequencies with intensity of selective pressure has been routinely cited as a signature of natural selection in human populations, see for example lactase persistence alleles and the establishment of dairy farming (Harvey *et al.*, 1998; Swallow, 2003) and blood pressure regulating alleles co-varying with latitude (Young *et al.*, 2005). Several authors have

identified a geographical cline of *PRNP* codon 129 allele frequency worldwide. Mead and colleagues first reported an approximate West-East reducing cline of the codon 129 valine allele, towards South East Asia and Oceania, identified through analysis of several world wide populations (Mead *et al.*, 2003). The valine allele frequency of the Fore population of PNG was found to be strikingly increased compared to neighbouring populations. Mead postulated that, taken with other data, one hypothesis describing the selective pressure responsible for creating and maintaining such a cline was the widespread occurrence of acquired prion disease, transmitted through cannibalism in prehistoric human populations and that in stark contrast the high valine frequency in the Fore represented a more recent episode of selection. This result was supported by the work of Soldevila and colleagues and Hardy and colleagues who investigated worldwide codon 129 allele frequencies in populations comprising the CEPH diversity project (Hardy *et al.*, 2006b; Soldevila *et al.*, 2003). Both Soldevila's and Hardy's data supported a longitudinal West-East cline in valine frequency and identified the highest known valine allele frequencies in several Central American populations with suspected histories of cannibalism. In addition, although Lucotte and Mercier's work investigating valine frequency in 12 French and Western European populations failed to identify a significant longitudinal cline, they did however identify a significant correlation of allele frequency with latitude (North-South) (Lucotte *et al.*, 2005). Population data from these and other international studies provided the opportunity to perform a combined analysis to assess worldwide clines in codon 129 allele frequency.

6.5.1 Variation of codon 129 valine allele frequency worldwide

Published codon 129 genotype data for normal worldwide populations were collected from the literature representing 41 countries. Data from 281 unexposed Fore individuals was obtained. Where data existed for distinct ethnic groups within a country, these were analysed separately. For simplicity, the geographical positions used for distance calculations were either (i) the country capital or (ii) the regional capital or largest regional town (for studied populations comprising of multiple ethnic groups). For example, several authors have studied *PRNP* variation in multiple Chinese ethnic groups including the Hui and the Uygur peoples, whose provincial capitals are separated by almost 2000 km and whose valine allele frequencies differ markedly by almost 15% (Figure 6.6).

The online map tool MultiMap (www.multimap.com, accessed 2006) was used to identify latitudinal and longitudinal coordinates in decimal degrees and distances from the Prime Meridian (at Greenwich, UK; 51.28N, 0E respectively), calculated using the Haversine formula employed in a java script (www.movable-type.co.uk/scripts/LatLong.html). Figure 6.7 illustrates the remarkable reducing cline seen in valine allele frequency worldwide. The correlation of allele frequency with

distance from the Prime Meridian was highly significant (Correlation coefficient R=0.80, R^2=0.65 and P=4x10^{-12}). The highest published valine frequency was found in Central America (Colombia 81% and Brazil 79%) (Hardy *et al.*, 2006b) and the lowest frequencies were found in East and South East Asia (Taiwan 1.5% and Japan 2%) (Mead *et al.*, 2003; Ohkubo *et al.*, 2003). In stark contrast to other populations at comparable distances east of the Prime Meridian, the Eastern Highlands valine allele frequency (based on the Fore population) significantly deviated from its predicted value.

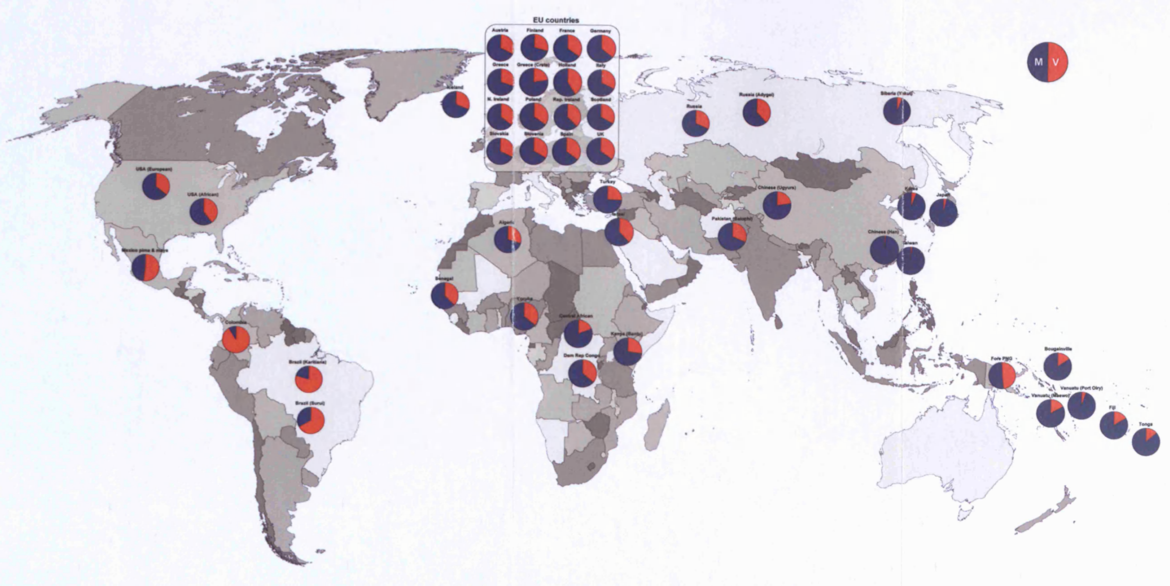

Figure 6.6 Worldwide *PRNP* codon 129 valine allele frequency

See Figure 6.7 legend

These data consolidate previous studies of worldwide variation of codon 129 and illustrate the Fore population of PNG as an outlier to this trend. As other authors have noted the two highest occurrences of valine allele frequency occur in the Fore population of PNG and in Central American populations, which all have documented cases of cannibalism.

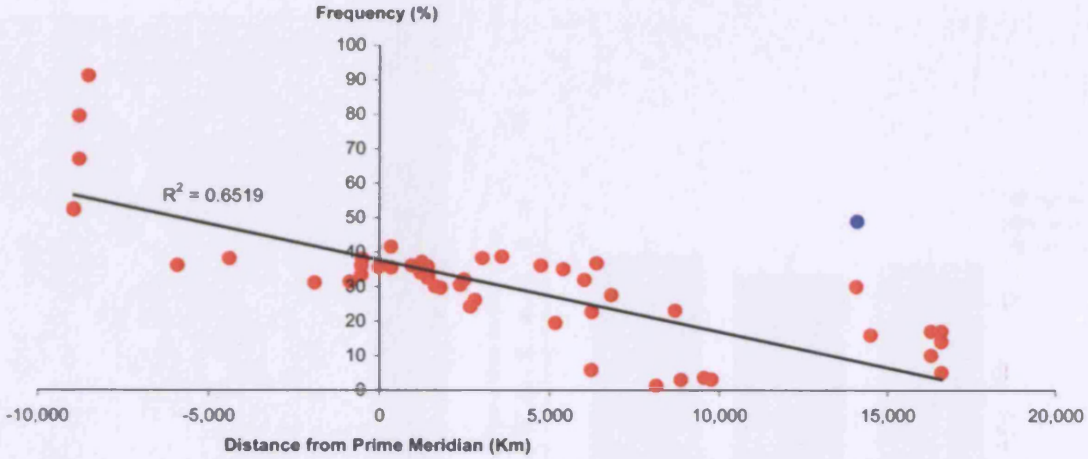

Figure 6.7 Variation of *PRNP* codon 129 valine allele frequency worldwide

Red data points: Austria (n=300) (Zimmermann *et al.*, 1999), China (Uygurs n=223; Han n=205) (Yu *et al.*, 2004), France (n=161) (Deslys *et al.*, 1994; Laplanche *et al.*, 1994), Germany (n=722) (Vollmert *et al.*, 2006), Greece (Crete n=205) (Plaitakis *et al.*, 2001), Greece (n=348) (Saetta *et al.*, 2006), Holland (n=117) (Bratosiewicz-Wasik *et al.*, 2007), Iceland (n=208) (Georgsson *et al.*, 2006), Italy (n=318) (Del Bo *et al.*, 2005), Japan (n=466) (Ohkubo *et al.*, 2003), Korea (n=529) (Jeong *et al.*, 2004), Poland (n=194) (Gacia *et al.*, 2006), Slovakia (n=613) (Mitrova *et al.*, 2005), Slovenia (n=97) (Galvani *et al.*, 2005), Spain (n=268) (Combarros *et al.*, 2000), Turkey (n=100) (Erginel-Unaltuna *et al.*, 2001), United Kingdom (n=406) (Collinge *et al.*, 1991), USA (n=86) (Brown *et al.*, 1994), Scotland (n=150), Northern Ireland (n=150), Republic of Ireland (n=203), Finland (n=1957) (Nurmi *et al.*, 2003), Mexico (Maya n=22; Pima n=25), Brazil (Surui n=21; Karitiana n=24), Colombia (n=11), Senegal (Mandenka n=24), Scotland (Orcadian n=16), Algeria (Mozabite n=30), Russia (n=25), Russia (Adygei n=17), Israel (Bedouin n=24), Central African Republic (Biaka Pygmy n=36), Cameroon (n=39) ,Yoruba (n=25), Pakistan (Balochi, n=26), Siberia (Yakut n=26), Democratic Republic of Congo (Mbuti Pygmy n=15), Kenya (Bantu n=20) (Hardy *et al.*, 2006b), Sri Lanka (n=35), Taiwan (n=70), PNG/Madang (n=83), Bougainville (n=22), Fiji (Taveuni n=10, other Fijian n=18), Tonga (n=22), Vanuatu (Port Olry n=33; Maewo n=32) (Mead, 2002). Blue data point: Papua New Guinea Fore population (n=281). Linear regression to the mean (R^2) indicated.

6.5.2 Variation of codon 129 valine allele frequency in the Eastern Highlands

As the results above show, the equilibrium valine allele frequency in the Eastern Highlands contrasts distinctly with the reducing cline seen worldwide particularly with neighbouring populations, including the costal PNG population of Madang (valine frequency 30%). Within the Eastern Highlands of PNG, kuru incidence is known to have varied geographically amongst the various linguistic groups that inhabit the region. The Fore linguistic groups comprised the epicentre of the kuru epidemic and the burden of kuru decreased, or was completely absent, in neighbouring linguistic groups. This geographical variation of kuru incidence afforded the opportunity to investigate the variation of *PRNP* codon 129 allele frequencies with kuru exposure amongst the linguistic groups of the Eastern Highlands, providing further evidence of the role of *PRNP* as a kuru susceptibility locus and a robust method for assessing other candidate susceptibility loci. Valine

allele frequency was calculated for each linguistic group and compared by exposure levels which were approximately proportional to distance from the focus of the epidemic in the South Fore region.

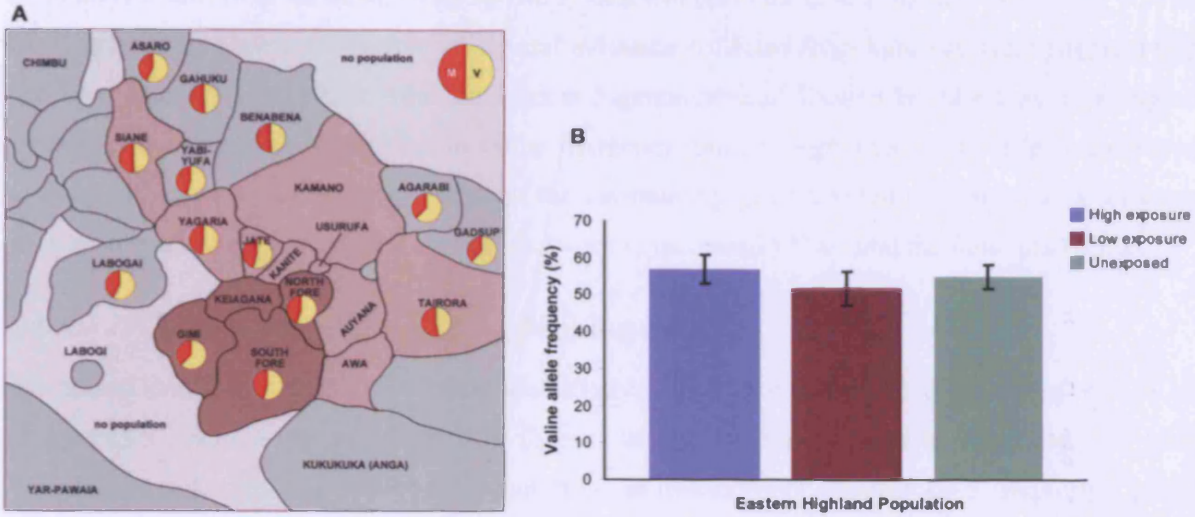

Figure 6.8 *PRNP* codon 129 valine frequencies across the Eastern Highlands

A. Linguistic groups with high exposure to kuru are shaded dark brown (Keiagana n=220; North Fore n=276; South Fore n=1279 and Gimi n=25). Low exposure linguistic groups are shaded light brown (Siane n=73; Tairora n=77; Yagaria n=114; Awa n=46 and Jate n=43). Unexposed linguistic groups are shaded green (Agarabi n=90; Yabiyufa n=30; Asaro n=26; BenaBena n=46; Gadsup n=42; Gahuku n=39; Labogai n=23 and Morae n=43). **B**. Mean valine allele frequency by kuru exposure level - no significant differences seen. Error bars are 1.96xSEM

Unexpectedly, an equilibrium valine allele frequency was identified across the linguistic groups of the Eastern Highlands, which was a surprising result (Figure 6.8A). There were no significant differences in allele frequency between those linguistic groups known to have been acutely exposed to kuru and those with low exposure (*T-test*, P=0.16) and unexposed groups (*T-test*, P=0.46) (Figure 6.8B). In addition there was no significant difference between the low exposed and unexposed groups (*T-test*, P=0.28). This intriguing result may have been due to: (i) demography – the uniform high valine frequency may reflect a historical bottleneck due migration and settling of the region rather than disease (ii) an older and more widespread incidence of kuru in the Eastern Highlands than previously reported (Jerome Whitfield, pers. comm.) and (iii) the absence of balancing selection – highly unlikely with evidence of HWE deviation presented earlier. In addition, the insensitivity of these analyses to the extent of kuru exposure of individual villages, as opposed to entire linguistic groups, may explain have confounded the results. It is known that within linguistic groups which experienced high occurrences of kuru, there were some villages that remained unexposed (Jerome Whitfield pers. comm.).

6.6 Linkage disequilibrium measures in PNG

Linkage disequilibrium was also investigated as a differentiating signature of kuru imposed selection. Under the balancing selection model, the frequency of the valine allele increased in the Fore populations from an initial value (possibly that similar to the costal Madang population ~30%) to its present equilibrium frequency. The oral evidence collected from kuru survivors suggests that the kuru epidemic was swift, affecting at most 3 generations of Eastern Highlanders, implying an equally dramatic and swift increase in valine frequency. Such a large increase in allele frequency at a locus can cause a "hitchhiking" effect of the surrounding genetic variation, known as a selective sweep. One consequence of such a selective sweep is increased LD around the functional allele.

6.6.1 LD between microsatellites flanking *PRNP*

Microsatellites 108 and 53*, previously identified by Dr Simon Mead 30 kb upstream and 24 kb downstream respectively of codon 129 (Mead, 2002), were genotyped in high and low kuru exposure populations and unexposed populations as described in Chapter 2.3.5. Haplotype phase was resolved by genotyping codon 129 homozygotes only. Mead previously demonstrated reduced microsatellite diversity and extended LD at both 108 and 53 in the Fore compared to European, Japanese and African populations. The additional samples and data on exposure index allowed LD comparisons across the Eastern Highlands to be made, controlling for differences due to demography of the international samples.

Microsatellites 108 and 53 and codon 129 were in significant LD (P_{exact} <0.000001, tested using the log likelihood method implemented in Arlequin) in all three groups examined on both haplotypic backgrounds. Similar patterns of allelic diversity and LD were seen in both directions for high, low and unexposed groups on both codon 129 methionine (Figure 6.9) and valine (Figure 6.10) allelic backgrounds. This result implied that either kuru had no effect on LD in the Eastern Highlands, or that the extent of LD surrounding *PRNP* in the Eastern Highland populations extends further than the two microsatellites examined and therefore, extended LD could not be detected. If the latter were true and kuru had affected LD surrounding *PRNP*, a reduction in allelic diversity would also be expected on the valine haplotype, which is not seen either.

* also referred to as a108990 and a54000 in (Mead, 2002)

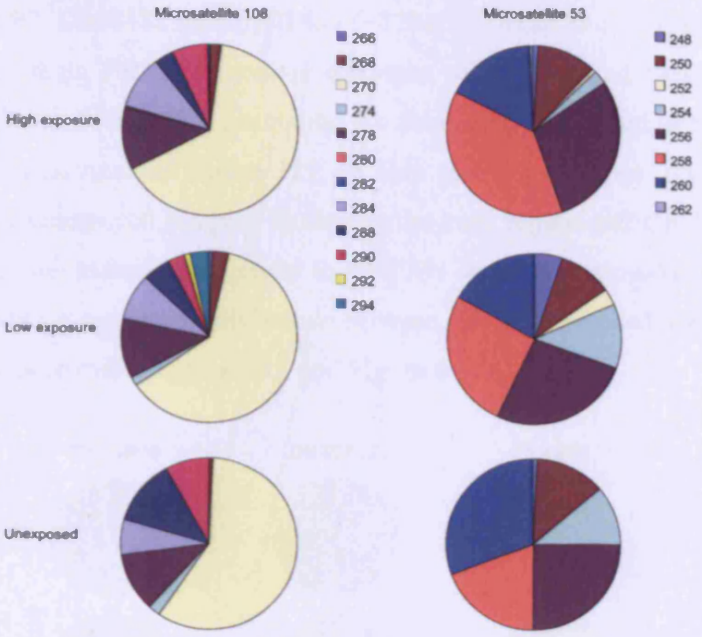

Figure 6.9 Microsatellite diversity upstream and downstream of the *PRNP* codon 129M allele

Allele frequencies at microsatellites 108 (upstream) and 53 (downstream) on the *PRNP* codon 129M haplotype. Maximum number of haplotypes: high exposure n=406, low exposure n=176 and unexposed n=136. No significant differences were seen in allele diversity or LD when compared between groups.

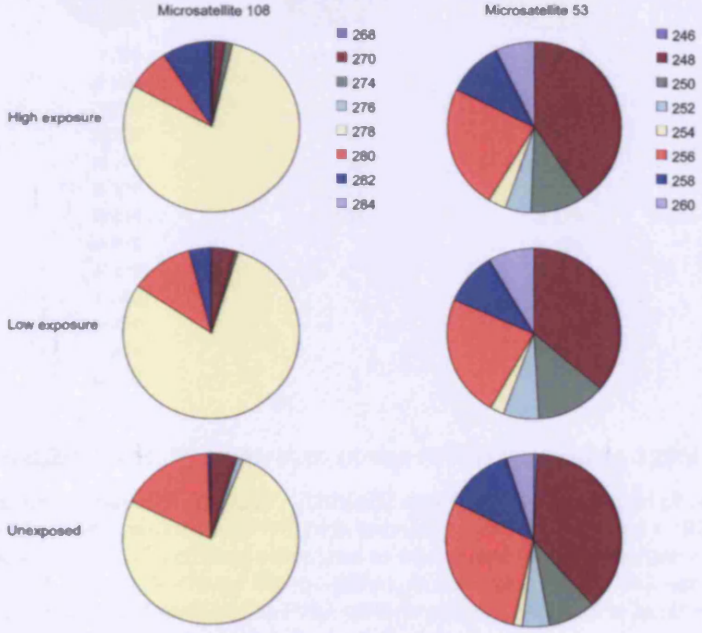

Figure 6.10 Microsatellite diversity upstream and downstream of the *PRNP* codon 129V allele

Allele frequencies at microsatellites 108 (upstream) and 53 (downstream) on the *PRNP* codon 129V haplotype. Maximum number of haplotypes: high exposure n=562, low exposure n=246 and unexposed n=162. No significant differences were seen in allele diversity or LD when compared between groups

Microsatellites D20S97, D20S482 and D20S889 (~720kb, ~161kb and ~143kb upstream of codon 129, respectively) flanking *PRNP* at greater distances were identified using the STS database UniSTS. These microsatellites were genotyped as previously discussed with help from James Uphill, in samples homozygous at codon 129, to help phase haplotypes: high exposure samples from the kuru region, unexposed samples bordering the kuru region and UK ECACC samples for comparison. Although microsatellite diversity in the PNG samples was markedly different form the UK samples, there was no significant difference between the kuru exposed and unexposed samples on both haplotypic backgrounds (Figure 6.11 and Figure 6.12).

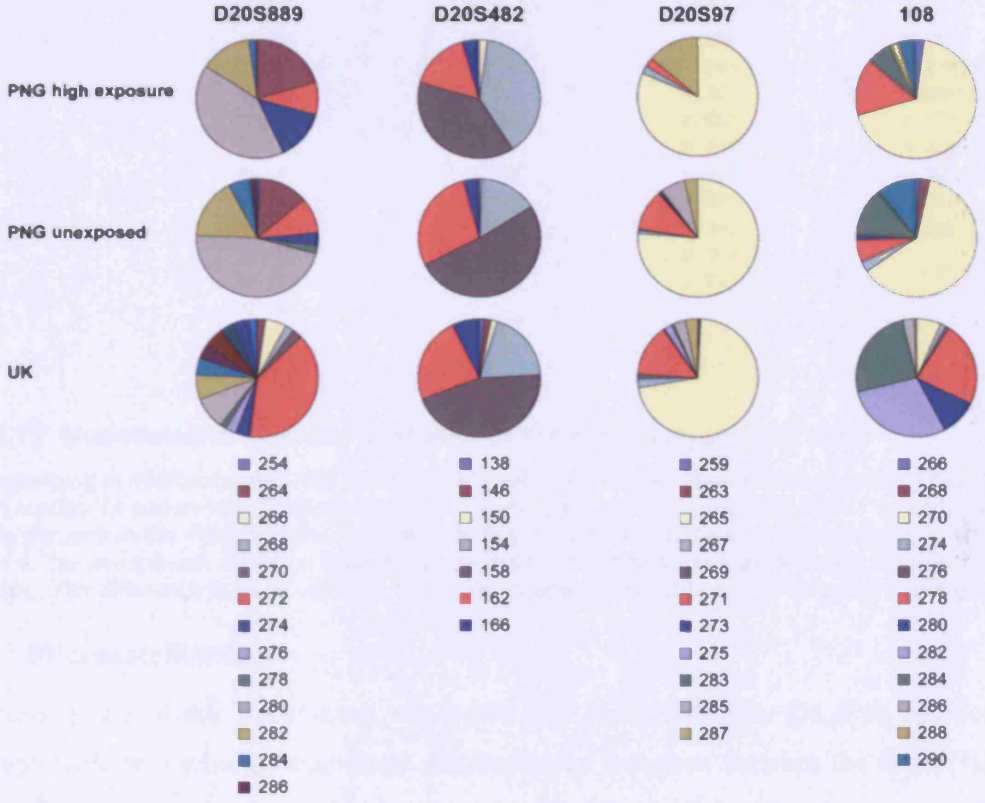

Figure 6.11 Microsatellite diversity upstream of the *PRNP* the codon 129M allele

Allele frequencies at microsatellites *108, D20S97, D20S482* and *D20S889* upstream of codon 129M allele. Maximum number of codon 129M haplotypes PNG high exposure n=44, unexposed n=228 and UK n=288. Allele diversity is reduced in the PNG samples compared to the UK and also in the high kuru exposed group compared to the unexposed. Although linkage disequilibrium is extensive in the PNG samples compared to the UK samples, little difference is seen between the PNG cohorts acutely exposed to kuru and those unexposed.

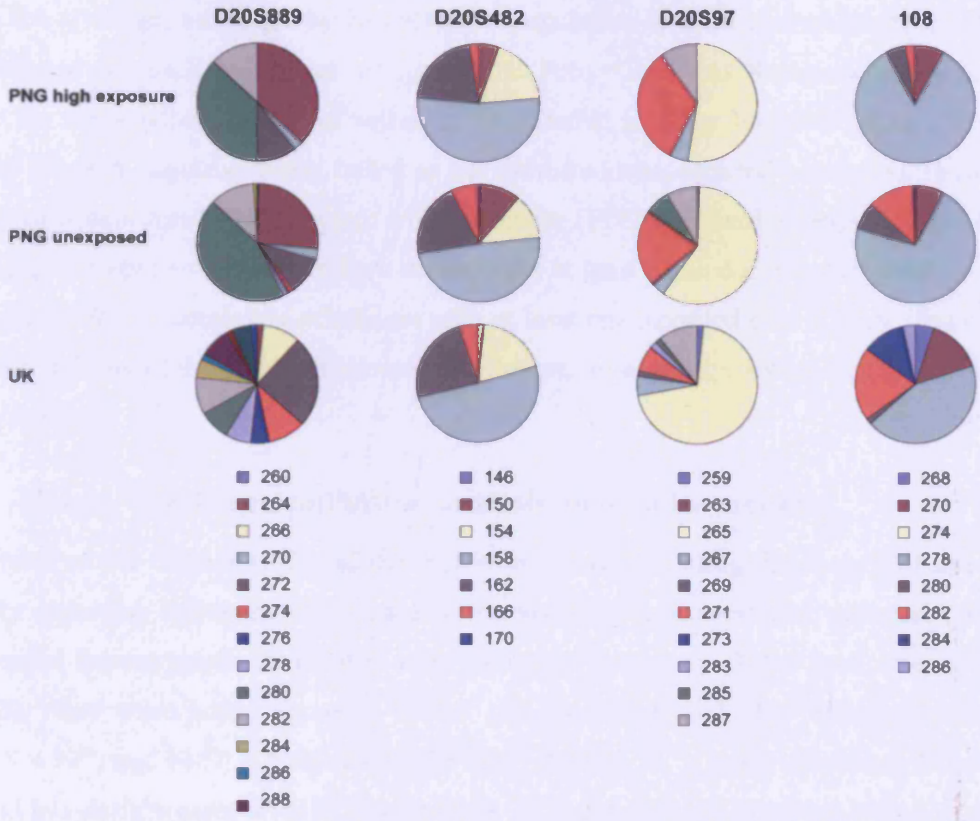

Figure 6.12 Microsatellite diversity upstream of the *PRNP* codon 129V allele

Allele frequencies at microsatellites *108, D20S97, D20S482* and *D20*S889 upstream of codon 129V allele. Maximum number of codon 129V haplotypes PNG high exposure n=40, unexposed n=344 and UK n=60. Allele diversity is reduced in the PNG samples compared to the UK and also in the high kuru exposed group compared to the unexposed. Although linkage disequilibrium is extensive in the PNG samples compared to the UK samples, little difference is seen between the PNG cohorts acutely exposed to kuru and those unexposed.

6.6.2 Microsatellite F_{ST}

F_{ST} analysis of the above populations was performed using Arlequin. On both methionine and valine haplotypic backgrounds significant differentiation was seen between the two PNG cohorts against the UK cohort ($P<<0.000001$, data not shown). Marginal significance was seen for valine associated alleles between kuru high exposure and unexposed ($P=0.02 \pm 0.02$) cohorts, indicating that some genetic differentiation exists between these two groups. The methionine comparison was not significant ($P=0.06 \pm 0.01$).

6.7 Refining the exposure of linguistic groups – exposure index

The continuing efforts of the MRC-PNGIMR field team collecting biological samples, clinical and historical data relating to the kuru epidemic permitted a refining of kuru exposure estimates to the level of individual villages within linguistic groups. A detailed explanation of how the new exposure index (EI) for each village was calculated is provided in the Materials and Methods. Briefly the EI for each village community was defined as the number of recorded kuru deaths in the

database for a village, normalise by its estimated population in 1958 and scaled by 1000. The EI was calculated for each individual village in the Fore, Gimi and Keiagana linguistic groups, however for the smaller number of villages, and deaths, in other linguistic groups the EI was calculated for each linguistic group, based on the estimated kuru-affected population. Broadly three levels of kuru exposure were adopted: high exposure (EI>200), medium exposure (30<EI<200) consisting of villages bordering the kuru region with at least some documented cases of kuru and low exposure (EI<30) consisting of villages with at least one recorded case of kuru. The new index permitted a refining of the level of exposure and the area of exposure, which may have confounded previous analyses.

6.7.1 Hardy-Weinberg equilibrium analysis indexed by exposure

A proportion of the Eastern Highland samples were reanalysed using the new EI (Table 6.2). As previously observed, increased homozygosity at codon 129 was associated with early onset kuru and increased heterozygosity associated with protection from kuru. 39/56 kuru cases with age at onset <20 years were homozygous at codon 129 compared to 39/125 elderly women EI>30 (P_{exact}=1.8 x 10^{-6}) and 14/50 elderly women EI>200 (P=3.4 x 10^{-5}). Hardy-Weinberg disequilibrium was found in elderly women with EI>30 (P=6.6 x 10^{-9}) and with EI>200 (P=0.004), increasing the significance which was a more significant deviation than that seen before in the linguistic group analysis. Loss of HWE was not found in a stratum of slightly younger women aged 40-50, born towards the end of the practice of mortuary feasts, and was also absent from elderly men and unexposed elderly women. As previously identified, a stratum of men aged 40-50, who would have participated in mortuary feasts as children, displayed marginal HWE deviations (P=0.016).

6.7.2 *PRNP* codon 129 valine allele frequency analysis indexed by exposure

Using the new EI classifications, codon 129 genotypes from 282 elderly women (>50 years old in 2000) from villages with EI>30 in the North Fore, South Fore, Keiagana and Gimi were obtained (referred hereafter as the kuru region; Figure 6.14). Codon 129 data were also obtained for low exposure populations, comprising individuals from Gimi (n=87), Jate (n=157), Keiagana (n=221), Kanite (n=35) and Awa (n=46) linguistic groups. Mean valine allele frequency was not significantly different between the kuru region and low exposure populations (57.4% and 54.3% respectively) by a two-tailed χ^2 test (Figure 6.13).

Additional Highland populations with no recoded cases of kuru comprising of individuals from villages speaking Asaro (n=19), BenaBena (n=20), Gadsup (n=22), Gahuku (n=42), Labogai

(n=47), Siane (n=29), Tairora (n=79), and Yabiyufa (n=27) were also tested against the mean allele counts of the kuru region data and found to be significant (two tailed χ^2 test P=0.004; Figure 6.13).

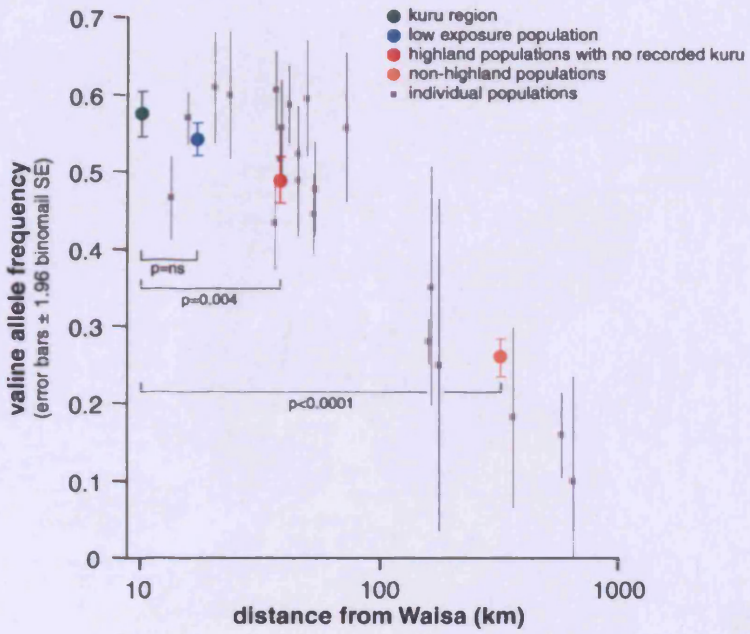

Figure 6.13 An increasing cline in codon 129 valine frequency within Papua New Guinea

Codon 129 allele counts were compared between the kuru region (n=282) and: low exposure populations (n=546), Highland populations with no recorded kuru (n=281) and non-highland populations (n=313). Subpopulations are shown in grey. (From Mead *et al.*, 2007).

Codon 129 genotypes were also obtained from more distant, non-Highland populations including: Vanimo/wewak (n=5), islands neighbouring PNG (n=44), Port Morseby (n=11), Western Highlands (n=4), Madang and its neighbouring inland area (n=239), and Lae (n=10) and comparison against the kuru region for allele count was highly significant (two tailed χ^2 test at P<0.0001; Figure 6.13). The mean distances between the villages examined and Waisa in the South Fore were calculated as previously described for each analysis group. Valine allele frequency significantly co-varied with distance from Waisa and exposure to kuru (correlation coefficient R=-0.99, P=0.007; Figure 6.13).

6.8 Additional *PRNP* susceptibility loci

During genetic screening studies of *PRNP* at the MRC Prion Unit by the Molecular Genetics Group, a novel coding change was detected in a highly conserved and structured region of PrP. The change at codon 127 of *PRNP* from glycine to valine was identified in elderly women >50 years from the geographically restricted region of the Purosa Valley and neighbouring villages (Figure 6.14). In this area, with the highest kuru exposure, G127V is a common variant, occurring at ~7% frequency and exclusively on the 129 methionine background (based on a retrospective analysis of Fore pedigrees collected prior to the discovery of the allele).

Figure 6.14 The kuru region divided into three zones of increasing exposure

Villages in grey with at least one recorded case of kuru but exposure index (EI) <30, a zone of EI >30<200, a high exposure zone with EI>200. Red points show the location of 127V individuals. (From Mead *et al.*, 2007).

The G127V change was genotyped by dideoxy resequencing in 161 WGA kuru samples and was found to be completely absent. This absence was significant when 127V-129M haplotype counts were compared by a two-tailed exact Pearson χ^2 test, to 125 elderly women (>50 years old in 2000) from the exposed region (P=0.005; Table 6.2). Based on the codon 129 heterozygous/homozygous resistance/susceptibility model, homozygosity at both loci was investigated. Homozygosity at both codon 127 and 129 was seen in 37/49 of the kuru cases <20 years old, compared to 39/125 of elderly women (<20 years old during the peak of the epidemic) which was highly significant (P=6.6x10^{-9}, exact χ^2 test, see Table 6.2). In addition, division of the kuru cohort by long (>30 years, onset after 1990) and short (aged <20 at sampling) average incubation time, illustrated that only 12/49 of the short incubation cohort were heterozygous at either codons 127, 129 or both, compared with 86/117 of elderly women (P=6.5 x 10^{-7}; exact χ^2 test, see Table 6.2).

		G127V			M129V		
	n	GG	GV	VV	MM	MV	VV
All Kuru[a]	**161**	**161**	**0**	**0**	**39**	**94**	**28**
Incubation <20[b] years	49	49	0	0	23	12	14
Incubation >30 years	10	10	0	0	1	8	1
Women >50[c] EI >30	125	119	6	0	16	86	23
Women >50[d] years EI >200	50	44	6	0	6	36	8
Women 40-50[e] years	150	144	6	0	30	80	40
Men >50[f] years	122	121	1	0	20	58	44
Men 40-50[g] years	83	81	2	0	14	53	16
Unexposed[h] women >50 years	50	50	0	0	13	28	19

Table 6.2 Genotypes of kuru patients and age-stratified healthy population controls

[a] all kuru vs. women >50 years, EI >30 (using 127V-129M haplotype counts) *P*=0.005
[b] kuru incubation <20 years vs. women >50 years, EI >30, *P*=6.6 x 10-9
[c] women >50 EI >30 exact test of HWE at codon 129, *P*=3.1 x 10-5
[d] women >50 EI >200, exact test of HWE at codon 129, *P*=0.004
[e] women 40-50 exact test of HWE at codon 129, *P*=0.42
[f] men >50 exact test of HWE at codon 129, *P*=1
[g] men 40-50 exact test of HWE at codon 129, *P*=0.016
[h] Unexposed women >50 years, exact test of HWE at codon 129 *P*=1.0
(From Mead *et al.*, 2007).

The relative fitness of each codon 127 and 129 haplotypic combination was calculated for the entire exposed population of both genders aged over 40 (n=472), which was chosen to be a large sample representative of the genetic effect of kuru on the descendent population. The relative fitness of each heterozygous combination (127GV-129MM, 127GG-129MV and 127GV-129MV) was assumed to be equal as there was insufficient data to calculate these separately. The relative fitness for 127GG-129MM was 0.64 and 127GG-129VV was 0.74, relative to a combination of the three heterozygous genotypic combinations. More highly kuru-exposed subgroups had an even lower relative fitness of homozygous genotypes: elderly exposed women (EI>30), 127GG-129MM relative fitness was 0.38, and 127GG-129VV was 0.48; elderly exposed women (EI>200), 127GG-129MM relative fitness was 0.23 and 127GG-129VV was 0.42.

6.8.1 Genealogy and codon 127

To confirm or refute the function of G127V mutation as a resistance factor, the incidence of kuru in the parents of the current living 127V probands, who would have lived through the kuru epidemic, was ascertained. This hypothesis was based on the assumption that as one of the parents would be expected to be a 127V carrier, an increased or reduced history of kuru in this generation would indicate whether 127V was acting as a susceptibility or resistance factor.

51 individuals carrying the 127V mutation, aged 16-78 years (mean age 35 years, 11 individuals aged 50 or older), were interviewed by an MRC-PNGIMR research nurse and none were found to

be symptomatic of dementia, ataxia or other evidence of neurodegenerative disease. Genealogies had been obtained, prior to the detection of the variant, from 18 probands with 127V. 127V genealogies were matched to all 127G pedigrees obtained from villages in the Purosa valley in which more than one 127V individual had been detected to obtain a control cohort. With the exception of Agakamatasa and Ilesa with moderate exposure, the village were all found in the region of highest kuru exposure. The village EI values were as follows: Purosa-Takai (172), Ai (221), Takai (362), Kamira (337), Ketabi (265), Ivaki (295), Mugaimuti (346), Kalu (200) and Waisa (217). Only 1/36 parents from 127V genealogies was recorded as dying from kuru, whereas 33/218 parents were recorded as dying from kuru in the matched 127G pedigrees (P=0.04; two tailed exact χ^2 test).

Given the apparent geographically restriction of the 127V mutation (Figure 6.14), it was suspected that there was a recent common ancestor of all alleles. 13 *PRNP* linked microsatellite markers were genotyped over 3 MB (*D20S181, D20S193, D20S473, D20S867, D20S889, D20S116, D20S482, D20S97, PRNP* Codon 129, *D20S895, D20S849, D20S873, D20S95* and *D20S194*) in all 127V individuals to test this hypothesis and haplotypes were identified using PHASE. 25/52 127V chromosomes shared at least one identical microsatellite allele across the region (Figure 6.15) consistent with a 127V-linked haplotype. The same haplotype was found in only 1/70 127G chromosomes.

The age of the 127V mutation was estimated by using the microsatellite data to find the time to most recent common ancestor (MCRA). Of the 13 microsatellites 4 were uninformative and one was excluded because of doubt over the genetic distance between this marker and *PRNP*. The time to MCRA was calculated by modelling recombination-mediated LD decay over time using the formula of Risch *et al.* (Risch *et al.*, 1990), as corrected by Colombo (Colombo, 2000). Importantly, this calculation did not consider the likelihood of selection acting on the variant and was therefore likely to be a conservative calculation. The median result of the 8 remaining markers gave a point estimate of the most recent common ancestor of 127V occurring within 13 generations (95% confidence intervals: 0 to 30 generations). Confidence intervals based on 10,000 bootstraps of the data (See Efron, 1993).

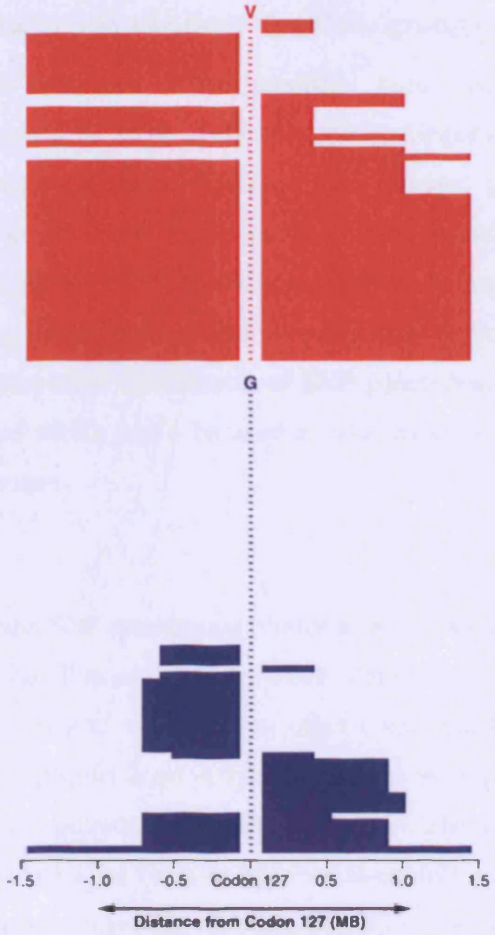

Figure 6.15 Size of 127V-linked haplotype compared with the same haplotype on 127G alleles

13 microsatellites linked to *PRNP* were genotyped and 8 were then used to date the most recent common ancestor which are illustrated here (*D20S181, D20S889, D20S116*, Codon 129, *D20S895, D20S849, D20S873, D20S95 and D20S194;* map locations relative to codon 129: -1494556, -720087, -613627, 419565, 527025, 929772, 1049310, 1475648). Codon 127-linked haplotypes were determined using PHASE software. The central dash refers to an individual haplotype, 127V-linked haplotypes are red and 127G are blue. Individuals are ordered by increasing size of linked haplotype. (From Mead *et al.*, 2007).

6.8.2 Additional *PRNP* independent susceptibility loci

The identification of the codon 127 mutation in the South Fore women supported the hypothesis that susceptibility factors other than codon 129 of *PRNP* may exist. The utility of examining neighbouring linguistic populations as a means of supporting the role of codons 127 and 129 in kuru susceptibility demonstrated the potential for this sample resource to identify *PRNP*-independent susceptibility loci using a genome-wide approach. Genome-wide SNP data for example could be used to obtain both an empirical distribution of "neutral" variation data and also be used to conduct genome-wide association studies.

6.9 Genome-wide analyses in the Fore linguistic group of Papua New Guinea

The analyses thus far have addressed *PRNP* mediated kuru susceptibility and the genomic signatures of variation that could be used to identify the participation of a locus. Developing a resource from the PNG Eastern Highland population, has allowed genetic variation at potential susceptibility loci to be to be examined for co-variance with exposure. Although this has been shown above to work effectively at *PRNP*, possibly because of its large effect size, other loci may be susceptible to confounding due to factors such as population demography. Therefore, attention was turned to obtaining an empirical distribution of SNP genotypes, against which signatures of selection may be assessed and which could be used to conduct whole-genome association studies and whole-genome selection scans.

6.9.1 Study design

Although several whole-genome SNP genotyping platforms were available, the opportunity arose to utilise the Affymetrix GeneChip Human Mapping 500K Array Sets*. The Affymetrix 500K array provided the greatest SNP density as compared to other commercial platforms with comparable genomic coverage. In total, 14 surplus NspI Affymetrix arrays were provided by Dr Simon Mead, each capable of genotyping approximately 250,000 SNPs each. The 14 arrays were used to pilot a kuru versus elderly kuru-exposed Fore females hyper-case-control study and so the study design was considerate of this and several other factors including time, cost and sample/array availability. 7 samples in each group were chosen for screening, permitting the analysis of common SNPs at MAF> 7.1% in the population. In addition the feasibility of using whole-genome amplified (WGA) kuru samples (required to maintain sufficient quantities of DNA for future research) could be tested.

6.9.2 Whole-genome amplification of kuru samples

The majority of kuru samples held at the MRC Prion Unit were collected in the years immediately following the peak of the epidemic, between 1957 and 1960 by investigators from the National Institutes of Health (Maryland, USA). Many of these samples had either degraded over time, which affected the quality of the DNA subsequently isolated, or were provided as blood sera, which typically yields low concentrations of DNA (compared to erythrocytes). To fully exploit these limited resources Multiple Displacement WGA was performed by Geneservice Ltd (Eng Ang *et al.*, 2007) on a subset of samples to investigate the efficacy of using amplified sample for genetic investigations. 8 kuru samples (PDGs 7450, 7456, 7468, 7470, 7504, 7520, 7595 and 7744), comprising 6 females and 2 males aged from 8 years to 40 years old, which were provided as genomic DNA extracted from sera, underwent WGA. The DNA yield was increased by 1000 fold

* Each Affymetrix 500k Array set comprises two 250K arrays which genotype SNPs proximal to either NspI or StyI restriction sites

and all samples passed Geneservice's quality control criteria except for PDG7520, which was dropped from further analysis due to allele drop-out.

6.9.3 Pre-hybridisation preparation of the PNG samples

The samples were prepared for hybridisation onto the Affymetrix chips as described in Materials and Methods (Chapter 2.3.12). During pre-hybridisation, PCRs of the adaptor-ligated fragments were visualised on 2% TBE agarose gel as shown in Figure 6.16. Prominent banding was seen at approximately 2.25kb and 2.75kb in all WGA samples only, possibly an artefact of the WGA process such as biased amplification.

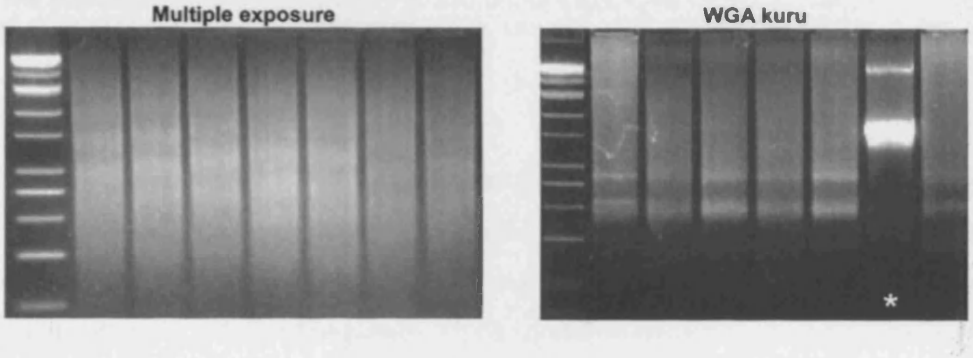

Figure 6.16 PCR of 7 South Fore multiple kuru exposure samples and 7 kuru samples

The multiple exposure and kuru samples were amplified in triplicate to provide a sufficient quantity of PCR product. The whole-genome amplified kuru samples amplified poorly compared to the multiple exposure samples with prominent bands at approximately 2.75kb and 2.25kb. *Sample PDG7595 showed an atypical band at 4kb. Run on 2% TBE agarose gel at 120V for 1 hour. Ladder sizes: 10kb, 8kb, 6kb, 5kb, 4kb, 3kb, 2.5kb, 2kb, 1.5kb, 1kb and 0.5kb.

WGA sample PDG7595 showed an atypical band at approximately 4kb. To exclude poor sample handling as a cause of the atypical band, the sample preparation was repeated with a second WGA sample with an untreated control. PDG7595 again showed an atypical band in contrast to the control samples (data not shown) however, it was retained for downstream hybridisation to identify what effect (if any) it might have on the genotyping call-rate. The PCR banding of PDG7595 had no effect on the fragmentation pattern (Figure 6.17).

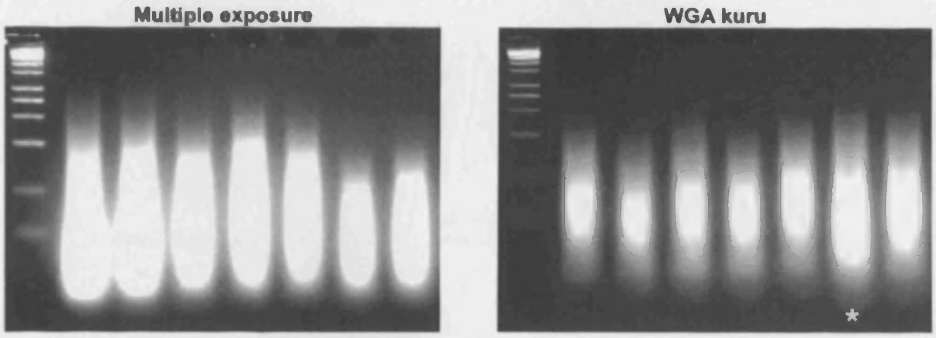

Figure 6.17 Fragmentation of ligated PCR products

Fragmentation of the ligated PCR amplicons resulted in a range of fragment sizes. The relative intensity of the multiple exposure samples compared to the WGA kuru samples reflects the differing amounts of starting material. *The fragmentation of sample PDG7595 was similar to the other WGA kuru samples. Run on 4% TBE agarose gel at 120V for 30 minutes. Ladder sizes: 10kb, 8kb, 6kb, 5kb, 4kb, 3kb, 2.5kb, 2kb, 1.5kb, 1kb and 0.5kb

6.9.3.1 Assigning calls and data analysis

As much of the data presented in the following sections rely on different SNP call assignments, a brief overview of how SNP genotypes are assigned is provided. Each 250K Affymetrix array contains over 6.5 million features*, each consisting of more than one million copies of a 25nt oligonucleotide probe of a defined sequence which is complimentary to the sequence surrounding a SNP. Probes are arranged as quartets comprising perfect match and mismatches to each allele and 6 or 10 probe quartets are used for each SNP at various locations on the array. SNP genotypes are called using an algorithm which utilises the fluorescent intensities of the 6 or 10 quartets distributed across the chip and the intensities of matches/mismatches within each quartet.

The hybridised arrays were scanned using a GeneChip Scanner 3000 and data analysis was conducted using the Affymetrix GeneChip DNA Analysis Software (GDAS). Genotypes were called using the Dynamic Model (DM) Mapping Algorithm employed within GDAS which also provided quality information for each call, based on the Wilcoxon's signed rank sum test. Data were obtained at three rank/confidence score thresholds (P=0.33, 0.16 and 0.1). Increasing the rank score threshold (moving the dashed line in Figure 6.18 towards the centre of the triangle) can increase the number of genotypes called, thus reducing the number of no calls, but may also reduce the confidence of these additional calls. The converse is also true.

* squares etched onto the glass array

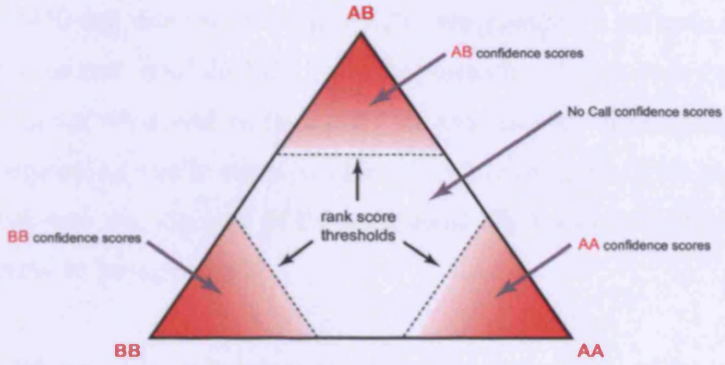

Figure 6.18 Dynamic Model scatter plot for calling genotypes

Graphical representation of the Dynamic Model (DM) algorithm. Genotypes are called based on measured fluorescence intensities, converted using the DM algorithm and tested against one of four genotype models (AA, AB, BB and null), with the rank score of the most likely model used to give a confidence measure in each called genotype. High confidence calls (~0) are plotted at the vertices and scores closer to 1 are near the centre of the triangle. Decreasing the rank score threshold (dashed line) increases the number of no calls and increasing the threshold decreases the number of no calls. Adapted from (Affymetrix, 2005b).

6.9.4 Hybridisation efficiency and call rates

Subsequent to scanning, each NspI array image was visually inspected for an assessment of quality. All samples were successfully scanned except for PDG7470 for which the array image was exceptionally dark (Figure 6.19). GDAS analysis was undertaken at a default threshold (P=0.19) and call rates obtained. WGA array call rates ranged from 49.6% to 72.9% (mean ~61%) and mean multiple exposure call rate was ~95% (good quality DNA with proper handling should yield call rates >93% (Affymetrix, 2005b)). With an atypical array image and a low call rate of 60%, PDG7470 was repeated for fear that post-hybridisation (staining and washing) reagents used for this chip only were contaminated. In addition, repeating the sample provided an opportunity to obtain a technical replicate, allowing the concordance rate* to be calculated between replicates and an assessment of assay repeatability on WGA samples.

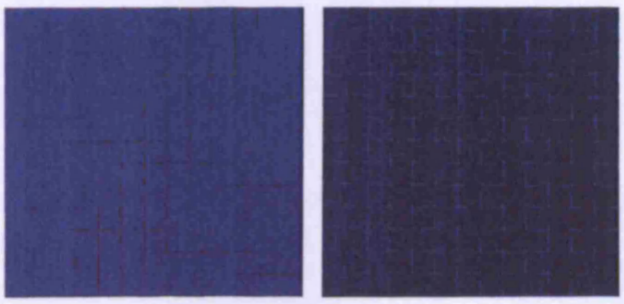

Figure 6.19 GeneChip NspI hybridisation array images for sample PDG7470

Labelled DNA hybridised poorly onto the NspI array (**right**) which gave a low genotype call rate. Repeating the sample gave a better call rate and a brighter array image.

* Concordance is calculated by identifying the fraction of SNPs which are assigned identical genotypes on a set of replicate arrays (two arrays hybridised with the same sample)

The repeated PDG7470 call rate improved to 69.8%, representing a net gain of 10,719 genotypes (37,081 SNP calls gained and 26,362 lost). Importantly, the majority of new calls were heterozygotes, which are often under-represented by fluorescence based detection due to bias in detecting a 50% decrease in allelic signal compared to homozygotes. This result implied that the cause of the low call rate was staining of the hybridised DNA molecules which resulted in lower fluorescence compared to background.

With 10% of the total concordance between the two arrays comprising of "no calls", the possibility of increasing the call rate by varying the stringency of the rank score threshold was examined. This would require a trade off between call rate and genotyping accuracy and therefore the relationship between these two variables was examined. Additional replicated NspI array genotyping data were obtained for 6 vCJD samples from Dr Mead and analysed with PDG7470. The 6 vCJD samples were not true technical replicates as one sample in each replicate was WGA treated however, they could provide data on WGA DNA performance on arrays. Analyses were conducted at thresholds 0.5, 0.3 and 0.19 and compared to a base-line analysis at 0.1 (Figure 6.20).

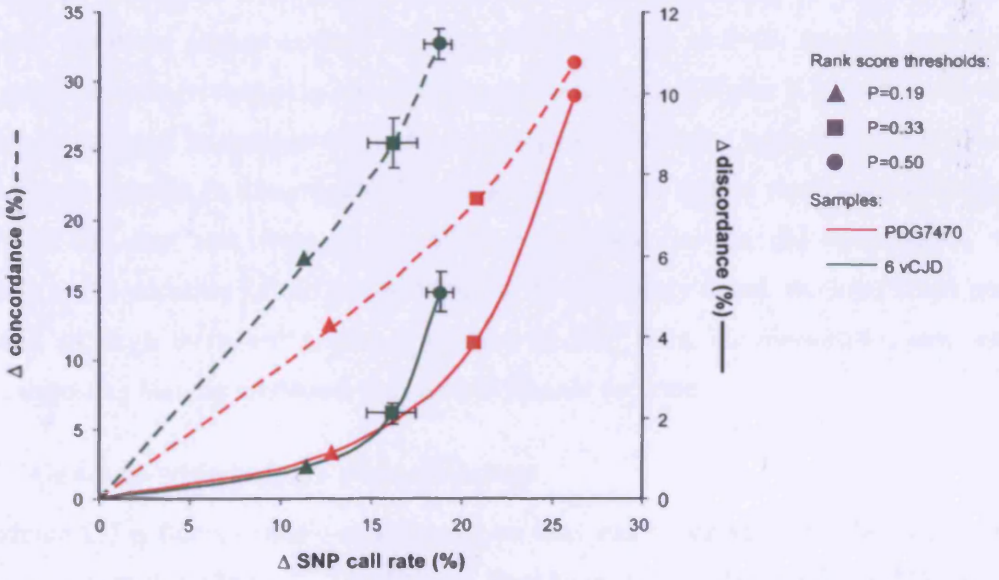

Figure 6.20 SNP gains and data reliability at various rank score thresholds

Increased call rates, relative those achieved at P=0.10, were seen for all threshold values. Mean values were calculated for the 6 vCJD samples. The maximum gain in SNP calls was achieved with P=0.19 with high SNP concordance and low discordance, after which increasing the threshold yielded diminishing returns. Error bars 1.96xSEM

The 6 WGA vCJD samples had similar call rates to their genomic replicates at various rank threshold values and comparing the genomic and WGA replicates, concordance varied directly with both threshold and call rate. At the most stringent threshold of P=0.1, a low mean call rate of 82.5% was seen with a low mean concordance rate of 72%. As the threshold stringency was decreased to

0.19, 0.33 and 0.5, both the mean call rate and concordance increased proportionally suggesting that genotypes were stable between replicates and therefore the majority of the data gained were accurate. Some increase in discordance was seen however as stringency was reduced (not including genotypes which were converted into "no calls" or vice versa). The mean discordance amongst the 6 arrays increased from 0.2% to 3.6% as stringency decreased. Taken together, these data suggest that for the vCJD samples, the WGA treatment had little effect on the quality of genotype data and that for chips with low call rates, the rank score threshold could be relaxed to obtain extra reliable data.

In comparison, the kuru chips performed poorly with, at P=0.5, a maximum mean call rate of 80%, concordance of 70% and an unacceptable high genotype discordance of 10%. At P=0.1, only 57% of the SNP genotypes were called and with only 40% concordance between chips. Whether this poor performance was due to the WGA of poor starting material or if it reflected the poor post-hybridisation treatment of the first chip, was not known.

To identify the optimal threshold value for WGA treated arrays – one that would accurately yield the maximum number of SNP genotypes with the minimum amount of discordance between replicates – the mean change in SNP call rate relative to that at P=0.1 baseline was examined, against mean percentage change in concordance and discordance (Figure 6.20). For both vCJD and kuru chips the greatest increase in call rate was seen at P=0.19 with a large increase in concordance and a marginal increase in discordance. Relaxing the threshold further yielded diminishing returns in terms of call rate and although concordance increased, so too did discordance, reducing confidence in the accuracy of the additional data. As previously noted, the kuru chips performed poorly and although there was a greater increase in SNP calls, the discordance rate was much greater, suggesting that the additional data gained was not accurate.

6.9.5 Genome-wide linkage disequilibrium

To determine LD patterns genome-wide, genotype data was exported from Affymetrix GeneChip Genotyping Analysis Software (GTYPE) into Haploview to calculate pairwise LD comparisons between SNPs. Unless stated, Affymetrix data was exported at a rank score threshold of P=0.33. Pairwise LD (D') was determined for loci with 85% completeness of genotype data, MAF>15% and for comparisons <100kb. The MAF cut-off of 15% was chosen based upon genome-wide data published for isolated population of Kosrae in which the allele frequency distribution of common alleles >15% was similar to other worldwide populations (Bonnen *et al.*, 2006) and was therefore not affected by SNP ascertainment bias. Mean pairwise LD was calculated for comparisons of increasing 2.5kb distances.

6.9.5.1 Genome-wide LD is inflated in small samples

Initially, pairwise LD was assessed for the 7 samples from elderly Fore women with multiple exposure to kuru with genotype data acquired at three different rank score thresholds (Figure 6.21). Varying the threshold had little effect on the genome-wide LD profile.

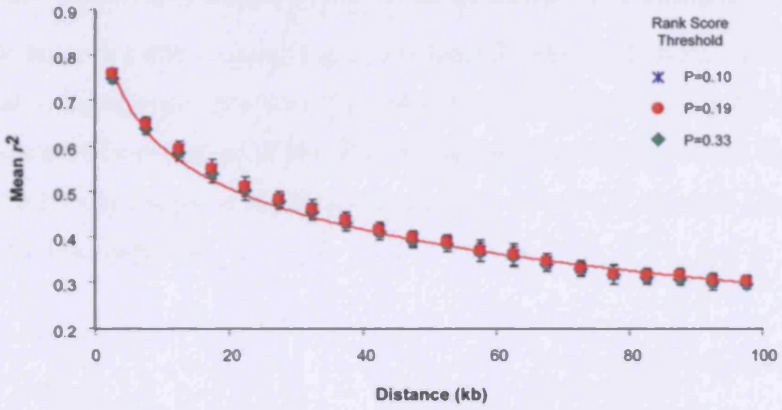

Figure 6.21 Pairwise LD in 7 elderly multiple kuru-exposed samples at different thresholds

Mean r^2 was calculated for pairwise comparisons between markers with minor allele frequencies ≥15% that fell within the same 2.5kb intermarker distance bins for 7 multiple kuru-exposed Fore females. The LD profile is similar at all three thresholds. Error bars are 1.96xSEM.

With only 7 samples available for analysis, it was expected that the mean LD would be inflated due to the small sample size (Jorde, 2000). To test the extent of sample size on genome-wide LD NspI array genotype data on from 90 UK control samples was obtained from Dr Simon Mead. Genome-wide LD was calculated for all 90 samples (genotypes called at threshold P=0.33) and for random sub-samples of 7 individuals which were sampled without replacement 4 times (Figure 6.22).

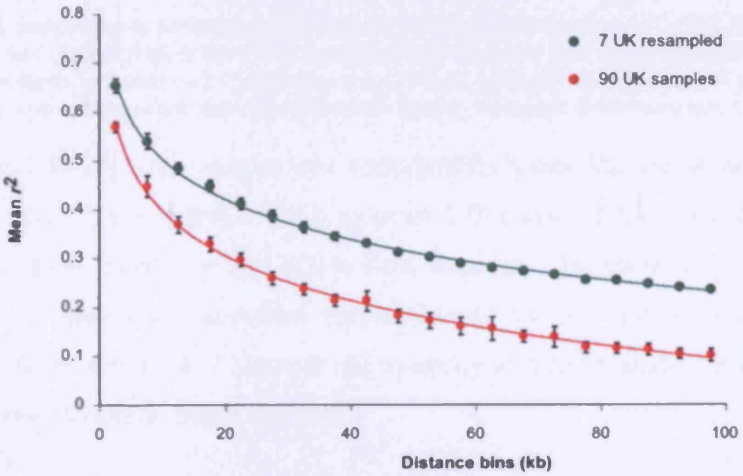

Figure 6.22 The effect of sample size on genome-wide pairwise LD

Mean r^2 was calculated for pairwise comparisons between markers with minor allele frequencies ≥15% that fell within the same 2.5kb intermarker distance bins for 90 UK samples and four sub-sampled sets of 7 UK individuals. Pairwise LD was found to be consistently inflated for the 7 sub-sampled cohorts compared to the complete data set at all distances. Error bars are 1.96xSEM.

LD was consistently inflated for the smaller 7 UK sub-sampled cohort than the full 90 UK sample data set. Furthermore, long range LD was more susceptible to inflation (230% inflation for 100kb comparisons) compared to short range LD (113% inflation for 5kb comparisons).

6.9.5.2 Genome-wide LD compared between PNG and UK samples

To overcome discrepancies due to sample size, LD from 7 individuals from the UK were compared to the 7 kuru and 7 elderly multiple kuru-exposure Fore females (Figure 6.23). The Fore females demonstrated elevated LD compared to the UK samples and the half-life of LD decay with genomic distance was substantially longer in the Fore women than in the UK samples (approximately 1.25-fold higher than the UK samples).

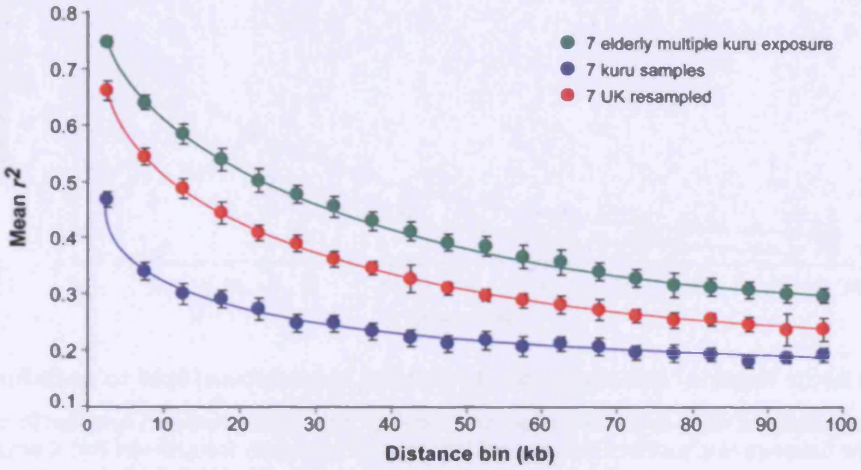

Figure 6.23 Linkage disequilibrium decay over distance

Mean r^2 for pairwise comparisons between markers with minor allele frequencies ≥15% that fell within the same 2.5kb intermarker distance bins, for 7 UK samples (sub-sampled four times from 90 samples), 7 WGA kuru and 7 elderly multiple kuru exposure Fore women. LD was greater in the 7 elderly Fore women compared to the 7 UK samples and LD amongst kuru samples was starkly reduced. Error bars are 1.96xSEM.

Pairwise LD in the 7 WGA kuru samples was considerably lower than the other samples and decay over distance occurred more rapidly. This reduced LD reflected the poor quality of the data obtained from the NspI arrays for the WGA kuru samples. The reduced LD is most likely an artefact of either (i) spuriously increased heterozygosity (which serves to reduce LD) due to genotyping inaccuracies across the 7 chips or (ii) a paucity of data to conduct a sufficient number of pairwise comparisons to obtain robust LD data.

6.9.5.3 Genome-wide LD between highly correlated SNPs

An important consideration for any future whole-genome PNG association study, using the Affymetrix 500k platform, is coverage. As the SNPs included on the Affymetrix array were ascertained in reference populations, it is important to assess how well these SNPs represent

variation within the PNG population. The importance of coverage and several methods of directly assessing this statistic are examined in detail in the discussion (the current study was too preliminary with too few samples to be able to utilise these methods). However, an approximate indicator of coverage was ascertained by examining the proportion of minor SNP alleles that were highly correlated ($r^2 \geq 0.8$) and therefore might serve as proxies for other unknown variants not directly genotyped on the array. The proportion of highly correlated pairwise comparisons (of the total comparisons made), within increasing 2.5kb genomic distance bins, was inflated in small samples of 7 individuals repeatedly sub-sampled from a total of 90 UK samples (Figure 6.24).

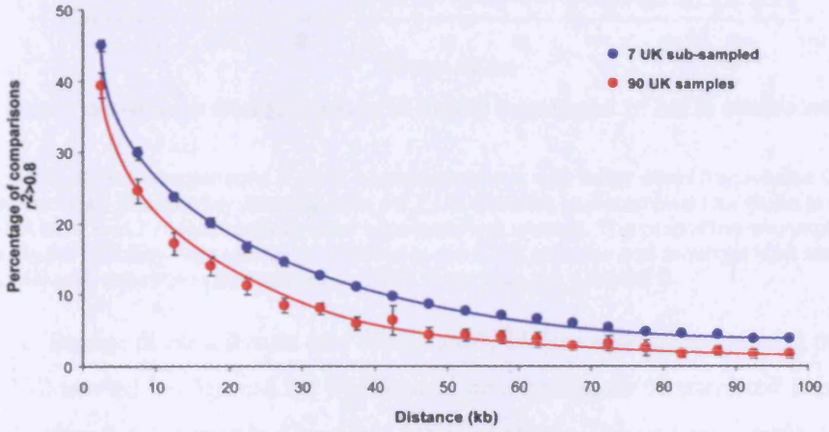

Figure 6.24 Inflation of highly correlated (r^2>0.8) LD comparisons in small sized samples

Mean proportion of pairwise comparisons $r^2 \geq 0.8$, between markers with minor allele frequencies ≥15% that fell within the same 2.5kb intermarker distance bins, for 90 UK samples and four sub-sampled sets of 7 UK individuals. Error bars are 1.96xSEM.

Comparing across the three sample sets, Figure 6.25 illustrates the increased LD in the elderly Fore women as compared to the UK samples and the relative paucity of highly correlated SNPs in the WGA kuru samples. The lack of highly correlated SNPs in the kuru samples, taken together with the lower overall LD, as compared to the 7 multiple-kuru exposure samples is likely to be attributable to poor genotyping of these samples (i.e. low call rates and a greater discordance) compared to the other PNG samples.

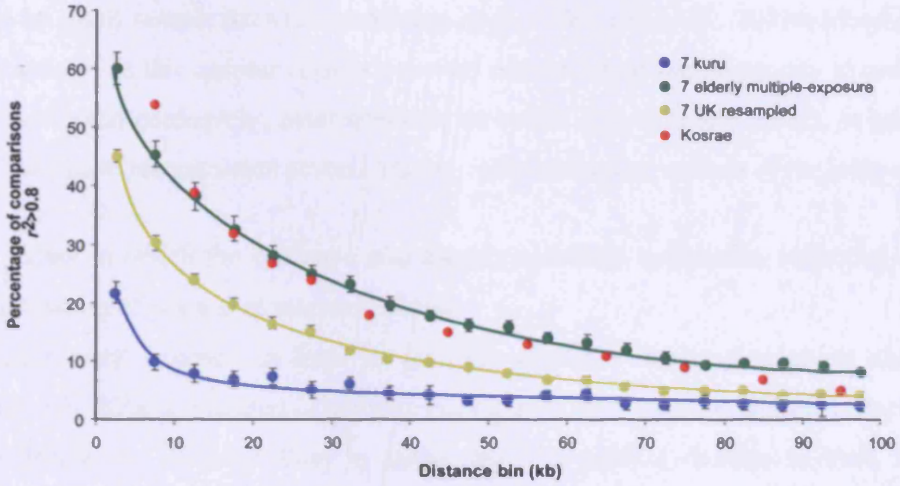

Figure 6.25 Decay of linkage disequilibrium of highly correlated ($r^2 \geq 0.8$) alleles with distance

Mean proportion of pairwise comparisons $r^2 \geq 0.8$, between markers with minor allele frequencies ≥15% that fell within the same 2.5kb intermarker distance bins, for 7 UK samples (sub-sampled four times from 90 samples), 7 WGA kuru and 7 elderly multiple kuru exposure Fore women. The proportion of comparisons $r^2 \geq 0.8$ was greater in the 7 elderly Fore women compared to the 7 UK samples and amongst kuru samples, was starkly reduced. Kosrae data from (Bonnen *et al.*, 2006). Error bars are 1.96xSEM.

For comparison, linkage disequilibrium data from a study of the isolated Micronesian population of Kosrae is also illustrated in Figure 6.25. The Kosrae data represents 60 unrelated individuals and was generated using the Affymetrix GeneChip 100K platform. The smaller sample size of the 7 elderly Fore women compared to the 60 Kosrae samples implies that LD on Kosrae will likely be greater than that on PNG, however, the lower SNP density 100K array may inflate LD estimates slightly as it is known that SNP density can affect the pattern and extent of LD. As the only whole-genome genotyping study of an isolated population, the Kosrae data will make an interesting comparison for future PNG data.

Several additional analyses that would provide information on the genetic diversity and the utility of the PNG samples could no be run due to small sample size

6.10 Discussion

The results presented in this chapter have expanded on previous investigations of the effect of kuru on the PNG Eastern Highland population and the effect of *PRNP* codon 129 on kuru survival. Moreover, the work presented in this chapter comprises the largest investigation of the genetic effect of kuru to date.

6.11 Codon 129 and kuru susceptibility

Analysis of 161 kuru samples and 125 elderly kuru-exposed females expanded on several published studies which observed significant correlation of *PRNP* codon 129 status with kuru survival but

were limited by small sample sizes (Cervenakova *et al.*, 1998; Lee *et al.*, 2001a; Mead *et al.*, 2003). The work presented in this chapter corroborates the correlation of homozygosity at codon 129 with early kuru onset (and conversely, heterozygosity at codon 129 with late onset). In addition, these genetic analyses have recapitulated several known epidemiological aspects of the kuru epidemic:

- the extent to which the epidemic was largely restricted to females, reflecting the majority participation of women at mortuary feasts
- females were exposed to kuru at multiple mortuary feasts throughout childhood and adulthood. This is reflected in both the peak age of kuru onset in females, which occurred a full decade in life later than in males and the gradual decline in kuru incidence in subsequent decades which, in contrast to the males' data, implies a sustained exposure to kuru through childhood and adulthood.
- male exposure to kuru largely occurred up to the age of 6 to 8 years. This is demonstrated by a peak age of male kuru onset at 11 to 20 years, given that the mean kuru incubation time is 12 years, and a rapid decline thereafter. This observation is consistent with reports that young males lived with and attended mortuary feasts with their mothers. Boys older than 6–8 years were taken from their mothers and brought up in the men's house and from this point on, they were exposed only to the same risk as adult men, who participated little in feasts and did not eat brain (the most infectious organ in kuru) (Collinge *et al.*, 2006). This practice explains why adult men in 1957–58 contributed only 2% to the total number of kuru cases. Consistent with a single peak period of male kuru exposure, the number of male kuru cases with onset in later decades declines rapidly

Within the surviving population from the kuru-exposed regions, highly significant deviations from HWE were seen in the surviving elderly population. The analysis of 125 women with multiple kuru exposure, corroborated and expanded the work of Lee *et al.* and Mead *et al.* demonstrating the protective advantage of heterozygosity at codon 129 and increasing the significance of this finding from the original observations (Lee *et al.*, 2001a; Mead *et al.*, 2003). Use of the EI classifications for elderly women from kuru exposed villages further increased the level of significance.

6.11.1 Codon 129 independent susceptibility?

The analyses of both the kuru-affected and surviving populations pose further questions of additional unidentified protective/susceptibility loci. The presence of MV heterozygotes in the kuru-affected cohort raises the possibility that these individuals may possess some other codon 129-independent susceptibility locus. Similarly, the presence of women homozygous at codon 129 in the surviving multiple-kuru-exposure population may be evidence of a codon-129 independent

protective factor, although long incubation times in these women cannot be discounted. Alternatively, the presence of these genotypes in either cohort may reflect non-uniform exposure within villages and linguistic groups i.e. a "hotspot" or "coldspot" of consumption within a village of linguistic group than is represented by an average exposure statistic.

6.11.2 *PRNP* and kuru-mediated signatures of selection

Several signatures of selection were tested on codon 129 data from 12 different linguistic groups of the Eastern Highlands, with limited success. Investigation of co-variation of Hardy-Weinberg disequilibrium with levels of kuru-exposure identified significant deviations from HWE in only the South Fore samples. South Fore women >50 years and men aged between 40-50 years showed significant departure from HWE disequilibrium. HWE was re-established in South Fore males born after 1960, demonstrating both the abrupt end to the kuru epidemic and the swift return of genotype proportions of return to HWE subsequent to removal of the selective pressure.

HWE was seen in other exposed linguistic groups including the North Fore, which is known to have experienced acute exposure to kuru second only to the South Fore. This may have been due to the early cessation of mortuary feasting in the communities of the North Fore in the 1950's or earlier, who were the first of the Fore people to lose their traditional practices in the wake of Australian administrative control (Collinge *et al.*, 2006).

HWE in non-Fore kuru-exposed linguistic groups is probably due to the absence of gender stratification which was precluded by small sample sizes. In addition, these analyses were insensitive to the differential exposure of villages within each linguistic group. Reclassification of the PNG samples using the new EI permitted a more robust analysis: women >50 years and men aged 40-50 years both remained highly significant results and no significant HWE deviations were seen for women between 40-50 years, men >50 years or unexposed women >50 years.

The analysis of codon 129 valine allele frequency worldwide and in PNG as a signature of selection provided an interesting result. The valine allele frequency demonstrated a significant cline worldwide to which the Fore clearly contrasted. Based on the early linguistic group analysis, an equilibrium valine allele frequency was seen across the Eastern Highlands, regardless of kuru exposure status. However, under the EI classification an increasing local PNG cline was seen from the non-Highland populations, to Eastern Highland populations with no record of kuru and the kuru exposed region itself. No significant difference was seen between the low and high kuru exposure populations from the Eastern Highlands. This may be due to a historically higher incidence of kuru in the low exposure populations than was recorded since the 1950s.

Investigating the extent of LD between microsatellites flanking *PRNP* did not yield conclusive results associated with the extent of kuru exposure. Kuru exposed and unexposed cohorts. Only microsatellite F_{ST} demonstrated marginal significance.

6.11.3 Additional susceptibility loci - *PRNP* G127V

The data presented in this chapter support the conclusion that G127V is a highly geographically restricted, but locally common, polymorphism that confers resistance to kuru in the heterozygous state. How glycine to valine change protects against kuru remains unclear. The polymorphism may result in a more bulky amino-acid side-chain which impedes beta-sheet formation and protects against prion formation, although this remains speculation and additional work would be needed, to clarify the effect on PrP structure and the mechanism of protection.

The possibility that, rather than protecting against kuru, the 127V polymorphism might have instead triggered the epidemic cannot be completely excluded. Given that life expectancy in the kuru region is 42 years, it is possible that 127V is associated with a late-onset and low penetrant inherited prion disease which might have triggered the kuru epidemic. There are few examples of mutations causative of autosomal dominant neurodegenerative disease that achieve the polymorphic frequency observed in the Purosa Valley (Wexler *et al.*, 2004). A wealth of data indicates that prion transmission is generally more efficient where there is complementarity between the primary PrP sequence of donor and host, implying that if 127V was pathogenic it would be expected to confer susceptibility to the corresponding acquired prion disease (Collinge, 2001). Additionally, the glycoform type of PrP^{Sc} in kuru, although restricted to a small number of autopsy samples, closely resembles sporadic CJD rather than point mutation inherited prion disease (Parchi, 2000). Finally, if 127V had triggered kuru, the localization to the southeastern part of the Fore linguistic group would be inconsistent with oral history that the first kuru patient was observed in the Keiagana linguistic group located to the northwest of the Fore.

6.11.4 Future study of PNG and kuru samples

An important issue that should be investigated further to conclusively resolve the use of genetic variation to identify kuru susceptibility loci is the description of "neutral" genetic variation against which variation at *PRNP* or other loci may be compared. The availability of 14 Affymetrix NspI arrays permitted the limited analysis of genomic variation in 7 Highland samples and the feasibility of utilising degraded kuru DNA through WGA.

6.11.4.1 The effect of whole-genome amplification of low quality material on whole-genome genotyping platforms

Recent studies at the MRC Prion Unit have proven the reliable use of WGA technologies for use on various genotyping arrays on high quality starting DNA. The results presented in this chapter have also illustrated the benefits of using WGA on good quality starting material but have shown that WGA on low concentration, degraded kuru DNA is not an effective method of increasing DNA quantity for Affymetrix NspI array analyses.

6.11.4.2 Ascertainment bias

All SNPs on the Affymetrix GeneChip arrays were pre-selected based on technical quality in the three HapMap reference populations (CEPH, Japanese/Chinese and Yoruban), essentially representing a quasi-random SNP set (Affymetrix, 2005a), and therefore it is unknown how representative the alleles ascertained in these reference populations are of common variation in PNG. Although the Affymetrix SNPs are likely to be representative of the majority of human SNP alleles, there is a possibility that a major class of common allele on PNG may not be represented on these arrays. Future work should concentrate on deep resequencing of several genomic regions in 16 PNG samples from unexposed PNG linguistic groups. Resequencing a subset of the ten 500kb regions investigated in the HapMap ENCODE resequencing project (www.hapmap.org) would permit a direct comparison of PNG genetic diversity against freely available data from African, European and Asian populations. The frequency distribution of all alleles could be compared to ensure that the Affymetrix 500k arrays also represent common variation in PNG. In addition, resequencing a subset of the 17 genomic regions studied in the Kosrae population would permit direct comparisons to be made with a second isolated population with available SNP data.

7 *PRNP* copy number polymorphisms and prion disease susceptibility

7.1 Introduction

This chapter investigates *PRNP* copy number as a mediator of sporadic CJD and kuru susceptibility. The chapter begins with a brief consideration of the relevance of copy number changes to neurodegenerative diseases and presents the hypotheses that *PRNP* duplications may mediate susceptibility to sporadic CJD, whilst deletion may afford protection against kuru. *PRNP* copy number was investigated using quantitative real-time PCR in 28 sporadic CJD samples and 104 elderly women from the Fore. A suspected triplication was identified in a sCJD sample and although no copy number changes were identified in the Fore women, a known polymorphism at codon 127 of *PRNP* was observed. This chapter ends with a brief discussion of the relevance of these results and the relevance of copy number polymorphisms to human prion disease.

7.1.1 Copy number polymorphisms in neurodegenerative disease

In recent years the insertion, deletion and duplication of DNA segments greater than 1 kb have been shown to occur frequently in the human genome (see for example (Conrad *et al.*, 2006; Freeman *et al.*, 2006; Khaja *et al.*, 2006)). With approximately 12% of the human genome undergoing dynamic rearrangements, these copy number polymorphisms (CNPs) can have dramatic phenotypic consequences, altering gene dosage, disrupting coding sequences, or perturbing long-range gene regulation (Redon *et al.*, 2006).

The accumulation and deposition of proteins is a common feature of many neurodegenerative diseases, and variability in the expression of an associated protein-coding gene is often related to the severity of neurodegeneration (i.e. age of onset, duration of disease etc.). This dosage hypothesis is supported by several examples of pathogenic copy number changes which have been observed to give rise to neurodegenerative diseases: (i) tandem duplication of a 1.5Mb region of the gene *PMP22* results in the dominantly inherited demyelinating neuropathy, Charcot–Marie–Tooth type 1A (CMT1A) (Lupski *et al.*, 1991), (ii) duplication of the amyloid precursor protein gene (*APP*) has been reported in five different families with autosomal dominant early onset Alzheimer's disease (Rovelet-Lecrux *et al.*, 2006), (iii) duplication of the proteolipid protein gene (*PLP*) in the rare X-linked dysmyelination disorder, Pelizaeus-Merzbacher disease (PMD) (Woodward *et al.*, 1998) and partial triplication of exons 2 to 4 of Parkin (*PARK2*). Perhaps most convincing support for a dosage hypothesis to neurodegenerative disease comes from the pathogenic multiplication the α-synuclein gene (*SCNA*) in autosomal dominant Parkinson's disease. Triplications of *SCNA* have been independently identified in two unrelated kindreds with onset in the fourth decade (Farrer *et*

al., 2004; Singleton *et al.*, 2003). In addition duplication of the *SCNA* locus has also been shown to be pathogenic in several families, with a less severe clinical phenotype than triplication families and with onset a decade later (Chartier-Harlin *et al.*, 2004; Ibanez *et al.*, 2004; Nishioka *et al.*, 2006).

7.1.2 Variability in *PRNP* expression and disease susceptibility

There are several lines of evidence that suggest that *PRNP* expression is correlated to disease outcome. In mice, the level of expression of *Prnp*, regardless of coding sequence, is a major determinant of incubation time. For example, transgenic mouse models with additional copies of the hamster PrP gene demonstrate an inverse correlation between PrP expression level and scrapie incubation time (Prusiner *et al.*, 1990). Bueler and colleagues importantly showed that *Prnp*-ablated mice are resistant to developing disease when inoculated with mouse scrapie (Bueler *et al.*, 1993) and that hemizygous *Prnp*-ablated mice have a greatly prolonged incubation time (Bueler *et al.*, 1993). Conversely, increasing *Prnp* expression by increasing *Prnp* transgene copy number in $Prnp^{a/b}$ mice, increases susceptibility to Rocky Mountain Laboratory (RML) prion infection (Fischer *et al.*, 1996). PrP levels following disease onset have also been able to modify disease outcome. Mice displaying disease following RML prion infection are seen to reverse spongiform pathology and cognitive and behavioural defects following depletion of neuronal PrP^{c} (Mallucci *et al.*, 2003; Mallucci *et al.*, 2007).

In addition, a QTL mapping study of inbred mouse strains has identified a region of chromosome 2, encompassing *Prnp*, as one of three major QTLs that determine prion-disease incubation time after intracerebral inoculation with mouse-adapted scrapie (Lloyd *et al.*, 2001). Intriguingly, this result has been replicated in humans - a 10kb prion haplotype confers risk to sporadic CJD (Mead *et al.*, 2001). Although it is not known if the associated haplotype results in altered expression of *PRNP*, it suggests that genetic variability in prion expression may contribute to sporadic disease risk.

Taken together, these data suggest that *PRNP* mediated disease susceptibility extends beyond polymorphisms of the amino acid sequence and that *PRNP* expression may influence human prion disease outcome. The genetic elements that determine *PRNP* expression have been studied. Mahal and colleagues were the first to isolate and characterise the human *PRNP* promoter, identifying by progressive 5' deletions of the promoter region, several candidate sites where nucleotide polymorphisms may influence expression (Mahal *et al.*, 2001). To date three SNPs in the regulatory region of the *PRNP* have been identified, a C to G transversion at position −101, a G to C transversion at position +310 and T to C transition at position +385. It has been shown that among sCJD patients homozygous for codon 129 methionine alleles, the numbers of who carried the rare promoter SNP alleles was higher than in controls, suggesting that the regulatory region

polymorphisms may be a risk factor for CJD (McCormack *et al.*, 2002). It has yet to be demonstrated if *PRNP* expression is mediated by copy number changes.

7.1.3 Copy number polymorphisms in sporadic CJD?

The majority of examples involving pathogenic copy number alterations in neurodegenerative diseases demonstrate familial or pseudo-familial inheritance. Conversely, the majority of neurodegenerative diseases including human prion disease occur sporadically, so can copy number changes explain sporadic disease? Essentially, the first appearance of a pathogenic copy number change is a sporadic *de novo* event which is subsequently inherited, for example the various *SCNA* families possess duplications and triplications of different allele sizes reflecting their independent origins. Reduced penetrance has been observed for several diseases that result from CNPs, including the 22q11 deletion DiGeorge syndrome (Gong *et al.*, 2001) as well as speech problems in patients with duplication of the Williams syndrome region (Gong *et al.*, 2001). Therefore, it is possible that incomplete penetrance may also be seen with potential *PRNP* copy number cases that have been diagnosed as sCJD.

7.1.4 *PRNP* copy number hypothesis

Two discrete hypotheses relating altered *PRNP* copy number to disease susceptibility were tested in this chapter:

(i) elderly Fore women (aged >50 years old in 2000), with acute exposure to kuru through attendance at multiple mortuary feasts, who were genotyped as codon 129 homozygotes, were actually hemizygous which afforded relative protection against kuru.

(ii) sporadic CJD patients who were heterozygous at codon 129 and should have essentially been less susceptible to disease, actually had a duplication of the $PRNP_{129M}$ allele

7.2 Quantitative Real Time PCR probe and primer design for *PRNP*

Selection of *PRNP* PCR primers and MGB probe sequences for quantitative PCR (qPCR) was performed as described in Materials and Methods 2.5.3. The probe was designed to anneal 5' to codon 129 in a region of *PRNP* without any known sequence variation (Figure 7.1). Primers identical to those used for codon 129 genotyping by allele discrimination were used and a methionine allele specific *PRNP* probe was also used. Ideally, the probe should have straddled an intron/exon boundary to amplify genomic DNA only (and not mRNA) however, by spanning codon 129 probe specificity could be tested by comparing detection of M and V codon 129 alleles.

RNA contamination was minimised by treating DNA samples with RNAse either during extraction from blood or (for samples obtained as DNA) following the identification of RNA impurities in

DNA by spectrophotometry. The house-keeping gene beta-actin (*β-Actin*; OMIM: 102630) was used as an endogenous control and *β-Actin* probe and primer sequences were taken from the literature (Suarez-Merino *et al.*, 2005).

Figure 7.1 *PRNP* and *β-Actin* quantitative real time PCR probes and primers

Probes are indicated in yellow boxes and forward and reverse primers are in grey boxes. The methionine specific $PRNP_{129M}$ probe is indicated by the black line. All *PRNP* probes were major groove binders (MGB) and were labelled with VIC fluorophore reporters. *β*-Actin probes were MGB and labelled with FAM fluorophore reporters.

To determine changes in *PRNP* copy number in relation to *β-Actin*, the comparative C_T* method ($2^{-\Delta\Delta C_T}$) was used see (Livak *et al.*, 2001). Although this method is usually used to quantify changes in gene expression it is also useful for quantifying genomic template changes and standardising assays across different experiments/plates. In brief, the difference between the threshold cycle of the *PRNP* target assay and the *β-Actin* endogenous reference assay (ΔC_T) is calculated for both the test and calibrator samples:

Equation 7.1 $\Delta C_T = C_T$ (target gene) - C_T (endogenous control)

The difference between the average ΔC_T value of a test sample and the average ΔC_T for the calibrator sample is calculated ($\Delta\Delta C_T$) and the expression fold value by:

Equation 7.2 $\Delta\Delta C_T$ (test sample) = ΔC_T (test sample) - ΔC_T (calibrator sample)

Equation 7.3 Expression fold value = $2^{-\Delta\Delta C_T}$

7.3 Validating qPCR probe efficiencies

For the $\Delta\Delta C_T$ calculation to be valid, the amplification efficiencies of the target and reference assays had to be approximately equal. A sensitive method for assessing if two amplicons have the same efficiency is to look at how ΔC_T varies with template dilution. $PRNP_{129M}$ and *PRNP* probe

* C_T or Threshold Cycle reflects the cycle number at which the fluorescence generated within a reaction crosses a baseline threshold of background fluorescence.

efficiency was validated by serially diluting a DNA sample of known concentration over a 32-fold range (approximately 200ng/μl to 6ng/μl – the working range of the majority of the samples used for the study). Assays were performed as described in Materials and Methods 2.6.7 and 5 replicates were conducted for each dilution. The average ΔC_T was calculated as explained above (Equation 7.1).

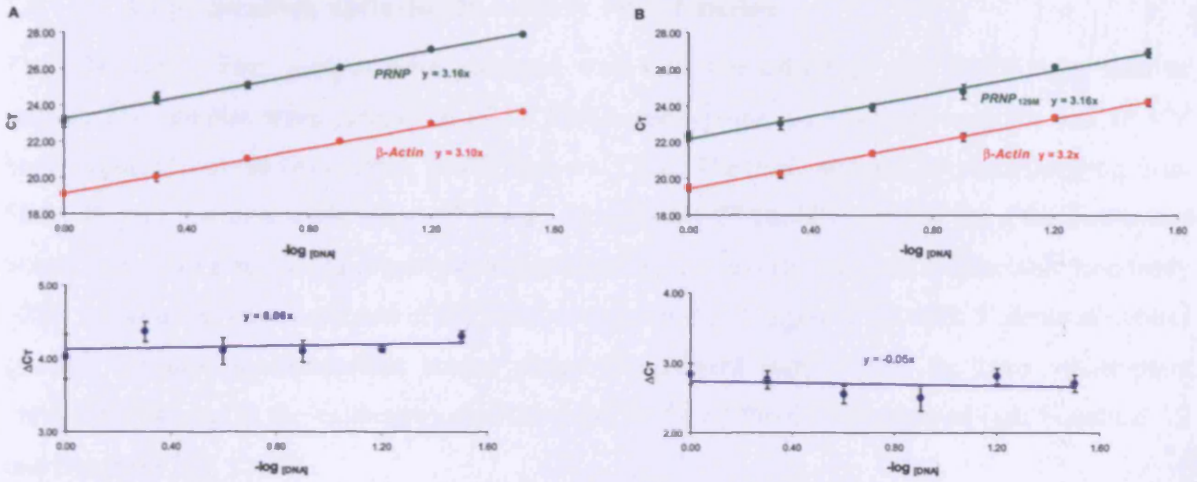

Figure 7.2 Relative efficiencies for *PRNP* and *PRNP*$_{129M}$ quantitative PCR probes

The efficiency of amplification of the *PRNP* (**A**) and *PRNP*$_{129M}$ (**B**) targets and endogenous control *β-Actin* by CT (**top**) and ΔCT (**bottom**). The data were fitted using least-squares linear regression analysis (N=5).

The relative efficiencies of the target and endogenous control probes, as calculated by the slope of the ΔC_T against graph, were approximately equal (Figure 7.2) and compared well to the acceptable efficiency of <0.1 established by the manufacturer of the real-time system (Applied Biosystems, 1997).

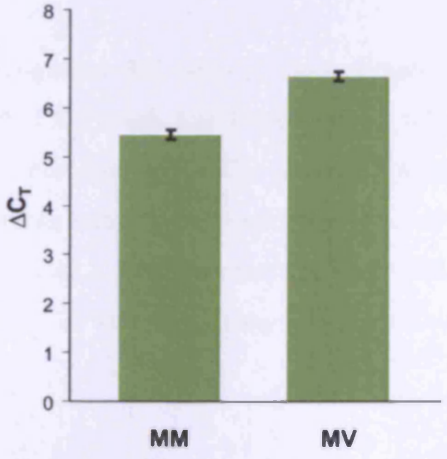

Figure 7.3 Average ΔC_T differences between *PRNP* codon 129 MM and MV CEPH samples

Error bars are ± 95% SEM. VV homozygote not shown. (N=11)

To ensure the assay was sensitive enough to detect a two-fold difference in template concentration, the methionine-specific *PRNP*$_{129M}$ probe was used to evaluate 23 CEPH samples blinded to codon

129 genotype (11 MM, 11 MV and one VV control sample). A highly significant difference between the ΔC_T of the MM and MV samples (T-test* $p<<0.0001$) was seen and, as expected, the valine homozygote controls failed to amplify with the $PRNP_{129M}$ probe (Figure 7.3). This result demonstrated that a two fold increase in genomic template (one cycle difference) could be detected.

7.4 Copy number variation in elderly Fore females

The 104 elderly Fore women were screened with both the $PRNP_{129M}$ and *PRNP* copy number probes. The samples were comprised of 17 MM homozygotes, 64 MV heterozygotes and 18 VV homozygotes from the North Fore, South Fore and Gimi. The mean age was 59 years (ranging from 50 to 82 years, with a median age 57 years). In addition, 25 healthy controls from the North and South Fore were screened to identify deletion/duplication polymorphisms at a detectable frequency >2%. All samples were screened in triplicate as described in Chapter 2.7.3, with 5 identical control samples included to standardise across plates (the control sample with the least within-plate variation was used as the calibrator), and the mean $2^{-\Delta\Delta C}{}_T \pm 1.96$xSEM calculated (see Equation 7.2 and Equation 7.3).

Initially, whilst waiting for reagents to arrive, 20 multiple-exposure samples were screened with the $PRNP_{129M}$ probe and three control samples (one MV, MM and VV). Samples were calibrated by an MM homozygote control. Methionine homozygotes generally fell within the $2^{-\Delta\Delta C}{}_T$ range 1.04 – 1.08 and heterozygotes between 2.04 – 2.14, however two MM samples were observed to not conform to the heterozygote group: sample PDG2711 (1.99 ± 0.07) and PDG9466 (1.57 ± 0.03) (Figure 7.4). Both of these samples were suggestive of a heterozygous methionine deletion.

On closer inspection it was recognised that both of these samples possessed a glycine to valine heterozygous mutation at codon 127, which had been recently found to occur in several samples from the Fore populations. The mutation was a G→ T transversion at the second position within codon 127 (GGC to GTC). As these samples had been genotyped as heterozygous at additional loci linked to codon 129 (data not shown), it was clear that the suspected deletion was a spurious result, most likely a consequence of the 127 mutation lying directly within the $PRNP_{129M}$ probe binding region.

* The data from replicates was tested for conformation to a normal distribution, proving that the use of statistical tests based on the normal distribution was valid.

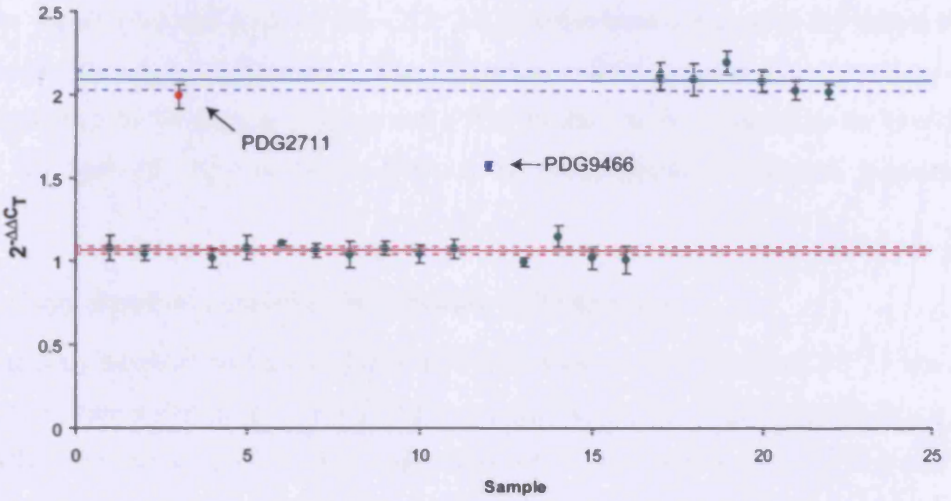

Figure 7.4 *PRNP* 129M copy number analysis of 25 Fore women over 50 years old repeatedly exposed to kuru

Samples calibrated by an MM homozygote. Red and blue lines give average homozygote and methionine heterozygote $2^{-\Delta\Delta C}T$ values respectively with dashed lines ±1.96xSEM.

When examined with the general *PRNP* probe, these samples were seen to lie within the population range. The difference in the $2^{-\Delta\Delta C}{}_T$ values of PDG2711 and PDG9466 from the MM average may reflect a stochastic effect of the 127 mutation spuriously affecting probe binding to the template. Although this result was due to an oversight in assembling the sample set, it also provided a precedent for the assay to detect sequence variations.

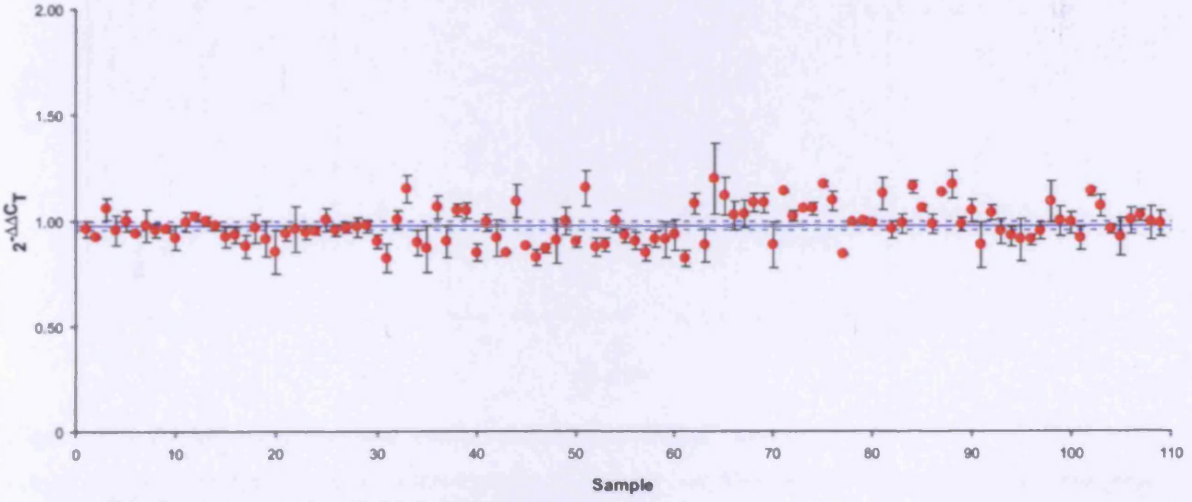

Figure 7.5 *PRNP* copy number analysis of Fore women over 50 years old repeatedly exposed to kuru

Samples calibrated by an MM homozygote control. 104 samples were screened with 5 control samples. The blue line gives average $2^{-\Delta\Delta C}{}_T$ value ±1.96xSEM. Error bars are ±1.96xSEM.

The 104 multiple kuru-exposure samples were screened as described above, with 5 control samples to ensure data were standardised between experiments (Figure 7.5). Mean $2^{-\Delta\Delta C}{}_T$ was 0.98 ± 0.02,

with values within a normal range of 0.8 – 1.2. All samples were observed to fall within the normal range and close to the population mean. The 25 healthy control samples also showed no difference in copy number (data not shown). The general *PRNP* probe was not affected by the G→ T mutation at codon 127 (possibly due to the position of the probe/template mismatch generated by the mutation).

7.5 Copy number variation in sporadic CJD samples

To examine copy number changes of *PRNP* as a pathogenic mechanism in sCJD, 28 brain- derived sCJD samples were screened with the *PRNP* copy number probe, with 4 healthy control samples from the UK. All samples were RNAse treated and qPCR was undertaken in triplicate as described above. As Figure 7.6 illustrates the majority of samples fell within the population mean of 0.95 ± 0.05 (±SEM) however, one sCJD sample (PDG2271) with average $2^{-\Delta\Delta C}{}_T$ value 3.77 ± 0.3 was clearly distinct from the others. PDG2271 was taken form an anonymous patient with confirmed sporadic CJD who was heterozygous at codon 129. As a consequence of anonymity of the sample, the patient's clinical information was not available. The average copy number of PDG2271 was approximately 4, which suggested that the patient would have possessed a triplication of **both** *PRNP* alleles.

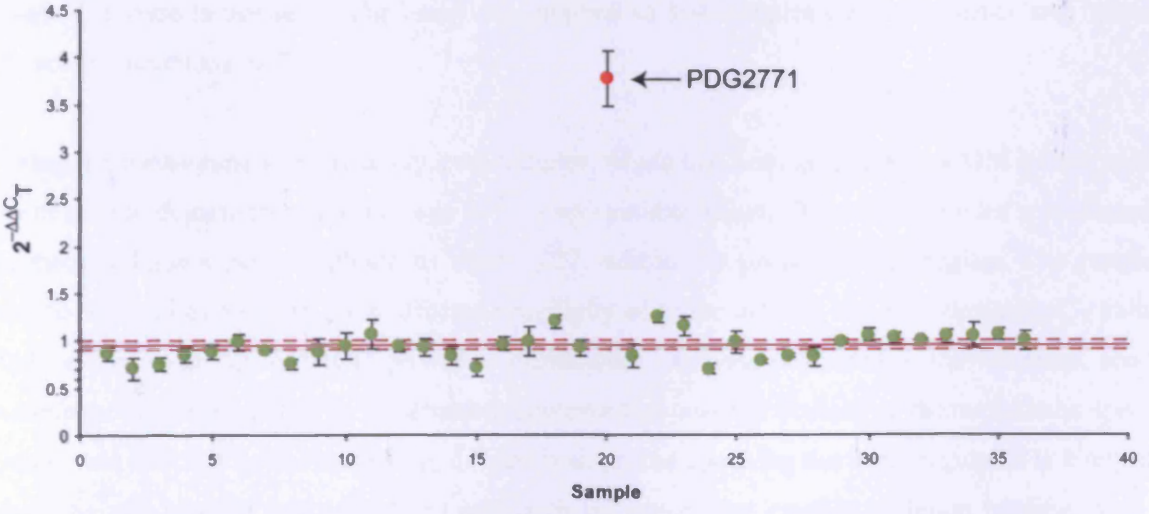

Figure 7.6 *PRNP* copy number analysis of sporadic CJD samples

A total of 28 sCJD samples and 4 control samples are shown (samples 29 to32 are controls). Red line gives average $2^{-\Delta\Delta C}$T value ±1.96xSEM. Error bars are 1.96xSEM.

The DNA quality of PDG2771 was rechecked as described in Materials and Methods 2.3.3 and the $^{260}/_{280}$ ratio was found to be sub-optimal at 1.64. A standard curve was constructed using a 32-fold serial dilution of PDG2271 (as described above) to dilute any impurities that may have affected the experiment. The standard curve produced for PDG2271 was within the tolerances described previously (data not shown) and therefore DNA quality could be excluded.

7.6 Discussion

This chapter describes the development of a robust assay to examine *PRNP* copy number as a novel mechanism for disease susceptibility in prion disease and extends the development of the PNG sample collection as a model to detect novel susceptibility loci. The *PRNP* and *β-Actin* probes and primers designed for this assay were demonstrated to effectively discriminate two or more fold differences in *PRNP* and $PRNP_{129M}$ copy number, from genomic DNA varying in concentration from 6ng/μl to 200ng/μl. This assay was applied to test two hypotheses, both based on the observation that codon 129 status alone is insufficient to explain disease susceptibility in several human prion diseases.

7.6.1 Hypothesis 1 – *PRNP* deletion mediates protection against kuru

The first hypothesis related to the elderly Fore women of the Eastern Highlands of PNG, who were repeatedly exposed to kuru at multiple mortuary feasts but failed to develop disease. Based on data from the previous chapter, ~30% of elderly kuru-exposed women possessed a susceptible codon 129 homozygous genotype and yet had not developed disease. The mechanism regulating protection may involve the deletion of a *PRNP* allele to effectively reduce PrP production to a level where the clinical disease is not seen. The assay was applied to 104 samples and 25 controls and failed to detect any deletions of *PRNP*.

Using the methionine specific assay, two samples, which had been genotyped as MM homozygotes, were seen to deviate from the average $2^{-\Delta\Delta C}{}_T$ copy number value. These two samples were found to harbour a known polymorphism at codon 127, within the probe-binding region. The resulting single-base mismatch may have affected specificity of probe binding and thus deviating C_T values. Indeed the sensitivity of MGB probes to mismatches has been described in the literature, see for example (Yao *et al.*, 2006). It is intriguing however that only the binding of the methionine specific probe was affected by the mismatch, despite both probes spanning the same region. It is likely that the type and relative position of the mismatch influences the kinetics of probe binding, such as altering melting temperatures, which can explain differential results such as these (Kutyavin *et al.*, 2000).

The absence of *PRNP* deletions in the elderly Fore females was a disappointing result however, the limit of detection of *PRNP* CNPs was 0.4%, implying that it is unlikely that *PRNP* deletion is a common protective mechanism against kuru.

7.6.2 Hypothesis 2 – *PRNP* duplication mediates susceptibility of codon 129 heterozygotes to sCJD

The hypothesis that those individuals heterozygous at codon 129 but who had succumbed to sCJD may have possessed a duplication of a *PRNP* allele (which would have gone undetected by genotyping codon 129 alone) was examined. Of the 28 UK sCJD samples tested, one potential triplication of *PRNP* was found. This was an intriguing result not least because the possible triplication had occurred on both alleles. The triplication of both *PRNP* alleles as a *de novo* event is incredibly unlikely (*de novo* CNP of two allelic loci is restricted to a few circumstances such as polyglutamine tract expansions). As witnessed in Parkinson's disease, triplications often result in an earlier age of onset and pseudo-autosomal inheritance (Lesage *et al.*, 2006; Lucking *et al.*, 2001). The inheritance of two triplicated loci is a possible mechanism, although without population frequency data it can only be assumed that the probability of acquiring such a genotype through random mating is small, implying therefore that the patient belonged to a consanguineous pedigree. Unfortunately, historical anonymisation of sCJD samples restricted the availability of clinical and familial data which would have helped to confirm this potential result.

Due to time limitations, additional work could not be undertaken to explore this sample further. However, future work to ensure that the result is genuine should explore the following avenues:

- the result should be replicated - the sample was originally extracted from autopsied brain material and should therefore be re-extracted to ensure that the result is replicated and not merely a product of inherent, undetected contamination.
- the assay could be repeated with different probes, both for the target and endogenous control, to ensure that unknown polymorphisms in the binding regions of the primers and probes are excluded and that the copy number of the beta actin gene does not vary.
- a second independent technique could be used to identify a duplication, such as FISH or extended homozygosity/heterozygosity.

7.6.3 Limitations of this approach and future work

There are limitations to the approach used in this chapter to detect CNPs and demonstrate that these are phenotypically relevant.

7.6.3.1 *PRNP* gene coverage

Despite the sensitivity of the copy number assay, it was limited to resolving information on relative copy number in a restricted region of the gene. *PRNP* spans approximately 15kb across chromosome 20 with a 12.5kb intron separating exons one and two. The assay amplified ~100bp of

exon two which therefore omitted information on, amongst other regions, the promoter. With regards to dosage effects and expression levels in neurodegenerative diseases, the promoter is an important region of the gene to assay – and with the promoter and other upstream elements implicated in sCJD (Mead *et al.*, 2001) hint. Therefore it may be necessary, for future work to design probes/primers that span the *PRNP* genomic locus representing in particular, the promoter region.

7.6.3.2 *PRNP* copy number and kuru

One attractive hypothesis would be to investigate potential duplications in individuals who succumbed to kuru despite being heterozygous at codon 129. Currently the availability of good quality DNA for such tests is limited although efforts are currently being pursued at the MRC Prion Unit to consolidate samples using whole genome amplification – although it is not known how gene copy numbers will be affected by these procedures.

7.6.3.3 A test for somatic mutation

The somatic mutation hypothesis is a likely mechanism to explain the majority of sCJD and the role of CNPs in these somatic mutations will only be elucidated by a sensitive test (such a sensitivity test was planned but limited time dictated that the test was not conducted). The copy number assay developed here should be tested for detection of less than two-fold increases in template. Brain tissue displaying somatic mosaicism is likely to comprise of subtle differences in templates and so the ability to detect a range of template concentrations should be investigated.

7.6.3.4 A test for other diseases associated with *PRNP*

The development of a copy number assay for the prion gene could also inform on the pathogenesis of other diseases in which the *PRNP* has been implicated. Inclusion body myositis (IBM) is one such disease, which was beyond the scope of this study (MIM: 147421). IBM is one of the most common inflammatory myopathies of late onset and is defined histologically by inclusions which are immunoreactive for several proteins including beta amyloid fragments. PrP immunoreactivity has also been noted within IBM inclusions and an association between codon 129 genotype and IBM has been proposed but not replicated (Lampe *et al.*, 1999; Orth *et al.*, 2000). Although the consequence of PrP deposition within inclusions in IBM is not known, a similar dosage mechanism to that hypothesised here for human prion diseases may exist and therefore, such a copy number assay may be able to elucidate the genetic mechanism responsible.

8 General discussion

The work presented in this thesis has attempted to apply evolving techniques and analyses used to investigate complex diseases to two different neurodegenerative diseases. As each set of experiments has been discussed individually, the purpose of this chapter is to review this work in context.

8.1 Evolving tools and techniques

A common thread throughout this thesis has been the rapid advance in our ability to analyse complex traits. Many of the tools and techniques evolved during or after the work in this thesis was carried out and therefore too late to impact this work. However, where this has happened, the implications of these changes have been discussed. The effect of large scale project and new resources such as the HapMap, on research carried out concomitantly is not a new phenomenon. Prior to the sequencing of the human genome, methods to localise Mendelian disease genes were extremely difficult and very expensive. For example, localising the cystic fibrosis gene cost several hundred million dollars because of the huge amounts of unknown DNA which needed cloning and careful analysis.

8.2 *DYNC1H1* and ALS

Mutation screening of *DYNC1H1* The preliminary aim of the work presented in the first results chapter was to elucidate the genomic structure of *DYNC1H1*, a candidate gene for ALS. The initial evidence implicating a role for *DYNC1H1* in ALS pathogenesis came from mouse models of neurodegeneration in which mutations were positionally cloned to the mouse homologue *Dync1h1*. More recently, mutations in FALS families have been identified in a subunit of dynactin, a binding partner of cytoplasmic dynein. Using in silico methods, a 78 exon genomic structure of *DYNC1H1* spanning 86.6kb was elucidated.

Subsequent work in this chapter aimed to screen *DYNC1H1* exons 8, 13 and 14 for disease-associated mutations in index cases from FALS, HSP and SMA families and controls. These exons were homologous to those harbouring mutations in the Loa and Cra1 mouse models of disease. Although two SNPs were identified in exons 8 and the intervening intron between exons 13 and 14, neither was seen to be associated with disease. This was essentially a direct association study and therefore unknown variants within the gene were not tested.

***DYNC1H1* association study** The second results chapter aimed to conduct an indirect association study, to investigate genetic variation across *DYNC1H1* for an association with SALS. SNPs were

ascertained, the underlying pattern of LD elucidated and tSNPs selected. Two tSNPs were found to be sufficient to tag the majority of variation across *DYNC1H1* and these were genotyped in SALS cases and controls. No significant association was seen.

During investigation of *DYNC1H1* the pattern of genetic variation – specifically, reduced diversity – was suggestive of an evolutionary signal of selection. Several indicators of selection were investigated including heterozygosity, F_{ST}, haplotype frequencies and LD decay, in northern Europeans, Cameroonians and Japanese populations. Although the results were suggestive of selection at this locus, due to ascertainment bias, no conclusive answers could be reached.

Genetic analysis of the cytoplasmic dynein subunit families The aim of this third results chapter was to conduct a phylogenetic study to clarify the relationships between the known cytoplasmic dynein subunits, clarify their mapping positions, identify novel members of the subunit families and clarify discreprencies in their nomenclature. In the absence of an association of *DYNC1H1* with both FALS and SALS, several additional components of the cytoplasmic dynein-dynactin complex were considered for further study. However, the available data on these subunits was found to be confusing and even erroneous. Interspecies phylogenetic comparisons and an exhaustive search for novel human and mouse homologs have clarified many existing discrepancies.

8.2.1 Is there a role for *DYNC1H1* in ALS?

The role of *DYNC1H1* in ALS remains unclear. The studies conducted in this thesis have identified no association of *DYNC1H1* with either FALS or SALS however, as previously discussed, it is highly likely that these studies were underpowered due to the lack of available samples and factors intrinsic to the study design.

Evidence is accumulating that suggests *DYNC1H1* remains a good candidate for ALS and potentially other neurodegenerative diseases by virtue of its importance in retrograde axonal transport. Defective axonal transport has been observed in models of ALS by several investigators (Jablonka *et al.*, 2004; Rao *et al.*, 2003; Williamson *et al.*, 1999) and defects in anterograde axonal transport are one of the earliest pathologies observed in SOD1 mice (Williamson *et al.*, 1999). The work of Hafezparast and colleagues directly linked *Dync1h1* mutations in both Loa and Cra1 mice with inhibited retrograde axonal transport and a progressive motor neuron degeneration phenotype (Hafezparast *et al.*, 2003). More recently, compelling data for the involvement of *DYNC1H1* in ALS pathogenesis has come from a surprising observation by Kieran and colleagues in a compound heterozygous mouse created by crossing a $SOD1^{G93A}$ mouse with a *Loa* heterozygous mouse (Kieran *et al.*, 2005). Kieran and colleagues noted that whilst heterozygous littermates of both

mutations displayed a normal disease phenotype with impaired axonal transport and motor neuron death, the compound heterozygote showed a 28% increase in lifespan (compared to $SOD1^{G93A}$ mice), increased motor neuron survival and rescued axonal transport deficits. The mechanism by which the dynein mutation induces amelioration in *Loa*/$SOD1^{G93A}$ mice is still under investigation, however Kieran postulates that amelioration of disease in Loa/$SOD1^{G93A}$ mice may result from the restoration of axonal homeostasis as the balance between anterograde and retrograde transport in double-heterozygote motor neurons is restored. In addition, the dynein mutation may result in abnormal intracellular transport, which in turn may change the interaction of mutant SOD1 with organelles such as mitochondria, thus delaying cell death.

8.2.1.1 The dynein-dynactin complex and ALS

Beyond *DYNC1H1* there is substantial evidence linking the cytoplasmic dynein-dynactin complex with ALS pathogenesis. Mutations in at least three different subunits of the complex, *Dync1h1*, dynamitin (p24) and dynactin (p150), have all been shown to result in motor neuron degeneration phenotypes (Hafezparast *et al.*, 2003; LaMonte *et al.*, 2002; Munch *et al.*, 2004; Munch *et al.*, 2005; Puls *et al.*, 2003; Puls *et al.*, 2005). In addition, the role of this complex as a retrograde motor protein makes it a good candidate in other axonal transport-mediated neurodegenerative diseases. For example, *DYNC1H1* has been found to colocalise with amyloid plaques in the brains of AD patients and transgenic mouse models of AD (Liao *et al.*, 2004). In addition, disrupted axonal transport has been witnessed in Huntington's disease in which the expanded mutant huntingtin protein is thought to disrupt axonal transport by interaction with the $p150^{Glued}$ subunit of dynactin indirectly, via the huntingtin-associated protein HAP1 (Engelender *et al.*, 1997). The expanded glutamine repeats in huntingtin have been proposed to disrupt the integrity of the dynein/dynactin complex, thus reducing the efficiency of neurotrophic factor transport and contributing to neuronal death (Gauthier *et al.*, 2004).

There is clearly some degree of genetic heterogeneity in the cytoplasmic dynein-dynactin complex and its associated neurodegeneration phenotype. Clarification of the genetic relationships of the cytoplasmic dynein subunits was undertaken with a view to conduct a future association study in which multiple members of the dynein-dynactin complex may be investigated in a 'candidate pathway' approach. Kasperavičiūtė and colleagues recently performed such a study, analysing 1277 putative functional and tSNPs in 134 genes, including 17 members of the dynein-dynactin complex, in 822 British SALS samples and 872 controls (Kasperaviciute *et al.*, 2007). 19 SNPs showed a trend of association in the initial screen and were genotyped in a replication sample of 580 German sporadic ALS patients and 361 controls, after which no strong evidence of association was seen. Despite this negative result, this study was only able to capture common SNPs (>5%) with

predicted moderate effect size. By genotyping only a subset of SNPs in the replication sample variants with lower effect size may have been missed and functional variants which were not represented well by the initially genotyped set of SNPs may have also been missed. Additionally, some variants are known to have population-specific effects, as is illustrated by the association of the *VEGF* gene promoter polymorphisms and ALS. These polymorphisms have been positively associated with disease in three studies (Sweden, Belgium, Birmingham) which has not been replicated in another four (London, Sheffield, The Netherlands, North America) (Brockington *et al.*, 2005; Chen *et al.*, 2006; Lambrechts *et al.*, 2003; Van Vught *et al.*, 2005). Therefore, the genes of the dynein-dynactin complex may be associated with disease in additional populations.

8.2.2 Are association studies the right approach for complex neurodegenerative diseases?

The application of association studies to complex diseases has had mixed success. Non-replication of association findings is common for complex diseases however, few association studies have been found to be consistently replicable (Table 8.1). The success of an association study is dependent on several factors including: sample size and sample homogeneity (phenotypic and therefore genetic homogeneity and population homogeneity); genotyping accuracy; statistical analyses (corrections for multiple candidate genes or genome-wide analyses) and study design /genetic architecture to name a few (Abou-Sleiman *et al.*, 2004; Hattersley *et al.*, 2005; Healy, 2006).

Disease	Gene	Polymorphism	Associated allele ~Freq	~OR	Reference
Thrombophilia	*F5*	Leiden Arg506Gln	0·03	4	(Bertina *et al.*, 1994)
Crohn's disease	*CARD15*	3 SNPs	0·06	4·6	(Hugot *et al.*, 2001)
Alzheimer's	*APOE*	e2/3/4	0·15	3·3	(Corder *et al.*, 1993; Farrer *et al.*, 1997; Rubinsztein *et al.*, 1999; Saunders *et al.*, 1993)
Osteoporotic fractures	*COL1A1*	Sp1 restriction site	0·19	1·3	(Mann *et al.*, 2001; Mann *et al.*, 2003)
Age-related macular degeneration	*HF1/CFH*	Tyr402His	0·30	2·5	(Edwards *et al.*, 2005; Hageman *et al.*, 2005; Haines *et al.*, 2005; Klein *et al.*, 2005; Zareparsi *et al.*, 2005)
Type 2 diabetes	*KCNJ11*	Glu23Lys	0·36	1·23	(Gloyn *et al.*, 2003)
Type 1 diabetes	*CTLA4*	Thr17Ala	0·36	1·27	(Marron *et al.*, 1997; Ueda *et al.*, 2003)
Graves' disease	*CTLA4*	Thr17Ala	0·36	1·6	(Chistiakov *et al.*, 2003)
Type 1 diabetes	*INS*	Variable 5" tandem repeats	0·67	1·2	(Bennett *et al.*, 1996)
Bladder cancer	*GSTM1*	Null (gene deletion)	0·70	1·28	(Engel *et al.*, 2002)
Type 2 diabetes	*PPARG*	Pro12Ala	0·85	1·23	(Altshuler *et al.*, 2000)

Table 8.1 Consistent associations with complex disease

Approximate disease associated polymorphism or haplotype frequency shown (~Freq) and odds ratio (~OR) shown

8.2.2.1 Sample size

Sample size is of particular concern in neurodegenerative disease and is often a limiting factor in association studies of these diseases including the *DYNC1H1* study described in this thesis. Sample size is a direct determinant of study power and therefore the study outcome. However, many neurodegenerative diseases have low disease prevalence with short survival times, which restricts the development of the large sample collections required to detect associated variants with moderate-to-low effect size or of low population frequency. As our understanding of the importance of sample size continues to develop, more multicentre and international collaborations have been undertaken. For example, the recent genome-wide association study in ALS undertaken by Kasperavičiūtė and colleagues was comprised of over 800 samples from collections across the UK and resultantly, their study had sufficient power to detect a causal variant with OR of 1.47 (Kasperaviciute *et al.*, 2007), In addition, WGA of these study samples was undertaken to increase DNA stock 300-fold and ensure that these limited resources were not depleted without any detrimental impact to genotyping quality or efficiency.

8.2.2.2 Statistical analyses

The availability of cheaper and more efficient genotyping platforms has recently made genome-wide association studies of complex diseases a reality. Several different platforms are now available which either employ fixed marker sets, such as the Affymetrix GeneChip arrays, or custom marker sets, such as the GoldenGate assays (reviewed in Syvanen, 2005) and these sets can also comprise HapMap tSNPs. However, the multiple testing of 100,000 or more SNPs increases the type I error rate and therefore the significance threshold must be corrected to reflect this. Several different methods of achieving an appropriate genome wide significance threshold exist but they all mean that low *P*-values (α-value) are required to achieve significance. This in turn affects the sample size required to detect an association at various susceptibility allele frequencies (Table 8.2). Genome-wide studies of rare neurodegenerative diseases may therefore require unfeasibly large sample sizes.

	Susceptibility allele frequency in controls					
α	1%	5%	10%	20%	30%	40%
0·05	13 599	2866	1533	886	694	623
0·01	19 258	4058	2171	1255	982	883
0·001	27 055	5702	3051	1763	1380	1240
5×10^{-6}	36 869	7770	4157	2403	1881	1690
5×10^{-8}	58 678	12 366	6617	3825	2994	2690

Table 8.2 Effect of differing statistical significance levels on sample size

Numbers indicate sample size needed to detect significant association (power=90%) for different values of α, assuming allelic odds ratio of 1·3, given differing allele frequencies for predisposing allele or haplotype. (From Hattersley *et al.*, 2005)

8.2.2.3 Rare diseases

Both the frequency and penetrance of causal alleles affect the statistical power to detect these alleles; power increases with increasing frequency and increasing penetrance. The power to detect an allele therefore depends on what is ultimately the most relevant measure of a genetic variant's contribution: the proportion of the phenotypic variance in the population that is explained by a particular variant. This means that rare variants with modest effects will be difficult to detect by any method because they explain only a small fraction of the variance in a trait.

Rare alleles might also be more difficult to detect by association for other reasons. Even if rare alleles have strong effects, they might be difficult to detect by association methods because they are less well represented in SNP databases and because tag SNP approaches are currently designed to tag common SNPs (usually with frequencies >5%).However, population-genetic considerations indicate that most rare alleles with frequencies <5% are likely to have arisen relatively recently (because old alleles tend to either disappear or become common), so there will have been less time for recombination and mutation to disrupt the haplotype on which they arose. Therefore, rare variants are expected to be on single, long haplotypes, as has been observed (Kamatani *et al.*, 2004).

However, as previously discussed, new techniques such as the exhaustive searching of all haplotypes employed in the EATDT approach could greatly increase power to detect rare variants (de Bakker *et al.*, 2005; Lin *et al.*, 2004). In addition, Vermeire and colleagues have shown that the alleles of *CARD15* with MAF<5% that contributes to IBD could have been detected indirectly with haplotypes composed of common variants (Vermeire *et al.*, 2002) and a rare (<3%) haplotype in the 11β-hydroxysteroid dehydrogenase type 1 gene (HSD11 β1) has been shown to be associated with a 6-fold increase in risk for sporadic AD

8.3 Identifying kuru susceptibility loci

Several different aims were investigated in the first kuru results chapter:

(i) **to perform a comprehensive analysis of *PRNP* codon 129 genotype data**

HWE analysis of 147 kuru samples corroborated the correlation of homozygosity at codon 129 with earlier kuru onset and conversely, the protective effect of heterozygosity at codon 129. Although only age of onset was available as a comparable phenotype, it is more likely that codon 129 status affected kuru incubation time of these cases, however, without knowing approximately when transmission occurred and at what dose, incubation time would be impossible to estimate. However, a recent study of long incubation time kuru deaths (deaths post-1960) by Collinge and colleagues identified a significant excess of codon 129 heterozygotes, suggesting that heterozygosity at codon 129 is associated with long incubation times (Collinge *et al.*, 2006). The protective effect of codon

129 was illustrated by analysis of 125 elderly Fore women who despite being exposed repeatedly to kuru at multiple mortuary feasts, did not succumb to disease. The codon 129 genotype in this cohort was highly enriched for heterozygotes and found to be extremely significant when compared to the genotype proportions expected under HWE.

(ii) **to identify signatures of selection at codon 129 as a paradigm for other candidate loci**

Several different tests of selection were undertaken at codon 129 and across the *PRNP* locus. The co-variation of these signatures of selection with the intensity of the selective force (i.e. kuru) was examined. HWE and heterozygosity analyses based on linguistic groups identified deviations from HWE in those groups known to have the highest exposure to kuru but not in those with moderate exposure to kuru. In addition, despite a world-wide cline in codon 129 valine allele frequency, no cline within the Eastern Highlands was seen. The establishment of an exposure index to account for the exposure of each individual village within a linguistic group consolidated the HWE data and identified a significant valine frequency cline between the highly exposed and unexposed Highland populations and non-Highland populations.

(iii) **to develop a PNG sample panel as a resource to test candidate genes**

The refinement of the PNG samples according to kuru exposure has provided a powerful resource for testing candidate genes against. The significant variation of valine allele frequency from non-Highland to Highland samples and within the Highlands from kuru-unexposed to kuru-exposed samples illustrates how potential susceptibility loci may be identified. Such clines in allele frequency or magnitude of other measures such as deviation from HWE or F_{ST} at candidate loci may be indicative of a susceptibility allele.

(iv) **to assess the feasibility of genome-wide genotyping on archived kuru samples**

The analysis of 7 kuru samples which had undergone WGA and 7 multiple exposure samples on Affymetrix NspI GeneChip arrays permitted several observations to be made. Despite the PCR banding patterns obtained following amplification of the WGA kuru DNA, fragmentation of the samples appeared relatively normal. The optimum rank score threshold for analysis of the WGA samples, compared to a baseline analysis at P=0.1, was found to be P=0.19. At this threshold, the greatest gain in SNP calls was seen with a minimal increase in discordance of calls. The analysis of pairwise LD identified that LD was insensitive to the rank score threshold used to analyse the data, possibly because the discordance seen at lower stringencies comprised a small fraction of the overall pairwise comparisons. The inflation of pairwise LD in a small sample size was seen to affect long-range LD to a greater extent compared to smaller pairwise intervals (230% inflation for 100kb comparisons compared to 113% inflation for 5kb comparisons). LD decay over distance for the 7

WGA kuru samples was markedly different to that of 7 UK and 7 multiple exposure samples, which probably reflected the failure of the WGA DNA samples to genotype accurately. Interestingly, the decay of LD in the 7 multiple exposure samples was 1.25-fold greater than that of the UK samples, with a similar distribution implying that LD is extends over a greater distance in these PNG samples.

8.3.1 Signatures of selection at *PRNP*

8.3.1.1 Evolutionary studies require good epidemiological evidence

All tests conducted for signatures of selection and for the influence of codon 129 on kuru incubation/onset have relied on good epidemiological data. For example, the protective effect of heterozygosity at codon 129 in women aged >50 years in 2000 required the documentation of the date of sample collection, age data and knowledge of the approximate cessation of the practice of endocannibalism. Together, these data allowed a powerful analysis of those women who lived during the peak of the kuru epidemic but who had not succumbed to kuru. Similarly, the HWE analysis of the surviving Eastern Highland population required knowledge of these data and appreciation of the selection model (i.e. sex specific balancing selection). These data permitted the stratification of data to provide a clearer signal of selection and resultantly, the HWE analysis recapitulated the known epidemiology of the disease.

The importance of precise epidemiological data was also highlighted in the investigation of a valine allele cline across the Eastern Highlands. Analysis of a valine allele cline, covarying with kuru exposure was undertaken within linguistic groups. This led to the observation of an equilibrium frequency for valine alleles across the Eastern Highlands. However, on application of the exposure index for each village within a linguistic group, a significant cline in valine allele frequency was seen.

8.3.1.2 Was evidence for selection seen at *PRNP*?

There were 3 key pieces of evidence that supported the role of selection at *PRNP*:

(i) a highly significant increase in codon 129 heterozygosity was seen in those exposed to kuru but not succumbing to disease.

(ii) a significant cline in valine allele frequency was seen with the highest value seen in the kuru exposed group suggesting that kuru may have been responsible for the increase.

(iii) although the microsatellite data did not yield any useful information regarding differences in LD between exposed and unexposed groups, marginal significance was seen with microsatellite F_{ST} on the valine chromosome, implying that a sudden increase in the valine haplotype may have resulted in a selective sweep of surrounding alleles.

8.3.1.3 *PRNP* selection study caveats

There are several caveats to the work carried out to identify selection at *PRNP*.

A necessarily limited amount of polymorphism data was analysed. Although it would have been preferable to have sequenced the *PRNP* ORF and flanking sequences to test for selection using measures based on the five main signatures of selection described by Sabeti and colleagues (Sabeti *et al.*, 2006)and summarised in Chapter 1, financial and time constraints dictated that available codon 129 data and microsatellite data was used. This restricted the analysis largely to single locus tests which omits data from surrounding polymorphisms.

The cline in valine frequency may be a demographic effect. The increase in valine frequency from costal PNG populations to within the Eastern Highlands could reflect the stochastic effects of genetic drift through migration and population bottlenecks. Unlinked loci should have been typed to ascertain if the increase in valine allele frequency was due to demography rather than selection, as following a population bottleneck a reduction in diversity will be seen across the genome at unlinked loci. Whereas following selection, only the genetic diversity related to the selected locus will be affected. Unlinked markers were not typed in this study as a whole-genome study in these samples was anticipated.

A population bottleneck cannot explain however, the significant difference seen in valine frequency between the Highland exposed and unexposed populations. Analysis by linguistic groups indicates that both of these cohorts have an equilibrium frequency however when grouped according to exposure index, a significant difference is seen.

Are the assumptions of Hardy-Weinberg equilibrium violated? Several of the tests applied to the *PRNP* data in this thesis and other published work have interrogated codon 129 data for departures from HWE and have attributed departures to a violation of the assumption of an absence of selection. However, as there is no written history in the Eastern Highlands, we cannot be clear about how the populations of the Eastern Highlands are structured, if migration occurs amongst them and if mating is truly random – at least prior to oral history being obtained by interview. Violation of these assumptions should be stated as a caveat to these data.

8.3.2 G127V is an additional *PRNP* susceptibility factor

The novel G127V polymorphism was found to be highly geographically restricted to the Purosa Valley, where it was a common variant occurring at ~7%. Analysis of the multiple exposure women and exposed men against the kuru samples illustrated that the polymorphism confers resistance to kuru in the heterozygous state. The mechanism of protection associated with this polymorphism is unclear: it may result steric hinderance from the addition of a bulky amino-acid side-chain which resultantly impedes beta-sheet formation and protect against prion formation.

The possibility that, rather than protecting against kuru, the 127V polymorphism might have instead triggered the epidemic cannot be completely excluded. Given that life expectancy in the kuru region is 42 years, it is possible that 127V is associated with a late-onset and low penetrant inherited prion disease which might have triggered the kuru epidemic. There are few examples of mutations causative of autosomal dominant neurodegenerative disease that achieve the polymorphic frequency observed in the Purosa Valley (Wexler *et al.*, 2004). A wealth of data indicates that prion transmission is generally more efficient where there is complementarity between the primary PrP sequence of donor and host, implying that if 127V was pathogenic it would be expected to confer susceptibility to the corresponding acquired prion disease (Collinge, 2001). Additionally, the glycoform type of PrP^{Sc} in kuru, although restricted to a small number of autopsy samples, closely resembles sCJD rather than point mutation inherited prion disease (Parchi, 2000). Finally, if 127V had triggered kuru, the localization to the southeastern part of the Fore linguistic group would be inconsistent with oral history that the first kuru patient was observed in the Keiagana linguistic group located to the northwest of the Fore. Future work should included the modelling of the 127 mutation in transgenic mouse lines and in cell-models to identify how this change may protect against disease.

8.3.3 Is selection a valid method for mapping loci in all neurodegenerative diseases?

The use of identifying a signature of selection for identifying loci involved in the pathogenesis of complex disease is an interesting concept but one that is not yet supported by concrete examples.

There are several reasons why signatures of selection may not be applicable to all complex neurodegenerative diseases. Perhaps the most significant is that pointed out by J.B.S. Haldane who recognised that late-onset genetic diseases in humans, such as Huntington's disease, encounter only weak selection (Haldane, 1941). Haldane's observation recognises that the principle driver of evolution is differential fitness or fecundity, meaning that an organism's ability to reproduce must be affected by mutation. However, the majority of cases of complex neurodegenerative diseases are late-onset, presenting after reproduction is completed and therefore are likely to be under little selection pressure.

For Mendelian diseases, which are usually caused by rare strongly deleterious mutations, a mutation-selection-balance model can be evoked, in which disease alleles are continuously generated by mutation and eliminated by purifying selection before reproduction. This model of purifying selection can also be extended to common late-onset diseases, by assuming that although onset occurs after reproduction is complete, the susceptibility genotypes still have weakly deleterious effects on fitness (Pritchard, 2001; Reich *et al.*, 2001b). Weak purifying selection is actually a pervasive mechanism underpinning patterns of variation in human populations, as non-synonymous variants occurring at evolutionarily conserved positions, tend to occur at lower frequencies compared with synonymous polymorphisms (Hughes *et al.*, 2003). Empirical data have also corroborated this model. In analysing nucleotide sequences of genes known to be mutated in Mendelian diseases and replicated genes in complex disease, Thomas and Kejariwal identified a preponderance for Mendelian disease-associated non-synonymous SNPs to occur at highly conserved positions in proteins compared to their complex disease counterparts (Thomas *et al.*, 2004). This result strongly suggests that, on average, the molecular effects of non-synonymous SNPs in complex diseases will be more subtle than the severe functional changes associated with most non-synonymous SNPs in Mendelian disease. In addition, under this mutation-selection-balance model multiple rare new alleles increasing risk are predicted to be found at trait loci. This has been observed at loci such as the *ABCA1* gene responsible for low HDL cholesterol (Cohen *et al.*, 2004).

In contrast, some mutations may have pleiotropic effects, which are beneficial in youth, but yield a greater subsequent risk of neurodegenerative disease. These mutations would then be incorporated into the population by selection, which will act more strongly on the early, beneficial effect. This can be considered an extension of James Neel's "thrifty gene" hypothesis which attempts to explain a tendency of certain populations towards obesity and diabetes (Neel, 1962). The hypothesis postulates that certain human genes have evolved to maximize metabolic efficiency which would thereby confer a survival advantage in times of food shortages. However, in times of abundance, the thrifty genotype no longer confers a survival advantage, instead predisposing carriers to diseases caused by excess nutritional intake, such as obesity and diabetes. This hypothesis has been used to explain ethnic variation in AD prevalence (Farrer *et al.*, 1997) linked to variation in the APOE ε4 allele frequency (Reviewed in Laws *et al.*, 2003). Briefly, APOE ε4 is associated with increased levels of dietary cholesterol and hypercholesterolaemia may play a role in the mechanism by which APOE e4 increases the risk for AD. Therefore, a change in dietary environment for populations possessing this "thrifty gene" may lead to an increased risk of AD, This phenomenon has been suggested to explain why Africans in Nigerian and East Africa show no association of APOE ε4 with AD whereas in African–Americans an association has been reported (Reviewed in Laws *et al.*, 2003).

A very strong signature of selection was found in the Fore, related to kuru. Perhaps those neurodegenerative diseases where signatures of selection may be of most use are diseases similar to kuru – epidemics with high mortality rates and high selection coefficients. ALS with Parkinsonism and dementia seen in Guam and a similar disease in the Kii peninsula of Japan of ALS with dementia are at first glance, good candidates, However despite having a historical prevalence ~400 per 100,000 population (Galasko *et al.*, 2000) and ~194 per 100,000 population (Yase *et al.*, 2001) respectively, onset and death occur after reproductive age is reached: mean age of onset is 55 years (Galasko *et al.*, 2000) in the Guamanian disease and 56.5 years in the Kii form of ALS (Yoshida *et al.*, 1998). The unique feature of prion disease – it's transmissibility – makes kuru exceptional amongst neurodegenerative diseases. K may be our best example of a neurodegenerative disease affected by selection and provide the first clues to novel susceptibility loci but it remains to be seen if evolutionary analyses will have utility in other neurodegenerative diseases.

8.4 Future directions for complex genetic analyses of neurodegenerative disease

It is likely that future studies of complex diseases will not be based solely on association studies or studies to identify evolutionary selection. A paper published within the last few weeks by David Reich and his group has illustrated the statistical power available to detect disease variants by combining these two approaches (Ayodo *et al.*, 2007). Reich and colleagues observed that power to

detect risk variants for malaria was increased by several orders of magnitude if case-control association studies were conducted with variants showing allele frequency differentiation between differently exposed populations, The applicability of this type of test to the majority of neurodegenerative diseases remains to be seen, however, kuru, which has been shown in this thesis to have caused codon 129 allele frequency differentiation in differently exposed populations, may be a good place to begin.

In conclusion, the work presented in this thesis aimed to investigate two complex neurodegenerative diseases by means of two very different methods – a candidate gene case-control association study and analyses based on the signatures of selection. The work presented in this thesis reflects the methods and study designs accepted and widely used at the time and therefore, this work is very much "of it's time". No association of *DYNC1H1* with FALS or SALS was seen, In the human prion disease kuru, strong balancing selection imposed by the disease was witnessed at codon 129 of *PRNP* and a new protective polymorphism was identified. And finally, the role of *PRNP* copy number polymorphisms was investigated as a potential pathogenic mechanism, in kuru and sCJD. From the data collected, it is likely that *PRNP* CNPs could account for a small minority of disease cases.

9 References

Abalkhail, H., Mitchell, J., Habgood, J. *et al.* (2003). A new familial amyotrophic lateral sclerosis locus on chromosome 16q12.1-16q12.2. *Am J Hum Genet.* **73**, 383-389

Abou-Sleiman, P.M., Healy, D.G., and Wood, N.W. (2004). Genetic approaches to solving common diseases. *J Neurol.* **251**, 1169-1172

Adkins, R.M. (2004). Comparison of the accuracy of methods of computational haplotype inference using a large empirical dataset. *BMC Genet.* **5**, 22

Affymetrix. (2005a). Affymetrix Data Sheet: GeneChip® Human Mapping 500K Array Set.

Affymetrix. (2005b). Affymetrix GeneChip® DNA Analysis Software: User's Guide Version 3.0.

Ahmad-Annuar, A., Shah, P., Hafezparast, M. *et al.* (2003). No association with common Caucasian genotypes in exons 8, 13 and 14 of the human cytoplasmic dynein heavy chain gene (*DNCHC1*) and familial motor neuron disorders. *Amyotroph Lateral Scler Other Motor Neuron Disord.* **4**, 150-157

Ahmadi, K.R., Weale, M.E., Xue, Z.Y. *et al.* (2005). A single-nucleotide polymorphism tagging set for human drug metabolism and transport. *Nat Genet.* **37**, 84-89

Akey, J.M., Zhang, G., Zhang, K. *et al.* (2002). Interrogating a high-density SNP map for signatures of natural selection. *Genome Res.* **12**, 1805-1814

Akey, J.M., Zhang, K., Xiong, M. *et al.* (2003). The effect of single nucleotide polymorphism identification strategies on estimates of linkage disequilibrium. *Mol Biol Evol.* **20**, 232-242

Al Chalabi, A., Andersen, P.M., Chioza, B. *et al.* (1998). Recessive amyotrophic lateral sclerosis families with the D90A SOD1 mutation share a common founder: evidence for a linked protective factor. *Hum Mol Genet.* **7**, 2045-2050

Al Chalabi, A., Andersen, P.M., Nilsson, P. *et al.* (1999). Deletions of the heavy neurofilament subunit tail in amyotrophic lateral sclerosis. *Hum Mol Genet.* **8**, 157-164

Al Chalabi, A., Enayat, Z.E., Bakker, M.C. *et al.* (1996). Association of apolipoprotein E epsilon 4 allele with bulbar-onset motor neuron disease. *Lancet.* **347**, 159-160

Al Chalabi, A., Scheffler, M.D., Smith, B.N. *et al.* (2003). Ciliary neurotrophic factor genotype does not influence clinical phenotype in amyotrophic lateral sclerosis. *Ann Neurol.* **54**, 130-134

Altmuller, J., Palmer, L.J., Fischer, G. *et al.* (2001). Genomewide scans of complex human diseases: true linkage is hard to find. *Am J Hum Genet.* **69**, 936-950

Altschul, S.F., Gish, W., Miller, W. *et al.* (1990). Basic local alignment search tool. *J Mol Biol.* **215**, 403-410

Altschul, S.F., Madden, T.L., Schaffer, A.A. *et al.* (1997). Gapped BLAST and PSI-BLAST: a new generation of protein database search programs. *Nucleic Acids Res.* **25**, 3389-3402

Altshuler, D., Hirschhorn, J.N., Klannemark, M. *et al.* (2000). The common PPARgamma Pro12Ala polymorphism is associated with decreased risk of type 2 diabetes. *Nat Genet.* **26**, 76-80

Andersen, P.M., Forsgren, L., Binzer, M. *et al.* (1996). Autosomal recessive adult-onset amyotrophic lateral sclerosis associated with homozygosity for Asp90Ala CuZn-superoxide dismutase mutation. A clinical and genealogical study of 36 patients. *Brain.* **119**, 1153-1172

Andersen, P.M., Nilsson, P., Ala-Hurula, V. *et al.* (1995). Amyotrophic lateral sclerosis associated with homozygosity for an Asp90Ala mutation in CuZn-superoxide dismutase. *Nat Genet.* **10**, 61-66

Andersen, P.M., Nilsson, P., Keranen, M.L. *et al.* (1997). Phenotypic heterogeneity in motor neuron disease patients with CuZn-superoxide dismutase mutations in Scandinavia. *Brain.* **120**, 1723-1737

Andersen, P.M., Sims, K.B., Xin, W.W. *et al.* (2003). Sixteen novel mutations in the Cu/Zn superoxide dismutase gene in amyotrophic lateral sclerosis: a decade of discoveries, defects and disputes. *Amyotroph Lateral Scler Other Motor Neuron Disord.* **4**, 62-73

Antonarakis, S.E. and Beckmann, J.S. (2006). Mendelian disorders deserve more attention. *Nat Rev Genet.* **7**, 277-282

Aoki, M., Lin, C.L., Rothstein, J.D. *et al.* (1998). Mutations in the glutamate transporter EAAT2 gene do not cause abnormal EAAT2 transcripts in amyotrophic lateral sclerosis. *Ann Neurol.* **43**, 645-653

Applied Biosystems. (1997). User Bulletin #2 ABI PRISM 7700 Sequence Detection System: Relative Quantitation of Gene Expression.

Ardlie, K.G., Lunetta, K.L., and Seielstad, M. (2002). Testing for population subdivision and association in four case-control studies. *Am J Hum Genet.* **71**, 304-311

Arnold, D.A., EDGREN, D.C., and PALLADINO, V.S. (1953). Amyotrophic lateral sclerosis; fifty cases observed on Guam. *J Nerv Ment Dis.* **117**, 135-139

Attenborough, R. D. and Alpers, M. P, (1992). *The Epidemiology of Malaria in Papua New Guinea* In:*Human Biology in Papua New Guinea.*Cattani, V. Oxford: Clarendon Press, 302:312

Ayodo, G., Price, A.L., Keinan, A. *et al.* (2007). Combining evidence of natural selection with association analysis increases power to detect malaria-resistance variants. *Am J Hum Genet.* **81**, 234-242

Bamshad, M. and Wooding, S.P. (2003). Signatures of natural selection in the human genome. *Nat Rev Genet.* **4**, 99-111

Bamshad, M.J., Mummidi, S., Gonzalez, E. *et al.* (2002). A strong signature of balancing selection in the 5' cis-regulatory region of CCR5. *Proc Natl Acad Sci U S A.* **99**, 10539-10544

Bennett, S.T. and Todd, J.A. (1996). Human type 1 diabetes and the insulin gene: principles of mapping polygenes. *Annu Rev Genet.* **30**, 343-370

Bersaglieri, T., Sabeti, P.C., Patterson, N. *et al.* (2004). Genetic signatures of strong recent positive selection at the lactase gene. *Am J Hum Genet.* **74**, 1111-1120

Bertina, R.M., Koeleman, B.P.C., Koster, T. *et al.* (1994). Mutation in blood coagulation factor V associated with resistance to activated protein C. *Nature.* **369**, 64-67

Biswas, S. and Akey, J.M. (2006). Genomic insights into positive selection. *Trends Genet.* **22**, 437-446

Blair, I.P., Bennett, C.L., Abel, A. *et al.* (2000). A gene for autosomal dominant juvenile amyotrophic lateral sclerosis (ALS4) localizes to a 500-kb interval on chromosome 9q34. *Neurogenetics.* **3**, 1-6

Boccardi, M., Sabattoli, F., Testa, C. *et al.* (2004). APOE and modulation of Alzheimer's and frontotemporal dementia. *Neurosci Lett.* **356**, 167-170

Bonnen, P.E., Pe'er, I., Plenge, R.M. *et al.* (2006). Evaluating potential for whole-genome studies in Kosrae, an isolated population in Micronesia. *Nat Genet.* **38**, 214-217

Bonnen, P.E., Wang, P.J., Kimmel, M. *et al.* (2002). Haplotype and linkage disequilibrium architecture for human cancer-associated genes. *Genome Res.* **12**, 1846-1853

Borroni, B., Yancopoulou, D., Tsutsui, M. *et al.* (2005). Association between tau H2 haplotype and age at onset in frontotemporal dementia. *Arch Neurol.* **62**, 1419-1422

Borthwick, G.M., Taylor, R.W., Walls, T.J. *et al.* (2006). Motor neuron disease in a patient with a mitochondrial tRNAIle mutation. *Ann Neurol.* **59**, 570-574

Bowman, A.B., Patel-King, R.S., Benashski, S.E. *et al.* (1999). Drosophila roadblock and Chlamydomonas LC7: a conserved family of dynein-associated proteins involved in axonal transport, flagellar motility, and mitosis. *J Cell Biol.* **146**, 165-180

Bozza, A., Malagu, S., Calzolari, E. *et al.* (1995). Expansion of a (CAG)n repeat region in a sporadic case of HD. *Acta Neurol Scand.* **92**, 132-134

Bratosiewicz-Wasik, J., Liberski, P.P., Golanska, E. *et al.* (2007). Regulatory sequences of the *PRNP* gene influence susceptibility to sporadic Creutzfeldt-Jakob disease. *Neurosci Lett.* **411**, 163-167

Brockington, A., Kirby, J., Eggitt, D. *et al.* (2005). Screening of the regulatory and coding regions of vascular endothelial growth factor in amyotrophic lateral sclerosis. *Neurogenetics.* **6**, 101-104

Bronfman, F.C., Escudero, C.A., Weis, J. *et al.* (2007). Endosomal transport of neurotrophins: Roles in signaling and neurodegenerative diseases. *Dev Neurobiol.* **67**, 1183-1203

Brookes, A.J., Lehvaslaiho, H., Siegfried, M. *et al.* (2000). HGBASE: a database of SNPs and other variations in and around human genes. *Nucleic Acids Res.* **28**, 356-360

Brookfield, J.F. (2003). Human evolution: a legacy of cannibalism in our genes? *Curr Biol.* **13**, R592-R593

Brooks, B.R. (1994). El Escorial World Federation of Neurology criteria for the diagnosis of amyotrophic lateral sclerosis. Subcommittee on Motor Neuron Diseases/Amyotrophic Lateral Sclerosis of the World Federation of Neurology Research Group on Neuromuscular Diseases and the El Escorial "Clinical limits of amyotrophic lateral sclerosis" workshop contributors. *J Neurol Sci.* **124**, 96-107

Brouwers, N., Sleegers, K., Engelborghs, S. *et al.* (2006). Genetic risk and transcriptional variability of amyloid precursor protein in Alzheimer's disease. *Brain.* **129**, 2984-2991

Brown, P., Cervenakova, L., Goldfarb, L.G. *et al.* (1994). Iatrogenic Creutzfeldt-Jakob disease: an example of the interplay between ancient genes and modern medicine. *Neurology.* **44**, 291-293

Bruce, M.E., Will, R.G., Ironside, J.W. *et al.* (1997). Transmissions to mice indicate that 'new variant' CJD is caused by the BSE agent. *Nature.* **389**, 498-501

Bruton, C.J., Bruton, R.K., Gentleman, S.M. *et al.* (1995). Diagnosis and incidence of prion (Creutzfeldt-Jakob) disease: a retrospective archival survey with implications for future research. *Neurodegeneration.* **4**, 357-368

Bueler, H., Aguzzi, A., Sailer, A. *et al.* (1993). Mice devoid of PrP are resistant to scrapie. *Cell.* **73**, 1339-1347

Burchard, E.G., Ziv, E., Coyle, N. *et al.* (2003). The importance of race and ethnic background in biomedical research and clinical practice. *N Engl J Med.* **348**, 1170-1175

Byers, H.R., Yaar, M., Eller, M.S. *et al.* (2000). Role of cytoplasmic dynein in melanosome transport in human melanocytes. *J Invest Dermatol.* **114**, 990-997

Cardon, L.R. and Palmer, L.J. (2003). Population stratification and spurious allelic association. *Lancet.* **361**, 598-604

Carlson, C.S., Eberle, M.A., Kruglyak, L. *et al.* (2004a). Mapping complex disease loci in whole-genome association studies. *Nature.* **429**, 446-452

Carlson, C.S., Eberle, M.A., Rieder, M.J. *et al.* (2003). Additional SNPs and linkage-disequilibrium analyses are necessary for whole-genome association studies in humans. *Nat Genet.* **33**, 518-521

Carlson, C.S., Eberle, M.A., Rieder, M.J. *et al.* (2004b). Selecting a maximally informative set of single-nucleotide polymorphisms for association analyses using linkage disequilibrium. *Am J Hum Genet.* **74**, 106-120

Carlson, C.S., Thomas, D.J., Eberle, M.A. *et al.* (2005). Genomic regions exhibiting positive selection identified from dense genotype data. *Genome Res.* **15**, 1553-1565

Carlson, G.A., Kingsbury, D.T., Goodman, P.A. *et al.* (1986). Linkage of prion protein and scrapie incubation time genes. *Cell.* **46**, 503-511

Cervenakova, L., Goldfarb, L.G., Garruto, R. *et al.* (1998). Phenotype-genotype studies in kuru: implications for new variant Creutzfeldt-Jakob disease. *Proc Natl Acad Sci U S A.* **95**, 13239-13241

Chakravarti, A. (1999). Population genetics--making sense out of sequence. *Nat Genet.* **21**, 56-60

Chamberlain, M., Baird, P., Dirani, M. *et al.* (2006). Unraveling a complex genetic disease: age-related macular degeneration. *Surv Ophthalmol.* **51**, 576-586

Chandler.L. (1961). Encephalopathy in mice produced by inoculation with scrapie brain material. *Lancet.* **1**, 1378-1379

Chapman, J.M., Cooper, J.D., Todd, J.A. *et al.* (2003). Detecting disease associations due to linkage disequilibrium using haplotype tags: a class of tests and the determinants of statistical power. *Hum Hered.* **56**, 18-31

Charlesworth, B., Morgan, M.T., and Charlesworth, D. (1993). The effect of deleterious mutations on neutral molecular variation. *Genetics.* **134**, 1289-1303

Chartier-Harlin, M.C., Kachergus, J., Roumier, C. *et al.* (2004). Alpha-synuclein locus duplication as a cause of familial Parkinson's disease. *Lancet.* **364**, 1167-1169

Chen, W., Saeed, M., Mao, H. *et al.* (2006). Lack of association of VEGF promoter polymorphisms with sporadic ALS. *Neurology.* **67**, 508-510

Chen, Y.Z., Bennett, C.L., Huynh, H.M. *et al.* (2004). DNA/RNA helicase gene mutations in a form of juvenile amyotrophic lateral sclerosis (ALS4). *Am J Hum Genet.* **74**, 1128-1135

Chesebro, B., Race, R., Wehrly, K. *et al.* (1985). Identification of scrapie prion protein-specific mRNA in scrapie-infected and uninfected brain. *Nature.* **315**, 331-333

Chioza, B.A., Ujfalusy, A., Csiszar, K. *et al.* (2001). Mutations in the lysyl oxidase gene are not associated with amyotrophic lateral sclerosis. *Amyotroph Lateral Scler Other Motor Neuron Disord.* **2**, 93-97

Chistiakov, D.A. and Turakulov, R.I. (2003). CTLA-4 and its role in autoimmune thyroid disease. *J Mol Endocrinol.* **31**, 21-36

Ciechanover, A. and Brundin, P. (2003). The ubiquitin proteasome system in neurodegenerative diseases: sometimes the chicken, sometimes the egg. *Neuron.* **40**, 427-446

Clark, A.G. (1990). Inference of haplotypes from PCR-amplified samples of diploid populations. *Mol Biol Evol.* **7**, 111-122

Clark, A.G., Hubisz, M.J., Bustamante, C.D. *et al.* (2005). Ascertainment bias in studies of human genome-wide polymorphism. *Genome Res.* **15**, 1496-1502

Clark, L.N., Poorkaj, P., Wszolek, Z. *et al.* (1998). Pathogenic implications of mutations in the tau gene in pallido-ponto-nigral degeneration and related neurodegenerative disorders linked to chromosome 17. *Proc Natl Acad Sci U S A.* **95**, 13103-13107

Clayton, D. (2004). SNPHAP: a program for estimating frequencies of large haplotypes of SNPs (Version 1.0).

Cleveland, D.W. and Rothstein, J.D. (2001). From Charcot to Lou Gehrig: deciphering selective motor neuron death in ALS. *Nat Rev Neurosci.* **2**, 806-819

Cohen, J.C., Kiss, R.S., Pertsemlidis, A. *et al.* (2004). Multiple rare alleles contribute to low plasma levels of HDL cholesterol. *Science.* **305**, 869-872

Cole, D.G. (2003). The intraflagellar transport machinery of Chlamydomonas reinhardtii. *Traffic.* **4**, 435-442

Collinge, J. (2001). Prion diseases of humans and animals: their causes and molecular basis. *Annu Rev Neurosci.* **24**, 519-550

Collinge, J. (2005). Molecular neurology of prion disease. *J Neurol Neurosurg Psychiatry.* **76**, 906-919

Collinge, J., Brown, J., Hardy, J. *et al.* (1992). Inherited prion disease with 144 base pair gene insertion. 2. Clinical and pathological features. *Brain.* **115**, 687-710

Collinge, J., Palmer, M.S., and Dryden, A.J. (1991). Genetic predisposition to iatrogenic Creutzfeldt-Jakob disease. *Lancet.* **337**, 1441-1442

Collinge, J., Sidle, K.C., Meads, J. *et al.* (1996). Molecular analysis of prion strain variation and the aetiology of 'new variant' CJD. *Nature.* **383**, 685-690

Collinge, J., Whitfield, J., McKintosh, E. *et al.* (2006). Kuru in the 21st century--an acquired human prion disease with very long incubation periods. *Lancet.* **367**, 2068-2074

Collins, F.S., Brooks, L.D., and Chakravarti, A. (1998). A DNA polymorphism discovery resource for research on human genetic variation. *Genome Res.* **8**, 1229-1231

Collins, F.S., Guyer, M.S., and Charkravarti, A. (1997). Variations on a theme: cataloging human DNA sequence variation. *Science.* **278**, 1580-1581

Colombo, R. (2000). Age and origin of the *PRNP* E200K mutation causing familial Creutzfeldt-Jacob disease in Libyan Jews. *Am J Hum Genet.* **67**, 528-531

Combarros, O., Sanchez-Guerra, M., Llorca, J. *et al.* (2000). Polymorphism at codon 129 of the prion protein gene is not associated with sporadic AD. *Neurology.* **55**, 593-595

Comi, G.P., Bordoni, A., Salani, S. *et al.* (1998). Cytochrome c oxidase subunit I microdeletion in a patient with motor neuron disease. *Ann Neurol.* **43**, 110-116

Conrad, D.F., Andrews, T.D., Carter, N.P. *et al.* (2006). A high-resolution survey of deletion polymorphism in the human genome. *Nat Genet.* **38**, 75-81

Corcia, P., Khoris, J., Couratier, P. *et al.* (2002a). SMN1 gene study in three families in which ALS and spinal muscular atrophy co-exist. *Neurology.* **59**, 1464-1466

Corcia, P., Mayeux-Portas, V., Khoris, J. *et al.* (2002b). Abnormal SMN1 gene copy number is a susceptibility factor for amyotrophic lateral sclerosis. *Ann Neurol.* **51**, 243-246

Corder, E.H., Saunders, A.M., Strittmatter, W.J. *et al.* (1993). Gene dose of apolipoprotein E type 4 allele and the risk of Alzheimer's disease in late onset families. *Science.* **261**, 921-923

Crackower, M.A., Sinasac, D.S., Xia, J. *et al.* (1999). Cloning and characterization of two cytoplasmic dynein intermediate chain genes in mouse and human. *Genomics.* **55**, 257-267

Cras-Meneur, C., Inoue, H., Zhou, Y. *et al.* (2004). An expression profile of human pancreatic islet mRNAs by Serial Analysis of Gene Expression (SAGE). *Diabetologia.* **47**, 284-299

Crepieux, P., Kwon, H., Leclerc, N. *et al.* (1997). I kappaB alpha physically interacts with a cytoskeleton-associated protein through its signal response domain. *Mol Cell Biol.* **17**, 7375-7385

Criswell, P.S., Ostrowski, L.E., and Asai, D.J. (1996). A novel cytoplasmic dynein heavy chain: expression of DHC1b in mammalian ciliated epithelial cells. *J Cell Sci.* **109**, 1891-1898

Cronin, S., Hardiman, O., and Traynor, B.J. (2007). Ethnic variation in the incidence of ALS: a systematic review. *Neurology.* **68**, 1002-1007

Cudkowicz, M.E., McKenna-Yasek, D., Sapp, P.E. *et al.* (1997). Epidemiology of mutations in superoxide dismutase in amyotrophic lateral sclerosis. *Ann Neurol.* **41**, 210-221

Cuillé, J. and Chelle, P.L. (1936). La maladie dite tremblante du mouton est-elle inocuable? *C R Acad Sci.* **203**, 1552-1554

Culver-Hanlon, T.L., Lex, S.A., Stephens, A.D. *et al.* (2006). A microtubule-binding domain in dynactin increases dynein processivity by skating along microtubules. *Nat Cell Biol.* **8**, 264-270

Curwen, V., Eyras, E., Andrews, T.D. *et al.* (2004). The Ensembl automatic gene annotation system. *Genome Res.* **14**, 942-950

Daly, M.J. and Rioux, J.D. (2004). New approaches to gene hunting in IBD. *Inflamm Bowel Dis.* **10**, 312-317

Daly, M.J., Rioux, J.D., Schaffner, S.F. *et al.* (2001). High-resolution haplotype structure in the human genome. *Nat Genet.* **29**, 229-232

Dausset, J., Cann, H., Cohen, D. *et al.* (1990). Centre d'etude du polymorphisme humain (CEPH): collaborative genetic mapping of the human genome. *Genomics.* **6**, 575-577

Davis, M.B., Bateman, D., Quinn, N.P. *et al.* (1994). Mutation analysis in patients with possible but apparently sporadic Huntington's disease. *Lancet.* **344**, 714-717

Dawson, E., Abecasis, G.R., Bumpstead, S. *et al.* (2002). A first-generation linkage disequilibrium map of human chromosome 22. *Nature.* **418**, 544-548

de Bakker, P.I., Yelensky, R., Pe'er, I. *et al.* (2005). Efficiency and power in genetic association studies. *Nat Genet.* **37**, 1217-1223

De La Vega, F.M., Isaac, H.I., and Scafe, C.R. (2006). A tool for selecting SNPs for association studies based on observed linkage disequilibrium patterns. *Pac Symp Biocomput.* 487-498

Dean, G. and Elian, M. (1993). Motor neuron disease and multiple sclerosis mortality in Australia, New Zealand and South Africa compared with England and Wales. *J Neurol Neurosurg Psychiatry.* **56**, 633-637

DeChiara, T.M., Vejsada, R., Poueymirou, W.T. *et al.* (1995). Mice lacking the CNTF receptor, unlike mice lacking CNTF, exhibit profound motor neuron deficits at birth. *Cell.* **83**, 313-322

Del Bo, R., Scarlato, M., Ghezzi, S. *et al.* (2005). Is M129V of *PRNP* gene associated with Alzheimer's disease? A case-control study and a meta-analysis. *Neurobiol Aging.*

Deslys, J.P., Marce, D., and Dormont, D. (1994). Similar genetic susceptibility in iatrogenic and sporadic Creutzfeldt-Jakob disease. *J Gen Virol.* **75**, 23-27

Devlin, B., Bacanu, S.A., and Roeder, K. (2004). Genomic Control to the extreme. *Nat Genet.* **36**, 1129-1130

Devlin, B. and Risch, N. (1995). A comparison of linkage disequilibrium measures for fine-scale mapping. *Genomics.* **29**, 311-322

Devlin, B. and Roeder, K. (1999). Genomic control for association studies. *Biometrics.* **55**, 997-1004

Dhaliwal, G.K. and Grewal, R.P. (2000). Mitochondrial DNA deletion mutation levels are elevated in ALS brains. *Neuroreport.* **11**, 2507-2509

Dick, T., Ray, K., Salz, H.K. *et al.* (1996a). Cytoplasmic dynein (ddlc1) mutations cause morphogenetic defects and apoptotic cell death in Drosophila melanogaster. *Mol Cell Biol.* **16**, 1966-1977

Dick, T., Ray, K., Salz, H.K. *et al.* (1996b). Cytoplasmic dynein (ddlc1) mutations cause morphogenetic defects and apoptotic cell death in Drosophila melanogaster. *Mol Cell Biol.* **16**, 1966-1977

Dole, V., Jakubzik, C.R., Brunjes, B. *et al.* (2000). A cDNA from the green alga Spermatozopsis similis encodes a protein with homology to the newly discovered Roadblock/LC7 family of dynein-associated proteins. *Biochim Biophys Acta.* **1490**, 125-130

Drory, V.E., Birnbaum, M., Korczyn, A.D. *et al.* (2001). Association of APOE epsilon4 allele with survival in amyotrophic lateral sclerosis. *J Neurol Sci.* **190**, 17-20

Drory, V.E., Birnbaum, M., Peleg, L. *et al.* (2003). Hexosaminidase A deficiency is an uncommon cause of a syndrome mimicking amyotrophic lateral sclerosis. *Muscle Nerve.* **28**, 109-112

Dunning, A.M., Durocher, F., Healey, C.S. *et al.* (2000). The extent of linkage disequilibrium in four populations with distinct demographic histories. *Am J Hum Genet.* **67**, 1544-1554

Durr, A., Dode, C., Hahn, V. *et al.* (1995). Diagnosis of "sporadic" Huntington's disease. *J Neurol Sci.* **129**, 51-55

Eberle, M.A., Rieder, M.J., Kruglyak, L. *et al.* (2006). Allele frequency matching between SNPs reveals an excess of linkage disequilibrium in genic regions of the human genome. *PLoS Genet.* **2**, e142-

Edwards, A.O., Ritter, R., III, Abel, K.J. *et al.* (2005). Complement factor H polymorphism and age-related macular degeneration. *Science.* **308**, 421-424

Efron, B. (1993). Bayes and likelihood calculations from confidence intervals. *Biometrika.* **80**, 3-26

Elian, M. and Dean, G. (1993). Motor neuron disease and multiple sclerosis among immigrants to England from the Indian subcontinent, the Caribbean, and east and west Africa. *J Neurol Neurosurg Psychiatry*. **56**, 454-457

Enard, W., Przeworski, M., Fisher, S.E. *et al.* (2002). Molecular evolution of FOXP2, a gene involved in speech and language. *Nature*. **418**, 869-872

Eng Ang, C., Jones, C., McBride, J. *et al.* (2007). Whole genome amplification of poor quality DNA rescues SNP microarray assays.

Engel, L.S., Taioli, E., Pfeiffer, R. *et al.* (2002). Pooled analysis and meta-analysis of glutathione S-transferase M1 and bladder cancer: a HuGE review. *Am J Epidemiol*. **156**, 95-109

Engelender, S., Sharp, A.H., Colomer, V. *et al.* (1997). Huntingtin-associated protein 1 (HAP1) interacts with the p150Glued subunit of dynactin. *Hum Mol Genet*. **6**, 2205-2212

Erginel-Unaltuna, N., Peoc'h, K., Komurcu, E. *et al.* (2001). Distribution of the M129V polymorphism of the prion protein gene in a Turkish population suggests a high risk for Creutzfeldt-Jakob disease. *Eur J Hum Genet*. **9**, 965-968

Escalante, A.A., Cornejo, O.E., Freeland, D.E. *et al.* (2005). A monkey's tale: the origin of Plasmodium vivax as a human malaria parasite. *Proc Natl Acad Sci U S A*. **102**, 1980-1985

Espindola, F.S., Suter, D.M., Partata, L.B. *et al.* (2000). The light chain composition of chicken brain myosin-Va: calmodulin, myosin-II essential light chains, and 8-kDa dynein light chain/PIN. *Cell Motil Cytoskeleton*. **47**, 269-281

Ewens, W.J. (1972). The sampling theory of selectively neutral alleles. *Theor Popul Biol*. **3**, 87-112

Eyre-Walker, A. and Keightley, P.D. (1999). High genomic deleterious mutation rates in hominids. *Nature*. **397**, 344-347

Farrer, L.A., Cupples, L.A., Haines, J.L. *et al.* (1997). Effects of age, sex, and ethnicity on the association between apolipoprotein E genotype and Alzheimer disease. A meta-analysis. APOE and Alzheimer Disease Meta Analysis Consortium. *JAMA*. **278**, 1349-1356

Farrer, M., Kachergus, J., Forno, L. *et al.* (2004). Comparison of kindreds with parkinsonism and alpha-synuclein genomic multiplications. *Ann Neurol*. **55**, 174-179

Feder, J.N., Gnirke, A., Thomas, W. *et al.* (1996). A novel MHC class I-like gene is mutated in patients with hereditary haemochromatosis. *Nat Genet*. **13**, 399-408

Feldman, B., Chapman, J., and Korczyn, A.D. (2006). Apolipoprotein epsilon4 advances appearance of psychosis in patients with Parkinson's disease. *Acta Neurol Scand*. **113**, 14-17

Fischer, M., Rulicke, T., Raeber, A. *et al.* (1996). Prion protein (PrP) with amino-proximal deletions restoring susceptibility of PrP knockout mice to scrapie. *EMBO J*. **15**, 1255-1264

Flowers, J.M., Leigh, P.N., Davies, A.M. *et al.* (1999). Mutations in the gene encoding human persyn are not associated with amyotrophic lateral sclerosis or familial Parkinson's disease. *Neurosci Lett.* **274**, 21-24

Flowers, J.M., Powell, J.F., Leigh, P.N. *et al.* (2001). Intron 7 retention and exon 9 skipping EAAT2 mRNA variants are not associated with amyotrophic lateral sclerosis. *Ann Neurol.* **49**, 643-649

Fracchiolla, N.S., Cortelezzi, A., and Lambertenghi-Deliliers, G. (1999). BitH, a human homolog of bithorax Drosophila melanogaster gene, on chromosome 20q. EMBL/GenBank/DDBJ databases.

Freeman, J.L., Perry, G.H., Feuk, L. *et al.* (2006). Copy number variation: new insights in genome diversity. *Genome Res.* **16**, 949-961

Fridolfsson, A.K., Hori, T., Wintero, A.K. *et al.* (1997). Expansion of the pig comparative map by expressed sequence tags (EST) mapping. *Mamm Genome.* **8**, 907-912

Fullerton, S.M., Clark, A.G., Weiss, K.M. *et al.* (2000). Apolipoprotein E variation at the sequence haplotype level: implications for the origin and maintenance of a major human polymorphism. *Am J Hum Genet.* **67**, 881-900

Futamura, N., Matsumura, R., Fujimoto, Y. *et al.* (1998). CAG repeat expansions in patients with sporadic cerebellar ataxia. *Acta Neurol Scand.* **98**, 55-59

Gabriel, S.B., Schaffner, S.F., Nguyen, H. *et al.* (2002). The structure of haplotype blocks in the human genome. *Science.* **296**, 2225-2229

Gacia, M., Safranow, K., Styczynska, M. *et al.* (2006). Prion protein gene M129 allele is a risk factor for Alzheimer's disease. *J Neural Transm.* **113**, 1747-1751

Gajdusek, D.C., Gibbs, C.J., Jr., and Alpers, M. (1967). Transmission and passage of experimenal "kuru" to chimpanzees. *Science.* **155**, 212-214

Gajewski, C.D., Lin, M.T., Cudkowicz, M.E. *et al.* (2003). Mitochondrial DNA from platelets of sporadic ALS patients restores normal respiratory functions in rho(0) cells. *Exp Neurol.* **179**, 229-235

Galasko, D., Salmon, D., Craig, U.K. *et al.* (2000). The clinical spectrum of Guam ALS and Parkinson-dementia complex: 1997-1999. *Ann N Y Acad Sci.* **920**, 120-125

Galvani, V., Rupreht, R.R., Serbec, V.C. *et al.* (2005). Genetic risk factors associated with Creutzfeld-Jakob disease in Slovenians and a rapid typing for *PRNP* codon 129 single nucleotide polymorphism. *Transfus Med.* **15**, 197-207

Garofalo, O., Figlewicz, D.A., Leigh, P.N. *et al.* (1993). Androgen receptor gene polymorphisms in amyotrophic lateral sclerosis. *Neuromuscul Disord.* **3**, 195-199

Gatz, M., Reynolds, C.A., Fratiglioni, L. *et al.* (2006). Role of genes and environments for explaining Alzheimer disease. *Arch Gen Psychiatry.* **63**, 168-174

Gauthier, L.R., Charrin, B.C., Borrell-Pages, M. *et al.* (2004). Huntingtin controls neurotrophic support and survival of neurons by enhancing BDNF vesicular transport along microtubules. *Cell.* **118**, 127-138

Georgsson, G., Tryggvason, T., Jonasdottir, A.D. *et al.* (2006). Polymorphism of *PRNP* codons in the normal Icelandic population. *Acta Neurol Scand.* **113**, 419-425

Gepner, J., Li, M., Ludmann, S. *et al.* (1996). Cytoplasmic dynein function is essential in Drosophila melanogaster. *Genetics.* **142**, 865-878

Ghani, A.C., Donnelly, C.A., Ferguson, N.M. *et al.* (2003). Updated projections of future vCJD deaths in the UK. *BMC Infect Dis.* **3**, 4-

Gibbons, B.H., Asai, D.J., Tang, W.J. *et al.* (1994). Phylogeny and expression of axonemal and cytoplasmic dynein genes in sea urchins. *Mol Biol Cell.* **5**, 57-70

Gibbons, I.R. (1995). Dynein family of motor proteins: present status and future questions. *Cell Motil Cytoskeleton.* **32**, 136-144

Giess, R., Beck, M., Goetz, R. *et al.* (2000). Potential role of LIF as a modifier gene in the pathogenesis of amyotrophic lateral sclerosis. *Neurology.* **54**, 1003-1005

Giess, R., Holtmann, B., Braga, M. *et al.* (2002). Early onset of severe familial amyotrophic lateral sclerosis with a SOD-1 mutation: potential impact of CNTF as a candidate modifier gene. *Am J Hum Genet.* **70**, 1277-1286

Gloyn, A.L., Weedon, M.N., Owen, K.R. *et al.* (2003). Large-scale association studies of variants in genes encoding the pancreatic beta-cell KATP channel subunits Kir6.2 (KCNJ11) and SUR1 (ABCC8) confirm that the KCNJ11 E23K variant is associated with type 2 diabetes. *Diabetes.* **52**, 568-572

Goldgaber, D., Lerman, M.I., McBride O.W. *et al.* (1987). Characterization and chromosomal localization of a cDNA encoding brain amyloid of Alzheimer's disease. *Science.* **20,** 877-80.

Goldstein, D.B., Ahmadi, K.R., Weale, M.E. *et al.* (2003a). Genome scans and candidate gene approaches in the study of common diseases and variable drug responses. *Trends Genet.* **19**, 615-622

Goldstein, D.B. and Weale, M.E. (2003b). Weale ME and Goldstein DB, TagIT Version 1.17 http://popgen.biol.ucl.ac.uk/software.

Gong, W., Gottlieb, S., Collins, J. *et al.* (2001). Mutation analysis of TBX1 in non-deleted patients with features of DGS/VCFS or isolated cardiovascular defects. *J Med Genet.* **38**, E45-

Gonnet, G.H., Cohen, M.A., and Benner, S.A. (1992). Exhaustive matching of the entire protein sequence database. *Science*. **256**, 1443-1445

Gottesman, I.I. and Gould, T.D. (2003). The endophenotype concept in psychiatry: etymology and strategic intentions. *Am J Psychiatry*. **160**, 636-645

Graham, A.J., Macdonald, A.M., and Hawkes, C.H. (1997). British motor neuron disease twin study. *J Neurol Neurosurg Psychiatry*. **62**, 562-569

Greenway, M.J., Alexander, M.D., Ennis, S. *et al.* (2004). A novel candidate region for ALS on chromosome 14q11.2. *Neurology*. **63**, 1936-1938

Grissom, P.M., Vaisberg, E.A., and McIntosh, J.R. (2002). Identification of a novel light intermediate chain (D2LIC) for mammalian cytoplasmic dynein 2. *Mol Biol Cell*. **13**, 817-829

Gros-Louis, F., Lariviere, R., Gowing, G. *et al.* (2004). A frameshift deletion in peripherin gene associated with amyotrophic lateral sclerosis. *J Biol Chem*. **279**, 45951-45956

Guindon, S. and Gascuel, O. (2003). A simple, fast, and accurate algorithm to estimate large phylogenies by maximum likelihood. *Syst Biol*. **52**, 696-704

Guyant-Marechal, L., Rovelet-Lecrux, A., Goumidi, L. *et al.* (2007). Variations in the APP gene promoter region and risk of Alzheimer disease. *Neurology*. **68**, 684-687

Hacia, J.G., Fan, J.B., Ryder, O. *et al.* (1999). Determination of ancestral alleles for human single-nucleotide polymorphisms using high-density oligonucleotide arrays. *Nat Genet*. **22**, 164-167

Hadano, S., Hand, C.K., Osuga, H. *et al.* (2001). A gene encoding a putative GTPase regulator is mutated in familial amyotrophic lateral sclerosis 2. *Nat Genet*. **29**, 166-173

Hafezparast, M., Klocke, R., Ruhrberg, C. *et al.* (2003). Mutations in dynein link motor neuron degeneration to defects in retrograde transport. *Science*. **300**, 808-812

Hageman, G.S., Anderson, D.H., Johnson, L.V. *et al.* (2005). A common haplotype in the complement regulatory gene factor H (HF1/CFH) predisposes individuals to age-related macular degeneration. *Proc Natl Acad Sci U S A*. **102**, 7227-7232

Haines, J.L., Hauser, M.A., Schmidt, S. *et al.* (2005). Complement factor H variant increases the risk of age-related macular degeneration. *Science*. **308**, 419-421

Haldane, J. B. S, (1941). *New Paths in Genetics.* George Allen & Unwin, London, UK

Halldorsson, B.V., Istrail, S., and De La Vega, F.M. (2004). Optimal selection of SNP markers for disease association studies. *Hum Hered*. **58**, 190-202

Hamblin, M.T., Thompson, E.E., and Di Rienzo, A. (2002). Complex signatures of natural selection at the Duffy blood group locus. *Am J Hum Genet*. **70**, 369-383

Hand, C.K., Devon, R.S., Gros-Louis, F. *et al.* (2003). Mutation screening of the ALS2 gene in sporadic and familial amyotrophic lateral sclerosis. *Arch Neurol.* **60**, 1768-1771

Hand, C.K., Khoris, J., Salachas, F. *et al.* (2002). A novel locus for familial amyotrophic lateral sclerosis, on chromosome 18q. *Am J Hum Genet.* **70**, 251-256

Harada, A., Takei, Y., Kanai, Y. *et al.* (1998). Golgi vesiculation and lysosome dispersion in cells lacking cytoplasmic dynein. *J Cell Biol.* **141**, 51-59

Hardy, J. and Orr, H. (2006a). The genetics of neurodegenerative diseases. *J Neurochem.* **97**, 1690-1699

Hardy, J., Scholz, S., Evans, W. *et al.* (2006b). Prion genotypes in Central America suggest selection for the V129 allele. *Am J Med Genet B Neuropsychiatr Genet.* **141**, 33-35

Hartl, D. L. and Clark, A. G, (2007). *Principles of Population Genetics.* Fourth Edition. Sinauer Associates, Sunderland, Massachusetts

Harvey, C.B., Hollox, E.J., Poulter, M. *et al.* (1998). Lactase haplotype frequencies in Caucasians: association with the lactase persistence/non-persistence polymorphism. *Ann Hum Genet.* **62**, 215-223

Hattersley, A.T. and McCarthy, M.I. (2005). What makes a good genetic association study? *Lancet.* **366**, 1315-1323

Hayward, C., Colville, S., Swingler, R.J. *et al.* (1999). Molecular genetic analysis of the APEX nuclease gene in amyotrophic lateral sclerosis. *Neurology.* **52**, 1899-1901

Healy, D.G. (2006). Case-control studies in the genomic era: a clinician's guide. *Lancet Neurol.* **5**, 701-707

Hedrick, P. (2004). Estimation of relative fitnesses from relative risk data and the predicted future of haemoglobin alleles S and C. *J Evol Biol.* **17**, 221-224

Hedrick, P.W. (2003). A heterozygote advantage. *Science.* **302**, 57-

Heilig, R., Eckenberg, R., Petit, J.L. *et al.* (2003). The DNA sequence and analysis of human chromosome 14. *Nature.* **421**, 601-607

Henikoff, S. and Henikoff, J.G. (1993). Performance evaluation of amino acid substitution matrices. *Proteins.* **17**, 49-61

Hentati, A., Bejaoui, K., Pericak-Vance, M.A. *et al.* (1994). Linkage of recessive familial amyotrophic lateral sclerosis to chromosome 2q33-q35. *Nat Genet.* **7**, 425-428

Hentati, A., Ouahchi, K., Pericak-Vance, M.A. *et al.* (1998). Linkage of a commoner form of recessive amyotrophic lateral sclerosis to chromosome 15q15-q22 markers. *Neurogenetics.* **2**, 55-60

HGNC. (2004). HUGO Gene Nomenclature Committee synonym entry, http://www.gene.ucl.ac.uk/cgi-bin/nomenclature/get_data.pl?hgnc_id=2961. *HGNC database.*

Hill, A.F., Desbruslais, M., Joiner, S. *et al.* (1997). The same prion strain causes vCJD and BSE. *Nature.* **389**, 448-50, 526

Hirschhorn, J.N. and Daly, M.J. (2005). Genome-wide association studies for common diseases and complex traits. *Nat Rev Genet.* **6**, 95-108

Holleran, E.A., Karki, S., and Holzbaur, E.L. (1998). The role of the dynactin complex in intracellular motility. *Int Rev Cytol.* **182**, 69-109

Holzbaur, E.L. (2004). Motor neurons rely on motor proteins. *Trends Cell Biol.* **14**, 233-240

Honig, L.S., Chambliss, D.D., Bigio, E.H. *et al.* (2000). Glutamate transporter EAAT2 splice variants occur not only in ALS, but also in AD and controls. *Neurology.* **55**, 1082-1088

Horikawa, Y., Oda, N., Cox, N.J. *et al.* (2000). Genetic variation in the gene encoding calpain-10 is associated with type 2 diabetes mellitus. *Nat Genet.* **26**, 163-175

Hosking, L., Lumsden, S., Lewis, K. *et al.* (2004). Detection of genotyping errors by Hardy-Weinberg equilibrium testing. *Eur J Hum Genet.* **12**, 395-399

Hosler, B.A., Sapp, P.C., Berger, R. *et al.* (1998). Refined mapping and characterization of the recessive familial amyotrophic lateral sclerosis locus (ALS2) on chromosome 2q33. *Neurogenetics.* **2**, 34-42

Hosler, B.A., Siddique, T., Sapp, P.C. *et al.* (2000). Linkage of familial amyotrophic lateral sclerosis with frontotemporal dementia to chromosome 9q21-q22. *JAMA.* **284**, 1664-1669

Howie, B.N., Carlson, C.S., Rieder, M.J. *et al.* (2006). Efficient selection of tagging single-nucleotide polymorphisms in multiple populations. *Hum Genet.* **120**, 58-68

Hsiao, K., Baker, H.F., Crow, T.J. *et al.* (1989). Linkage of a prion protein missense variant to Gerstmann-Straussler syndrome. *Nature.* **338**, 342-345

Huang, X., Chen, P., Kaufer, D.I. *et al.* (2006). Apolipoprotein E and dementia in Parkinson disease: a meta-analysis. *Arch Neurol.* **63**, 189-193

Hubbard, T., Barker, D., Birney, E. *et al.* (2002). The Ensembl genome database project. *Nucleic Acids Res.* **30**, 38-41

Hughes, A.L., Packer, B., Welch, R. *et al.* (2003). Widespread purifying selection at polymorphic sites in human protein-coding loci. *Proc Natl Acad Sci U S A.* **100**, 15754-15757

Hughes, S.M., Vaughan, K.T., Herskovits, J.S. *et al.* (1995). Molecular analysis of a cytoplasmic dynein light intermediate chain reveals homology to a family of ATPases. *J Cell Sci.* **108**, 17-24

Hugot, J.P., Chamaillard, M., Zouali, H. *et al.* (2001). Association of NOD2 leucine-rich repeat variants with susceptibility to Crohn's disease. *Nature.* **411**, 599-603

Huttley, G.A., Smith, M.W., Carrington, M. *et al.* (1999). A scan for linkage disequilibrium across the human genome. *Genetics.* **152**, 1711-1722

Hutton, M., Lendon, C.L., Rizzu, P. *et al.* (1998). Association of missense and 5'-splice-site mutations in tau with the inherited dementia FTDP-17. *Nature.* **393**, 702-705

Ibanez, P., Bonnet, A.M., Debarges, B. *et al.* (2004). Causal relation between alpha-synuclein gene duplication and familial Parkinson's disease. *Lancet.* **364**, 1169-1171

International HapMap Consortium. (2003). The International HapMap Project. *Nature.* **426**, 789-796

Jablonka, S., Wiese, S., and Sendtner, M. (2004). Axonal defects in mouse models of motoneuron disease. *J Neurobiol.* **58**, 272-286

Jackson, G.S., Beck, J.A., Navarrete, C. *et al.* (2001). HLA-DQ7 antigen and resistance to variant CJD. *Nature.* **414**, 269-270

Jackson, M., Al Chalabi, A., Enayat, Z.E. *et al.* (1997). Copper/zinc superoxide dismutase 1 and sporadic amyotrophic lateral sclerosis: analysis of 155 cases and identification of a novel insertion mutation. *Ann Neurol.* **42**, 803-807

Jackson, M., Morrison, K.E., Al Chalabi, A. *et al.* (1996). Analysis of chromosome 5q13 genes in amyotrophic lateral sclerosis: homozygous NAIP deletion in a sporadic case. *Ann Neurol.* **39**, 796-800

Jackson, M., Steers, G., Leigh, P.N. *et al.* (1999). Polymorphisms in the glutamate transporter gene EAAT2 in European ALS patients. *J Neurol.* **246**, 1140-1144

Jaffrey, S.R. and Snyder, S.H. (1996). PIN: An Associated Protein Inhibitor of Neuronal Nitric Oxide Synthase. *Science.* **274**, 774-777

Jeffreys, A.J., Kauppi, L., and Neumann, R. (2001). Intensely punctate meiotic recombination in the class II region of the major histocompatibility complex. *Nat Genet.* **29**, 217-222

Jeong, B.H., Nam, J.H., Lee, Y.J. *et al.* (2004). Polymorphisms of the prion protein gene (*PRNP*) in a Korean population. *J Hum Genet.* **49**, 319-324

Jiang, J., Yu, L., Huang, X. *et al.* (2001). Identification of two novel human dynein light chain genes, DNLC2A and DNLC2B, and their expression changes in hepatocellular carcinoma tissues from 68 Chinese patients. *Gene.* **281**, 103-113

Johnson, G.C., Esposito, L., Barratt, B.J. *et al.* (2001). Haplotype tagging for the identification of common disease genes. *Nat Genet.* **29**, 233-237

Johnston, C.A., Stanton, B.R., Turner, M.R. *et al.* (2006). Amyotrophic lateral sclerosis in an urban setting: a population based study of inner city London. *J Neurol.* **253**, 1642-1643

Jones, C.T., Shaw, P.J., Chari, G. *et al.* (1994a). Identification of a novel exon 4 SOD1 mutation in a sporadic amyotrophic lateral sclerosis patient. *Mol Cell Probes.* **8**, 329-330

Jones, C.T., Swingler, R.J., and Brock, D.J. (1994b). Identification of a novel SOD1 mutation in an apparently sporadic amyotrophic lateral sclerosis patient and the detection of Ile113Thr in three others. *Hum Mol Genet.* **3**, 649-650

Jorde, L.B. (2000). Linkage disequilibrium and the search for complex disease genes. *Genome Res.* **10**, 1435-1444

Jorde, L.B., Watkins, W.S., and Bamshad, M.J. (2001). Population genomics: a bridge from evolutionary history to genetic medicine. *Hum Mol Genet.* **10**, 2199-2207

Julien, J.P., Cote, F., and Collard, J.F. (1995). Mice overexpressing the human neurofilament heavy gene as a model of ALS. *Neurobiol Aging.* **16**, 487-490

Kamatani, N., Sekine, A., Kitamoto, T. *et al.* (2004). Large-scale single-nucleotide polymorphism (SNP) and haplotype analyses, using dense SNP Maps, of 199 drug-related genes in 752 subjects: the analysis of the association between uncommon SNPs within haplotype blocks and the haplotypes constructed with haplotype-tagging SNPs. *Am J Hum Genet.* **75**, 190-203

Kamel, F., Umbach, D.M., Lehman, T.A. *et al.* (2003). Amyotrophic lateral sclerosis, lead, and genetic susceptibility: polymorphisms in the delta-aminolevulinic acid dehydratase and vitamin D receptor genes. *Environ Health Perspect.* **111**, 1335-1339

Kamel, F., Umbach, D.M., Munsat, T.L. *et al.* (2002). Lead exposure and amyotrophic lateral sclerosis. *Epidemiology.* **13**, 311-319

Karki, S. and Holzbaur, E.L. (1999). Cytoplasmic dynein and dynactin in cell division and intracellular transport. *Curr Opin Cell Biol.* **11**, 45-53

Karki, S., LaMonte, B., and Holzbaur, E.L. (1998). Characterization of the p22 subunit of dynactin reveals the localization of cytoplasmic dynein and dynactin to the midbody of dividing cells. *J Cell Biol.* **142**, 1023-1034

Kasperaviciute, D., Weale, M.E., Shianna, K.V. *et al.* (2007). Large-scale pathways-based association study in amyotrophic lateral sclerosis. *Brain.*

Ke, X., Hunt, S., Tapper, W. *et al.* (2004). The impact of SNP density on fine-scale patterns of linkage disequilibrium. *Hum Mol Genet.* **13**, 577-588

Kelley, J.L., Madeoy, J., Calhoun, J.C. *et al.* (2006). Genomic signatures of positive selection in humans and the limits of outlier approaches. *Genome Res.* **16**, 980-989

Khaja, R., Zhang, J., MacDonald, J.R. *et al.* (2006). Genome assembly comparison identifies structural variants in the human genome. *Nat Genet.* **38**, 1413-1418

Khoris, J., Boukaftane, Y., Moulard, B. *et al.* (1997). Familial amyotrophic lateral sclerosis associated with either homozygous or heterozygous Asp90Ala Cu/Zn-superoxide dismutase mutation. *Proceedings of the 8th International Symposium on ALS/MND, Abstract Booklet.* 46-

Kidd, J.R., Pakstis, A.J., Zhao, H. *et al.* (2000). Haplotypes and linkage disequilibrium at the phenylalanine hydroxylase locus, PAH, in a global representation of populations. *Am J Hum Genet.* **66**, 1882-1899

Kieran, D., Hafezparast, M., Bohnert, S. *et al.* (2005). A mutation in dynein rescues axonal transport defects and extends the life span of ALS mice. *J Cell Biol.* **169**, 561-567

Kimura, K. (1961). Endemiological and geomedical studies on amyotrophic lateral sclerosis and allied diseases in Kii Peninsula, Japan (preliminary report). *Folia Psychiatr Neurol Jpn.* **15**, 175-181

Kimura, M. (1968). Genetic variability maintained in a finite population due to mutational production of neutral and nearly neutral isoalleles. *Genet Res.* **11**, 247-269

Kimura, M. and Ota, T. (1973). The age of a neutral mutant persisting in a finite population. *Genetics.* **75**, 199-212

Kimura, M. and Ota, T. (1974). On some principles governing molecular evolution. *Proc Natl Acad Sci U S A.* **71**, 2848-2852

King, S.J. and Schroer, T.A. (2000). Dynactin increases the processivity of the cytoplasmic dynein motor. *Nat Cell Biol.* **2**, 20-24

King, S.M., Barbarese, E., Dillman, J.F., III *et al.* (1996b). Brain cytoplasmic and flagellar outer arm dyneins share a highly conserved Mr 8,000 light chain. *J Biol Chem.* **271**, 19358-19366

King, S.M., Barbarese, E., Dillman, J.F., III *et al.* (1996a). Brain cytoplasmic and flagellar outer arm dyneins share a highly conserved Mr 8,000 light chain. *J Biol Chem.* **271**, 19358-19366

King, S.M., Dillman, J.F., III, Benashski, S.E. *et al.* (1996c). The mouse t-complex-encoded protein Tctex-1 is a light chain of brain cytoplasmic dynein. *J Biol Chem.* **271**, 32281-32287

King, S.M. and Patel-King, R.S. (1995). The M(r) = 8,000 and 11,000 outer arm dynein light chains from Chlamydomonas flagella have cytoplasmic homologues. *J Biol Chem.* **270**, 11445-11452

Kingsbury, D.T., Kasper, K.C., Stites, D.P. *et al.* (1983). Genetic control of scrapie and Creutzfeldt-Jakob disease in mice. *J Immunol.* **131**, 491-496

Kitada, T., Asakawa, S., Hattori, N. *et al.* (1998). Mutations in the parkin gene cause autosomal recessive juvenile parkinsonism. *Nature.* **392**, 605-608

Klein, R.J., Zeiss, C., Chew, E.Y. *et al.* (2005). Complement Factor H Polymorphism in Age-Related Macular Degeneration. *Science.* **308**, 385-389

Kondo, K. (1996). Rising prevalence of neurodegenerative diseases worldwide. *Intern Med.* **35**, 238-

Kong, A., Gudbjartsson, D.F., Sainz, J. *et al.* (2002). A high-resolution recombination map of the human genome. *Nat Genet.* **31**, 241-247

Koonin, E.V. (2005). Orthologs, paralogs, and evolutionary genomics. *Annu Rev Genet.* **39**, 309-338

Koonin, E.V. and Aravind, L. (2000). Dynein light chains of the Roadblock/LC7 group belong to an ancient protein superfamily implicated in NTPase regulation. *Curr Biol.* **10**, R774-R776

Kowalska, A., Konagaya, M., Sakai, M. *et al.* (2003). Familial amyotrophic lateral sclerosis and parkinsonism-dementia complex--tauopathy without mutations in the tau gene? *Folia Neuropathol.* **41**, 59-64

Kozak, M. (1981). Possible role of flanking nucleotides in recognition of the AUG initiator codon by eukaryotic ribosomes. *Nucleic Acids Res.* **9**, 5233-5252

Kozak, M. (1984). Compilation and analysis of sequences upstream from the translational start site in eukaryotic mRNAs. *Nucleic Acids Res.* **12**, 857-872

Kozak, M. (1986). Point mutations define a sequence flanking the AUG initiator codon that modulates translation by eukaryotic ribosomes. *Cell.* **44**, 283-292

Kreitman, M. (2000). Methods to detect selection in populations with applications to the human. *Annu Rev Genomics Hum Genet.* **1**, 539-559

Kruglyak, L. (1999). Prospects for whole-genome linkage disequilibrium mapping of common disease genes. *Nat Genet.* **22**, 139-144

Kunst, C.B., Messer, L., Gordon, J. *et al.* (2000). Genetic mapping of a mouse modifier gene that can prevent ALS onset. *Genomics.* **70**, 181-189

Kutyavin, I.V., Afonina, I.A., Mills, A. *et al.* (2000). 3'-minor groove binder-DNA probes increase sequence specificity at PCR extension temperatures. *Nucleic Acids Res.* **28**, 655-661

Lader, E., Ha, H.S., O'Neill, M. *et al.* (1989). tctex-1: a candidate gene family for a mouse t complex sterility locus. *Cell.* **58**, 969-979

Lai, C.H., Chou, C.Y., Ch'ang, L.Y. *et al.* (2000). Identification of Novel Human Genes Evolutionarily Conserved in Caenorhabditis elegans by Comparative Proteomics. *Genome Res.* **10**, 703-713

Lambrechts, D., Storkebaum, E., Morimoto, M. *et al.* (2003). VEGF is a modifier of amyotrophic lateral sclerosis in mice and humans and protects motoneurons against ischemic death. *Nat Genet.* **34**, 383-394

LaMonte, B.H., Wallace, K.E., Holloway, B.A. *et al.* (2002). Disruption of dynein/dynactin inhibits axonal transport in motor neurons causing late-onset progressive degeneration. *Neuron.* **34**, 715-727

Lampe, J., Kitzler, H., Walter, M.C. *et al.* (1999). Methionine homozygosity at prion gene codon 129 may predispose to sporadic inclusion-body myositis. *Lancet.* **353**, 465-466

Lampe, J.B., Gossrau, G., Herting, B. *et al.* (2003). HLA typing and Parkinson's disease. *Eur Neurol.* **50**, 64-68

Lander, E.S. (1996). The new genomics: global views of biology. *Science.* **274**, 536-539

Lander, E.S. and Schork, N.J. (1994). Genetic dissection of complex traits. *Science.* **265**, 2037-2048

Laplanche, J.L., Delasnerie-Laupretre, N., Brandel, J.P. *et al.* (1994). Molecular genetics of prion diseases in France. French Research Group on Epidemiology of Human Spongiform Encephalopathies. *Neurology.* **44**, 2347-2351

Laplanche, J.L., Lepage, V., Peoc'h, K. *et al.* (2003). HLA in French patients with variant Creutzfeldt-Jakob disease. *Lancet.* **361**, 531-532

Laws, S.M., Hone, E., Gandy, S. *et al.* (2003). Expanding the association between the APOE gene and the risk of Alzheimer's disease: possible roles for APOE promoter polymorphisms and alterations in APOE transcription. *J Neurochem.* **84**, 1215-1236

Lee, H.S., Brown, P., Cervenakova, L. *et al.* (2001a). Increased susceptibility to Kuru of carriers of the *PRNP* 129 methionine/methionine genotype. *J Infect Dis.* **183**, 192-196

Lee, N., Daly, M.J., Delmonte, T. *et al.* (2001b). A genomewide linkage-disequilibrium scan localizes the Saguenay-Lac-Saint-Jean cytochrome oxidase deficiency to 2p16. *Am J Hum Genet.* **68**, 397-409

Lee, W.C. (2003). Searching for disease-susceptibility loci by testing for Hardy-Weinberg disequilibrium in a gene bank of affected individuals. *Am J Epidemiol.* **158**, 397-400

Lehmann, D.J., Barnardo, M.C., Fuggle, S. *et al.* (2006). Replication of the association of HLA-B7 with Alzheimer's disease: a role for homozygosity? *J Neuroinflammation.* **3**, 33-

Lesage, S., Durr, A., Tazir, M. *et al.* (2006). LRRK2 G2019S as a cause of Parkinson's disease in North African Arabs. *N Engl J Med.* **354**, 422-423

Leung, C.L., He, C.Z., Kaufmann, P. *et al.* (2004). A pathogenic peripherin gene mutation in a patient with amyotrophic lateral sclerosis. *Brain Pathol.* **14**, 290-296

Li, Y.J., Hauser, M.A., Scott, W.K. *et al.* (2004). Apolipoprotein E controls the risk and age at onset of Parkinson disease. *Neurology.* **62**, 2005-2009

Li, Y.J., Scott, W.K., Hedges, D.J. *et al.* (2002). Age at onset in two common neurodegenerative diseases is genetically controlled. *Am J Hum Genet.* **70**, 985-993

Liao, L., Cheng, D., Wang, J. *et al.* (2004). Proteomic characterization of postmortem amyloid plaques isolated by laser capture microdissection. *J Biol Chem.* **279**, 37061-37068

Ligon, L.A., LaMonte, B.H., Wallace, K.E. *et al.* (2005). Mutant superoxide dismutase disrupts cytoplasmic dynein in motor neurons. *Neuroreport.* **16**, 533-536

Lin, C.L., Bristol, L.A., Jin, L. *et al.* (1998). Aberrant RNA processing in a neurodegenerative disease: the cause for absent EAAT2, a glutamate transporter, in amyotrophic lateral sclerosis. *Neuron.* **20**, 589-602

Lin, F.H., Lin, R., Wisniewski, H.M. *et al.* (1992). Detection of point mutations in codon 331 of mitochondrial NADH dehydrogenase subunit 2 in Alzheimer's brains. *Biochem Biophys Res Commun.* **182**, 238-246

Lin, S., Chakravarti, A., and Cutler, D.J. (2004). Exhaustive allelic transmission disequilibrium tests as a new approach to genome-wide association studies. *Nat Genet.* **36**, 1181-1188

Liu, Z., Lin, S., and Tan, M. (2006). Genome-wide tagging SNPs with entropy-based Monte Carlo method. *J Comput Biol.* **13**, 1606-1614

Livak, K.J. and Schmittgen, T.D. (2001). Analysis of relative gene expression data using real-time quantitative PCR and the 2(-Delta Delta C(T)) Method. *Methods.* **25**, 402-408

Lloyd, S.E. and Collinge, J. (2005). Genetic Susceptibility to Prion Diseases in Humans and Mice. *Current Genomics.* **6**, 1-11

Lloyd, S.E., Onwuazor, O.N., Beck, J.A. *et al.* (2001). Identification of multiple quantitative trait loci linked to prion disease incubation period in mice. *Proc Natl Acad Sci U S A.* **98**, 6279-6283

Lloyd, S.E., Thompson, S.R., Beck, J.A. *et al.* (2004). Identification and characterization of a novel mouse prion gene allele. *Mamm Genome.* **15**, 383-389

Lloyd, S.E., Uphill, J.B., Targonski, P.V. *et al.* (2002). Identification of genetic loci affecting mouse-adapted bovine spongiform encephalopathy incubation time in mice. *Neurogenetics.* **4**, 77-81

Lohmueller, K.E., Pearce, C.L., Pike, M. *et al.* (2003). Meta-analysis of genetic association studies supports a contribution of common variants to susceptibility to common disease. *Nat Genet.* **33**, 177-182

Lucking, C.B., Bonifati, V., Periquet, M. *et al.* (2001). Pseudo-dominant inheritance and exon 2 triplication in a family with parkin gene mutations. *Neurology.* **57**, 924-927

Lucotte, G. and Mercier, G. (2005). The population distribution of the Met allele at the *PRNP*129 polymorphism (a high risk factor for Creutzfeldt-Jakob disease) in various regions of France and in West Europe. *Infect Genet Evol.* **5**, 141-144

Lunin, V.V., Munger, C., Wagner, J. *et al.* (2004). The structure of the MAPK scaffold, MP1, bound to its partner, p14. A complex with a critical role in endosomal map kinase signaling. *J Biol Chem.* **279**, 23422-23430

Lupski, J.R., Oca-Luna, R.M., Slaugenhaupt, S. *et al.* (1991). DNA duplication associated with Charcot-Marie-Tooth disease type 1A. *Cell.* **66**, 219-232

MacGregor, A.J., Snieder, H., Schork, N.J. *et al.* (2000). Twins. Novel uses to study complex traits and genetic diseases. *Trends Genet.* **16**, 131-134

Mahal, S.P., Asante, E.A., Antoniou, M. *et al.* (2001). Isolation and functional characterisation of the promoter region of the human prion protein gene. *Gene.* **268**, 105-114

Majoor-Krakauer, D., Ottman, R., Johnson, W.G. *et al.* (1994). Familial aggregation of amyotrophic lateral sclerosis, dementia, and Parkinson's disease: evidence of shared genetic susceptibility. *Neurology.* **44**, 1872-1877

Mallucci, G., Dickinson, A., Linehan, J. *et al.* (2003). Depleting neuronal PrP in prion infection prevents disease and reverses spongiosis. *Science.* **302**, 871-874

Mallucci, G.R., White, M.D., Farmer, M. *et al.* (2007). Targeting cellular prion protein reverses early cognitive deficits and neurophysiological dysfunction in prion-infected mice. *Neuron.* **53**, 325-335

Maltais, L.J., Blake, J.A., Eppig, J.T. *et al.* (1997). Rules and guidelines for mouse gene nomenclature: a condensed version. International Committee on Standardized Genetic Nomenclature for Mice. *Genomics.* **45**, 471-476

Mandich, P., Di Maria, E., Bellone, E. *et al.* (1996). Molecular analysis of the IT15 gene in patients with apparently 'sporadic' Huntington's disease. *Eur Neurol.* **36**, 348-352

Manfredi, G. and Beal, M.F. (2000). The role of mitochondria in the pathogenesis of neurodegenerative diseases. *Brain Pathol.* **10**, 462-472

Mann, V., Hobson, E.E., Li, B. *et al.* (2001). A COL1A1 Sp1 binding site polymorphism predisposes to osteoporotic fracture by affecting bone density and quality. *J Clin Invest.* **107**, 899-907

Mann, V. and Ralston, S.H. (2003). Meta-analysis of COL1A1 Sp1 polymorphism in relation to bone mineral density and osteoporotic fracture. *Bone.* **32**, 711-717

Manolakou, K., Beaton, J., McConnell, I. *et al.* (2001). Genetic and environmental factors modify bovine spongiform encephalopathy incubation period in mice. *Proc Natl Acad Sci U S A.* **98**, 7402-7407

Manson, J., West, J.D., Thomson, V. *et al.* (1992). The prion protein gene: a role in mouse embryogenesis? *Development.* **115**, 117-122

Marenholz, I., Heizmann, C.W., and Fritz, G. (2004). S100 proteins in mouse and man: from evolution to function and pathology (including an update of the nomenclature). *Biochem Biophys Res Commun.* **322**, 1111-1122

Marron, M.P., Raffel, L.J., Garchon, H.J. *et al.* (1997). Insulin-dependent diabetes mellitus (IDDM) is associated with CTLA4 polymorphisms in multiple ethnic groups. *Hum Mol Genet.* **6**, 1275-1282

Masters, C.L., Harris, J.O., Gajdusek, D.C. *et al.* (1979). Creutzfeldt-Jakob disease: patterns of worldwide occurrence and the significance of familial and sporadic clustering. *Ann Neurol.* **5**, 177-188

Masu, Y., Wolf, E., Holtmann, B. *et al.* (1993). Disruption of the CNTF gene results in motor neuron degeneration. *Nature.* **365**, 27-32

Mateu, E., Calafell, F., Lao, O. *et al.* (2001). Worldwide genetic analysis of the CFTR region. *Am J Hum Genet.* **68**, 103-117

Mawrin, C., Kirches, E., and Dietzmann, K. (2003). Single-cell analysis of mtDNA in amyotrophic lateral sclerosis: towards the characterization of individual neurons in neurodegenerative disorders. *Pathol Res Pract.* **199**, 415-418

Mawrin, C., Kirches, E., Krause, G. *et al.* (2004). Single-cell analysis of mtDNA deletion levels in sporadic amyotrophic lateral sclerosis. *Neuroreport.* **15**, 939-943

McCormack, J.E., Baybutt, H.N., Everington, D. *et al.* (2002). *PRNP* contains both intronic and upstream regulatory regions that may influence susceptibility to Creutzfeldt-Jakob Disease. *Gene.* **288**, 139-146

McDermott, C.J., Roberts, D., Tomkins, J. *et al.* (2003). Spastin and paraplegin gene analysis in selected cases of motor neurone disease (MND). *Amyotroph Lateral Scler Other Motor Neuron Disord.* **4**, 96-99

McGowan, J.P. (1922). Scrapie in sheep. *Scott J Agric.* **5**, 365-375

Mead, S. (2002). Molecular Genetic Analysis of the Prion Protein Gene in Human Prion Disease.

Mead, S. (2006). Prion disease genetics. *Eur J Hum Genet.* **14**, 273-281

Mead, S., Beck, J., Dickinson, A. *et al.* (2000). Examination of the human prion protein-like gene doppel for genetic susceptibility to sporadic and variant Creutzfeldt-Jakob disease. *Neurosci Lett.* **290**, 117-120

Mead, S., Mahal, S.P., Beck, J. *et al.* (2001). Sporadic--but not variant--Creutzfeldt-Jakob disease is associated with polymorphisms upstream of *PRNP* exon 1. *Am J Hum Genet.* **69**, 1225-1235

Mead, S., Shah, P., Whitfield, J. *et al.* (2007). A novel protective prion protein variant co-localises with kuru exposure. *Nature.* In press

Mead, S., Stumpf, M.P., Whitfield, J. *et al.* (2003). Balancing selection at the prion protein gene consistent with prehistoric kurulike epidemics. *Science.* **300**, 640-643

Mesngon, M.T., Tarricone, C., Hebbar, S. *et al.* (2006). Regulation of cytoplasmic dynein ATPase by Lis1. *J Neurosci.* **26**, 2132-2139

Meyer, D., Single, R.M., Mack, S.J. *et al.* (2006). Signatures of demographic history and natural selection in the human major histocompatibility complex Loci. *Genetics.* **173**, 2121-2142

Meyer, M.A. and Potter, N.T. (1995). Sporadic ALS and chromosome 22: evidence for a possible neurofilament gene defect. *Muscle Nerve.* **18**, 536-539

Meyer, T., Fromm, A., Munch, C. *et al.* (1999). The RNA of the glutamate transporter EAAT2 is variably spliced in amyotrophic lateral sclerosis and normal individuals. *J Neurol Sci.* **170**, 45-50

Meyer, T., Munch, C., Volkel, H. *et al.* (1998). The EAAT2 (GLT-1) gene in motor neuron disease: absence of mutations in amyotrophic lateral sclerosis and a point mutation in patients with hereditary spastic paraplegia. *J Neurol Neurosurg Psychiatry.* **65**, 594-596

Meyer, T., Schwan, A., Dullinger, J.S. *et al.* (2005). Early-onset ALS with long-term survival associated with spastin gene mutation. *Neurology.* **65**, 141-143

MGI. (2004). Dnch1 MGI Entry: mKIAA0325 synonym. *Mouse Genome Informatics.*

Mikami, A., Paschal, B.M., Mazumdar, M. *et al.* (1993). Molecular cloning of the retrograde transport motor cytoplasmic dynein (MAP 1C). *Neuron.* **10**, 787-796

Mikami, A., Tynan, S.H., Hama, T. *et al.* (2002a). Molecular structure of cytoplasmic dynein 2 and its distribution in neuronal and ciliated cells. *J Cell Sci.* **115**, 4801-4808

Mikami, A., Tynan, S.H., Hama, T. *et al.* (2002b). Molecular structure of cytoplasmic dynein 2 and its distribution in neuronal and ciliated cells. *J Cell Sci.* **115**, 4801-4808

Miki, H., Okada, Y., and Hirokawa, N. (2005). Analysis of the kinesin superfamily: insights into structure and function. *Trends Cell Biol.* **15**, 467-476

Miller, R.G., Munsat, T.L., Swash, M. *et al.* (1999). Consensus guidelines for the design and implementation of clinical trials in ALS. World Federation of Neurology committee on Research. *J Neurol Sci.* **169**, 2-12

Mitchell, D.R. and Kang, Y. (1991). Identification of oda6 as a Chlamydomonas dynein mutant by rescue with the wild-type gene. *J Cell Biol.* **113**, 835-842

Mitrova, E., Mayer, V., Jovankovicova, V. *et al.* (2005). Creutzfeldt-Jakob disease risk and *PRNP* codon 129 polymorphism: necessity to revalue current data. *Eur J Neurol.* **12**, 998-1001

Moreno, C.R., Lantier, F., Lantier, I. *et al.* (2003). Detection of new quantitative trait Loci for susceptibility to transmissible spongiform encephalopathies in mice. *Genetics.* **165**, 2085-2091

Morgenstern, B., Rinner, O., Abdeddaim, S. *et al.* (2002). Exon discovery by genomic sequence alignment. *Bioinformatics.* **18**, 777-787

Morita, M., Al Chalabi, A., Andersen, P.M. *et al.* (2006). A locus on chromosome 9p confers susceptibility to ALS and frontotemporal dementia. *Neurology.* **66**, 839-844

Moulard, B., Sefiani, A., Laamri, A. *et al.* (1996). Apolipoprotein E genotyping in sporadic amyotrophic lateral sclerosis: evidence for a major influence on the clinical presentation and prognosis. *J Neurol Sci.* **139 Suppl**, 34-37

Mount, S.M. (1982). A catalogue of splice junction sequences. *Nucleic Acids Res.* **10**, 459-472

Mouse Genome Informatics. (2004). Mouse Genome Database (MGD), Mouse Genome Informatics Web Site, The Jackson Laboratory, Bar Harbor, Maine. World Wide Web (URL: http://www.informatics.jax.org). Data Retrieved March, 2004,

Mueller, S., Cao, X., Welker, R. *et al.* (2002). Interaction of the poliovirus receptor CD155 with the dynein light chain Tctex-1 and its implication for poliovirus pathogenesis. *J Biol Chem.* **277**, 7897-7904

Mui, S., Rebeck, G.W., McKenna-Yasek, D. *et al.* (1995). Apolipoprotein E epsilon 4 allele is not associated with earlier age at onset in amyotrophic lateral sclerosis. *Ann Neurol.* **38**, 460-463

Munch, C., Rosenbohm, A., Sperfeld, A.D. *et al.* (2005). Heterozygous R1101K mutation of the DCTN1 gene in a family with ALS and FTD. *Ann Neurol.* **58**, 777-780

Munch, C., Sedlmeier, R., Meyer, T. *et al.* (2004). Point mutations of the p150 subunit of dynactin (DCTN1) gene in ALS. *Neurology.* **63**, 724-726

Myers, R.H., MacDonald, M.E., Koroshetz, W.J. *et al.* (1993). De novo expansion of a (CAG)n repeat in sporadic Huntington's disease. *Nat Genet.* **5**, 168-173

Nagase, T., Ishikawa, K., Nakajima, D. *et al.* (1997). Prediction of the coding sequences of unidentified human genes. VII. The complete sequences of 100 new cDNA clones from brain which can code for large proteins in vitro. *DNA Res.* **4**, 141-150

Naisbitt, S., Valtschanoff, J., Allison, D.W. *et al.* (2000b). Interaction of the postsynaptic density-95/guanylate kinase domain-associated protein complex with a light chain of myosin-V and dynein. *J Neurosci.* **20**, 4524-4534

Naisbitt, S., Valtschanoff, J., Allison, D.W. *et al.* (2000a). Interaction of the postsynaptic density-95/guanylate kinase domain-associated protein complex with a light chain of myosin-V and dynein. *J Neurosci.* **20**, 4524-4534

Narayan, D., Desai, T., Banks, A. *et al.* (1994). Localization of the human cytoplasmic dynein heavy chain (DNECL) to 14qter by fluorescence in situ hybridization. *Genomics.* **22**, 660-661

NCBI. (2004a). D2LIC GenBank entry: LIC3, CGI-60, DKFZP564A033 synonyms. *GenBank.*

NCBI. (2004b). Dlc2 GenBank Entry: 6720463E02Rik and 1700064A15Rik synonym. *GenBank.*

NCBI. (2004c). Dlc2 GenBank Entry: MGC17810 synonym. *GenBank.*

NCBI. (2004d). DNCL2A GenBank Entry: MGC15113 synonym. *GenBank.*

NCBI. (2004e). DNCLI1 LocusLink Entry: Dynein Light Chain A synonym. *NCBI LocusLink.*

NCBI. (2004f). Dnclic1 GenBank Entry: MGC32416 synonym. *GenBank.*

NCBI. (2004g). Mouse D2LIC entry: D2LIC, mD2LIC, MGC7211, MGC40646, 4933404O11Rik synonyms. *GenBank.*

NCBI: Online Citation assigned by submitter. (1998). http://www.ncbi.nlm.nih.gov/entrez/viewer.fcgi?db=nucleotide&val=31743626&txt=on.

Nebert, D.W., Sophos, N.A., Vasiliou, V. *et al.* (2004). Cyclophilin nomenclature problems, or, 'a visit from the sequence police'. *Hum Genomics.* **1**, 381-388

Nebert, D.W. and Wain, H.M. (2003). Update on human genome completion and annotations: gene nomenclature. *Hum Genomics.* **1**, 66-71

Neel, J.V. (1962). Diabetes mellitus: A "thrifty" genotype rendered detrimental by "progress"? *Am J Hum Genet.* **14**, 353-362

Neesen, J., Koehler, M.R., Kirschner, R. *et al.* (1997). Identification of dynein heavy chain genes expressed in human and mouse testis: chromosomal localization of an axonemal dynein gene. *Gene.* **200**, 193-202

Nei, M., Xu, P., and Glazko, G. (2001). Estimation of divergence times from multiprotein sequences for a few mammalian species and several distantly related organisms. *Proc Natl Acad Sci U S A.* **98**, 2497-2502

Nelson, L.M. (1995). Epidemiology of ALS. *Clin Neurosci.* **3**, 327-331

Nicholl, D.J., Bennett, P., Hiller, L. *et al.* (1999). A study of five candidate genes in Parkinson's disease and related neurodegenerative disorders. European Study Group on Atypical Parkinsonism. *Neurology.* **53**, 1415-1421

Nielsen, D.M., Ehm, M.G., and Weir, B.S. (1998). Detecting marker-disease association by testing for Hardy-Weinberg disequilibrium at a marker locus. *Am J Hum Genet.* **63**, 1531-1540

Nielsen, R. (2001). Statistical tests of selective neutrality in the age of genomics. *Heredity.* **86**, 641-647

Nielsen, R., Williamson, S., Kim, Y. *et al.* (2005). Genomic scans for selective sweeps using SNP data. *Genome Res.* **15**, 1566-1575

Nikulina, K., Patel-King, R.S., Takebe, S. *et al.* (2004). The roadblock light chains are ubiquitous components of cytoplasmic dynein that form homo- and heterodimers. *Cell Motil Cytoskeleton.* **57**, 233-245

Nishimura, A.L., Mitne-Neto, M., Silva, H.C. *et al.* (2004a). A novel locus for late onset amyotrophic lateral sclerosis/motor neurone disease variant at 20q13. *J Med Genet.* **41**, 315-320

Nishimura, A.L., Mitne-Neto, M., Silva, H.C. *et al.* (2004b). A mutation in the vesicle-trafficking protein VAPB causes late-onset spinal muscular atrophy and amyotrophic lateral sclerosis. *Am J Hum Genet.* **75**, 822-831

Nishioka, K., Hayashi, S., Farrer, M.J. *et al.* (2006). Clinical heterogeneity of alpha-synuclein gene duplication in Parkinson's disease. *Ann Neurol.* **59**, 298-309

Nistico, L., Buzzetti, R., Pritchard, L.E. *et al.* (1996). The CTLA-4 gene region of chromosome 2q33 is linked to, and associated with, type 1 diabetes. Belgian Diabetes Registry. *Hum Mol Genet.* **5**, 1075-1080

Nixon, R.A. (2005). Endosome function and dysfunction in Alzheimer's disease and other neurodegenerative diseases. *Neurobiol Aging.* **26**, 373-382

Noonan, C.W., White, M.C., Thurman, D. *et al.* (2005). Temporal and geographic variation in United States motor neuron disease mortality, 1969-1998. *Neurology.* **64**, 1215-1221

Nurmi, M.H., Bishop, M., Strain, L. *et al.* (2003). The normal population distribution of *PRNP* codon 129 polymorphism. *Acta Neurol Scand.* **108**, 374-378

Oesch, B., Westaway, D., Walchli, M. *et al.* (1985). A cellular gene encodes scrapie PrP 27-30 protein. *Cell.* **40**, 735-746

Ohara, O., Nagase, T., Ishikawa, K. *et al.* (1997). Construction and characterization of human brain cDNA libraries suitable for analysis of cDNA clones encoding relatively large proteins. *DNA Res.* **4**, 53-59

Ohkubo, T., Sakasegawa, Y., Asada, T. *et al.* (2003). Absence of association between codon 129/219 polymorphisms of the prion protein gene and Alzheimer's disease in Japan. *Ann Neurol.* **54**, 553-554

Okazaki, N., Kikuno, R., Ohara, R. *et al.* (2003). Prediction of the coding sequences of mouse homologues of KIAA gene: II. The complete nucleotide sequences of 400 mouse KIAA-homologous cDNAs identified by screening of terminal sequences of cDNA clones randomly sampled from size-fractionated libraries. *DNA Res.* **10**, 35-48

Online Citation assigned by submitter. (1998). http://www.ncbi.nlm.nih.gov/entrez/viewer.fcgi?db=nucleotide&val=31744556&txt=on.

Oosthuyse, B., Moons, L., Storkebaum, E. *et al.* (2001). Deletion of the hypoxia-response element in the vascular endothelial growth factor promoter causes motor neuron degeneration. *Nat Genet.* **28**, 131-138

Orrell, R.W., Habgood, J.J., de Belleroche, J.S. *et al.* (1997a). The relationship of spinal muscular atrophy to motor neuron disease: investigation of SMN and NAIP gene deletions in sporadic and familial ALS. *J Neurol Sci.* **145**, 55-61

Orrell, R.W., Habgood, J.J., Gardiner, I. *et al.* (1997b). Clinical and functional investigation of 10 missense mutations and a novel frameshift insertion mutation of the gene for copper-zinc superoxide dismutase in UK families with amyotrophic lateral sclerosis. *Neurology.* **48**, 746-751

Orrell, R.W., King, A.W., Lane, R.J. *et al.* (1995). Investigation of a null mutation of the CNTF gene in familial amyotrophic lateral sclerosis. *J Neurol Sci.* **132**, 126-128

Orru, S., Mascia, V., Casula, M. *et al.* (1999). Association of monoamine oxidase B alleles with age at onset in amyotrophic lateral sclerosis. *Neuromuscul Disord.* **9**, 593-597

Orth, M., Tabrizi, S.J., and Schapira, A.H. (2000). Sporadic inclusion body myositis not linked to prion protein codon 129 methionine homozygosity. *Neurology.* **55**, 1235-

Ota, T., Suzuki, Y., Nishikawa, T. *et al.* (2004). Complete sequencing and characterization of 21,243 full-length human cDNAs. *Nat Genet.* **36**, 40-45

Owen, F., Poulter, M., Lofthouse, R. *et al.* (1989). Insertion in prion protein gene in familial Creutzfeldt-Jakob disease. *Lancet.* **1**, 51-52

Page, R.D.M. (1996). TREEVIEW: An application to display phylogenetic trees on personal computers. *Computer Applications in the Biosciences*. **12**, 357-358

Palmer, M.S., Dryden, A.J., Hughes, J.T. *et al.* (1991). Homozygous prion protein genotype predisposes to sporadic Creutzfeldt-Jakob disease. *Nature*. **352**, 340-342

Pamilo, P. and Nei, M. (1988). Relationships between gene trees and species trees. *Mol Biol Evol*. **5**, 568-583

Panas, M., Karadima, G., Kalfakis, N. *et al.* (2000). Genotyping of presenilin-1 polymorphism in amyotrophic lateral sclerosis. *J Neurol*. **247**, 940-942

Parboosingh, J.S., Meininger, V., McKenna-Yasek, D. *et al.* (1999). Deletions causing spinal muscular atrophy do not predispose to amyotrophic lateral sclerosis. *Arch Neurol*. **56**, 710-712

Pardi, F., Lewis, C.M., and Whittaker, J.C. (2005). SNP selection for association studies: maximizing power across SNP choice and study size. *Ann Hum Genet*. **69**, 733-746

Parkinson, N., Ince, P.G., Smith, M.O. *et al.* (2006). ALS phenotypes with mutations in CHMP2B (charged multivesicular body protein 2B). *Neurology*. **67**, 1074-1077

Parsian, A., Racette, B., Goldsmith, L.J. *et al.* (2002). Parkinson's disease and apolipoprotein E: possible association with dementia but not age at onset. *Genomics*. **79**, 458-461

Parton, M.J., Broom, W., Andersen, P.M. *et al.* (2002). D90A-SOD1 mediated amyotrophic lateral sclerosis: a single founder for all cases with evidence for a Cis-acting disease modifier in the recessive haplotype. *Hum Mutat*. **20**, 473-

Paschal, B.M., Mikami, A., Pfister, K.K. *et al.* (1992b). Homology of the 74-kD cytoplasmic dynein subunit with a flagellar dynein polypeptide suggests an intracellular targeting function. *J Cell Biol*. **118**, 1133-1143

Paschal, B.M., Mikami, A., Pfister, K.K. *et al.* (1992a). Homology of the 74-kD cytoplasmic dynein subunit with a flagellar dynein polypeptide suggests an intracellular targeting function. *J Cell Biol*. **118**, 1133-1143

Paschal, B.M. and Vallee, R.B. (1987). Retrograde transport by the microtubule-associated protein MAP 1C. *Nature*. **330**, 181-183

Patil, N., Berno, A.J., Hinds, D.A. *et al.* (2001). Blocks of limited haplotype diversity revealed by high-resolution scanning of human chromosome 21. *Science*. **294**, 1719-1723

Pazour, G.J., Wilkerson, C.G., and Witman, G.B. (1998). A dynein light chain is essential for the retrograde particle movement of intraflagellar transport (IFT). *J Cell Biol*. **141**, 979-992

Peltonen, L., Palotie, A., and Lange, K. (2000). Use of population isolates for mapping complex traits. *Nat Rev Genet*. **1**, 182-190

Pennisi, E. (1999). Keeping genome databases clean and up to date. *Science*. **286**, 447-450

Pepys, M.B., Bybee, A., Booth, D.R. *et al.* (2003). MHC typing in variant Creutzfeldt-Jakob disease. *Lancet*. **361**, 487-489

Petrucelli, L. and Dawson, T.M. (2004). Mechanism of neurodegenerative disease: role of the ubiquitin proteasome system. *Ann Med*. **36**, 315-320

Pfister, K.K., Fisher, E.M., Gibbons, I.R. *et al.* (2005a). Cytoplasmic dynein nomenclature. *J Cell Biol*. **171**, 411-413

Pfister, K.K., Hummerich, H., King, S.M. *et al.* (2005b). Mammalian cytoplasmic dyneins: subunits, genetics and molecular phylogeny. *J Cell Biol*.

Piontkivska, H., Rooney, A.P., and Nei, M. (2002). Purifying selection and birth-and-death evolution in the histone H4 gene family. *Mol Biol Evol*. **19**, 689-697

Plaitakis, A., Viskadouraki, A.K., Tzagournissakis, M. *et al.* (2001). Increased incidence of sporadic Creutzfeldt-Jakob disease on the island of Crete associated with a high rate of *PRNP* 129-methionine homozygosity in the local population. *Ann Neurol*. **50**, 227-233

Polymeropoulos, M.H., Higgins, J.J., Golbe, L.I. *et al.* (1996). Mapping of a gene for Parkinson's disease to chromosome 4q21-q23. *Science*. **274**, 1197-1199

Poorkaj, P., Tsuang, D., Wijsman, E. *et al.* (2001). TAU as a susceptibility gene for amyotropic lateral sclerosis-parkinsonism dementia complex of Guam. *Arch Neurol*. **58**, 1871-1878

Porter, M.E., Bower, R., Knott, J.A. *et al.* (1999). Cytoplasmic Dynein Heavy Chain 1b Is Required for Flagellar Assembly in Chlamydomonas. *Molecular Biology of the Cell*. **10**, 693-712

Poulter, M., Baker, H.F., Frith, C.D. *et al.* (1992). Inherited prion disease with 144 base pair gene insertion. 1. Genealogical and molecular studies. *Brain*. **115**, 675-685

Pritchard, J.K. (2001). Are rare variants responsible for susceptibility to complex diseases? *Am J Hum Genet*. **69**, 124-137

Pritchard, J.K. and Cox, N.J. (2002). The allelic architecture of human disease genes: common disease-common variant...or not? *Hum Mol Genet*. **11**, 2417-2423

Pritchard, J.K. and Przeworski, M. (2001). Linkage disequilibrium in humans: models and data. *Am J Hum Genet*. **69**, 1-14

Prusiner, S.B. (1982). Novel proteinaceous infectious particles cause scrapie. *Science*. **216**, 136-144

Prusiner, S.B., Scott, M., Foster, D. *et al.* (1990). Transgenetic studies implicate interactions between homologous PrP isoforms in scrapie prion replication. *Cell*. **63**, 673-686

Puckett, C., Concannon, P., Casey, C. *et al.* (1991). Genomic structure of the human prion protein gene. *Am J Hum Genet.* **49**, 320-329

Puls, I., Jonnakuty, C., LaMonte, B.H. *et al.* (2003). Mutant dynactin in motor neuron disease. *Nat Genet.* **33**, 455-456

Puls, I., Oh, S.J., Sumner, C.J. *et al.* (2005). Distal spinal and bulbar muscular atrophy caused by dynactin mutation. *Ann Neurol.* **57**, 687-694

Purcell, S., Cherny, S.S., and Sham, P.C. (2003). Genetic Power Calculator: design of linkage and association genetic mapping studies of complex traits. *Bioinformatics.* **19**, 149-150

Qin, Z.S., Niu, T., and Liu, J.S. (2002). Partition-ligation-expectation-maximization algorithm for haplotype inference with single-nucleotide polymorphisms. *Am J Hum Genet.* **71**, 1242-1247

Quackenbush, J., Cho, J., Lee, D. *et al.* (2001). The TIGR Gene Indices: analysis of gene transcript sequences in highly sampled eukaryotic species. *Nucleic Acids Res.* **29**, 159-164

Rao, M.V. and Nixon, R.A. (2003). Defective neurofilament transport in mouse models of amyotrophic lateral sclerosis: a review. *Neurochem Res.* **28**, 1041-1047

Redon, R., Ishikawa, S., Fitch, K.R. *et al.* (2006). Global variation in copy number in the human genome. *Nature.* **444**, 444-454

Reich, D.E., Cargill, M., Bolk, S. *et al.* (2001a). Linkage disequilibrium in the human genome. *Nature.* **411**, 199-204

Reich, D.E. and Lander, E.S. (2001b). On the allelic spectrum of human disease. *Trends Genet.* **17**, 502-510

Reuter, J.E., Nardine, T.M., Penton, A. *et al.* (2003). A mosaic genetic screen for genes necessary for Drosophila mushroom body neuronal morphogenesis. *Development.* **130**, 1203-1213

Riemenschneider, M., Klopp, N., Xiang, W. *et al.* (2004). Prion protein codon 129 polymorphism and risk of Alzheimer disease. *Neurology.* **63**, 364-366

Rioux, J.D., Daly, M.J., Silverberg, M.S. *et al.* (2001). Genetic variation in the 5q31 cytokine gene cluster confers susceptibility to Crohn disease. *Nat Genet.* **29**, 223-228

Risch, N., De Leon, D., Ozelius, L. *et al.* (1995). Genetic analysis of idiopathic torsion dystonia in Ashkenazi Jews and their recent descent from a small founder population. *Nat Genet.* **9**, 152-159

Risch, N.J. (2000). Searching for genetic determinants in the new millennium. *Nature.* **405**, 847-856

Risch, N.J., Bressman, S.B., deLeon, D. *et al.* (1990). Segregation analysis of idiopathic torsion dystonia in Ashkenazi Jews suggests autosomal dominant inheritance. *Am J Hum Genet.* **46**, 533-538

Ro, L.S., Lai, S.L., Chen, C.M. *et al.* (2003). Deleted 4977-bp mitochondrial DNA mutation is associated with sporadic amyotrophic lateral sclerosis: a hospital-based case-control study. *Muscle Nerve.* **28**, 737-743

Robakis, N.K., Sawh, P.R., Wolfe, G.C. *et al.* (1986). Isolation of a cDNA clone encoding the leader peptide of prion protein and expression of the homologous gene in various tissues. *Proc Natl Acad Sci U S A.* **83**, 6377-6381

Robberecht, W., Aguirre, T., Van Den, B.L. *et al.* (1996). D90A heterozygosity in the SOD1 gene is associated with familial and apparently sporadic amyotrophic lateral sclerosis. *Neurology.* **47**, 1336-1339

Roberts, R.J., Belfort, M., Bestor, T. *et al.* (2003). A nomenclature for restriction enzymes, DNA methyltransferases, homing endonucleases and their genes. *Nucleic Acids Res.* **31**, 1805-1812

Rockman, M.V., Hahn, M.W., Soranzo, N. *et al.* (2004). Positive selection on MMP3 regulation has shaped heart disease risk. *Curr Biol.* **14**, 1531-1539

Rodgers, B.D., Roalson, E.H., Weber, G.M. *et al.* (2007). A proposed nomenclature consensus for the myostatin gene family. *Am J Physiol Endocrinol Metab.* **292**, E371-E372

Ronquist, F. and Huelsenbeck, J.P. (2003). MrBayes 3: Bayesian phylogenetic inference under mixed models. *Bioinformatics.* **19**, 1572-1574

Rooke, K., Figlewicz, D.A., Han, F.Y. *et al.* (1996). Analysis of the KSP repeat of the neurofilament heavy subunit in familiar amyotrophic lateral sclerosis. *Neurology.* **46**, 789-790

Rosen, D.R., Siddique, T., Patterson, D. *et al.* (1993). Mutations in Cu/Zn superoxide dismutase gene are associated with familial amyotrophic lateral sclerosis. *Nature.* **362**, 59-62

Ross, C.A. and Pickart, C.M. (2004). The ubiquitin-proteasome pathway in Parkinson's disease and other neurodegenerative diseases. *Trends Cell Biol.* **14**, 703-711

Roux, A.F., Rommens, J., McDowell, C. *et al.* (1994). Identification of a gene from Xp21 with similarity to the tctex-1 gene of the murine t complex
9049. *Hum Mol Genet.* **3**, 257-263

Rovelet-Lecrux, A., Hannequin, D., Raux, G. *et al.* (2006). APP locus duplication causes autosomal dominant early-onset Alzheimer disease with cerebral amyloid angiopathy. *Nat Genet.* **38**, 24-26

Roy, S., Zhang, B., Lee, V.M. *et al.* (2005). Axonal transport defects: a common theme in neurodegenerative diseases. *Acta Neuropathol (Berl).* **109**, 5-13

Rubinsztein, D.C. and Easton, D.F. (1999). Apolipoprotein E Genetic Variation and Alzheimer's Disease. *Dement Geriatr Cogn Disord.*

Ruddy, D.M., Parton, M.J., Al Chalabi, A. *et al.* (2003). Two families with familial amyotrophic lateral sclerosis are linked to a novel locus on chromosome 16q. *Am J Hum Genet.* **73**, 390-396

Sabeti, P.C., Reich, D.E., Higgins, J.M. *et al.* (2002). Detecting recent positive selection in the human genome from haplotype structure. *Nature.* **419**, 832-837

Sabeti, P.C., Schaffner, S.F., Fry, B. *et al.* (2006). Positive natural selection in the human lineage. *Science.* **312**, 1614-1620

Saetta, A.A., Michalopoulos, N.V., Malamis, G. *et al.* (2006). Analysis of *PRNP* gene codon 129 polymorphism in the Greek population. *Eur J Epidemiol.* **21**, 211-215

Sakharkar, M.K., Chow, V.T., and Kangueane, P. (2004). Distributions of exons and introns in the human genome. *In Silico Biol.* **4**, 387-393

Salvatore, M., Genuardi, M., Petraroli, R. *et al.* (1994). Polymorphisms of the prion protein gene in Italian patients with Creutzfeldt-Jakob disease. *Hum Genet.* **94**, 375-379

Sankoff, D. (2001). Gene and genome duplication. *Curr Opin Genet Dev.* **11**, 681-684

Sapp, P.C., Hosler, B.A., McKenna-Yasek, D. *et al.* (2003). Identification of two novel loci for dominantly inherited familial amyotrophic lateral sclerosis. *Am J Hum Genet.* **73**, 397-403

Saunders, A.M., Strittmatter, W.J., Schmechel, D. *et al.* (1993). Association of apolipoprotein E allele epsilon 4 with late-onset familial and sporadic Alzheimer's disease. *Neurology.* **43**, 1467-1472

Saunderson, R., Yu, B., Trent, R.J. *et al.* (2004). A polymorphism in the poliovirus receptor gene differs in motor neuron disease. *Neuroreport.* **15**, 383-386

Schafer, J.C., Haycraft, C.J., Thomas, J.H. *et al.* (2003). XBX-1 encodes a dynein light intermediate chain required for retrograde intraflagellar transport and cilia assembly in Caenorhabditis elegans
9037. *Mol Biol Cell.* **14**, 2057-2070

Schon, E.A. and Manfredi, G. (2003). Neuronal degeneration and mitochondrial dysfunction. *J Clin Invest.* **111**, 303-312

Schroer, T.A. (2004). Dynactin. *Annu Rev Cell Dev Biol.* **20**, 759-779

Schwartz, S., Elnitski, L., Li, M. *et al.* (2003). MultiPipMaker and supporting tools: Alignments and analysis of multiple genomic DNA sequences. *Nucleic Acids Res.* **31**, 3518-3524

Schwartz, S., Zhang, Z., Frazer, K.A. *et al.* (2000). PipMaker--a web server for aligning two genomic DNA sequences. *Genome Res.* **10**, 577-586

Shah, P.R., Ahmad-Annuar, A., Ahmadi, K.R. *et al.* (2006). No association of DYNC1H1 with sporadic ALS in a case-control study of a northern European derived population: a tagging SNP approach. *Amyotroph Lateral Scler.* **7**, 46-56

Sham, P.C. and Curtis, D. (1995). Monte Carlo tests for associations between disease and alleles at highly polymorphic loci. *Ann Hum Genet.* **59**, 97-105

Shaw, P.J. (2005). Molecular and cellular pathways of neurodegeneration in motor neurone disease. *J Neurol Neurosurg Psychiatry.* **76**, 1046-1057

Shibata, K., Itoh, M., Aizawa, K. *et al.* (2000). RIKEN integrated sequence analysis (RISA) system--384-format sequencing pipeline with 384 multicapillary sequencer
9053. *Genome Res.* **10**, 1757-1771

Shibuya, S., Higuchi, J., Shin, R.W. *et al.* (1998). Codon 219 Lys allele of *PRNP* is not found in sporadic Creutzfeldt-Jakob disease. *Ann Neurol.* **43**, 826-828

Shows, T.B., Alper, C.A., Bootsma, D. *et al.* (1979). International system for human gene nomenclature (1979) ISGN (1979). *Cytogenet Cell Genet.* **25**, 96-116

Siddique, T., Figlewicz, D.A., Pericak-Vance, M.A. *et al.* (1991). Linkage of a gene causing familial amyotrophic lateral sclerosis to chromosome 21 and evidence of genetic-locus heterogeneity. *N Engl J Med.* **324**, 1381-1384

Siddique, T. and Hentati, A. (1995). Familial amyotrophic lateral sclerosis. *Clin Neurosci.* **3**, 338-347

Siddique, T., Hong, S., Brooks, B.R. *et al.* (1998a). X-linked dominant locus for late-onset familial amyotrophic lateral sclerosis. *Am J Hum Genet.* **S63**, A308-

Siddique, T., Pericak-Vance, M.A., Caliendo, J. *et al.* (1998b). Lack of association between apolipoprotein E genotype and sporadic amyotrophic lateral sclerosis. *Neurogenetics.* **1**, 213-216

Siddons, M.A., Pickering-Brown, S.M., Mann, D.M. *et al.* (1996). Debrisoquine hydroxylase gene polymorphism frequencies in patients with amyotrophic lateral sclerosis. *Neurosci Lett.* **208**, 65-68

Silahtaroglu, A.N., Brondum-Nielsen, K., Gredal, O. *et al.* (2002). Human CCS gene: genomic organization and exclusion as a candidate for amyotrophic lateral sclerosis (ALS). *BMC Genet.* **3**, 5-

Silva, J.C., Loreto, E.L., and Clark, J.B. (2004). Factors that affect the horizontal transfer of transposable elements. *Curr Issues Mol Biol.* **6**, 57-71

Simpson, C.L. and Al Chalabi, A. (2006). Amyotrophic lateral sclerosis as a complex genetic disease. *Biochim Biophys Acta*. **1762**, 973-985

Singleton, A.B., Farrer, M., Johnson, J. *et al.* (2003). alpha-Synuclein locus triplication causes Parkinson's disease. *Science*. **302**, 841-

Skibinski, G., Parkinson, N.J., Brown, J.M. *et al.* (2005). Mutations in the endosomal ESCRTIII-complex subunit CHMP2B in frontotemporal dementia. *Nat Genet*. **37**, 806-808

Skovronsky, D.M., Lee, V.M., and Trojanowski, J.Q. (2006). Neurodegenerative Diseases: New Concepts of Pathogenesis and Their Therapeutic Implications. *Annual Review of Pathology: Mechanisms of Disease*. **1**, 151-170

Smigielski, E.M., Sirotkin, K., Ward, M. *et al.* (2000). dbSNP: a database of single nucleotide polymorphisms. *Nucleic Acids Res*. **28**, 352-355

Smith, D.J. and Lusis, A.J. (2002). The allelic structure of common disease. *Hum Mol Genet*. **11**, 2455-2461

Smith, J.M. and Haigh, J. (1974). The hitch-hiking effect of a favourable gene. *Genet Res*. **23**, 23-35

Soldevila, M., Andres, A.M., Ramirez-Soriano, A. *et al.* (2006). The prion protein gene in humans revisited: lessons from a worldwide resequencing study. *Genome Res*. **16**, 231-239

Soldevila, M., Calafell, F., Andres, A.M. *et al.* (2003). Prion susceptibility and protective alleles exhibit marked geographic differences. *Hum Mutat*. **22**, 104-105

Spielman, R.S., McGinnis, R.E., and Ewens, W.J. (1993). Transmission test for linkage disequilibrium: the insulin gene region and insulin-dependent diabetes mellitus (IDDM). *Am J Hum Genet*. **52**, 506-516

Stefansson, H., Sigurdsson, E., Steinthorsdottir, V. *et al.* (2002). Neuregulin 1 and susceptibility to schizophrenia. *Am J Hum Genet*. **71**, 877-892

Stephens, J.C., Schneider, J.A., Tanguay, D.A. *et al.* (2001). Haplotype variation and linkage disequilibrium in 313 human genes. *Science*. **293**, 489-493

Stephens, M. and Donnelly, P. (2003). A comparison of bayesian methods for haplotype reconstruction from population genotype data. *Am J Hum Genet*. **73**, 1162-1169

Stephenson, D.A., Chiotti, K., Ebeling, C. *et al.* (2000). Quantitative trait loci affecting prion incubation time in mice. *Genomics*. **69**, 47-53

Strachan, T. and Read, A, (1999). *Human Molecular Genetics.* Second Edition. Bios Scientific Publishers Ltd, Abingdon, Oxfordshire, UK

Strausberg, R.L., Feingold, E.A., Grouse, L.H. *et al.* (2002). Generation and initial analysis of more than 15,000 full-length human and mouse cDNA sequences
9043. *Proc Natl Acad Sci U S A.* **99**, 16899-16903

Suarez-Merino, B., Hubank, M., Revesz, T. *et al.* (2005). Microarray analysis of pediatric ependymoma identifies a cluster of 112 candidate genes including four transcripts at 22q12.1-q13.3. *Neuro-oncol.* **7**, 20-31

Susalka, S.J., Nikulina, K., Salata, M.W. *et al.* (2002). The roadblock light chain binds a novel region of the cytoplasmic Dynein intermediate chain. *J Biol Chem.* **277**, 32939-32946

Swallow, D.M. (2003). Genetics of lactase persistence and lactose intolerance. *Annu Rev Genet.* **37**, 197-219

Swerdlow, R.H., Parks, J.K., Cassarino, D.S. *et al.* (1998). Mitochondria in sporadic amyotrophic lateral sclerosis. *Exp Neurol.* **153**, 135-142

Syvanen, A.C. (2005). Toward genome-wide SNP genotyping. *Nat Genet.* **37 Suppl**, S5-10

Szmuness, W., Prince, A.M., Hirsch, R.L. *et al.* (1973). Familial clustering of hepatitis B infection. *N Engl J Med.* **289**, 1162-1166

Tajima, F. (1983). Evolutionary relationship of DNA sequences in finite populations. *Genetics.* **105**, 437-460

Takahashi, R., Yokoji, H., Misawa, H. *et al.* (1994). A null mutation in the human CNTF gene is not causally related to neurological diseases. *Nat Genet.* **7**, 79-84

Tan, E.K., Matsuura, T., Nagamitsu, S. *et al.* (2000). Polymorphism of NACP-Rep1 in Parkinson's disease: an etiologic link with essential tremor? *Neurology.* **54**, 1195-1198

Tan, E.K., Tan, C., Shen, H. *et al.* (2003). Alpha synuclein promoter and risk of Parkinson's disease: microsatellite and allelic size variability. *Neurosci Lett.* **336**, 70-72

Tanaka, Y., Zhang, Z., and Hirokawa, N. (1995). Identification and molecular evolution of new dynein-like protein sequences in rat brain
9022. *J Cell Sci.* **108 (Pt 5)**, 1883-1893

Tang, G., Xie, H., Xu, L. *et al.* (2002a). Genetic study of apolipoprotein E gene, alpha-1 antichymotrypsin gene in sporadic Parkinson disease. *Am J Med Genet.* **114**, 446-449

Tang, Q., Staub, C.M., Gao, G. *et al.* (2002b). A novel transforming growth factor-beta receptor-interacting protein that is also a light chain of the motor protein dynein
9044. *Mol Biol Cell.* **13**, 4484-4496

Tanzi, R.E., Gusella, J.F., Watkins, P.C., *et al.* (1987). Amyloid beta protein gene: cDNA, mRNA distribution, and genetic linkage near the Alzheimer locus. *Science.* **20,** 880-4

Taylor, J.P., Hardy, J., and Fischbeck, K.H. (2002). Toxic proteins in neurodegenerative disease. *Science*. **296**, 1991-1995

Taylor, J.S. and Raes, J. (2004). Duplication and divergence: the evolution of new genes and old ideas. *Annu Rev Genet*. **38**, 615-643

Terry, P.D., Kamel, F., Umbach, D.M. *et al.* (2004). VEGF promoter haplotype and amyotrophic lateral sclerosis (ALS). *J Neurogenet*. **18**, 429-434

The International HapMap Consortium. (2005). A haplotype map of the human genome. *Nature*. **437**, 1299-1320

Thomas, P.D. and Kejariwal, A. (2004). Coding single-nucleotide polymorphisms associated with complex vs. Mendelian disease: evolutionary evidence for differences in molecular effects. *Proc Natl Acad Sci U S A*. **101**, 15398-15403

Thompson, J.D., Higgins, D.G., and Gibson, T.J. (1994). CLUSTAL W: improving the sensitivity of progressive multiple sequence alignment through sequence weighting, position-specific gap penalties and weight matrix choice. *Nucleic Acids Res*. **22**, 4673-4680

Tishkoff, S.A., Reed, F.A., Ranciaro, A. *et al.* (2007). Convergent adaptation of human lactase persistence in Africa and Europe. *Nat Genet*. **39**, 31-40

Tomkins, J., Banner, S.J., McDermott, C.J. *et al.* (2001). Mutation screening of manganese superoxide dismutase in amyotrophic lateral sclerosis. *Neuroreport*. **12**, 2319-2322

Tomkins, J., Usher, P., Slade, J.Y. *et al.* (1998). Novel insertion in the KSP region of the neurofilament heavy gene in amyotrophic lateral sclerosis (ALS). *Neuroreport*. **9**, 3967-3970

Ueda, H., Howson, J.M., Esposito, L. *et al.* (2003). Association of the T-cell regulatory gene CTLA4 with susceptibility to autoimmune disease. *Nature*. **423**, 506-511

Vadlamudi, R.K., Bagheri-Yarmand, R., Yang, Z. *et al.* (2004). Dynein light chain 1, a p21-activated kinase 1-interacting substrate, promotes cancerous phenotypes. *Cancer Cell*. **5**, 575-585

Vaisberg, E.A., Grissom, P.M., and McIntosh, J.R. (1996a). Mammalian cells express three distinct dynein heavy chains that are localized to different cytoplasmic organelles. *J Cell Biol*. **133**, 831-842

Vaisberg, E.A., Grissom, P.M., and McIntosh, J.R. (1996b). Mammalian cells express three distinct dynein heavy chains that are localized to different cytoplasmic organelles. *J Cell Biol*. **133**, 831-842

Vaisberg, E.A., Koonce, M.P., and McIntosh, J.R. (1993). Cytoplasmic dynein plays a role in mammalian mitotic spindle formation
9012. *J Cell Biol*. **123**, 849-858

Vallee, R.B., Williams, J.C., Varma, D. *et al.* (2004). Dynein: An ancient motor protein involved in multiple modes of transport. *J Neurobiol.* **58**, 189-200

van Duijn, C.M., Delasnerie-Laupretre, N., Masullo, C. *et al.* (1998). Case-control study of risk factors of Creutzfeldt-Jakob disease in Europe during 1993-95. European Union (EU) Collaborative Study Group of Creutzfeldt-Jakob disease (CJD). *Lancet.* **351**, 1081-1085

Van Vught, P.W., Sutedja, N.A., Veldink, J.H. *et al.* (2005). Lack of association between VEGF polymorphisms and ALS in a Dutch population. *Neurology.* **65**, 1643-1645

Vance, C., Al Chalabi, A., Ruddy, D. *et al.* (2006). Familial amyotrophic lateral sclerosis with frontotemporal dementia is linked to a locus on chromosome 9p13.2-21.3. *Brain.* **129**, 868-876

Vanin, E.F. (1985). Processed pseudogenes: characteristics and evolution. *Annu Rev Genet.* **19**, 253-272

Vaughan, K.T., Mikami, A., Paschal, B.M. *et al.* (1996). Multiple mouse chromosomal loci for dynein-based motility. *Genomics.* **36**, 29-38

Vaughan, K.T. and Vallee, R.B. (1995). Cytoplasmic dynein binds dynactin through a direct interaction between the intermediate chains and p150Glued
9067. *J Cell Biol.* **131**, 1507-1516

Vechio, J.D., Bruijn, L.I., Xu, Z. *et al.* (1996). Sequence variants in human neurofilament proteins: absence of linkage to familial amyotrophic lateral sclerosis. *Ann Neurol.* **40**, 603-610

Veldink, J.H., Kalmijn, S., Van der Hout, A.H. *et al.* (2005). SMN genotypes producing less SMN protein increase susceptibility to and severity of sporadic ALS. *Neurology.* **65**, 820-825

Veldink, J.H., van den Berg, L.H., Cobben, J.M. *et al.* (2001). Homozygous deletion of the survival motor neuron 2 gene is a prognostic factor in sporadic ALS. *Neurology.* **56**, 749-752

Vermeire, S., Wild, G., Kocher, K. *et al.* (2002). CARD15 genetic variation in a Quebec population: prevalence, genotype-phenotype relationship, and haplotype structure. *Am J Hum Genet.* **71**, 74-83

Verrelli, B.C. and Tishkoff, S.A. (2004). Signatures of selection and gene conversion associated with human color vision variation. *Am J Hum Genet.* **75**, 363-375

Vollmert, C., Windl, O., Xiang, W. *et al.* (2006). Significant association of a M129V independent polymorphism in the 5' UTR of the *PRNP* gene with sporadic Creutzfeldt-Jakob disease in a large German case-control study. *J Med Genet.* **43**, e53-

Wain, H.M., Bruford, E.A., Lovering, R.C. *et al.* (2002). Guidelines for human gene nomenclature. *Genomics.* **79**, 464-470

Wang, W.Y. and Todd, J.A. (2003). The usefulness of different density SNP maps for disease association studies of common variants. *Hum Mol Genet.* **12**, 3145-3149

Wang, X.S., Lee, S., Simmons, Z. *et al.* (2004). Increased incidence of the Hfe mutation in amyotrophic lateral sclerosis and related cellular consequences. *J Neurol Sci.* **227**, 27-33

Watanabe, T.K., Fujiwara, T., Shimizu, F. *et al.* (1996). Cloning, expression, and mapping of TCTEL1, a putative human homologue of murine Tctel, to 6q. *Cytogenet Cell Genet.* **73**, 153-156

Waterston, R.H., Lindblad-Toh, K., Birney, E. *et al.* (2002). Initial sequencing and comparative analysis of the mouse genome. *Nature.* **420**, 520-562

Watterson, G.A. (1978). The homozygosity test of neutrality. *Genetics.* **88**, 405-417

Watterson, G.A. (1986). The homozygosity test after a change in population size. *Genetics.* **112**, 899-907

Weale, M.E., Depondt, C., Macdonald, S.J. *et al.* (2003). Selection and evaluation of tagging SNPs in the neuronal-sodium-channel gene SCN1A: implications for linkage-disequilibrium gene mapping. *Am J Hum Genet.* **73**, 551-565

Weiss, K.M. and Clark, A.G. (2002). Linkage disequilibrium and the mapping of complex human traits. *Trends Genet.* **18**, 19-24

Westaway, D., Goodman, P.A., Mirenda, C.A. *et al.* (1987). Distinct prion proteins in short and long scrapie incubation period mice. *Cell.* **51**, 651-662

Wheeler, D.L., Church, D.M., Federhen, S. *et al.* (2003). Database resources of the National Center for Biotechnology. *Nucleic Acids Res.* **31**, 28-33

Wiedemann, F.R., Manfredi, G., Mawrin, C. *et al.* (2002). Mitochondrial DNA and respiratory chain function in spinal cords of ALS patients. *J Neurochem.* **80**, 616-625

Wilhelmsen, K.C., Forman, M.S., Rosen, H.J. *et al.* (2004). 17q-linked frontotemporal dementia-amyotrophic lateral sclerosis without tau mutations with tau and alpha-synuclein inclusions. *Arch Neurol.* **61**, 398-406

Will, R.G., Alperovitch, A., Poser, S. *et al.* (1998). Descriptive epidemiology of Creutzfeldt-Jakob disease in six European countries, 1993-1995. EU Collaborative Study Group for CJD. *Ann Neurol.* **43**, 763-767

Williamson, T.L. and Cleveland, D.W. (1999). Slowing of axonal transport is a very early event in the toxicity of ALS-linked SOD1 mutants to motor neurons. *Nat Neurosci.* **2**, 50-56

Wilson, M.J., Salata, M.W., Susalka, S.J. *et al.* (2001). Light chains of mammalian cytoplasmic dynein: identification and characterization of a family of LC8 light chains. *Cell Motil Cytoskeleton.* **49**, 229-240

Wilson, P.A., Gardner, S.D., Lambie, N.M. *et al.* (2006). Characterization of the human patatin-like phospholipase family. *J Lipid Res.* **47**, 1940-1949

Windl, O., Dempster, M., Estibeiro, J.P. *et al.* (1996). Genetic basis of Creutzfeldt-Jakob disease in the United Kingdom: a systematic analysis of predisposing mutations and allelic variation in the *PRNP* gene. *Hum Genet.* **98**, 259-264

Windl, O., Giese, A., Schulz-Schaeffer, W. *et al.* (1999). Molecular genetics of human prion diseases in Germany. *Hum Genet.* **105**, 244-252

Witherden, A.S., Hafezparast, M., Nicholson, S.J. *et al.* (2002). An integrated genetic, radiation hybrid, physical and transcription map of a region of distal mouse chromosome 12, including an imprinted locus and the 'Legs at odd angles' (Loa) mutation. *Gene.* **283**, 71-82

Wolfe, K.H. (2001). Yesterday's polyploids and the mystery of diploidization. *Nat Rev Genet.* **2**, 333-341

Wood, E.T., Stover, D.A., Slatkin, M. *et al.* (2005). The beta -globin recombinational hotspot reduces the effects of strong selection around HbC, a recently arisen mutation providing resistance to malaria. *Am J Hum Genet.* **77**, 637-642

Wooding, S., Stone, A.C., Dunn, D.M. *et al.* (2005). Contrasting effects of natural selection on human and chimpanzee CC chemokine receptor 5. *Am J Hum Genet.* **76**, 291-301

Woodward, K., Kendall, E., Vetrie, D. *et al.* (1998). Pelizaeus-Merzbacher disease: identification of Xq22 proteolipid-protein duplications and characterization of breakpoints by interphase FISH. *Am J Hum Genet.* **63**, 207-217

Wopfner, F., Weidenhofer, G., Schneider, R. *et al.* (1999). Analysis of 27 mammalian and 9 avian PrPs reveals high conservation of flexible regions of the prion protein. *J Mol Biol.* **289**, 1163-1178

Yang, Y., Hentati, A., Deng, H.X. *et al.* (2001). The gene encoding alsin, a protein with three guanine-nucleotide exchange factor domains, is mutated in a form of recessive amyotrophic lateral sclerosis. *Nat Genet.* **29**, 160-165

Yao, Y., Nellaker, C., and Karlsson, H. (2006). Evaluation of minor groove binding probe and Taqman probe PCR assays: Influence of mismatches and template complexity on quantification. *Mol Cell Probes.* **20**, 311-316

Yase, Y., Yoshida, S., Kihira, T. *et al.* (2001). Kii ALS dementia. *Neuropathology.* **21**, 105-109

Yen, A.A., Simpson, E.P., Henkel, J.S. *et al.* (2004). HFE mutations are not strongly associated with sporadic ALS. *Neurology.* **62**, 1611-1612

Yoshida, S., Uebayashi, Y., Kihira, T. *et al.* (1998). Epidemiology of motor neuron disease in the Kii Peninsula of Japan, 1989-1993: active or disappearing focus? *J Neurol Sci.* **155**, 146-155

Young, J.H., Chang, Y.P., Kim, J.D. *et al.* (2005). Differential susceptibility to hypertension is due to selection during the out-of-Africa expansion. *PLoS Genet.* **1**, e82-

Yu, F., Sabeti, P.C., Hardenbol, P. *et al.* (2005). Positive selection of a pre-expansion CAG repeat of the human SCA2 gene. *PLoS Genet.* **1**, e41-

Yu, S.L., Jin, L., Sy, M.S. *et al.* (2004). Polymorphisms of the *PRNP* gene in Chinese populations and the identification of a novel insertion mutation. *Eur J Hum Genet.* **12**, 867-870

Zareparsi, S., Branham, K.E., Li, M. *et al.* (2005). Strong association of the Y402H variant in complement factor H at 1q32 with susceptibility to age-related macular degeneration. *Am J Hum Genet.* **77**, 149-153

Zareparsi, S., James, D.M., Kaye, J.A. *et al.* (2002). HLA-A2 homozygosity but not heterozygosity is associated with Alzheimer disease. *Neurology.* **58**, 973-975

Zhang, J., Rowe, W.L., Clark, A.G. *et al.* (2003). Genomewide distribution of high-frequency, completely mismatching SNP haplotype pairs observed to be common across human populations. *Am J Hum Genet.* **73**, 1073-1081

Zhang, J., Webb, D.M., and Podlaha, O. (2002). Accelerated protein evolution and origins of human-specific features: Foxp2 as an example. *Genetics.* **162**, 1825-1835

Zhang, Q.H., Ye, M., Wu, X.Y. *et al.* (2000). Cloning and functional analysis of cDNAs with open reading frames for 300 previously undefined genes expressed in CD34+ hematopoietic stem/progenitor cells. *Genome Res.* **10**, 1546-1560

Zhao, J.H. and Sham, P.C. (2002). Faster haplotype frequency estimation using unrelated subjects. *Hum Hered.* **53**, 36-41

Zimmermann, K., Turecek, P.L., and Schwarz, H.P. (1999). Genotyping of the prion protein gene at codon 129. *Acta Neuropathol (Berl).* **97**, 355-358

10 Appendices

SNP				Amplicon	Genotype			Minor
Number	ID	Position (bp)	Alleles	size (bp)	AA	AB	BB	allele
1	rs2180511	27670	A/T	535	14	2	0	6.0%
2	rs1678034	30289	A/C	566	14	2	0	6.3%
3	rs2180513	61497	C/T	622	16	0	0	0%
4	rs1956297	74179	C/T	453	16	0	0	0%
5	rs2474677	75613	C/T	360	16	0	0	0%
6	rs2474678	75617	A/G		16	0	0	0%
7	rs2448241	76261	C/T		16	0	0	0%
8	rs2093025	76319	C/T	500	16	0	0	0%
9	rs2474679	76323	C/T		16	0	0	0%
10	rs1044838	76846	A/C		16	0	0	0%
11	rs2281539	76858	C/T	510	16	0	0	0%
12	rs2273434	76920	C/G		16	0	0	0%
13	rs2273435	77049	A/G		15	1	0	3.1%
14	rs2448240	77419	C/G	360	16	0	0	0%
15	rs2448239	79006	A/G	520	16	0	0	0%
16	rs1741151	81081	C/T	320	14	2	0	6.3%
17	rs2403015	89054	A/G	591	16	0	0	0%
18	rs1622886	89874	A/G	420	16	0	0	0%
19	**rs1741155**	89892	A/G		12	3	1	15.6%
20	rs2749911	90216	C/T		16	0	0	0%
21	rs2720193	90225	A/G	460	12	4	0	12.5%
22	rs2720194	90295	A/G		12	4	0	12.5%
23	rs2448242	91338	A/G	440	16	0	0	0%
24	**rs2273438**	107101	C/T	390	12	4	0	12.5%
25	rs2273439	107195	C/T	380	16	0	0	0%
26	rs2720218	109449	A/C	190	16	0	0	0%
27	**rs2749890**	114824	A/G	200	12	4	0	**12.5%**
28	rs2749894	119522	A/C	211	16	0	0	0%
29	rs2720206	119787	C/T	260	16	0	0	0%
30	rs2720213	126498	C/G	160	15	1	0	3.1%
31	**rs2251644**	129341	A/G	280	12	4	0	**12.5%**
32	rs2749896	132256	A/G		16	0	0	0%
33	rs2749897	138855	A/G	380	16	0	0	0%
34	rs2720197	139455	A/G		16	0	0	0%
35	**rs3742426*†**	147536	A/G	600	12	4	0	**12.5%**
36	**rs2180510**	147694	A/G		12	4	0	**12.5%**
37	rs2749899	150639	A/G	453	16	0	0	0%
38	rs2749900	151540	C/G	365	16	0	0	0%
39	rs2720198	151863	A/C	440	16	0	0	0%
40	rs2403016	153341	C/T	359	16	0	0	0%
41	rs2295445	157537	C/G	367	16	0	0	0%
42	rs754598	160726	A/G	498	16	0	0	0%
43	rs941632	163482	A/G	275	16	0	0	0%
44	rs2093024	167571	A/C	530	16	0	0	0%
45	**rs941793**	168955	C/T	260	12	4	1	**17.6%**
46	rs1190605	171447	C/G	420	16	0	0	0%
47	rs1043455	172220	C/T	327	16	0	0	0%
48	**rs13749**	175721	C/T	430	12	4	0	**12.5%**
49	rs2273656	175929	A/C		16	0	0	0%
50	**rs941792***	176207	C/T		12	3	1	**15.6%**
51	rs1127284	176475	C/T	380	16	0	0	0%
52	**rs1004903**	176509	A/G		12	3	1	**15.6%**
53	**rs10135238***	180364	C/T	530	12	4	1	**17.6%**
54	**rs1190610**	180468	A/G		12	3	1	**15.6%**
55	**rs1190613**	183028	C/T	440	12	4	1	**17.6%**
56	bp183293*‡	183293	A/T		15	1	0	3.1%
57	rs1190614	185042	A/T	570	13	3	0	9.4%
58	rs11849604*	185073	A/T		13	3	0	9.4%
59	rs1203482	193407	C/T	360	16	0	0	0%
60	**rs1190618***	193460	C/G		12	4	1	**17.6%**

Appendix 1. Full genotypes for 60 SNPs across *DYNC1H1*

* SNPs previously absent from the SNP databases which have since been added
† rs3742426 was merged with rs12895291 in May 2006
‡ no information available for this SNP in SNP databases

Primer name	Forward sequence	Reverse sequence	T_m (°c)	Amplicon size (bp)
rs1741155	ggaatttccagggagtgga	gactctggctccagcacac	60	604
rs2720193	gtcagcttggggtgtgct	ggccatccaccatctgag	60	752
rs2720194	gtcagcttggggtgtgct	ggccatccaccatctgag	60	752
rs2273438	cagtagctctcatgtactaaag	cggctcactagcgttacc	60	444
rs2749890	agggaggaggacccttttgta	gctgtcgtatgcatctggtc	60	767
rs2251644	ggagcctgtcatctgtggt	acagtgaaagcgtgggagac	60	401
rs3742426	agcataaagtgagcagcttgaa	gcaccacctggctctaactt	60	589
rs2180510	agcataaagtgagcagcttgaa	gcaccacctggctctaactt	60	589
rs941793	ggaaaccacttagggagatcg	tgctcacttcctgagaacacc	60	503
rs13749	tcccagtgtggactcactca	ctggacacctgctctgaggt	60	633
rs941792	acacaagctcggttccaagt	ctgtctgcacgtggtgct	60	850
rs1004903	acacaagctcggttccaagt	ctgtctgcacgtggtgct	60	850
rs10135238	cctgagctcaagtggtcctc	tctctgggtgacatgagctg	60	677
rs1190610	cctgagctcaagtggtcctc	tctctgggtgacatgagctg	60	677
rs1190613	tctttcctagcccaggtcaa	ggggtgctgaaacagatgtc	63	562
rs1190618	catgcccagcctaatgttt	tctgggaacagaggaagctc	60	458
rs2251644CBDay	tgaagcgattgtcaaggatg	aatacggagagagcttcatgg	60	392
DYNC1H1 Exon 8	ttaaagccttcgtttggtcag	agctcgctattacagtgctt	60	1190
DYNC1H1 Exon 13 and 14	gtggtgaaagacatgaaccttc	ctggccgtgtgtctactgagtg	60	655

Appendix 2. *DYNC1H1* informative primers

11 Publications

ALS and other motor neuron disorders 2003 4, 150–157
 ISSN 1466-0822

Original Research

No association with common Caucasian genotypes in exons 8, 13 and 14 of the human cytoplasmic dynein heavy chain gene (*DNCHC1*) and familial motor neuron disorders

Azlina Ahmad-Annuar,[1] Paresh Shah,[1] Majid Hafezparast,[1] Holger Hummerich,[1] Abi S Witherden,[1] Karen E Morrison,[2] Pamela J Shaw,[3] Janine Kirby,[3] Thomas T Warner,[4] Andrew Crosby,[5] Christos Proukakis,[4] Philip Wilkinson,[5] Richard W Orrell,[4] Lloyd Bradley,[4] Joanne E Martin,[6] and Elizabeth MC Fisher[1]

OPEN ACCESS Freely available online

PLoS GENETICS

Review

Genetic Analysis of the Cytoplasmic Dynein Subunit Families

K. Kevin Pfister*, Paresh R. Shah, Holger Hummerich, Andreas Russ, James Cotton, Azlina Ahmad Annuar, Stephen M. King, Elizabeth M. C. Fisher

ABSTRACT

Cytoplasmic dyneins, the principal microtubule minus-end-directed motor proteins of the cell, are involved in many essential cellular processes. The major form of this enzyme is a complex of at least six protein subunits, and in mammals all but one of the subunits are encoded by at least two genes. Here we review current knowledge concerning the subunits, their interactions, and their functional roles as derived from biochemical and genetic analyses. We also carried out extensive database searches to look for new genes and to clarify anomalies in the databases. Our analysis documents evolutionary relationships among the dynein subunits of mammals and other model organisms, and sheds new light on the role of this diverse group of proteins, highlighting the existence of two cytoplasmic dynein complexes with distinct cellular roles.

Introduction

Dyneins are large multi-subunit protein complexes that undertake a wide range of roles within the cell. They are adenosine triphosphate (ATP)–driven, microtubule minus-end-directed molecular motors that can be divided, based on function, into two classes: axonemal and cytoplasmic dyneins [1–7] (reviewed in [8,9]). Axonemal dyneins are responsible for the movement of cilia and flagella. Two cytoplasmic dynein complexes have been identified. The most abundant cytoplasmic dynein complex, cytoplasmic dynein 1, is involved in functions as diverse as spindle-pole organization and nuclear migration during mitosis, the positioning and functioning of the endoplasmic reticulum, the Golgi apparatus, and the nucleus, and also the minus-end-directed transport of vesicles, including endosomes and lysosomes, along microtubules and retrograde axonal transport in neurons. A second cytoplasmic dynein complex, cytoplasmic dynein 2, has a role in intraflagellar transport (IFT), a process required for ciliary/flagellar assembly (reviewed in [10]).

The core of the cytoplasmic dynein 1 complex is a homodimer of two heavy chain polypeptides and associated intermediate, light intermediate, and light chain polypeptides, which are defined and named by their molecular mass and mobility in SDS-PAGE gels (Figure 1A). The protein subunits are encoded by families of at least two genes, and the expression patterns of the individual family members are different in various cell types. At least one of the light chains, DYNLL1 (LC8), has multiple cellular roles independent of its participation in a dynein complex. Cytoplasmic dynein 1 interacts with various other proteins including a second multimer, dynactin, to form the dynein–dynactin complex. Dynactin is comprised of at least seven different proteins, which together act as an adaptor that connects the cytoplasmic dynein motor to a range of cargoes (for review, see [11]). Interaction with dynactin also increases dynein motor processivity [12]. Furthermore, dynactin functions independently of dynein, anchoring microtubules at the centrosome [13]. Current evidence suggests that the second cytoplasmic dynein complex, cytoplasmic dynein 2, is also a homodimer of a distinct heavy chain, DYNC2H1, with associated light intermediate chain, DYNC2LI1 (Figure 1B). No other subunits have yet been identified for this complex, and it does not appear to interact with the dynactin complex [14–16].

The cytoplasmic dynein proteins are fundamental to the functioning of all cells, and have recently been shown to be causally mutated in forms of neurodegeneration [17–19]. They are thus of great interest for mammalian genetic, and other, studies. We therefore sought to examine the role of cytoplasmic dynein subunits from a genetic perspective. During this analysis, we noted considerable confusion in the human and mouse gene and protein names and mapping positions. Therefore, we reexamined the mapping locations for the subunit genes and clarified and updated entries in the various sequence databases. In doing so, we utilized the revised consensus nomenclature developed for the cytoplasmic dynein subunits and their genes (Table 1). We also defined, as far as possible with current data, homologous genes in model organisms, including *Drosophila*, *Caenorhabditis*

Citation: Pfister KK, Shah PR, Hummerich H, Russ A, Cotton J, et al. (2006) Genetic analysis of the cytoplasmic dynein subunit families. PLoS Genet 2(1): e1.

DOI: 10.1371/journal.pgen.0020001

Abbreviations: ATP, adenosine triphosphate; BBSRC, Biotechnology and Biological Sciences Research Council; IFT, intraflagellar transport; JTT, Jones, Taylor, and Thornton; MGI, Mouse Genome Informatics; Mr, relative mobility; NCBI, National Center for Biotechnology Information; NIH, National Institutes of Health; nNOS, neuronal nitric oxide synthase; PSI-BLAST, position-specific iterative BLAST; RefSeq, Reference Sequence

K. Kevin Pfister is in the Department of Cell Biology, School of Medicine, University of Virginia, Charlottesville, Virginia, United States of America. Paresh R. Shah is in the Department of Neurodegenerative Disease and in the MRC Prion Unit, Institute of Neurology, London, United Kingdom. Holger Hummerich is in the MRC Prion Unit, Institute of Neurology, London, United Kingdom. Andreas Russ is in the Genetics Unit, Department of Biochemistry, University of Oxford, Oxford, United Kingdom. James Cotton is in the Department of Zoology, the Natural History Museum, London, United Kingdom. Azlina Ahmad Annuar and Elizabeth M. C. Fisher are in the Department of Neurodegenerative Disease, Institute of Neurology, London, United Kingdom. Stephen M. King is in the Department of Molecular, Microbial, and Structural Biology, University of Connecticut Health Center, Farmington, Connecticut, United States of America.

* To whom correspondence should be addressed. E-mail: kkp9w@virginia.edu

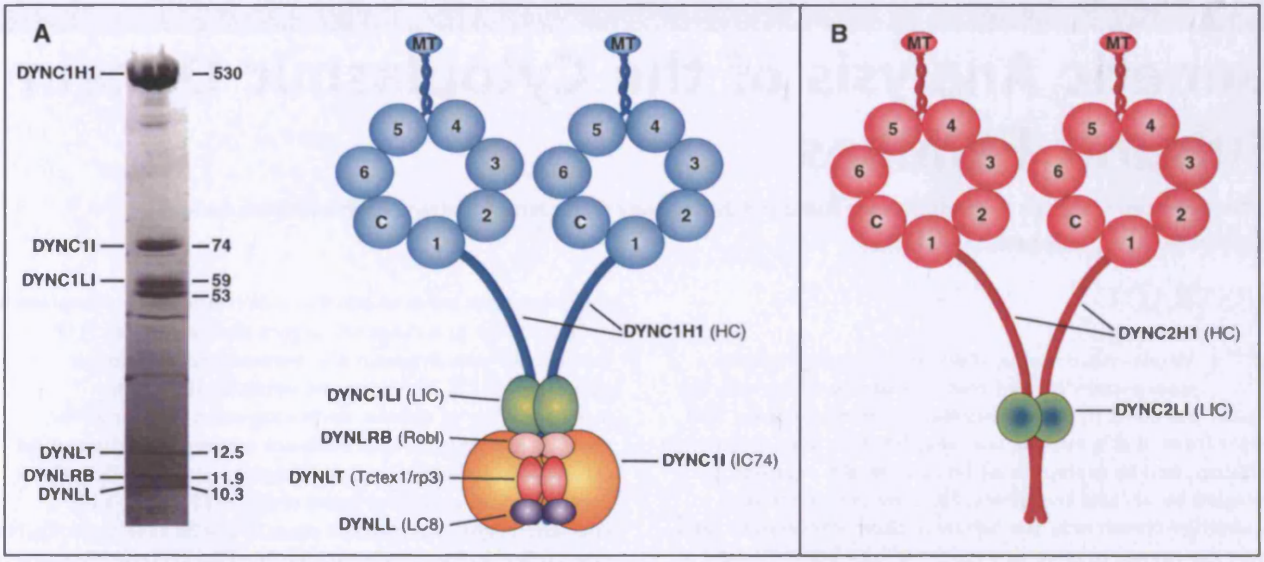

DOI: 10.1371/journal.pgen.0020001.g001

Figure 1. The Mammalian Cytoplasmic Dynein Complexes

(A) Cytoplasmic dynein. (Left panel) Polypeptides of immunoaffinity-purified rat brain cytoplasmic dynein. Polypeptide mass (in kDa) is indicated on the right side of the gel, and the consensus family names are indicated on the left. (Right panel) Structural model for the association of the cytoplasmic dynein complex subunits. The core of the cytoplasmic dynein complex is made of two DYNC1H1 heavy chains which homodimerize via regions in their N-termini. The motor domains are at the C-termini of the heavy chains, the large globular heads of ~350 kDa that are composed of a ring of seven densities surrounding a central cavity; six of the densities are AAA domains (numbered 1–6). AAA domain 1 is the site of ATP hydrolysis. The microtubule-binding domain is a projection found on the opposite side of the ring between AAA domains 4 and 5. C is the C-terminus of the heavy chain that would form the 7th density. Two DYNC1I intermediate chains (IC74) and DYNC1LI light intermediate chains bind at overlapping regions of the N-terminus of the heavy chain, overlapping with the heavy chain dimerization domains. Dimers of the three light chain families; DYNLT, the Tctex1 light chains; DYNLRB, the Roadblock light chains; and DYNLL, the LC8 light chains, bind to the intermediate chain dimers.

(B) Cytoplasmic dynein 2 complex, structural model for subunit association. This dynein complex has a unique role in IFT and is sometimes known as IFT dynein. Structural predictions indicate that the heavy chain, DYNC2H1, is similar to the cytoplasmic and axonemal dyneins. The only known subunit of this complex is a 33- to 47-kDa polypeptide, DYNC2LI1, which is related to the cytoplasmic dynein light intermediate chains. No intermediate chain or light chains have yet been identified [16].

elegans, *Chlamydomonas*, and yeast. To further our understanding of the function of cytoplasmic dynein subunits, we also briefly examined mutations in this group of proteins in a variety of model organisms. We do not discuss dynein-binding proteins such as dynactin, LIS1, or various kinases, which while important for dynein function, have not yet been shown to be stoichiometric components of the cytoplasmic dynein complex.

Human and mouse cytoplasmic dynein subunit genes. The subunits of the cytoplasmic dynein complexes are resolved into subunit polypeptides of ~530 kDa (heavy chains), ~74 kDa (intermediate chains), ~33–59 kDa (light intermediate chains), and ~10–14 kDa (light chains) in SDS-PAGE gels (Figure 1A). Research on the cytoplasmic dynein subunits has been undertaken in a wide range of organisms from yeast to humans. The nomenclature of the mammalian genes encoding these proteins has drawn on homologs in other organisms and, consequently, a number of aliases have been found for any given human or mouse cytoplasmic dynein subunit. Much of the early research into dynein genetics was conducted in the biflagellate green alga *Chlamydomonas* on the dyneins found in the flagellar axoneme, and therefore some cytoplasmic dynein nomenclature derives from these studies. For example, mammalian members of the cytoplasmic light chain families DYNLRB and DYNLL have commonly been referred to as LC7 and LC8, respectively, which are the names of homologous *Chlamydomonas* axonemal dynein subunits.

Nomenclature. The revised classification system for mammalian cytoplasmic dynein (Table 1) recognizes the two distinct dynein complexes, cytoplasmic dynein 1 and cytoplasmic dynein 2, and the fact that cytoplasmic dynein light chains are shared with some axonemal dyneins. Cytoplasmic dynein subunits are also classified into polypeptide families according to sequence similarity within groups of similarly sized proteins; thus there is sequence similarity within the dynein gene families (and when cytoplasmic and axonemal members of the same gene families are compared) but not among them.

This nomenclature has been approved by the Human Genome Organization Nomenclature Committee [20] and the International Committee on Standardized Nomenclature for Mice. In accordance with their policy, the designation of each unique cytoplasmic dynein subunit starts with **DYNC** for dynein, cytoplasmic, followed by the specific dynein complex subtype **1** or **2**; for example, cytoplasmic dynein 2 is designated **DYNC2**. The shared light chains start with **DYN**. Each subunit is designated with a letter(s) for the size of the polypeptides, **H** for the heavy chain, **I** for the intermediate chain, **LI** for the light intermediate chain, and **L** for the light chain. Additional letters (**T**, **RB**, and **L**) are used to distinguish the three distinct light chain families as described in the text. Individual members of the gene families are assigned numbers. Standard human and mouse gene nomenclature is used: italicized upper case for human gene symbols (for

Table 1. Human and Mouse Cytoplasmic Dynein Genes and Map Positions

Cytoplasmic Dynein Gene Family	Official or Proposed Gene Name HUGO[a] (Human)	Aliases	Location: Human (Hsa) NCBI[b]/Mouse (Mmu) MGI[c]	Entrez Gene ID[d] (Human and Mouse)/ MGI ID (Mouse)	mRNA (NCBI RefSeq Accession Numbers)	Protein (NCBI/ SwissProt[e] Accession Numbers)
Cytoplasmic dynein 1 heavy chain	Human *DYNC1H1*	DNCHC1 [177]; DNECL [178]; Hp22 [43]; pM7 [98]; Rk3–8 [98]; DHC1 [23]; DHC1a [61]; MAP1C [3]; DNCL [20]; HL-3 [98]; KIAA0325 [21]; AB002323 [179]; Dyh1 [180]; cDHC [44]; DYHC_HUMAN[f]	Hsa14q32	1778	NM_001376	NP_001367/*Q14204*
	Mouse *Dync1h1*	Dnchc1 [98]; cDHC [44]; Loa [181]; Rk9–32 [98]; Dnec1 [20]; DNCL [182]; MAP1C [41]; mKIAA0325 [183,184]; DYHC_MOUSE[f]	Mmu12 (55cM)	13424/103147	NM_030238	NP_084514/*Q9JHU4*
Cytoplasmic dynein 2 heavy chain	Human *DYNC2H1*	DHC2 [23,74]; DHC1b [74]; DLP4 [69]; DYH1B [8]; Dyh2 [180]; hdhc11 [185]; FLJ11756 [186]	Hsa11q21-q22.1	79659	XM_370652[g]	XP_370652[g]/O00432
	Mouse *Dync2h1*	Dnchc2 [187]; Mdhc11 [185]	Mmu9 (1cM)	110350/107736	XM_358380	XP_358380/O08822
Cytoplasmic dynein 1 intermediate chain	Human *DYNC1I1*	IC1 [79]; IC74 [76]; IC74–1 [40]; D1 IC74 [14]; DH IC-1 [188]; DNCI1 [94]; DYI1_HUMAN[f]	Hsa7q21.3-q22.1	1780	NM_004411	NP_004402/O14576
	Mouse *Dync1i1*	Dncic1 [187]; Dnci1 [94]; DYI1_MOUSE[f]	Mmu6 (4cM)	13426/107743	NM_010063	NP_034193/O88485
	Human *DYNC1I2*	IC2 [79]; IC74–2 [40]; DH IC-2 [189]; DYI2_HUMAN[f]	Hsa2q31.1	1781	NM_001378	NP_001369/Q13409
	Mouse *Dync1i2*	Dncic2 [187]; Dnci2 [94]; DYI2_MOUSE[f]	Mmu2 (41cM)	13427/107750	NM_010064	NP_034194/O88487
Cytoplasmic dynein 1 light intermediate chain	Human *DYNC1LI1*	Light chain A [190]; D1LIC [14]; LIC57/59 [102]; LIC-1 [102]; DYJ1_HUMAN[f]	Hsa3p22.3	51143	NM_016141	NP_057225
	Mouse *Dync1li1*	Dnclic1 [187]; MGC32416 [191]	Mmu9 F3	235661/2135610	NM_146229	NP_666341
	Human *DYNC1LI2*	LIC53/55 [102]; LIC-2 [102]; DYJ2_HUMAN[f]	Hsa16q22.1	1783	NM_006141	NP_006132/O43237
	Mouse *Dync1li2*	Dnclic2 [187]	Mmu8 (50cM)	110801 (and see 234663)/*107738*	XM_134573[g]	XP_134573[g]
Cytoplasmic dynein 2 light intermediate chain	Human *DYNC2LI1*	D2LIC [14]; LIC3 [15]; CGI-60 [15,192]; DKFZP564A033 [192]	Hsa2p25.1-p24.1	51626	NM_016008 (isoform 1)/ NM_015522 (isoform 2)	NP_057092 (isoform 1)/ NP_056337 (isoform 2)
	Mouse *Dync2li1*	4933404O11Rik [193]; D2LIC [193]; mD2LIC [193]; MGC7211 [193]; MGC40646 [193]	Mmu17 E4	213575/1913996	NM_172256	NP_758460
Cytoplasmic dynein Tctex1 light chain	Human *DYNLT1*	TCTEL1 [194]; Tctex1 [114,116]; Protein CW-1 [195]; DYLX_HUMAN[f]	Hsa6q25.3	6993	NM_006519	NP_006510/Q15763
	Mouse *Dynlt1*	Tctex1 [116]; Tcd1 [114,116]; DYLX_MOUSE[f]	Mmu17 (4cM)	21648/98643	NM_009342	NP_033368/P51807
	Human *DYNLT3*	TCTE1L [126]; rp3 [126]; TCTEX1-L [126]; TCTL_HUMAN[f]	HsaXp21	6990	NM_006520	NP_006511/P51808
	Mouse *Dynlt3*	Tcte1l [187]; 2310075M16Rik [196]; TCTL_MOUSE[f]	MmuX A1.1	67117/1914367	NM_025975	NP_080251/P56387
Cytoplasmic dynein light chain Roadblock	Human *DYNLRB1*	MGC15113 [197]; DNCL2A [142] (bithoraxoid-like protein) [135,198]; BITH [199]; hkm23/mLC7–1 [144]; Robl1 [143]; Roadblock(robl)/LC7 [135]; HSPC162 [200,201]; DL2A_HUMAN[f]	Hsa20q11.21	83658	NM_014183 (isoform a)/ NM_177953 (isoform b)/ NM_177954 (isoform c)	NP_054902/Q9NP97 (isoform a)/ NP_808852 (isoform b)/ NP_808853 (isoform c)
	Mouse *Dynlrb1*	Dncl2a [187]; Dnclc2A; km23/mLC7–1 [144]; 2010012N15Rik [196]; 2010320M17Rik [196]; DL2A_MOUSE[f]	Mmu2 H1	67068/1914318	NM_025947	NP_080223/O88567
	Human *DYNLRB2*	DNCL2B [142] (bithoraxoid-like protein) [135,198]; Robl2 [143]; LC7-like [142]; mLC7–2 [144]; DL2B_HUMAN[f]	Hsa16q23.3	83657	NM_130897	NP_570967/Q8TF09
	Mouse *Dynlrb2*	Dncl2b [187]; DL2B_MOUSE[f]	Mmu8 E1	75465/1922715	NM_029297	NP_083573/Q9DAJ5/AAH48623
Cytoplasmic dynein light chain LC8	Human *DYNLL1*	DCL1 [149]; DNLC1; DNCL1 [202]; M, 8000 LC [104]; M, 8000 DLC [147]; DLC8 [152]; LC8 [72]; LC8a [148]; PIN [153]; hdlc1 [162]; Dlc-1 [203]; DYL1_HUMAN[f]	Hsa12q24.31	8655	NM_003746	NP_003737/Q15701
	Mouse *Dynll1*	Dnclc1 [187]	Mmu5 F	56455/1861457	NM_019682	NP_062656/Q9D6F6
	Human *DYNLL2*	DLC2 [149]; LC8b [148]; MGC17810 [204]	Hsa17q23.2	140735	NM_080677	NP_542408
	Mouse *Dynll2*	Dlc2 [187]; 1700064A15Rik [205]; 6720463E02Rik [205]	Mmu11 C	68097/1915347	NM_026556	NP_080832

"MGC" prefixes are from the NIH Mammalian Gene Collection (MGC) as part of an initiative to identify and sequence cDNA clones containing a full-length open reading frame for human, mouse, and rat [206]. "CGI" prefixes are assigned by the Comparative Gene Identification study, which uses the C. elegans proteome as an alignment template to assist in novel human gene identification from human EST nucleotide databases [207]. "Rik" suffixes are gene aliases assigned by the Riken Genomic Sciences Center (http://genome.gsc.riken.jp). Source: Pfister et al. [210].

[a]HUGO: http://www.gene.ucl.ac.uk/nomenclature. Accessed 25 November 2005.

[b]NCBI: http://www.ncbi.nlm.nih.gov. Accessed 25 November 2005.

[c]MGI: http://www.informatics.jax.org. Accessed 25 November 2005. Mapping position shown in cM or cytogenetic band.

[d]NCBI Entrez Gene: http://www.ncbi.nih.gov/entrez/query.fcgi?db=gene. Accessed 25 November 2005.

[e]SwissProt: http://ca.expasy.org/sprot. Accessed 25 November 2005.

[f]Name as given by SwissProt

[g]Human *DYNC2H1* sequences XM_370652 and XP_370652 are predicted by analysis of genomic sequence (NT_033899) using the NCBI gene-prediction method GNOMON, supported by mRNA and EST evidence. Mouse *Dync1li2* sequences XM_134573 and XP_134573 are predicted by analysis of genomic sequence (NT_033899) using the NCBI gene-prediction method GNOMON, supported by mRNA and EST evidence.

DOI: 10.1371/journal.pgen.0020001.t001

example, *DYNC1H1*), italicized initial upper case and then lower-case letters for mouse *(Dync1h1)*, and for proteins of both species, the same symbols in upper case, upright (DYNC1H1). In accordance with the International Union of Pure and Applied Chemistry standards, isoforms of the intermediate chain gene products are referred to with letters. This nomenclature system can be expanded to other subunits as appropriate. We refer to mapping positions using the prefixes Hsa *(Homo sapiens)* for human and Mmu *(Mus musculus)* for mouse, followed by the chromosomal localization e.g. Hsa2q11, Mmu11.

Table 1 lists the aliases, map position, and protein/DNA-sequence accession data for each known mouse and human cytoplasmic dynein gene. The greatest number of aliases was observed for the cytoplasmic dynein 1 heavy chain 1 *(DYNC1H1)* for which we identified 15 different names. Some alternative cytoplasmic dynein gene names have come from large-scale gene and transcript identification efforts such as the partial *DYNC1H1* clone KIAA0325 and its mouse homolog "mKIA00325," generated by the Kazusa cDNA project [21]. A small number of gene names have been derived from the names of DNA markers and cDNA clones used to identify the genes, for example, cytoplasmic dynein 2 light intermediate chain 1, *DYNC2LI1*, was named DKFZp564A033 after the cDNA sequence and clone of the same name. The heavy chain gene *DYNC1H1* has also been referred to by the name of a marker, Hp22, generated from its human cDNA sequence, as well as the rat-derived marker Rk3-8 and a cDNA clone named HL-3.

Cytoplasmic Dynein Heavy Chain Gene Family *(DYNC1H1, DYNC2H1)*

Figure 2A shows the phylogenetic relationships amongst the dynein heavy chain protein sequences from various organisms. The heavy chain sequences fall into two distinct clades, and the relationships within each clade are generally consistent with known evolutionary distances between the organisms shown. We note that our phylogeny fits well with and extends previous phylogenetic analyses of the heavy chain proteins [22,23]. This analysis indicates that the partial human sequence DNAH12, (AAB09729) [23], is unlikely to be a cytoplasmic dynein.

Cytoplasmic dynein heavy chain 1, DYNC1H1. DYNC1H1, cytoplasmic dynein 1 heavy chain 1, is the largest cytoplasmic dynein subunit, having ~4,600 residues and a molecular weight of >530 kDa. First identified in rat spinal cord and brain and termed Microtubule Associated Protein 1C (MAP1C) [24], DYNC1H1 is a distant member of the AAA family of ATPases and is the cytoplasmic counterpart to axonemal dynein heavy chains [3,25]. DYNC1H1 associates as a homodimer within the cytoplasmic dynein complex and effects the contact and translocation of the dynein complex along microtubules via its large motor domain [8,26] (Figure 1B).

The C-terminal region of DYNC1H1 is the motor domain of the dynein complex and is conserved in all cytoplasmic and axonemal dynein heavy chains. This region is arranged as a heptameric ring with six AAA domains and a seventh domain, the identity of which remains a matter of discussion (Figure 1B) [12,25,27,28]. AAA domains are regions of ATP binding and hydrolysis, and thus they generate the energy required for translocation [29–31]. While the first AAA domain is essential for motor activity [32], reviewed in [30], the first four AAA domains are potentially capable of binding and hydrolysing ATP [33–35]. Contact of the heavy chain with a microtubule is established via an ~15-nm projection that extends between the fourth and fifth AAA domains [28,36]. The N-terminal region of DYNC1H1 is known as the stem, and force production, and therefore translocation, is thought to be achieved through the contact and shift of a 10-nm fold of the stem closest to the first AAA domain [37]. DYNC1H1 dimerization also occurs in the stem, and the intermediate chains and light intermediate chains bind in this region as well [38,39]. The three light chains bind to the intermediate chains [40]. Collectively the five smaller dynein subunits that bind to the N-terminus of DYNC1H1 make up the cargo-binding portion of the dynein complex.

The sequence of full-length mammalian DYNC1H1 was first obtained in rat and mouse [41,42]. Human *DYNC1H1* was identified by screening an adenocarcinoma library with a partial human cDNA [23,43]. As yet, the only mutations reported in mammalian heavy chains have been in the mouse: the *Loa* and *Cra1* strains have allelic point mutations in *Dync1h1* that cause late-onset motor neuron degeneration in heterozygotes and neuronal apoptosis in homozygotes [17]. The loss of both copies of *Dync1h1* has been shown to be lethal during early embryonic development, with disorganization of the Golgi complex, improper distribution of endosomes and lysosomes, and defects in cell proliferation; no phenotype has yet been reported for heterozygote knock-out mice [44].

In *Drosophila*, the dynein heavy chain gene, *Dhc64C*, functions in oogenesis [45,46], oocyte differentiation [47], centrosome attachment during mitosis [48], eye development, cell development in thorax, abdomen, and wing [45], and axonal transport [49]. Homozygous mutations induced by the mutagen ethyl methane sulfonate in *Dhc64C* are larval/pupal lethal, whilst heterozygotes have defects in bristle formation, eye development, and fertility [45]. In *C. elegans*, dynein heavy chain *(dhc-1)* is an essential gene, also known as *let-354* (LEThal) [50]. Extensive mutational analysis has been conducted on *dhc-1* to produce a range of variants from recessive/dominant lethals to temperature-sensitive mutants. The resultant phenotypes invariably include embryonic lethality, spindle orientation defects, polar body abnormalities, and excessive blebbing in the early embryo [51–54].

In the yeast *Saccharomyces cerevisiae*, heavy chain function ensures the alignment and orientation of mitotic spindles. Mutation of the *S. cerevisiae* heavy chain gene *dyn1*, which has 50% similarity (28% identity) to DYNC1H1 over 80% of the protein's length, has been shown to disrupt spindle orientation and reduce the fidelity of nuclear segregation during mitosis [55,56]. Despite this phenotype, *dyn1* mutants remain viable, although *dyn1* and kinesin double mutants are lethal [57]. This observation suggests some functional redundancy for dynein by kinesin motors in yeast. No cytoplasmic dynein 1 heavy chain 1 homolog has unambiguously been identified in *Chlamydomonas*, and neither have dyneins been found in either the Arabidopsis or rice genomes [58,59] (reviewed in [60]). There are many dynein heavy chains in the *Chlamydomonas* genome. However, with the exception of *DYNC2H1*, they appear to be components of the axonemal dyneins.

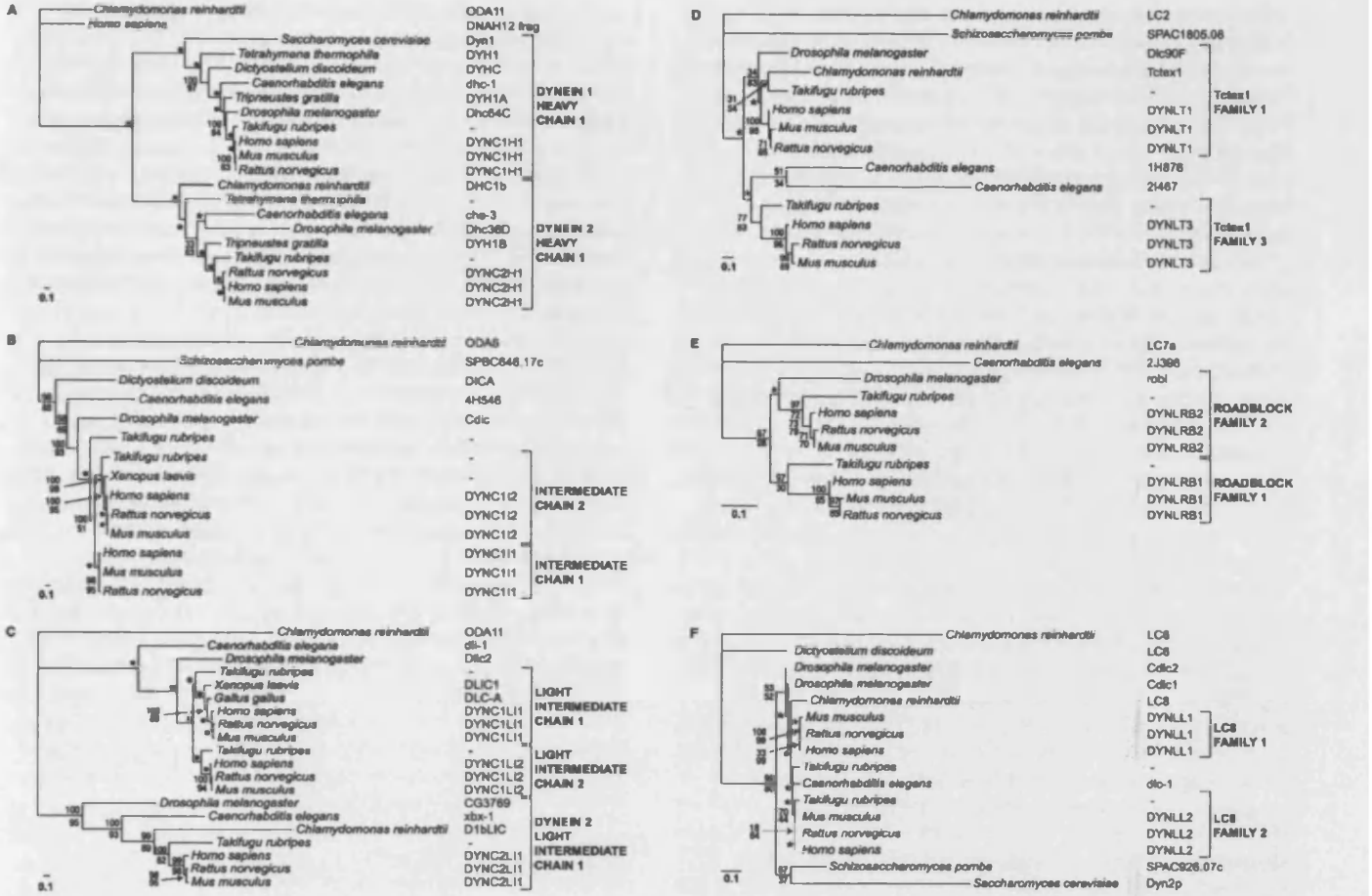

DOI: 10.1371/journal.pgen.0020001.g002

Figure 2. Panel Showing the Protein-Based Phylogenies of the Cytoplasmic Dynein Subunit Families

Species names are shown with NCBI/GenBank gene/protein names. NCBI/GenBank protein-sequence accession numbers are given in Table S1. Orthologous human, mouse, and rat gene names use the revised systematized consensus nomenclature (e.g. DYNC1H1 in humans, mouse, and rat). Relationships amongst dynein sequences of different species do *not* necessarily reflect the evolutionary relationships amongst species; see [208] and [209] for further details. Named clades are indicated in the right margins. Bayesian and maximum-likelihood bootstrap values are shown as percentages (top and bottom, respectively), adjacent to branch points. Asterisks denote bootstraps below 50%. Filled circles denote bootstraps at 100%. Scale-bar represents evolutionary distance (estimated numbers of amino-acid substitutions per site).

(A) Cytoplasmic dynein heavy chain family. *Chlamydomonas* outer arm heavy chain *(ODA11)* is used as the outgroup. DNAH12frag is the partial axonemal heavy chain fragment taken from [23]. For mouse DYNC2H1, XP_35830, only partial protein sequence (336aa) was available in the GenBank database. Adding this partial sequence to our analysis resulted in spurious clustering, therefore we obtained an extended, putative sequence by using BLAST (TBLASTN) against the mouse genome (Build 32) with human and rat sequences XP_370652 and NP_075413, respectively. Incomplete mouse genomic assembly at the *DYNC2H1* locus yielded a truncated sequence 3455 amino acids in length, 85% the length of human DYNC2H1.

(B) Cytoplasmic dynein intermediate chain family. The *Chlamydomonas* IC2 *(ODA6)* is used as the outgroup.

(C) Cytoplasmic dynein light intermediate chain family. There does not appear to be a sufficiently distant homolog in *Chlamydomonas* to be used as an outgroup in this analysis, therefore ODA11 (Q39610, a heavy chain protein) was chosen as the outgroup for this tree.

(D) Cytoplasmic dynein light chain Tctex1 family. The *Chlamydomonas* LC2 light chain is used as the outgroup.

(E) Cytoplasmic dynein light chain Roadblock family. The *Chlamydomonas* outer arm dynein LC7a, is used as the outgroup.

(F) Cytoplasmic dynein light chain LC8 family. The *Chlamydomonas* Q39579 sequence is used as an outgroup. This phylogeny is poorly resolved, with low bootstrap support values and posterior clade probabilities, most likely due to there being little variation amongst the ingroup sequences. We found good support for the LC8 light chain 1 clade, and some support for the LC8 light chain 2 clade, of four vertebrate sequences. The relationships of the two sequences, C. elegans and *Takifugu* were poorly resolved, and therefore we have not included these in the LC8 light chain 2 clade.

Cytoplasmic dynein 2 heavy chain 1, DYNC2H1. The cytoplasmic dynein 2 heavy chain, DYNC2H1, was originally identified in sea urchin embryos by Gibbons and colleagues and was termed DYH1b [61]. It is much less abundant than DYNC1H1 and does not appear to heterodimerize with DYNC1H1; biochemical analyses suggest that DYNC2H1 is a homodimer [16]. DYNC2H1 contains regions characteristic of cytoplasmic dyneins, for example, human DYNC1H1 and DYNC2H1 sequences are similar within both the motor region and around the light intermediate chain–binding site [15]. However, the expression of its mRNA increases during embryonic reciliation, a property typical of axonemal dyneins, suggesting a flagellar role for an otherwise cytoplasmic-like dynein heavy chain. The flagellar properties of DYNC2H1 were clarified with its identification as the motor responsible for retrograde (tip to base) IFT, in *Chlamydomonas*, a process required for assembly and maintenance of the eukaryotic cilium/flagellum [6,22].

DYNC2H1 is also important in modified ciliary structures such as nematode mechanosensory neurons [62] and vertebrate photoreceptors [63,64]. In *C. elegans*, the DYNC2H1 homolog, che-3, is expressed in ciliated sensory neurons which are thought to be involved in odorant chemotaxis [65]. Mutations of che-3 affect IFT, the establishment and maintenance of sensory cilia, which are stunted and swollen in the mutants, [62,66], chemotactic behavior [67], and formation of the third larval stage, dauer formation [68].

The first mammalian DYNC2H1 gene was described in rat, designated DLP4 [69], and full-length sequence has been obtained [15]. Genetic and biochemical studies suggest that DYNC2H1 associates with a member of the light intermediate chain family, DYNC2LI1 (Figure 1B, and see discussion of the light intermediate chain family below) [14,16,70–73] and possibly also with DYNLL1 (LC8) light chain [72]. In mice *Dync2h1*, mRNA is abundant in the olfactory epithelium and the ependymal layer of the neural tube; antibodies against DYNC2H1 and DYNC2LI1 strongly stain these tissues and connecting cilia in the retina as well as primary cilia of non-neuronal cultured cells [15]. The co-localization of DYNC2H1, DYNC2LI1, and homologs of the IFT pathway in mammalian ciliated tissues supports a specific role for DYNC2H1 in the generation and maintenance of mammalian cilia [14,16]. Other antibody studies suggest that DYNC2H1 localizes to the cytoplasm of apical regions of ciliated rat tracheal epithelial cells, but not in the cilia themselves [74]. In non-ciliated human COS cells, antibodies against DYNC2H1 show Golgi localization and induce Golgi dispersion, suggesting a cytoplasmic role for DYNC2H1 [23].

Cytoplasmic Dynein Intermediate Chain Gene Family *(DYNC1I1, DYNC1I2)*

Intermediate chains are present in axonemal and/or cytoplasmic dyneins from yeast to mammals (Figure 2B). Protein-sequence data demonstrate evolutionary distant relationships between axonemal and cytoplasmic dynein intermediate chains; for example, rat DYNC1I1 has 48% similarity to the *Chlamydomonas* IC2 axonemal outer arm dynein intermediate chain encoded by the ODA6 locus [75,76]. Figure 2B shows the dynein intermediate chain protein phylogeny. The intermediate chain sequences fall into two distinct clades, intermediate chains 1 and 2, comprised of vertebrate species only. An alternative placement of a *Takifugu* sequence, as a member of the intermediate chain 1 clade, is almost as well supported by the data as the placement shown in Figure 2B (49% bootstrap support against 51% support). In view of this and with all non-vertebrate species falling outside these clades, the data suggest a recent evolutionary origin for the split into intermediate chain gene 1 and intermediate chain gene 2, perhaps as part of a "2R" event of genome duplication (see [77] for review). The absence of an amphibian *(Xenopus)* intermediate chain 1 protein may be due to the current paucity of *X. laevis* sequences in the GenBank sequence database (http://www.ncbi.nlm.nih.gov/Genbank).

The cytoplasmic dynein 1 intermediate chains have a molecular weight of ~74 kDa [5] and associate in the cytoplasmic dynein complex with a stoichiometry of two intermediate chains per complex [40,78]. DYNC1I1 and DYNC1I2 proteins are thought to help assemble the cytoplasmic dynein complex and to bind various cargoes. The intermediate chains interact with the dynein activator, dynactin, via their conserved N-termini [79]. The DYNC1I C-termini contain a WD repeat domain [76,80,81] that is conserved between cytoplasmic and axonemal intermediate chains and is important for intermediate chain–binding to the heavy chains [76,82]. The dynein light chains, DYNLL1 (LC8) and DYNLT1 (Tctex1), bind near the N-termini of the intermediate chains [83–85], and the DYNLRB (Roadblock) light chains bind just upstream of the WD repeat region [40]. The DYNC1I are phosphorylated, and phosphorylation at one site regulates DYNC1I2 interaction with the p150 subunit of dynactin [86,87].

The *Chlamydomonas* IC2 axonemal intermediate chain was localized to the base of the dynein heavy chain dimer by immunoelectron microscopy [88]. Steffen and colleagues identified a similar location for the cytoplasmic dynein intermediate chain and found that antibodies to it block dynein binding to membrane-bound organelles [89,90]. These data indicate a role for DYNC1I in targeting the dynein complex to various cargoes, including membranous organelles and kinetochores [76,79,89]. In *Drosophila*, mutations in dynein intermediate chain, Cdic (also referred to as cDic and Dic), lead to larval lethality, demonstrating that this intermediate chain provides an essential function. Cdic mutations dominantly enhance the rough-eye phenotype of *Glued*, a dominant mutation in the p150 subunit of dynactin [91]. *Shortwing (sw)* is an allele of the dynein intermediate chain gene but, unlike other Cdic alleles, *sw* is homozygous viable and gives rise to a recessive, temperature-sensitive defect in eye and wing development [91].

We note that in *Drosophila*, the Cdic gene lies in the 19DE region of the X chromosome, adjacent to several dynein intermediate chain-like sequences. These sequences are derived from a 7-kb duplication/deletion event involving Cdic and its proximal gene annexin X, which encodes a cell-surface-adhesion protein [92]. The duplication/deletion of this 7-kb region resulted in the formation of a de novo coding sequence, under the control of a testes-specific promoter, called sperm-specific dynein intermediate chain gene *(Sdic)* [93]. The de novo region has undergone at least 10-fold tandem duplication, which has given rise to a multi-gene family comprising at least four classes of *Sdic* gene, of which more than one class is functional [93].

Cytoplasmic dynein 1 intermediate chain 1, DYNC1I1. Multiple DYNC1I1 isoforms exist in mammals. They are the products of alternative splicing of the N-terminal region of a single *DYNC1I1* gene and phosphorylation [76,79,86]. In humans, alternate splicing may arise from cryptic splice-acceptor sites located within exon 4 of this 17-exon gene [94]. Two DYNC1I1 isoforms were found in rat brain and DYNC1I1 mRNA, and protein isoform expression is regulated during rat brain development, and a single DYNC1I1 isoform is found in testis. DYNC1I1 expression is also cell-specific: cultured rat neurons express at least two DYNC1I1 alternative splicing variants and their phosphorylated isoforms, while cultured glial astrocytes do not express any *DYNC1I1* gene products [95–97]. In the mouse, expression of *Dync1i1* has been shown to be restricted primarily to the brain, with weak expression in testis [94], further supporting possible neuronal specificity for *Dync1i1*. As with the other dynein subunits, the isoform diversity of the intermediate chain is thought to result in specific populations of dynein

molecules that have specific functions; for example, both DYNC1I1 isoforms are components of cytoplasmic dynein found in the slow component of axonal transport in the optic nerves [95]. Multiple isoforms of the *Drosophila* intermediate chains are also produced by alternative splicing of the single gene [92].

Cytoplasmic dynein 1 intermediate chain 2, DYNC1I2. Vaughan and Vallee used a partial human cDNA sequence with identity to the already known *DYNC1I1* gene as a probe to isolate a rat *Dync1i2* cDNA; predicted human and rat *DYNC1I2* sequences are 94% identical [79], and the existence of two genes was supported by mapping data that placed *Dync1i1* and *Dync1i2* at distinct loci within the mouse genome [98]. Like *Dync1i1*, *Dync1i2* produces different splice isoforms: alternative splice sites lie at two positions within the N-terminal region. The expression of *Dync1i2* isoforms is ubiquitous with the rat DYNC1I2C isoform being expressed in all tissues and cells examined [79,94,96,97]. During rat brain development, DYNC1I2C is the only isoform found before E14 (embryonic day 14) and it is often the only isoform observed in cultured cells [96,99]. During nerve growth-factor stimulation of PC12 cell differentiation and neurite extension, there is a change in relative expression levels of the DYNC1I2 isoforms [100]. In the rat optic nerve, it has been shown that the DYNC1I2C isoform is the only intermediate chain involved in the fast component of anterograde transport to the axon tip [95,99].

The strong expression of *Dync1i2* in the mouse developing limb bud led to the suggestion that DYNC1I2 may play a role in limb development and digit patterning and/or in establishing cell polarity [94]; dynein may not do this directly, but may mediate these processes by orientating intracellular components correctly [101].

Cytoplasmic Dynein Light Intermediate Chain Gene Family *(DYNC1LI1, DYNC1LI2, DYNC2LI1)*

Figure 2C shows the phylogenetic relationships amongst the dynein light intermediate chain protein sequences from various organisms. The light intermediate chains can be separated into three distinct groups: the two light intermediate chains that are components of cytoplasmic dynein 1, DYNC1LI1 and DYNC1LI2, are more closely related to each other than to the cytoplasmic dynein 2 light intermediate chain, DYNC2LI1. Hughes and colleagues first proposed the name light intermediate chains for these subunits [102], although these polypeptides were also referred to as light chains [103] prior to the discovery of the smaller light chains [104]. The mammalian cytoplasmic dynein complex contains four species with molecular masses of 50–60 kDa that resolve into numerous isoforms on 2D gels [86,102]. The multiple isoforms observed in 1D and 2D gels are thought to be the result of post-translational phosphorylation, although the possibility of alternate splicing has not been eliminated [86,102,103]. A third gene, *DYNC2LI1*, has recently been described which encodes a protein that appears to exclusively associate with DYNC2H1 in the cytoplasmic dynein 2 complex [14–16,71]. Unlike the other subunits of cytoplasmic dynein, homologs of the DYNC1LIs have not yet been identified in the axonemal dyneins [105]. The function of the DYNC1LIs has yet to be determined, although it has been suggested that they may regulate the interactions of dynein with dynactin, or with sub-cellular cargoes of dynein-mediated motility. DYNC1LI1 and DYNC1LI2 form only homo-oligomers, and their mutually exclusive binding to the N-terminal base of the dynein heavy chain is consistent with a role in cargo binding [38].

C. elegans appears to have one light intermediate chain *(dli-1)* for cytoplasmic dynein (DYNC1H1-based complexes), and one *(xbx-1)* for cytoplasmic dynein 2 (DYNC2H1-based complexes) [73]. *dli*-1 is required for dynein function during mitosis, pronuclear migration, centrosome separation, and centrosome association with the male pronuclear envelope [106], as well as retrograde axonal transport. Mutations in dli-1 lead to an accumulation of cargo at axonal terminals [52]. Disruption of *xbx-1* results in ciliary defects and causes behavioral abnormalities that are observed in other cilia mutants [14]. Binding of dli-1 to ZYG-12 is thought to be the mechanism for dynein binding to the nuclear envelope [107].

Cytoplasmic dynein 1 light intermediate chain 1, DYNC1LI1. DYNC1LI1 was cloned from rat [38] and found to have a P-loop motif, which is one of the major conserved motifs making up the nucleotide-binding domain found in numerous proteins, including ATPases and kinases [108]. DYNC1LI1, however, lacks other essential motifs associated with ATPase activity, which itself has not been assayed. Tynan showed that pericentrin, a known dynein cargo, binds DYNC1LI1 and not DYNC1LI2 [38]. DYNC1LI and its phospho-isoform are exclusively found with dynein in the slow component of axonal transport in rat optic nerves [95]. In HeLa cells, DYNC1LI1 localizes to the microtubule organizing centre and mitotic spindle, co-localizing with the GTPase Rab4a (which interacts with the central domain of DYNC1LI1 [109]); thus DYNC1LI1 may be implicated in the regulation of membrane-receptor recycling. Phosphorylation of the *Xenopus* DYNC1LI has been implicated in regulation of dynein binding to membrane-bound organelles [110]. It is thought that *Xenopus* melanosomes contain a distinct dynein light intermediate chain protein, possibly a version of DYNC1LI1 [111]. In the chicken *(Gallus gallus)* DYNC1LI1 has been called DLC-A, as part of the DLC-A group of light chains [103].

Cytoplasmic dynein 1 light intermediate chain 2, DYNC1LI2. DYNC1LI2 is paralogous to DYNC1LI1 and is also thought to be post-translationally modified by phosphorylation [86,102,103]. DYNC1LI2 is found in both the fast and slow components of axonal transport in rat optic nerves, although its phospho-isoforms are found only in the slow component of axonal transport. During nerve growth-factor stimulation of PC12 cell differentiation and neurite extension, *DYNC1LI2* gene expression is up-regulated [112], and phosphorylation of both DYNC1LI1 and DYNC1LI2 is increased [100]. Like DYNC1LI1, the chicken *(G. gallus)* DYNC1LI2 has also been termed DLC-A, as part of the DLC-A group of light chains [103].

Cytoplasmic dynein 2 light intermediate chain 1, DYNC2LI1. *DYNC2LI1* is a light intermediate chain that was identified in mammals by two groups and was originally designated D2LIC [14] and LIC3 [15]. DYNC2LI1 is the light intermediate chain that associates with DYNC2H1 in the cytoplasmic dynein 2 complex: Grissom and colleagues observed that DYNC2LI1 co-immunoprecipitated specifically with DYNC2H1 and co-localized with DYNC2H1 at the Golgi

apparatus. Mikami and coworkers [15] found the 350-amino acid LIC3 polypeptide (AAD34055) had a 24% similarity to rat DYNC1LI2 but failed to observe Golgi localization. DYNC2LI1 has been identified in mouse, *C. elegans*, *Drosophila*, and *Chlamydomonas* [14,16]. A targeted deletion of *Dync2li1* in mouse affects development, in particular ventral cell fates and axis establishment in the early embryo [113]. In *Chlamydomonas*, DYNC2LI1 (D1bLIC) is essential for retrograde IFT [71]. As mentioned above, DYNC2LI1 appears to bind exclusively with DYNC2H1; in agreement with this, we find DYNC2LI1 homologs in species that have DYNC2H1. The exclusive association of DYNC2H1 and DYNC2LI1 with one another, and not with any of the other cytoplasmic dynein subunits, emphasizes the distinct cellular identities and roles of these separate DYNC1H1 and DYNC2H1 dynein complexes.

Cytoplasmic Dynein Light Chain Gene Families

There are three known dynein light chain gene families that are components of cytoplasmic dynein 1: (1) the *t*-complex-associated family *(DYNLT1, DYNLT3)*, (2) the Roadblock family *(DYNLRB1, DYNLRB2)*, and (3) the LC8 family *(DYNLL1, DYNLL2)*. The gene families are named according to their original discovery, through the effect of mutations in mouse (*t*-complex associated, Tctex1) and *Drosophila* (Roadblock), or according to the size of the protein in *Chlamydomonas* (LC8) as discussed below. We present each family by molecular weight, starting with the largest light chain protein gene family, the *t*-complex-associated family (~113 amino acids), through to the Roadblock family (~96 amino acids) and the smallest light chain proteins, the LC8 family (~89 amino acids). As described below, some of the light chains have cellular functions that are independent of their role in the cytoplasmic dynein 1 complex.

Cytoplasmic Dynein Light Chain Tctex1 Gene Family *(DYNLT1, DYNLT3)*

Figure 2D shows the phylogenetic relationships amongst the dynein light chain Tctex1-family protein sequences from various organisms. Our phylogeny shows distinct clades for DYNLT1-like and DYNLT3-like sequences. Tctex2-like sequences lie closer to the outgroup than they do to the DYNLT1 and DYNLT3 clades (not shown).

Cytoplasmic dynein light chain Tctex1, DYNLT1. *Tctex1* (*t*-complex *t*estis-*ex*pressed) gene was originally identified within the mouse *t-complex* (a 30- to 40-Mb region of Mmu17) as a candidate for one of the "distorter" products responsible for the non-Mendelian transmission of variant *t* haplotypes [114]. Lader et al. [114] and O'Neill and Artzt [115] found evidence of four copies of *Dynlt1 (Tctex1)* in the mouse genome; we found that the current genomic sequence databases appear to contain only one such locus that maps to Mmu 17, although a processed pseudogene has also been described on Mmu6. Subsequently, DYNLT1 was found to be an integral component of cytoplasmic dynein [116], and has since also been identified within axonemal inner and outer arm dyneins [117,118]. DYNLT1 binds to the N-terminus of the intermediate chain DYNC1I [85]. Many studies have identified DYNLT1 as a binding partner for various cellular proteins, and it has been suggested that it may attach specific proteins or cellular components to cytoplasmic dynein; for example, DYNLT1, but not its homolog DYNLT3 (see below), binds to the C-terminal domain of rhodopsin and is required for the trafficking of this visual pigment within photoreceptors [119]. The two DYNLT1 polypeptides in the cytoplasmic dynein complex dimerize, and their dimer structure is similar to that of the DYNLL1, LC8, dimer [116,120–122]. The evidence suggests that the same *Dynlt1* gene product is a component of both axonemal and cytoplasmic dyneins in mouse [117]. The binding site on DYNC1I for DYNLT1 has been mapped to a 19-amino acid region at the N-terminus [85].

The *Schizosaccharomyces pombe* DYNLT-like gene SPAC1805.08 (also referred to as Dlc1) is involved in movement of nuclear material during meiotic prophase and is expressed in astral microtubules and microtubule-anchoring sites on the cell cortex. The Dlc1 localization pattern is similar to that of cytoplasmic dynein heavy chain Dhc1 [123]. Dlc1 null mutants are viable but have irregular nuclear movement during meiosis and defects in sporulation, recombination, and karyogamy [123]. Genetic analyses in *Drosophila*, which appears to have only one member of the DYNLT family, suggest that DYNLT1 is not essential for cytoplasmic dynein function, as the null mutation is not lethal. However, the mutants do have sperm-motility defects, suggesting they do have an essential role in axonemal dynein [124,125]. In *Chlamydomonas*, Tctex1 is an axonemal inner arm dynein component [117], and recently a variant form has been identified in axonemal outer arm dynein (DiBella et al., in press).

Cytoplasmic dynein light chain, DYNLT3. Closely related to *DYNLT1* is *DYNLT3*, also known as rp3 because it was initially a candidate for causing X-linked retinitis pigmentosa type 3 [126]. However, the actual gene that is defective in this disease was later identified as a guanine nucleotide exchange factor that is unrelated to *DYNLT3* [127]. Subsequently, King and colleagues found that DYNLT3 is a cytoplasmic dynein light chain that is differentially expressed in a cell- and tissue-specific manner [78,116]. Interestingly, while many proteins have been identified as binding partners for DYNLT1, none have been identified as binding exclusively to DYNLT3, though recently the *Herpes simplex* virus capsid protein VP26 has been shown to bind both DYNLT1 and DYNLT3 [128]. There is no evidence that DYNLT3 is a component of axonemal dyneins.

Axonemal dynein light chain, *Tctex2*. To avoid confusion with Tctex2, an axonemal dynein subunit, the DYNLT2 designation is not used: a third human *t*-complex *t*estis-*ex*pressed gene, originally characterized by Rappold and colleagues [129,130], was given the name *Tctex2*, and is also known as LC2, *TCTE3*, and *Tcd3*. Patel-King and colleagues demonstrated that it has 35% identity to the 19,000-M_r (relative mobility) axonemal outer arm dynein light chain (LC2) of *Chlamydomonas* [131], and that it is distantly related to cytoplasmic light chains DYNLT1 and DYNLT3 [116,120]. LC2 is essential for outer arm dynein assembly [132]. There is evidence that Tctex2 may interact substoichiometrically with cytoplasmic dynein, but there has not yet been a definitive demonstration that it is a cytoplasmic dynein subunit.

In mice, expression of *Tctex2* is testis-specific, particularly in later spermatogenic stages, and isoforms are thought to be generated by alternative splicing [130]. As yet, isoforms of the human homolog have not been identified, and its expression

is restricted to tissues containing cilia and flagella [133]. Mutations in *Tctex2* have been implicated in the autosomal recessive disorder primary ciliary dyskinesia, which results in the impairment of ciliary and flagellar function, although these mutations are thought not to be the primary cause of the disorder [133].

Mouse *Tctex2* lies within the Mmu17 *t*-complex in a central region containing the distorter/sterility locus *Tcd3* [134]. Human *Tctex2* maps to the long arm of Chromosome 6 [129] and, interestingly, is a neighbor of the two genes, *TCP1* and *TCP10,* which are also homologs of mouse *t*-complex loci found adjacent to mouse *Tctex2*. This conservation of gene order suggests that the region of Chromosome 6q containing these genes is syntenic to the homologous central region of mouse Chromosome 17. In contrast, DYNLT1 and DYNLT3 are located on human Chromosome 6p and show synteny to the distal portion of the mouse *t*-complex, suggesting that the middle and distal portions of the mouse *t*-complex are syntenic to the long and short arms of human Chromosome 6, respectively [129].

Cytoplasmic Dynein Light Chain Roadblock Gene Family *(DYNLRB1, DYNLRB2)*

The first Roadblock gene was identified in *Drosophila* through mutational analyses, and from biochemical and sequence comparisons with the *Chlamydomonas* outer arm dynein LC7a light chain [135,136]. *Drosophila* has at least six Roadblock homologs, including bithoraxoid, which has been implicated in thoracic and abdominal parasegment development. These proteins belong to an ancient family that has been implicated in NTPase regulation in bacteria [137]. Mutations in the Roadblock genes result in the accumulation of axonal cargoes, mitotic defects, female sterility, and either larval or pupal lethality [135]. Roadblock mutations also affect neuroblast proliferation and result in reduced dendritic complexity, as well as in defects in axonal transport [138]. Mutational analysis in *Chlamydomonas* suggests that DYNLRB (LC7a) is involved in axonemal outer arm dynein assembly, and a related protein (LC7b) is associated with dynein regulatory elements [136,139].

Figure 2E shows the phylogenetic relationships amongst the dynein light chain Roadblock-family protein sequences from various organisms. The Roadblock sequences are remarkably well conserved between different organisms, with 96% of pair-wise sequence comparisons amongst all sequences shown in Figure 2E demonstrating an identity greater than 50% (data not shown). The high conservation of Roadblock-family sequences presumably arises from functional constraints on the proteins. We note that genes in mammals and in other species incorporate conserved and complete Roadblock sequences (known as Roadblock domains) within their coding regions [135,137]. However, these genes are not thought to be cytoplasmic dyneins; for example, MAPBPIP in human and mouse appears to function mainly in the endosome/lysosome pathway [140]. Both DYNLRB polypeptides are found in mammalian cytoplasmic dynein, but it is not yet known if just one, or both, are utilized in mammalian axonemal dyneins.

Cytoplasmic dynein light chain Roadblock1, DYNLRB1. Database searches [135,141] (Figure 2E) revealed there are two Roadblock-related proteins in mammals, DYNLRB1 and DYNLRB2 (also termed DYNLC2A and DYNLC2B) [142]. Biochemical studies suggest that in mammals both Roadblocks exist as homo- and heterodimers that associate with cytoplasmic dynein [143] through specific binding sites on the intermediate chains, distinct from those for the DYNLL (LC8) and DYNLT (Tctex1) light chains [40]. Expression studies in humans have identified tissue-specific differences in the expression of the two human Roadblock-like genes, with strong expression of *DYNLRB1* in heart, liver, and brain, and up-regulation in hepatocellular carcinoma tissues [142]. In a role that may be independent of its association with cytoplasmic dynein, TGFb phosphorylation of human DYNLRB1 (termed mLC7–1/km23 by Tang and colleagues [144]) results in the human DYNLRB1 binding to the TGFb receptor that mediates TGFb responses including JNK activation, c-JUN phosphorylation, and growth inhibition.

Cytoplasmic dynein light chain Roadblock 2, DYNLRB2. *DYNLRB2* was identified by EST database searches for sequences homologous to *Chlamydomonas* LC7a [135,141]; human *DYNLRB2* was cloned in 2001 [142] and was found to be differentially expressed in various tissues, including hepatocellular carcinomas.

Cytoplasmic Dynein Light Chain LC8 Gene Family *(DYNLL1, DYNLL2)*

Cytoplasmic dynein light chain LC8 1, DYNLL1. DYNLL (the light chain that has been known as LC8, as well as LC8a and PIN) is a component of many enzyme systems, and it has a long and somewhat confusing history. This protein was originally identified, using biochemical methods, as a light chain of the *Chlamydomonas* axonemal outer arm dynein [145,146]. The term LC8 derives from the observation that this component migrates at ~8 kDa in SDS-PAGE gels, and it is also the smallest of the eight light chains then known within this *Chlamydomonas* axonemal dynein. It was first cloned from *Chlamydomonas,* and closely related sequences were identified in mouse and nematode along with more distantly related proteins in higher plants [147,148]. Using biochemical and immunochemical methods, DYNLL was also identified as an integral component of brain cytoplasmic dynein [104]. Only recently, it has been realized that mammals have two closely related DYNLL genes, and that the protein products of both genes are components of cytoplasmic dynein [148,149]. Thus, most of the studies on the cellular roles of DYNLL do not distinguish between the two DYNLL polypeptides.

Another factor complicating efforts to elucidate the role of the DYNLL polypeptides in dynein function was the realization that large amounts of DYNLL1 in brain, and presumably cells in general, are not associated with the dynein complex [104]. In fact, the DYNLL polypeptides have other important functions unrelated to their role in axonemal and cytoplasmic dyneins. DYNLL1 is a subunit of the flagellar radial spokes which are involved in control of axonemal dynein motor function [150]. DYNLL1 is also a substrate of a p21-activating kinase, and its interaction with the kinase may be important for cell survival [151]. A DYNLL is an integral component of the actin-based motor myosin V [152]. Immunostaining shows that a DYNLL is concentrated in dendritic spines and growth cones, and it is proposed that this is due to its association with the actin-based motor

myosin V [149]. DYNLL1 was identified within neuronal nitric oxide synthase (nNOS) [14] and named "PIN" for "protein inhibitor of nNOS" [153]. However, it is unclear whether it is actually an inhibitor of nNOS or is merely a component of the nNOS complex, as DYNLL1 appears to be required for the stability of various multimeric enzyme complexes. DYNLL1 has been found to interact with a wide variety of other cytoplasmic components, including the pro-apoptotic factor Bim [154], *Drosophila* swallow [155,156], and rabies virus P protein [157], and it may act to attach them to the dynein and/or myosin-V molecular motors. In addition, there are *many* other DYNLL-interacting proteins not mentioned here that have been identified using yeast two-hybrid screens and other methods.

There are two copies of DYNLL in the cytoplasmic dynein complex, and the crystal and NMR structures of the DYNLL dimer with bound peptide are known [104,158–160]. Both monomers contribute to the formation of two symmetrical grooves in the dimer that are the binding sites for two DYNC1I polypeptides reviewed in [161]. Adding DYNLL to an N-terminal polypeptide of DYNC1I in vitro increases the structural order of DYNC1I, suggesting that DYNLL is important for the assembly of a functional dynein complex [84].

Figure 2F shows the phylogenetic relationships amongst the dynein light chain LC8-family protein sequences from various organisms. Our phylogeny shows that the mammalian LC8 light chain family falls into two distinct clades containing DYNLL1- and DYNLL2-like genes. DYNLL is highly conserved from alga and humans, and homologs are required for sensory axon projection and other developmental events in *Drosophila* [162,163], nuclear migration in *Aspergillus* [164], and retrograde IFT in *Chlamydomonas* [72]. The phenotype of partial loss-of-function mutants in *Drosophila* revealed a wide array of pleiomorphic developmental defects; the total loss-of-function mutation was embryonic lethal [162]. The *Drosophila* dynein light chain 1 (Cdlc1, also known as ddlc1 and "cut-up" *[ctp]*) is ubiquitously expressed during development and in adult tissue, and is required for proper embryogenesis and cellular differentiation. Mutations in this gene result in female sterility, which may be due to the severely disordered cytoskeletons of ovarian and embryonic cells [162]. A high degree of sequence similarity (92%) exists between *Drosophila* Cdlc1 and the 8-kDa flagellar outer arm dynein light chain from *Chlamydomonas*, and with human and *C. elegans* light chain 1 (91%), suggesting this gene has been under strong selective pressure [162]. *S. pombe* has a single known DYNLL homolog, SPAC926.07c (also referred to as Dlc2); it is transcribed during the vegetative phase, induced at low level in the sexual phase, and is enriched at the nuclear periphery [123]. A Dlc2 null mutant has been described with marginally reduced recombination in meiosis, but no other reported phenotype [123].

During the course of homology searches for this paper, we noted that *DYNLL1* has related sequences in several locations in the human genome (data not shown); none of these appear to be associated with expressed sequences and thus may be pseudogenes. There was also a discrepancy in the likely mapping position of *DYNLL1*, and therefore we carried out a sequence analysis of *DYNLL1*-related genomic loci and show that the cognate human locus lies on Hsa12q24.31 (data not shown), which agrees with the mouse mapping result of *Dynll1* on Mmu5.

Cytoplasmic dynein light chain LC8 2, DYNLL2. DYNLL2, also known as DYNLL2 and LC8b, is the second member of this light chain family. It was identified by micro-sequencing of polypeptides from purified brain cytoplasmic dynein [148] and a yeast two-hybrid screen [149]. Mammalian DYNLL1 and DYNLL2 have 93% identity, differing by only six amino acids out of 89. Indicative of the extraordinary conservation of these proteins, the amino acid sequences of both DYNLL1 and DYNLL2 from human, mouse, rat, pig, and cow are identical [148]. Human DYNLL2 was identified in a yeast two-hybrid screen using the guanylate kinase–associated protein (GKAP) as bait and may mediate the interaction between GKAP and actin- and microtubule-based motors, allowing GKAP and its associated proteins to be translocated as a cargo, although DYNLL1 also binds to GKAP [149]. DYNLL2 binds the pro-apoptotic factor Bmf, which binds Bcl2, neutralizing its antiapoptotic activity, a role comparable to that reported for the binding of Bim to DYNLL1 [165]. However, it has also been observed that Bim and Bmf have identical binding affinities for both DYNLL1 and DYNLL2 [166].

It has further been proposed that DYNLL1 binds specifically to the dynein intermediate chain DYNC1I, while DYNLL2 binds to the myosin-V heavy chain. However, DYNLL2 co-purifies with cytoplasmic dynein from various rat tissues [148], and DYNLL1- and DYNLL2-GST are equally effective in binding myosin V [149]. Furthermore, DYNLL1 and DYNLL2 bind with equal affinity to DYNC1I in pair-wise yeast two-hybrid studies (K. W. Lo and K. K. Pfister, unpublished data). It is not yet known if one, or both, of the DYNLL polypeptides are associated with axonemal dyneins; however, DYNLL1 is enriched in testes and lung—tissues that have large numbers of cilia or flagella [148].

Human and Mouse Cytoplasmic Dyneins: Nomenclature, Map Positions, and Sequences

To create Table 1, we cataloged, by literature searches, all known gene and protein names for the cytoplasmic dyneins in mouse and human. In addition, aliases were recorded from the single-query interface LocusLink (http://www.ncbi.nlm.nih.gov/LocusLink) and the Mouse Genome Informatics (MGI) website (http://www.informatics.jax.org). We also included aliases previously approved by the HUGO Gene Nomenclature Committee (http://www.gene.ucl.ac.uk/nomenclature) as well as aliases referenced in sequence submissions to the GenBank (http://www.ncbi.nlm.nih.gov/Genbank) and Entrez (http://www.ncbi.nlm.nih.gov/entrez) sequence databases [167].

Human and mouse orthologs in Table 1 are taken from the literature and databases. Human and mouse chromosomal locations were obtained from the literature and from the MGI and LocusLink databases. The OMIM numbers given for gene and disease loci in humans refers to the unique accession numbers in the On-line Mendelian Inheritance in Man database (http://www.ncbi.nlm.nih.gov/entrez/query.fcgi?db=OMIM). Nucleotide and protein sequences (prefix NM__ and NP__, respectively) are National Center for Biotechnology Information (NCBI) Reference Sequence (RefSeq, http://www.ncbi.nlm.nih.gov/RefSeq) and Swiss-Prot accession numbers (http://www.ebi.ac.uk/swissprot), respectively [167]. The NCBI RefSeq project provides a non-redundant and comprehensive collection of nucleotide and

protein sequences drawn from the primary-sequence database GenBank. RefSeq collates and summarizes primary-sequence data to give a minimal tiling path for individual transcripts, using available cDNA and genomic sequence whilst removing mutations, sequencing errors, and cloning artifacts. Sequences are validated in silico by NCBI's Genome Annotation project to confirm that any genomic sequence incorporated into a RefSeq cDNA matches primary cDNA sequences in GenBank, and that the coding region really can be translated into the corresponding protein sequence. Accession numbers beginning with the prefix XM__ (mRNA) and XP__ (protein) are RefSeq sequences of transcripts and proteins that are annotated on NCBI genomic contigs; these may have incomplete cDNA-tiling-sequence data or contig sequences [168]. For dyneins with known isoforms, isoform-sequence accession numbers available within nucleotide and protein databases are given.

Included in the heavy chains that we found were "Cell Division Cycle 23, yeast homolog" *(CDC23)* and "Cell Division Cycle 22, yeast homolog" *(CDC22)*, which are GenBank aliases for human and mouse dynein heavy chain 1, respectively. We found no evidence in the literature to support the "CDC" designation of these genes and their products in terms of either "Cell Division Cycle" or "Cytoplasmic Dynein Chain". We compared mouse and human heavy chain 1 cDNA and protein sequences with mouse, human, and yeast CDC23 and CDC22 sequences and found no similarity to support this designation (data not shown). We concluded that the synonym CDC had most likely been attributed in error, and we contacted NCBI who, in agreement with our findings, removed the CDC designation from the sequences involved.

Human/Mouse Homology Searches

Homology searches of human cytoplasmic dynein subunit genes were conducted using position-specific iterative BLAST (PSI-BLAST) [169] at NCBI (http://www.ncbi.nlm.nih.gov/BLAST; Table 2). The PSI-BLAST program identifies families of related proteins using an iterative BLAST procedure [170]. In an initial search, a position-specific scoring matrix is constructed from a multiple sequence alignment of the highest scoring hits. Subsequent iterations using the position-specific scoring matrix are performed in a new BLAST query to refine the profile and find additional related sequences. We used nucleotide and protein sequences from each known human dynein gene to query the human and mouse non-redundant sequence databases at GenBank, using default parameters and the BLOSUM-62 substitution matrix, which has been shown to be the most effective substitution matrix to identify new members of a protein family [171]. Where dynein isoforms were present, the longest sequence was used to search the databases.

Phylogenetic Analysis

To establish gene family groupings, we investigated the phylogenetic relationships between dynein protein homologs in various organisms. Homologous sequences were identified by searching the GenBank non-redundant protein database, with the human protein using PSI-BLAST with default parameters and the BLOSUM-62 substitution matrix. Searches of pufferfish sequence *Takifugu rubripes* (commonly known as *Fugu rubripes*), for which little transcribed sequence exists although a usable genome assembly is present, were performed using the BLAST (TBLASTN) feature at the Ensembl Fugu Genome Browser (version 2.0; http://www.ensembl.org/Fugu_rubripes), searching with human protein sequence against a translated nucleotide database.

Protein sequences were aligned for comparison across their full lengths using the multiple sequence alignment program CLUSTALW [172] (http://www.ebi.ac.uk/clustalw) and applying the GONNET250 matrix as default. The GONNET250 is a widely used matrix for performing protein-sequence alignments, allowing 250 accepted point mutations per 100 amino acids, using scoring tables based on the PAM250 matrix [173].

Two different phylogenetic methods were used to analyse the dynein gene family alignments. Maximum-likelihood trees were inferred under the Jones, Taylor, and Thornton (JTT) empirical model of amino-acid substitution using PHYML version 2.4.3 [174], as was non-parametric bootstrapping using 100 resampled alignments for each gene family. Bayesian analyses were performed using MrBayes version 3.0B4 [175], using the default Bayesian priors on tree topologies and branch lengths. Two different sets of analyses were performed for each gene family, the first allowing the Markov-chain Monte-Carlo algorithm to move between the 11 different amino-acid substitution models available in MrBayes, and another specifying the JTT model. The first analysis allows the chain to take into account uncertainty in the substitution process. For all analyses performed here, the posterior probability of the JTT model was at least 99%, confirming that this model best describes the evolution of the dynein sequences—so only results from the fixed-JTT model analyses are shown here.

For each analysis, three chains of 1,000,000 generations each were run, sampling parameters every 100 generations and discarding the first 100,000 generations as a burn-in period. Running these multiple independent chains allowed visual confirmation that the chains had reached a stationary state by ensuring that all three chains were moving around a region of similar likelihood. For one of the gene families (cytoplasmic dynein heavy chain), the three chains had reached different likelihood values after 1,000,000 generations, suggesting failure to converge. Running another three independent chains resulted in five out of six chains agreeing on the likelihood values, suggesting that only one chain had not converged properly. In all cases, the phylogeny presented is the majority-rule consensus of the posterior sample of tree topologies from all three Markov chains, drawn using TreeView [176] with posterior clade probabilities and maximum-likelihood bootstrap values shown for each clade on these trees.

Searching for Function and Mutant Phenotypes

As well as literature searches, information on protein function was taken from the Gene Ontology database (http://www.geneontology.org), which provides data on function and processes associated with a search protein. Mutant-phenotype data were obtained from the literature and the following sources: Online Mendelian Inheritance in Man at NCBI for human (http://www.ncbi.nlm.nih.gov/entrez/query.fcgi?db=OMIM); MGI for mouse (http://www.informatics.jax.org); FlyBase for *Drosophila* (http://www.flybase.org); and WormBase for *C. elegans* (http://www.wormbase.org).

Conclusions

In this paper, we have provided an overview of the two cytoplasmic dynein complexes, cytoplasmic dynein 1 and cytoplasmic dynein 2, from a genetic perspective. We have highlighted the unique subunit compositions and cellular functions of the two cytoplasmic dyneins, and we have emphasized the unique role of cytoplasmic dynein 2 in IFT. We have described the different mammalian dynein gene families, and have shown the phylogenetic and functional relationships between members of individual families. We carried out initial database searches and clarified and corrected anomalous data. We have also discussed known functions and mutations of these proteins, and we have highlighted both their fundamental importance to the cell and the fact that much research remains to be carried out to define the roles of individual proteins.

Supporting Information

Table S1. Species Names, NCBI/GenBank Protein-Sequence Accession Numbers, and NCBI/GenBank Gene/Protein Names for Figures 2A–F

Found at DOI: 10.1371/journal.pgen.0020001.st001 (53 KB DOC).

Accession Numbers

The Entrez Gene database (http://www.ncbi.nlm.nih.gov/entrez) accession numbers for the proteins discussed in this paper are Cdic (also referred to as cDic and Dic) (44160); che-3 (DYNC2H1 homolog) (172593); DYNC1I1 (1780); DYNC1I2 (1781); DYNC1LI1 (51143); DYNC1LI2, (1783); DYNC2H1, (79659); DYNC2LI1 (51626); DYNLL1 (LC8) (8655); DYNLL2 (also known as DYNLL2 and LC8b) (140735); DYNLRB1 (also termed DYNLC2A) (83658); DYNLRB2 (also termed DYNLC2B) (83657); DYNLT1 (Tctex1) (6993); MAPBPIP (28956); SPAC1805.08 (also referred to as Dlc1) (3361491).

The Entrez Gene database (http://www.ncbi.nlm.nih.gov/entrez) accession numbers for the genes discussed in this paper are *Dhc64C* (38580); *dli-1* (178260); *dyn1* (853928); *Dync1h1* (13424); *DYNC1H1* (1778) ; *Dync1i1* (13426); *Dync1i2* (13427); *Dync2li1* (213575); *Dynlt1* (*Tctex1*) in the mouse genome (21648); *DYNLT3* (6990); human *Tctex2* (also known as LC2, *TCTE3*, and *Tcd3*) (6991); mouse *Tctex2* (21647); *xbx-1* (184080).

The Entrez Protein database (http://www.ncbi.nlm.nih.gov/entrez/query.fcgi?db=protein&cmd=search&term=) accession numbers for the proteins discussed in this paper are *C. elegans* LC8 sequence (49822); *C. elegans* light chain 1 (498422); Cdlc1 (525075); *Chlamydomonas* 19,000-M_r axonemal outer arm dynein light chain (LC2) (AAB58383); rat DYNC1I1 (062107); rat DYNC1LI2 (112288).

The OMIM (http://www.ncbi.nlm.nih.gov/entrez/query.fcgi?db=OMIM) accession numbers for the proteins discussed in this paper are autosomal recessive disorder primary ciliary dyskinesia (242650); Bim (603827); Bmf (606266); X-linked retinitis pigmentosa type 3 (300389).

The Ensembl (http://www.ensembl.org/Fugu_rubripes/textview) accession number for the *Takifugu* LC8 sequence is SINFRUP0000015498.

The SwissProt (http://ca.expasy.org/sprot/) accession numbers for the *Chlamydomonas* 8-kDa flagellar outer arm dynein light chain and the *Chlamydomonas* LC2 light chain used as the outgroup in Figure 2 are Q39580 and T08216, respectively. ■

Acknowledgments

PRS, HH, and EMCF are supported by the UK Medical Research Council, the Motor Neurone Disease Association, and the American Amyotrophic Lateral Sclerosis Association. KKP is supported by a grant from the National Institute of Neurological Disorders and Stroke, at the National Institutes of Health (NIH). SMK is supported by grants (GM51293 and GM63548) from the National Institutes of General Medical Sciences, NIH, and is an investigator of the Patrick and Catherine Weldon Donaghue Medical Research Foundation. JC is supported by the Biotechnology and Biological Sciences Research Council (BBSRC), grant 40/G18385. AR is supported by grants from the BBSRC and the Royal Society. We are most grateful to Lois Maltais of the Mouse Genomic Nomenclature Committee and to Mathew Wright of the Human Genome Organization Gene Nomenclature Committee for their help and support in preparing this manuscript. We thank Ray Young for supplying graphics.

References

1. Gibbons IR (1965) Chemical dissection of cilia. Arch Biol (Liege) 76: 317–352.
2. Sale WS, Satir P (1977) Direction of active sliding of microtubules in *Tetrahymena* cilia. Proc Natl Acad Sci U S A 74: 2045–2049.
3. Paschal BM, Shpetner HS, Vallee RB (1987) MAP 1C is a microtubule-activated ATPase which translocates microtubules in vitro and has dynein-like properties. J Cell Biol 105: 1273–1282.
4. Paschal BM, King SM, Moss AG, Collins CA, Vallee RB, et al. (1987) Isolated flagellar outer arm dynein translocates brain microtubules in vitro. Nature 330: 672–674.
5. Paschal BM, Vallee RB (1987) Retrograde transport by the microtubule-associated protein MAP 1C. Nature 330: 181–183.
6. Pazour GJ, Dickert BL, Witman GB (1999) The DHC1b (DHC2) isoform of cytoplasmic dynein is required for flagellar assembly. J Cell Biol 144: 473–481.
7. Sakakibara H, Kojima H, Sakai Y, Katayama E, Oiwa K (1999) Inner arm dynein c of *Chlamydomonas* flagella is a single-headed processive motor. Nature 400: 586–590.
8. Gibbons IR (1995) Dynein family of motor proteins: Present status and future questions. Cell Motil Cytoskeleton 32: 136–144.
9. Vallee RB, Williams JC, Varma D, Barnhart LE (2004) Dynein: An ancient motor protein involved in multiple modes of transport. J Neurobiol 58: 189–200.
10. Cole DG (2003) The intraflagellar transport machinery of *Chlamydomonas reinhardtii*. Traffic 4: 435–442.
11. Karki S, Holzbaur EL (1999) Cytoplasmic dynein and dynactin in cell division and intracellular transport. Curr Opin Cell Biol 11: 45–53.
12. King SJ, Schroer TA (2000) Dynactin increases the processivity of the cytoplasmic dynein motor. Nat Cell Biol 2: 20–24.
13. Quintyne NJ, Schroer TA (2002) Distinct cell cycle-dependent roles for dynactin and dynein at centrosomes. J Cell Biol 159: 245–254.
14. Grissom PM, Vaisberg EA, McIntosh JR (2002) Identification of a novel light intermediate chain (D2LIC) for mammalian cytoplasmic dynein 2. Mol Biol Cell 13: 817–829.
15. Mikami A, Tynan SH, Hama T, Luby-Phelps K, Saito T, et al. (2002) Molecular structure of cytoplasmic dynein 2 and its distribution in neuronal and ciliated cells. J Cell Sci 115: 4801–4808.
16. Perrone CA, Tritschler D, Taulman P, Bower R, Yoder BK, et al. (2003) A novel dynein light intermediate chain colocalizes with the retrograde motor for intraflagellar transport at sites of axoneme assembly in *Chlamydomonas* and mammalian cells. Mol Biol Cell 14: 2041–2056.
17. Hafezparast M, Klocke R, Ruhrberg C, Marquardt A, Ahmad-Annuar A, et al. (2003) Mutations in dynein link motor neuron degeneration to defects in retrograde transport. Science 300: 808–812.
18. Puls I, Jonnakuty C, LaMonte BH, Holzbaur EL, Tokito M, et al. (2003) Mutant dynactin in motor neuron disease. Nat Genet 33: 455–456.
19. Munch C, Sedlmeier R, Meyer T, Homberg V, Sperfeld AD, et al. (2004) Point mutations of the p150 subunit of dynactin (DCTN1) gene in ALS. Neurology 63: 724–726.
20. HUGO Gene Nomenclature Committee (2004) HGNC database symbol report: DYNC1H1synonym entry. London: HUGO Gene Nomenclature Committee, University College London. Available: http://www.gene.ucl.ac.uk/cgi-bin/nomenclature/get_data.pl?hgnc_id=2961. Accessed 25 November 2005.
21. Ohara O, Nagase T, Ishikawa K, Nakajima D, Ohira M, et al. (1997) Construction and characterization of human brain cDNA libraries suitable for analysis of cDNA clones encoding relatively large proteins. DNA Res 4: 53–59.
22. Porter ME, Bower R, Knott JA, Byrd P, Dentler W (1999) Cytoplasmic dynein heavy chain 1b is required for flagellar assembly in *Chlamydomonas*. Mol Biol Cell 10: 693–712.
23. Vaisberg EA, Grissom PM, McIntosh JR (1996) Mammalian cells express three distinct dynein heavy chains that are localized to different cytoplasmic organelles. J Cell Biol 133: 831–842.
24. Bloom GS, Schoenfeld TA, Vallee RB (1984) Widespread distribution of the major polypeptide component of MAP 1 (microtubule-associated protein 1) in the nervous system. J Cell Biol 98: 320–330.
25. Neuwald AF, Aravind L, Spouge JL, Koonin EV (1999) AAA+: A class of chaperone-like ATPases associated with the assembly, operation, and disassembly of protein complexes. Genome Res 9: 27–43.
26. Neely MD, Erickson HP, Boekelheide K (1990) HMW-2, the Sertoli cell cytoplasmic dynein from rat testis, is a dimer composed of nearly identical subunits. J Biol Chem 265: 8691–8698.
27. Samso M, Radermacher M, Frank J, Koonce MP (1998) Structural characterization of a dynein motor domain. J Mol Biol 276: 927–937.
28. Samso M, Koonce MP (2004) 25 Angstrom resolution structure of a cytoplasmic dynein motor reveals a seven-member planar ring. J Mol Biol 340: 1059–1072.

29. Mitchell DR, Brown KS (1994) Sequence analysis of the *Chlamydomonas* alpha and beta dynein heavy chain genes. J Cell Sci 107: 635–644.
30. Sakato M, King SM (2004) Design and regulation of the AAA+ microtubule motor dynein. J Struct Biol 146: 58–71.
31. Saraste M, Sibbald PR, Wittinghofer A (1990) The P-loop—A common motif in ATP- and GTP-binding proteins. Trends Biochem Sci 15: 430–434.
32. Eshel D (1995) Functional dissection of the dynein motor domain. Cell Motil Cytoskeleton 32: 133–135.
33. Kon T, Nishiura M, Ohkura R, Toyoshima YY, Sutoh K (2004) Distinct functions of nucleotide-binding/hydrolysis sites in the four AAA modules of cytoplasmic dynein. Biochemistry 43: 11266–11274.
34. Mocz G, Gibbons IR (1996) Phase partition analysis of nucleotide binding to axonemal dynein. Biochemistry 35: 9204–9211.
35. Takahashi Y, Edamatsu M, Toyoshima YY (2004) Multiple ATP-hydrolyzing sites that potentially function in cytoplasmic dynein. Proc Natl Acad Sci U S A 101: 12865–12869.
36. Gee MA, Heuser JE, Vallee RB (1997) An extended microtubule-binding structure within the dynein motor domain. Nature 390: 636–639.
37. Burgess SA, Walker ML, Sakakibara H, Knight PJ, Oiwa K (2003) Dynein structure and power stroke. Nature 421: 715–718.
38. Tynan SH, Purohit A, Doxsey SJ, Vallee RB (2000) Light intermediate chain 1 defines a functional subfraction of cytoplasmic dynein which binds to pericentrin. J Biol Chem 275: 32763–32768.
39. Habura A, Tikhonenko I, Chisholm RL, Koonce MP (1999) Interaction mapping of a dynein heavy chain. Identification of dimerization and intermediate chain binding domains. J Biol Chem 274: 15447–15453.
40. Susalka SJ, Nikulina K, Salata MW, Vaughan PS, King SM, et al. (2002) The roadblock light chain binds a novel region of the cytoplasmic Dynein intermediate chain. J Biol Chem 277: 32939–32946.
41. Mikami A, Paschal BM, Mazumdar M, Vallee RB (1993) Molecular cloning of the retrograde transport motor cytoplasmic dynein (MAP 1C). Neuron 10: 787–796.
42. Zhang Z, Tanaka Y, Nonaka S, Aizawa H, Kawasaki H, et al. (1993) The primary structure of rat brain (cytoplasmic) dynein heavy chain, a cytoplasmic motor enzyme. Proc Natl Acad Sci U S A 90: 7928–7932.
43. Vaisberg EA, Koonce MP, McIntosh JR (1993) Cytoplasmic dynein plays a role in mammalian mitotic spindle formation. J Cell Biol 123: 849–858.
44. Harada A, Takei Y, Kanai Y, Tanaka Y, Nonaka S, et al. (1998) Golgi vesiculation and lysosome dispersion in cells lacking cytoplasmic dynein. J Cell Biol 141: 51–59.
45. Gepner J, Li M, Ludmann S, Kortas C, Boylan K, et al. (1996) Cytoplasmic dynein function is essential in *Drosophila melanogaster*. Genetics 142: 865–878.
46. Li M, McGrail M, Serr M, Hays TS (1994) *Drosophila* cytoplasmic dynein, a microtubule motor that is asymmetrically localized in the oocyte. J Cell Biol 126: 1475–1494.
47. McGrail M, Hays TS (1997) The microtubule motor cytoplasmic dynein is required for spindle orientation during germline cell divisions and oocyte differentiation in *Drosophila*. Development 124: 2409–2419.
48. Robinson JT, Wojcik EJ, Sanders MA, McGrail M, Hays TS (1999) Cytoplasmic dynein is required for the nuclear attachment and migration of centrosomes during mitosis in *Drosophila*. J Cell Biol 146: 597–608.
49. Martin M, Iyadurai SJ, Gassman A, Gindhart JG Jr, Hays TS, et al. (1999) Cytoplasmic dynein, the dynactin complex, and kinesin are interdependent and essential for fast axonal transport. Mol Biol Cell 10: 3717–3728.
50. Hamill DR, Severson AF, Carter JC, Bowerman B (2002) Centrosome maturation and mitotic spindle assembly in *C. elegans* require SPD-5, a protein with multiple coiled-coil domains. Dev Cell 3: 673–684.
51. Mains PE, Sulston IA, Wood WB (1990) Dominant maternal-effect mutations causing embryonic lethality in *Caenorhabditis elegans*. Genetics 125: 351–369.
52. Koushika SP, Schaefer AM, Vincent R, Willis JH, Bowerman B, et al. (2004) Mutations in *Caenorhabditis elegans* cytoplasmic dynein components reveal specificity of neuronal retrograde cargo. J Neurosci 24: 3907–3916.
53. Schmidt DJ, Rose DJ, Saxton WM, Strome S (2005) Functional analysis of cytoplasmic dynein heavy chain in *Caenorhabditis elegans* with fast-acting temperature-sensitive mutations. Mol Biol Cell 16: 1200–1212.
54. Mains PE, Kemphues KJ, Sprunger SA, Sulston IA, Wood WB (1990) Mutations affecting the meiotic and mitotic divisions of the early *Caenorhabditis elegans* embryo. Genetics 126: 593–605.
55. Eshel D, Urrestarazu LA, Vissers S, Jauniaux JC, Vliet-Reedijk JC, et al. (1993) Cytoplasmic dynein is required for normal nuclear segregation in yeast. Proc Natl Acad Sci U S A 90: 11172–11176.
56. Li YY, Yeh E, Hays T, Bloom K (1993) Disruption of mitotic spindle orientation in a yeast dynein mutant. Proc Natl Acad Sci U S A 90: 10096–10100.
57. Saunders WS, Koshland D, Eshel D, Gibbons IR, Hoyt MA (1995) *Saccharomyces cerevisiae* kinesin- and dynein-related proteins required for anaphase chromosome segregation. J Cell Biol 128: 617–624.
58. Lawrence CJ, Morris NR, Meagher RB, Dawe RK (2001) Dyneins have run their course in plant lineage. Traffic 2: 362–363.
59. International Rice Genome Sequencing Project (2005) The map-based sequence of the rice genome. Nature 436: 793–800.
60. Vale RD (2003) The molecular motor toolbox for intracellular transport. Cell 112: 467–480.
61. Gibbons BH, Asai DJ, Tang WJ, Hays TS, Gibbons IR (1994) Phylogeny and expression of axonemal and cytoplasmic dynein genes in sea urchins. Mol Biol Cell 5: 57–70.
62. Signor D, Wedaman KP, Orozco JT, Dwyer ND, Bargmann CI, et al. (1999) Role of a class DHC1b dynein in retrograde transport of IFT motors and IFT raft particles along cilia, but not dendrites, in chemosensory neurons of living *Caenorhabditis elegans*. J Cell Biol 147: 519–530.
63. Baker SA, Freeman K, Luby-Phelps K, Pazour GJ, Besharse JC (2003) IFT20 links kinesin II with a mammalian intraflagellar transport complex that is conserved in motile flagella and sensory cilia. J Biol Chem 278: 34211–34218.
64. Rosenbaum JL, Cole DG, Diener DR (1999) Intraflagellar transport: The eyes have it. J Cell Biol 144: 385–388.
65. Bargmann CI, Hartwieg E, Horvitz HR (1993) Odorant-selective genes and neurons mediate olfaction in *C. elegans*. Cell 74: 515–527.
66. Collet J, Spike CA, Lundquist EA, Shaw JE, Herman RK (1998) Analysis of osm-6, a gene that affects sensory cilium structure and sensory neuron function in *Caenorhabditis elegans*. Genetics 148: 187–200.
67. Wicks SR, de Vries CJ, van Luenen HG, Plasterk RH (2000) CHE-3, a cytosolic dynein heavy chain, is required for sensory cilia structure and function in *Caenorhabditis elegans*. Dev Biol 221: 295–307.
68. Albert PS, Brown SJ, Riddle DL (1981) Sensory control of dauer larva formation in *Caenorhabditis elegans*. J Comp Neurol 198: 435–451.
69. Tanaka Y, Zhang Z, Hirokawa N (1995) Identification and molecular evolution of new dynein-like protein sequences in rat brain. J Cell Sci 108: 1883–1893.
70. Adams MD, Celniker SE, Holt RA, Evans CA, Gocayne JD, et al. (2000) The genome sequence of *Drosophila melanogaster*. Science 287: 2185–2195.
71. Hou Y, Pazour GJ, Witman GB (2004) A dynein light intermediate chain, D1bLIC, is required for retrograde intraflagellar transport. Mol Biol Cell 15: 4382–4394.
72. Pazour GJ, Wilkerson CG, Witman GB (1998) A dynein light chain is essential for the retrograde particle movement of intraflagellar transport (IFT). J Cell Biol 141: 979–992.
73. Schafer JC, Haycraft CJ, Thomas JH, Yoder BK, Swoboda P (2003) XBX-1 encodes a dynein light intermediate chain required for retrograde intraflagellar transport and cilia assembly in *Caenorhabditis elegans*. Mol Biol Cell 14: 2057–2070.
74. Criswell PS, Ostrowski LE, Asai DJ (1996) A novel cytoplasmic dynein heavy chain: Expression of DHC1b in mammalian ciliated epithelial cells. J Cell Sci 109: 1891–1898.
75. Mitchell DR, Kang Y (1991) Identification of oda6 as a *Chlamydomonas* dynein mutant by rescue with the wild-type gene. J Cell Biol 113: 835–842.
76. Paschal BM, Mikami A, Pfister KK, Vallee RB (1992) Homology of the 74-kD cytoplasmic dynein subunit with a flagellar dynein polypeptide suggests an intracellular targeting function. J Cell Biol 118: 1133–1143.
77. Wolfe KH (2001) Yesterday's polyploids and the mystery of diploidization. Nat Rev Genet 2: 333–341.
78. King SM, Barbarese E, Dillman JF III, Benashski SE, Do KT, et al. (1998) Cytoplasmic dynein contains a family of differentially expressed light chains. Biochemistry 37: 15033–15041.
79. Vaughan KT, Vallee RB (1995) Cytoplasmic dynein binds dynactin through a direct interaction between the intermediate chains and p150Glued. J Cell Biol 131: 1507–1516.
80. Wilkerson CG, King SM, Koutoulis A, Pazour GJ, Witman GB (1995) The 78,000 M(r) intermediate chain of *Chlamydomonas* outer arm dynein is a WD-repeat protein required for arm assembly. J Cell Biol 129: 169–178.
81. Yang P, Sale WS (1998) The Mr 140,000 intermediate chain of *Chlamydomonas* flagellar inner arm dynein is a WD-repeat protein implicated in dynein arm anchoring. Mol Biol Cell 9: 3335–3349.
82. Ma S, Trivinos-Lagos L, Graf R, Chisholm RL (1999) Dynein intermediate chain mediated dynein-dynactin interaction is required for interphase microtubule organization and centrosome replication and separation in *Dictyostelium*. J Cell Biol 147: 1261–1274.
83. Lo KW, Naisbitt S, Fan JS, Sheng M, Zhang M (2001) The 8-kDa dynein light chain binds to its targets via a conserved (K/R)XTQT motif. J Biol Chem 276: 14059–14066.
84. Makokha M, Hare M, Li M, Hays T, Barbar E (2002) Interactions of cytoplasmic dynein light chains Tctex-1 and LC8 with the intermediate chain IC74. Biochemistry 41: 4302–4311.
85. Mok YK, Lo KW, Zhang M (2001) Structure of Tctex-1 and its interaction with cytoplasmic dynein intermediate chain. J Biol Chem 276: 14067–14074.
86. Dillman JF III, Pfister KK (1994) Differential phosphorylation in vivo of cytoplasmic dynein associated with anterogradely moving organelles. J Cell Biol 127: 1671–1681.
87. Vaughan PS, Leszyk JD, Vaughan KT (2001) Cytoplasmic dynein intermediate chain phosphorylation regulates binding to dynactin. J Biol Chem 276: 26171–26179.
88. King SM, Witman GB (1990) Localization of an intermediate chain of outer arm dynein by immunoelectron microscopy. J Biol Chem 265: 19807–19811.
89. Steffen W, Hodgkinson JL, Wiche G (1996) Immunogold localisation of

the intermediate chain within the protein complex of cytoplasmic dynein. J Struct Biol 117: 227–235.
90. Steffen W, Karki S, Vaughan KT, Vallee RB, Holzbaur EL, et al. (1997) The involvement of the intermediate chain of cytoplasmic dynein in binding the motor complex to membranous organelles of *Xenopus* oocytes. Mol Biol Cell 8: 2077–2088.
91. Boylan KL, Hays TS (2002) The gene for the intermediate chain subunit of cytoplasmic dynein is essential in *Drosophila*. Genetics 162: 1211–1220.
92. Nurminsky DI, Nurminskaya MV, Benevolenskaya EV, Shevelyov YY, Hartl DL, et al. (1998) Cytoplasmic dynein intermediate chain isoforms with different targeting properties created by tissue-specific alternative splicing. Mol Cell Biol 18: 6816–6825.
93. Ranz JM, Ponce AR, Hartl DL, Nurminsky D (2003) Origin and evolution of a new gene expressed in the *Drosophila* sperm axoneme. Genetica 118: 233–244.
94. Crackower MA, Sinasac DS, Xia J, Motoyama J, Prochazka M, et al. (1999) Cloning and characterization of two cytoplasmic dynein intermediate chain genes in mouse and human. Genomics 55: 257–267.
95. Dillman JF III, Dabney LP, Pfister KK (1996) Cytoplasmic dynein is associated with slow axonal transport. Proc Natl Acad Sci U S A 93: 141–144.
96. Pfister KK, Salata MW, Dillman JF III, Torre E, Lye RJ (1996) Identification and developmental regulation of a neuron-specific subunit of cytoplasmic dynein. Mol Biol Cell 7: 331–343.
97. Pfister KK, Salata MW, Dillman JF III, Vaughan KT, Vallee RB, et al. (1996) Differential expression and phosphorylation of the 74-kDa intermediate chains of cytoplasmic dynein in cultured neurons and glia. J Biol Chem 271: 1687–1694.
98. Vaughan KT, Mikami A, Paschal BM, Holzbaur EL, Hughes SM, et al. (1996) Multiple mouse chromosomal loci for dynein-based motility. Genomics 36: 29–38.
99. Susalka SJ, Pfister KK (2000) Cytoplasmic dynein subunit heterogeneity: Implications for axonal transport. J Neurocytol 29: 819–829.
100. Salata MW, Dillman JF III, Lye RJ, Pfister KK (2001) Growth factor regulation of cytoplasmic dynein intermediate chain subunit expression preceding neurite extension. J Neurosci Res 65: 408–416.
101. Levin M, Nascone N (1997) Two molecular models of initial left-right asymmetry generation. Med Hypotheses 49: 429–435.
102. Hughes SM, Vaughan KT, Herskovits JS, Vallee RB (1995) Molecular analysis of a cytoplasmic dynein light intermediate chain reveals homology to a family of ATPases. J Cell Sci 108: 17–24.
103. Gill SR, Cleveland DW, Schroer TA (1994) Characterization of DLC-A and DLC-B, two families of cytoplasmic dynein light chain subunits. Mol Biol Cell 5: 645–654.
104. King SM, Barbarese E, Dillman JF III, Patel-King RS, Carson JH, et al. (1996) Brain cytoplasmic and flagellar outer arm dyneins share a highly conserved Mr 8,000 light chain. J Biol Chem 271: 19358–19366.
105. King SJ, Bonilla M, Rodgers ME, Schroer TA (2002) Subunit organization in cytoplasmic dynein subcomplexes. Protein Sci 11: 1239–1250.
106. Yoder JH, Han M (2001) Cytoplasmic dynein light intermediate chain is required for discrete aspects of mitosis in *Caenorhabditis elegans*. Mol Biol Cell 12: 2921–2933.
107. Malone CJ, Misner L, Le Bot N, Tsai MC, Campbell JM, et al. (2003) The *C. elegans* hook protein, ZYG-12, mediates the essential attachment between the centrosome and nucleus. Cell 115: 825–836.
108. Walker JE, Saraste M, Runswick MJ, Gay NJ (1982) Distantly related sequences in the alpha- and beta-subunits of ATP synthase, myosin, kinases and other ATP-requiring enzymes and a common nucleotide binding fold. EMBO J 1: 945–951.
109. Bielli A, Thornqvist PO, Hendrick AG, Finn R, Fitzgerald K, et al. (2001) The small GTPase Rab4A interacts with the central region of cytoplasmic dynein light intermediate chain-1. Biochem Biophys Res Commun 281: 1141–1153.
110. Niclas J, Allan VJ, Vale RD (1996) Cell cycle regulation of dynein association with membranes modulates microtubule-based organelle transport. J Cell Biol 133: 585–593.
111. Reilein AR, Serpinskaya AS, Karcher RL, Dujardin DL, Vallee RB, et al. (2003) Differential regulation of dynein-driven melanosome movement. Biochem Biophys Res Commun 309: 652–658.
112. Angelastro JM, Klimaschewski L, Tang S, Vitolo OV, Weissman TA, et al. (2000) Identification of diverse nerve growth factor-regulated genes by serial analysis of gene expression (SAGE) profiling. Proc Natl Acad Sci U S A 97: 10424–10429.
113. Rana AA, Martinez Barbera JP, Rodriguez TA, Lynch D, Hirst E, et al. (2004) Targeted deletion of the novel cytoplasmic dynein mD2LIC disrupts the embryonic organiser, formation of the body axes and specification of ventral cell fates. Development 131: 4999–5007.
114. Lader E, Ha HS, O'Neill M, Artzt K, Bennett D (1989) Tctex-1: A candidate gene family for a mouse t complex sterility locus. Cell 58: 969–979.
115. O'Neill MJ, Artzt K (1995) Identification of a germ-cell-specific transcriptional repressor in the promoter of Tctex-1. Development 121: 561–568.
116. King SM, Dillman JF III, Benashski SE, Lye RJ, Patel-King RS, et al. (1996) The mouse t-complex-encoded protein Tctex-1 is a light chain of brain cytoplasmic dynein. J Biol Chem 271: 32281–32287.
117. Harrison A, Olds-Clarke P, King SM (1998) Identification of the t complex-encoded cytoplasmic dynein light chain Tctex1 in inner arm I1 supports the involvement of flagellar dyneins in meiotic drive. J Cell Biol 140: 1137–1147.
118. Kagami O, Gotoh M, Makino Y, Mohri H, Kamiya R, et al. (1998) A dynein light chain of sea urchin sperm flagella is a homolog of mouse Tctex 1, which is encoded by a gene of the t complex sterility locus. Gene 211: 383–386.
119. Tai AW, Chuang JZ, Bode C, Wolfrum U, Sung CH (1999) Rhodopsin's carboxy-terminal cytoplasmic tail acts as a membrane receptor for cytoplasmic dynein by binding to the dynein light chain Tctex-1. Cell 97: 877–887.
120. DiBella LM, Benashski SE, Tedford HW, Harrison A, Patel-King RS, et al. (2001) The Tctex1/Tctex2 class of dynein light chains. Dimerization, differential expression, and interaction with the LC8 protein family. J Biol Chem 276: 14366–14373.
121. Williams JC, Xie H, Hendrickson WA (2005) Crystal structure of dynein light chain TcTex-1. J Biol Chem 280: 21981–21986.
122. Wu H, Maciejewski MW, Takebe S, King SM (2005) Solution structure of the Tctex1 dimer reveals a mechanism for dynein-cargo interactions. Structure (Camb) 13: 213–223.
123. Miki F, Okazaki K, Shimanuki M, Yamamoto A, Hiraoka Y, et al. (2002) The 14-kDa dynein light chain-family protein Dlc1 is required for regular oscillatory nuclear movement and efficient recombination during meiotic prophase in fission yeast. Mol Biol Cell 13: 930–946.
124. Caggese C, Moschetti R, Ragone G, Barsanti P, Caizzi R (2001) Dtctex-1, the *Drosophila melanogaster* homolog of a putative murine t-complex distorter encoding a dynein light chain, is required for production of functional sperm. Mol Genet Genomics 265: 436–444.
125. Li MG, Serr M, Newman EA, Hays TS (2004) The *Drosophila* Tctex-1 light chain is dispensable for essential cytoplasmic dynein functions but is required during spermatid differentiation. Mol Biol Cell 15: 3005–3014.
126. Roux AF, Rommens J, McDowell C, Anson-Cartwright L, Bell S, et al. (1994) Identification of a gene from Xp21 with similarity to the Tctex-1 gene of the murine t complex. Hum Mol Genet 3: 257–263.
127. Meindl A, Dry K, Herrmann K, Manson F, Ciccodicola A, et al. (1996) A gene (RPGR) with homology to the RCC1 guanine nucleotide exchange factor is mutated in X-linked retinitis pigmentosa (RP3). Nat Genet 13: 35–42.
128. Douglas MW, Diefenbach RJ, Homa FL, Miranda-Saksena M, Rixon FJ, et al. (2004) *Herpes simplex* virus type 1 capsid protein VP26 interacts with dynein light chains RP3 and Tctex1 and plays a role in retrograde cellular transport. J Biol Chem 279: 28522–28530.
129. Rappold GA, Trowsdale J, Lichter P (1992) Assignment of the human homologue of the mouse t-complex gene TCTE3 to human chromosome 6q27. Genomics 13: 1337–1339.
130. Huw LY, Goldsborough AS, Willison K, Artzt K (1995) Tctex2: A sperm tail surface protein mapping to the t-complex. Dev Biol 170: 183–194.
131. Patel-King RS, Benashski SE, Harrison A, King SM (1997) A *Chlamydomonas* homologue of the putative murine t complex distorter Tctex-2 is an outer arm dynein light chain. J Cell Biol 137: 1081–1090.
132. Pazour GJ, Koutoulis A, Benashski SE, Dickert BL, Sheng H, et al. (1999) LC2, the *Chlamydomonas* homologue of the t complex-encoded protein Tctex2, is essential for outer dynein arm assembly. Mol Biol Cell 10: 3507–3520.
133. Neesen J, Drenckhahn JD, Tiede S, Burfeind P, Grzmil M, et al. (2002) Identification of the human ortholog of the t-complex-encoded protein TCTE3 and evaluation as a candidate gene for primary ciliary dyskinesia. Cytogenet Genome Res 98: 38–44.
134. Rappold GA, Stubbs L, Labeit S, Crkvenjakov RB, Lehrach H (1987) Identification of a testis-specific gene from the mouse t-complex next to a CpG-rich island. EMBO J 6: 1975–1980.
135. Bowman AB, Patel-King RS, Benashski SE, McCaffery JM, Goldstein LS, et al. (1999) *Drosophila* roadblock and *Chlamydomonas* LC7: A conserved family of dynein-associated proteins involved in axonal transport, flagellar motility, and mitosis. J Cell Biol 146: 165–180.
136. DiBella LM, Sakato M, Patel-King RS, Pazour GJ, King SM (2004) The LC7 light chains of *Chlamydomonas* flagellar dyneins interact with components required for both motor assembly and regulation. Mol Biol Cell 15: 4633–4646.
137. Koonin EV, Aravind L (2000) Dynein light chains of the Roadblock/LC7 group belong to an ancient protein superfamily implicated in NTPase regulation. Curr Biol 10: R774–R776.
138. Reuter JE, Nardine TM, Penton A, Billuart P, Scott EK, et al. (2003) A mosaic genetic screen for genes necessary for *Drosophila* mushroom body neuronal morphogenesis. Development 130: 1203–1213.
139. Pazour GJ, Witman GB (2000) Forward and reverse genetic analysis of microtubule motors in *Chlamydomonas*. Methods 22: 285–298.
140. Lunin VV, Munger C, Wagner J, Ye Z, Cygler M, et al. (2004) The structure of the MAPK scaffold, MP1, bound to its partner, p14. A complex with a critical role in endosomal map kinase signaling. J Biol Chem 279: 23422–23430.
141. Ye F, Zangenehpour S, Chaudhuri A (2000) Light-induced down-

regulation of the rat class 1 dynein-associated protein robl/LC7-like gene in visual cortex. J Biol Chem 275: 27172–27176.
142. Jiang J, Yu L, Huang X, Chen X, Li D, et al. (2001) Identification of two novel human dynein light chain genes, DNLC2A and DNLC2B, and their expression changes in hepatocellular carcinoma tissues from 68 Chinese patients. Gene 281: 103–113.
143. Nikulina K, Patel-King RS, Takebe S, Pfister KK, King SM (2004) The roadblock light chains are ubiquitous components of cytoplasmic dynein that form homo- and heterodimers. Cell Motil Cytoskeleton 57: 233–245.
144. Tang Q, Staub CM, Gao G, Jin Q, Wang Z, et al. (2002) A novel transforming growth factor-beta receptor-interacting protein that is also a light chain of the motor protein dynein. Mol Biol Cell 13: 4484–4496.
145. Pfister KK, Fay RB, Witman GB (1982) Purification and polypeptide composition of dynein ATPases from *Chlamydomonas* flagella. Cell Motil 2: 525–547.
146. Piperno G, Luck DJ (1982) Outer and inner arm dyneins from flagella of *Chlamydomonas reinhardtii*. Prog Clin Biol Res 80: 95–99.
147. King SM, Patel-King RS (1995) The M(r) = 8,000 and 11,000 outer arm dynein light chains from *Chlamydomonas* flagella have cytoplasmic homologues. J Biol Chem 270: 11445–11452.
148. Wilson MJ, Salata MW, Susalka SJ, Pfister KK (2001) Light chains of mammalian cytoplasmic dynein: Identification and characterization of a family of LC8 light chains. Cell Motil Cytoskeleton 49: 229–240.
149. Naisbitt S, Valtschanoff J, Allison DW, Sala C, Kim E, et al. M (2000) Interaction of the postsynaptic density-95/guanylate kinase domain-associated protein complex with a light chain of myosin-V and dynein. J Neurosci 20: 4524–4534.
150. Yang P, Diener DR, Rosenbaum JL, Sale WS (2001) Localization of calmodulin and dynein light chain LC8 in flagellar radial spokes. J Cell Biol 153: 1315–1326.
151. Vadlamudi RK, Bagheri-Yarmand R, Yang Z, Balasenthil S, Nguyen D, et al. (2004) Dynein light chain 1, a p21-activated kinase 1-interacting substrate, promotes cancerous phenotypes. Cancer Cell 5: 575–585.
152. Espindola FS, Suter DM, Partata LB, Cao T, Wolenski JS, et al. (2000) The light chain composition of chicken brain myosin-Va: Calmodulin, myosin-II essential light chains, and 8-kDa dynein light chain/PIN. Cell Motil Cytoskeleton 47: 269–281.
153. Jaffrey SR, Snyder SH (1996) PIN: An associated protein inhibitor of neuronal nitric oxide synthase. Science 274: 774–777.
154. Puthalakath H, Huang DC, O'Reilly LA, King SM, Strasser A (1999) The proapoptotic activity of the Bcl-2 family member Bim is regulated by interaction with the dynein motor complex. Mol Cell 3: 287–296.
155. Schnorrer F, Bohmann K, Nusslein-Volhard C (2000) The molecular motor dynein is involved in targeting swallow and bicoid RNA to the anterior pole of *Drosophila* oocytes. Nat Cell Biol 2: 185–190.
156. Wang L, Hare M, Hays TS, Barbar E (2004) Dynein light chain LC8 promotes assembly of the coiled-coil domain of swallow protein. Biochemistry 43: 4611–4620.
157. Raux H, Flamand A, Blondel D (2000) Interaction of the rabies virus P protein with the LC8 dynein light chain. J Virol 74: 10212–10216.
158. Benashski SE, Harrison A, Patel-King RS, King SM (1997) Dimerization of the highly conserved light chain shared by dynein and myosin V. J Biol Chem 272: 20929–20935.
159. Liang J, Jaffrey SR, Guo W, Snyder SH, Clardy J (1999) Structure of the PIN/LC8 dimer with a bound peptide. Nat Struct Biol 6: 735–740.
160. Fan J, Zhang Q, Tochio H, Li M, Zhang M (2001) Structural basis of diverse sequence-dependent target recognition by the 8 kDa dynein light chain. J Mol Biol 306: 97–108.
161. Wu H, King SM (2003) Backbone dynamics of dynein light chains. Cell Motil Cytoskeleton 54: 267–273.
162. Dick T, Ray K, Salz HK, Chia W (1996) Cytoplasmic dynein (ddlc1) mutations cause morphogenetic defects and apoptotic cell death in *Drosophila melanogaster*. Mol Cell Biol 16: 1966–1977.
163. Phillis R, Statton D, Caruccio P, Murphey RK (1996) Mutations in the 8 kDa dynein light chain gene disrupt sensory axon projections in the *Drosophila* imaginal CNS. Development 122: 2955–2963.
164. Beckwith SM, Roghi CH, Liu B, Ronald MN (1998) The "8-kD" cytoplasmic dynein light chain is required for nuclear migration and for dynein heavy chain localization in *Aspergillus nidulans*. J Cell Biol 143: 1239–1247.
165. Puthalakath H, Villunger A, O'Reilly LA, Beaumont JG, Coultas L, et al. (2001) Bmf: A proapoptotic BH3-only protein regulated by interaction with the myosin V actin motor complex, activated by anoikis. Science 293: 1829–1832.
166. Day CL, Puthalakath H, Skea G, Strasser A, Barsukov I, et al. (2004) Localization of dynein light chains 1 and 2 and their pro-apoptotic ligands. Biochem J 377: 597–605.
167. Wheeler DL, Church DM, Federhen S, Lash AE, Madden TL, et al. (2003) Database resources of the National Center for Biotechnology. Nucleic Acids Res 31: 28–33.
168. Pruitt KD, Tatusova T, Maglott DR (2003) NCBI Reference Sequence Project: Update and current status. Nucleic Acids Res 31: 34–37.
169. Altschul SF, Madden TL, Schaffer AA, Zhang J, Zhang Z, et al. (1997) Gapped BLAST and PSI-BLAST: A new generation of protein database search programs. Nucleic Acids Res 25: 3389–3402.
170. Altschul SF, Gish W, Miller W, Myers EW, Lipman DJ (1990) Basic local alignment search tool. J Mol Biol 215: 403–410.
171. Henikoff S, Henikoff JG (1993) Performance evaluation of amino acid substitution matrices. Proteins 17: 49–61.
172. Thompson JD, Higgins DG, Gibson TJ (1994) CLUSTAL W: Improving the sensitivity of progressive multiple sequence alignment through sequence weighting, position-specific gap penalties and weight matrix choice. Nucleic Acids Res 22: 4673–4680.
173. Gonnet GH, Cohen MA, Benner SA (1992) Exhaustive matching of the entire protein sequence database. Science 256: 1443–1445.
174. Guindon S, Gascuel O (2003) A simple, fast, and accurate algorithm to estimate large phylogenies by maximum likelihood. Syst Biol 52: 696–704.
175. Ronquist F, Huelsenbeck JP (2003) MrBayes 3: Bayesian phylogenetic inference under mixed models. Bioinformatics 19: 1572–1574.
176. Page RDM (1996) TREEVIEW: An application to display phylogenetic trees on personal computers. Comput Appl Biosci 12: 357–358.
177. Ahmad-Annuar A, Shah P, Hafezparast M, Hummerich H, Witherden AS, et al. (2003) No association with common Caucasian genotypes in exons 8, 13 and 14 of the human cytoplasmic dynein heavy chain gene (DNCHC1) and familial motor neuron disorders. Amyotroph Lateral Scler Other Motor Neuron Disord 4: 150–157.
178. Narayan D, Desai T, Banks A, Patanjali SR, Ravikumar TS, et al. (1994) Localization of the human cytoplasmic dynein heavy chain (DNECL) to 14qter by fluorescence in situ hybridization. Genomics 22: 660–661.
179. Nagase T, Ishikawa K, Nakajima D, Ohira M, Seki N, et al. (1997) Prediction of the coding sequences of unidentified human genes. VII. The complete sequences of 100 new cDNA clones from brain which can code for large proteins in vitro. DNA Res 4: 141–150.
180. Byers HR, Yaar M, Eller MS, Jalbert NL, Gilchrest BA (2000) Role of cytoplasmic dynein in melanosome transport in human melanocytes. J Invest Dermatol 114: 990–997.
181. Witherden AS, Hafezparast M, Nicholson SJ, Ahmad-Annuar A, Bermingham N, et al. (2002) An integrated genetic, radiation hybrid, physical and transcription map of a region of distal mouse Chromosome 12, including an imprinted locus and the "Legs at odd angles" (Loa) mutation. Gene 283: 71–82.
182. Fridolfsson AK, Hori T, Wintero AK, Fredholm M, Yerle M, et al. (1997) Expansion of the pig comparative map by expressed sequence tags (EST) mapping. Mamm Genome 8: 907–912.
183. The Jackson Laboratory (2004) Mouse Genome Database gene detail: Dync1h1(mKIAA0325 synonym). Bar Harbor (Maine): The Jackson Laboratory. Available: http://www.informatics.jax.org/searches/accession__report.cgi?id=MGI:103147. Accessed 25 November 2005.
184. Okazaki N, Kikuno R, Ohara R, Inamoto S, Aizawa H, et al. (2003) Prediction of the coding sequences of mouse homologues of KIAA gene: II. The complete nucleotide sequences of 400 mouse KIAA-homologous cDNAs identified by screening of terminal sequences of cDNA clones randomly sampled from size-fractionated libraries. DNA Res 10: 35–48.
185. Neesen J, Koehler MR, Kirschner R, Steinlein C, Kreutzberger J, et al. (1997) Identification of dynein heavy chain genes expressed in human and mouse testis: Chromosomal localization of an axonemal dynein gene. Gene 200: 193–202.
186. Ota T, Suzuki Y, Nishikawa T, Otsuki T, Sugiyama T, et al. (2004) Complete sequencing and characterization of 21,243 full-length human cDNAs. Nat Genet 36: 40–45.
187. The Jackson Laboratory (2004) Mouse Genome Database, Mouse Genome Informatics Web site. Bar Harbor (Maine): The Jackson Laboratory. Available: http://www.informatics.jax.org. Accessed 25 November 2005. Version 3.0 retrieved March 2004.
188. National Center for Biotechnology Information (1998) Homo sapiens cDNA clone MPMGp800I08506 5' similar to DYNEIN INTERMEDIATE CHAIN 1. Bethesda (Maryland): National Center for Biotechnology Information. Available: http://www.ncbi.nlm.nih.gov/entrez/viewer.fcgi?db=nucleotide&val=31744556&txt=on. Accessed 25 November 2005.
189. National Center for Biotechnology Information (1998) Homo sapiens cDNA clone MPMGp800C22508 5' similar to DYNEIN INTERMEDIATE CHAIN 2. Bethesda (Maryland): National Center for Biotechnology Information. Available: http://www.ncbi.nlm.nih.gov/entrez/viewer.fcgi?db=nucleotide&val=31743626&txt=on. Accessed 25 November 2005.
190. National Center for Biotechnology Information (2004) Entrez Gene DNC1LI1 LocusLink entry: Dynein Light Chain A synonym. Bethesda (Maryland): National Center for Biotechnology Information. Available: http://www.ncbi.nlm.nih.gov/LocusLink/LocRpt.cgi?l=51143. Accessed 25 November 2005.
191. National Center for Biotechnology Information (2004) Entrez Nucleotide database Dync1li1 entry: MGC32416 synonym. Bethesda (Maryland): National Center for Biotechnology Information. Available: http://www.ncbi.nlm.nih.gov/entrez/viewer.fcgi?db=nucleotide&val=22122794. Accessed 25 November 2005.
192. National Center for Biotechnology Information (2004) Entrez Nucleotide database DYNC2LI1 entry: D2LIC, LIC3, CGI-60, DKFZP564A033 synonyms. Bethesda (Maryland): National Center for Biotechnology Information. Available: http://www.ncbi.nlm.nih.gov/entrez/viewer.fcgi?db=nucleotide&val=40548412. Accessed 25 November 2005.
193. National Center for Biotechnology Information (2004) Entrez Nucleotide

database mouse Dync2li1 entry: D2LIC, mD2LIC, MGC7211, MGC40646, 4933404O11Rik synonyms. Bethesda (Maryland): National Center for Biotechnology Information. Available: http://www.ncbi.nlm.nih.gov/entrez/viewer.fcgi?db=nucleotide&val=26986540. Accessed 25 November 2005.
194. Watanabe TK, Fujiwara T, Shimizu F, Okuno S, Suzuki M, et al. (1996) Cloning, expression, and mapping of TCTEL1, a putative human homologue of murine Tctel, to 6q. Cytogenet Cell Genet 73: 153–156.
195. Mueller S, Cao X, Welker R, Wimmer E (2002) Interaction of the poliovirus receptor CD155 with the dynein light chain Tctex-1 and its implication for poliovirus pathogenesis. J Biol Chem 277: 7897–7904.
196. Shibata K, Itoh M, Aizawa K, Nagaoka S, Sasaki N, et al. (2000) RIKEN integrated sequence analysis (RISA) system—384-format sequencing pipeline with 384 multicapillary sequencer. Genome Res 10: 1757–1771.
197. National Center for Biotechnology Information (2004) DNCL2A GenBank entry: MGC15113 synonym. Bethesda (Maryland): National Center for Biotechnology Information. Available: http://www.ncbi.nlm.nih.gov/entrez/viewer.fcgi?29570778:NCBI:5998190. Accessed 25 November 2005.
198. Dole V, Jakubzik CR, Brunjes B, Kreimer G (2000) A cDNA from the green alga *Spermatozopsis similis* encodes a protein with homology to the newly discovered Roadblock/LC7 family of dynein-associated proteins. Biochim Biophys Acta 1490: 125–130.
199. Fracchiolla NS, Cortelezzi A, Lambertenghi-Deliliers G (1999) BitH, a human homolog of bithorax *Drosophila melanogaster* gene, on Chromosome 20q. Available: EMBL Nucleotide Sequence Database (http://www.ebi.ac.uk/embl), GenBank (http://www.ncbi.nlm.nih.gov/Genbank), and DNA Data Bank of Japan (DDBJ) (http://www.ddbj.nig.ac.jp) databases. Accessed 25 November 2005.
200. Quackenbush J, Cho J, Lee D, Liang F, Holt I, et al. (2001) The TIGR gene indices: Analysis of gene transcript sequences in highly sampled eukaryotic species. Nucleic Acids Res 29: 159–164.
201. Zhang QH, Ye M, Wu XY, Ren SX, Zhao M, et al. (2000) Cloning and functional analysis of cDNAs with open reading frames for 300 previously undefined genes expressed in CD34+ hematopoietic stem/progenitor cells. Genome Res 10: 1546–1560.
202. Cras-Meneur C, Inoue H, Zhou Y, Ohsugi M, Bernal-Mizrachi E, et al. (2004) An expression profile of human pancreatic islet mRNAs by serial analysis of gene expression (SAGE). Diabetologia 47: 284–299.
203. Crepieux P, Kwon H, Leclerc N, Spencer W, Richard S, et al. (1997) I kappaB alpha physically interacts with a cytoskeleton-associated protein through its signal response domain. Mol Cell Biol 17: 7375–7385.
204. National Center for Biotechnology Information (2004) GenBank DIC2 entry: MGC17810 synonym. Bethesda (Maryland): National Center for Biotechnology Information. Available: http://www.ncbi.nlm.nih.gov/entrez/viewer.fcgi?db=nucleotide&val=18087854. Accessed 25 November 2005.
205. National Center for Biotechnology Information (2004) GenBank Dlc2 entry: 6720463E02Rik and 1700064A15Rik synonym. Bethesda (Maryland): National Center for Biotechnology Information. Available: http://www.ncbi.nlm.nih.gov/entrez/viewer.fcgi?db=nucleotide&val=31542030. Accessed 25 November 2005.
206. Strausberg RL, Feingold EA, Grouse LH, Derge JG, Klausner RD, et al. (2002) Generation and initial analysis of more than 15,000 full-length human and mouse cDNA sequences. Proc Natl Acad Sci U S A 99: 16899–16903.
207. Lai CH, Chou CY, Ch'ang LY, Liu CS, Lin Wc (2000) Identification of novel human genes evolutionarily conserved in *Caenorhabditis elegans* by comparative proteomics. Genome Res 10: 703–713.
208. Tajima F (1983) Evolutionary relationship of DNA sequences in finite populations. Genetics 105: 437–460.
209. Pamilo P, Nei M (1988) Relationships between gene trees and species trees. Mol Biol Evol 5: 568–583.
210. Pfister KK, Fisher EM, Gibbons IR, Hays TS, Holzbaur EL, et al. (2005) Cytoplasmic dynein nomenclature. J Cell Biol 171: 411–413.

Amyotrophic Lateral Sclerosis. 2006; 7: 46–56

Taylor & Francis
Taylor & Francis Group

ORIGINAL ARTICLE

No association of *DYNC1H1* with sporadic ALS in a case-control study of a northern European derived population: A tagging SNP approach

PARESH R. SHAH[1,2], AZLINA AHMAD-ANNUAR[1], KOUROSH R. AHMADI[3], CARSTEN RUSS[4], PETER C. SAPP[5], H. ROBERT HORVITZ[5], ROBERT H. BROWN JR[4], DAVID B. GOLDSTEIN[3] & ELIZABETH M. C. FISHER[1]

ISSN 1748-2968 print/ISSN 1471-180X online
DOI: 10.1080/14660820500397057